MINIATURISED SYSTEM FOR DNA ANALYSIS

ABBAS ALI SALMAN
Doctor of Philosophy (PhD)

Teesside University

January 2013

This research project was carried out within the Nanotechnology group at Teesside University.

ABSTRACT

The growing markets for analytical techniques in areas such as pathogen detection, clinical analysis, forensic investigation, environmental analysis and food analysis require the development of devices with simultaneous high performance, speed, simplicity and low cost. Analysis of deoxyribonucleic acid (DNA) has been enhanced by use of the polymerase chain reaction (PCR) technique, which is now a widely used tool for *in vitro* amplification of nucleic acids.

In this work, a miniaturised PCR system comprising a microfluidic PCR chip, novel heating method and fluorescence detection unit was developed. PCR chip with reactants were shunted along three temperature zones in a fine polycarbonate chip. The polycarbonate PCR chip was fabricated using milling and thermal fusion binding for sealing of the cover. Thermal-cycling within the microfluidic chip was achieved by programmable shunting of the chip between three double side temperature zones with different temperatures to accomplish the denaturation, annealing and elongation steps necessary for PCR amplification. This thermal-cycling model potentially improves PCR efficacy because it increases the ramping rates for heating and cooling the PCR mixture. The detection unit comprises a photo-detector and Light Emitting Diode (LED) as the source of excitation. The detection limit of the system was determined on the PCR chip using Fluorescein isothiocyanate (FITC) as a fluorophore dye. The detection limit achieved was 7.8 pg ml^{-1} or (19.7 pmol) of FITC. The chromosomal DNA used in this work was extracted from non-pathogenic K-12 subtype of *Escherichia coli* (E. *coli*). The investigations showed that the system was capable of performing PCR amplification with different annealing temperature ranging from 54 to 68 °C, targeting three different sizes of PCR products of 250, 552 and 1500 bp. The prototype thermal-cycler and PCR chip were used successfully to amplify the three sizes and the results were compared with same fragments amplified on a conventional PCR .thermal-cycler machine. The method used for comparison was gel electrophoresis. In addition, a fluorescence detection system was employed for detecting of PCR products using SYBR Green I fluorescent dye. The whole system allows for developments of low cost, easy to use and portable instruments.

Key words: PCR shunting system, Portable PCR device, DNA analysis, Minturization, lab-on-a-chip**.**

Author's Declaration

I confirm that all novel material presented in this thesis is solely the work of the author

Name: Abbas Ali Abdulwahab Salman

Signature

Abbas

Acknowledgment

Foremost, I would like to express my sincere gratitude to my director of study Dr. Helen Carney for the continuous support of my PhD study and research, for his patience, motivation, enthusiasm, and immense knowledge. Her guidance helped me in all the time of research and writing of this thesis. I could not have imagined having a better advisor and mentor for my PhD study.

Besides my advisor, I would like to thank the other supervisors, Prof. Zulfiqur Ali and Dr. Simon Bateson, for their encouragement, insightful comments, and challenging questions. Many thanks and appreciation offered to my adviser Dr. Ralebitso-Senior, Komang and Dr. Sarker, Mosharraf.

I thank my fellow lab-mates, Henderson Andrew; Lakey Andrew; Bajuszova Zuzana; Pasirayi, Godfrey; Rashid Mamun; Abujaafar Elhashmi, for the stimulating discussions and for we have had in the last four years. Many thank to the entire Laboratory and the workshop technicians in Teesside University specially those who supported me in any respect during the completion of the project.

TABLE OF CONTENTS

List of Figures

List of Tables

Glossary

The following important terms have been used frequently in the thesis:

Deoxyribonucleic Acid (DNA) The chemical building blocks (molecules) of which genes (i.e., paired nucleotide units that code for a protein to be produced by a cell's machinery, such as its ribosome's) are constructed. Every inherited characteristic has its origin somewhere in the code of the organism's complement of DNA. The code is made up of subunits, called nucleic acids. Certain molecular machines (systems) to produce the proteins required by an organism interpret the sequence of the four nucleic acids. James Watson, Francis Crick, and Maurice Wilkins elucidated the structure of the DNA molecule in 1953. The DNA molecule is a linear polymer made up of deoxyribonucleotide repeating units (composed of the sugar 2-deoxyribose, phosphate, and a Purine or pyrimidine base). The bases are linked by a phosphate group, joining the 3' position of one sugar to the 5' position of the next sugar. Most molecules are double-stranded and anti-parallel, resulting in a right-handed helix structure that is held together by hydrogen bonds between a purine on one chain and pyrimidine on the other chain. DNA is the carrier of genetic information, which is encoded in the sequence of bases; it is present in chromosomes and chromosomal material of cell organelles such as mitochondria and chloroplasts, and also present in some viruses. More details were discussed in the introduction of the thesis.

Gene A natural unit of the hereditary material, which is the physical basis for the transmission of the characteristics of living organisms from one generation to another. The basic genetic material is fundamentally the same in all living organisms: it consists of chain-like molecules of nucleic acids- deoxyribonucleic acid (DNA) in most organisms and ribonucleic acid (RNA) in certain viruses- and is usually associated in a linear arrangement that (in part) constitutes a chromosome. The segment of DNA is involved in producing a polypeptide chain. It includes regions preceding and following the coding region (leader and trailer) as well as intervening sequences (introns) between individual coding segments (exons).

Base Pair (bp): Two nucleotides that are in different nucleic acid chains and whose bases pair (interact) by hydrogen bonding. In DNA, the nucleotide bases are adenine (which pairs with thymine) and guanine (which pairs with cytosine).

Chromosomes: Discrete units of the genome carrying many genes, consisting of (histone) proteins and a very long molecule of DNA. Found in the nucleus of every plant and animal cell.

Kilo base Pairs (Kbp): A unit of DNA equals to 1,000 base pairs.

Primer (DNA): A short sequence deoxyribonucleic acid (DNA) that is paired with one strand of the template DNA, in the Polymerase Chain Reaction (PCR) technique. In PCR testing the primer is selected to be complementary to the analytically-relevant sequence of DNA. It is the growing end of the DNA chain and it simply provides a free 3'- OH end at which the enzyme DNA polymerase adds on deoxyribonucleotides units (monomers). Which deoxyribonucleotides are added is dictated by base pairing to the

template DNA chain. Without a DNA primer sequence a new DNA chain cannot form since DNA polymerase is not able to initiate DNA chains.

Polymerase Chain Reaction (PCR): A reaction that uses the enzyme DNA polymerase to catalyze the formation of more DNA strands from an original one by the execution of repeated cycles of DNA synthesis. Functionally, this is accomplished by heating and melting double-stranded (hydrogen bonded) DNA into single-stranded (non-hydrogen bonded) DNA and producing an oligonucleotide primer complementary to each DNA strand. The primers bind to the DNA and mark it in such a way that the addition of DNA polymerase and deoxynucleoside triphosphates (dNTPs) causes a new strand of DNA to form which is complementary to the target section of DNA. The process described previously is repeated (trait, product, etc.) again and again to produce millions of copies (amplicons) of the desired strand of DNA. PCR and its registered trademarks are the property of F. Hoffmann-La Roche and Co. AG, Basel, Switzerland.

Template: In general terms, it is a pattern that can be copied or its shape reproduced. When used with reference to molecular dimensions, it is a macromolecular pattern for the synthesis of another macromolecule.

Detection limit (LOD) is the minimum amount of analyte can be detected or the minimum amount of analyte can produce a significant signal by a system or method.

Detector is a "device that responds to some characteristic of the system under observation and convert that responds into a measurable signal".(Skoog *et al*, 2004).

Molarity (M) is the number of mole of specific chemical dissolved in one litter of solution.

Mole is the amount of chemical substance that contained 6.022×10^{23} molecule of the substance.

CTAB (Hexadecyl Trimethyl Ammonium Bromide) extraction method (Murray HG and Thompson, 1980)

MEMS MicroElectroMechanical System is a fabrication technique used for developing Micro and Nano systems.

µ-TAS Miniaturized Total Analysis System.

$\mathbf{T_g}$ glass transition Temperature it is a temperature required to transfer the materials from a hard and relatively brittle state into a molten -like state

PC polycarbonate

PDMS poly (dimethylsiloxane).

PE polyethylene.

COC cycloolefincopolymer.

PEEK polyetheretherketone.

PEPE perfluoropolyether.

PI polyamide.

PMMA poly(methyl methacrylate).

POC point of care.

PP polypropylene.

PMMA Poly(methyl methacralate)

PTFE Poly Tetrafluoroethlene

PET Polyethylene terephthalate
PP Polypropylene
PDMS Poly(dimethylsiloxane)
CE Capillary Electrophoresis is a It is the most efficient separation technique available for the analysis of both large and small molecules.
OLED Organic Light Emitting Device.
PMT photomultiplier tube convert photons to an electrical signal. They have a high internal gain and are sensitive detectors for low-intensity applications such as fluorescence spectroscopy.
CCD charge-coupled device it is a device for the movement of electrical charge to typically to digital value.
LED light-emitting diode is a semiconductor light source.
LOD Lower Detection limit
ADC Analog-to-Digital Converter
Thermistor is a type of resistor whose resistance varies significantly with temperature, more so than in standard resistors
ISO International Organization for Standardization
AutoCAD is an industrial leader in 2D and 3D CAD design used for drafting, modeling, architectural drawing, and engineering software.
FITC Fluorescein isothiocyanate isomer I is a green fluorescent dye.
SAW Surface Acoustic Waves is a fabrication technique used to develop passive wireless sensors.
IDT Inter-Digital Transducer or Piezoacoustic IDT are a key component of SAWdevices, which are used for measurement of material properties and signal processing.
E. coli Escherichia coli is a gram-negative bactria.
TE buffer is a commonly used buffer solution in molecular biology"TE" is derived from its components: Tris, a common pH buffer, and EDTA, a molecule that chelates cations like magnesium ion.
EDTA is abbreviation of chemical name (Ethylenediaminetetraacetic acid).
MRSA Methicillin-resistant *Staphylococcus aureus* is a bacterium that causes infections in different parts of the body.
UV is the Ultra Violet light.
POC it is a Point of care device or portable device**.**

Chapter 1 Introduction

1.0 Introduction

The growing markets for analytical techniques in areas such as pathogen detection, clinical analysis, forensic investigation, environmental analysis and food analysis require the development of devices with simultaneous high performance, speed, simplicity and low cost. Analysis of nucleic acids has been substantially enhanced by the development of a technique called polymerase chain reaction (PCR). This technique is now an indispensable tool for *in vitro* amplification of nucleic acids. Current applications of PCR include forensic investigations, the detection of genetically modified foods, the detection of food authenticity and medical applications: for example, the identification of cancer-associated genes, viral sub-typing for AIDS and hepatitis, bacterial drug susceptibility research and the determination of genetic disorders. PCR is the most popular nucleic acid amplification method due to its simplicity; however, the commonly used Peltier effect, or metal-block-based PCR system, is characterized by high thermal mass, a large reaction volume and, thus, slow heating/cooling rates. The PCR process can be improved by increasing the heat transfer rate or decreasing the thermal mass.

This chapter is intended to provide background knowledge of PCR as an analytical technique that is relevant to biological analysis. The later sections present an overview of techniques in microfluidics, which may be applicable to PCR-on-a-chip. In particular, the focus will be on discussing common methods of fabrication and on-a-chip functions.

1.1 Background

In order to clarify PCR technique it is helpful to start by introducing the nucleic acids. The two main nucleic acids are Deoxyribonucleic acid (DNA) and Ribonucleic acid (RNA). Nucleic acids either DNA or RNA are molecules available in all living cells mainly in the nucleus of the cells and containing the genetic information vital for all cellular functions and heredity. Nucleic acids are consisting of either one or two long chains of repeating units called nucleotides (Stryer, 1981).

James Watson and Francis Crick elucidated the chemical structure of DNA in 1953. A molecule of DNA consists of a very long threadlike double strand molecule made from a large number of nucleotides. The backbone of the single stranded DNA molecule consists of nucleotide monomers illustrated in Figure 1.1 and linked by phosphodiester bridges (phosphate bonds). The nucleotide is a nitrogen base molecule bonded with a deoxyribose sugar molecule. The phosphodiester bridges linking the 3´- hydroxyl of the sugar with 5´- hydroxyl of the adjacent sugar as can be seen in the Figure 1.2 below (Stryer, 1981).

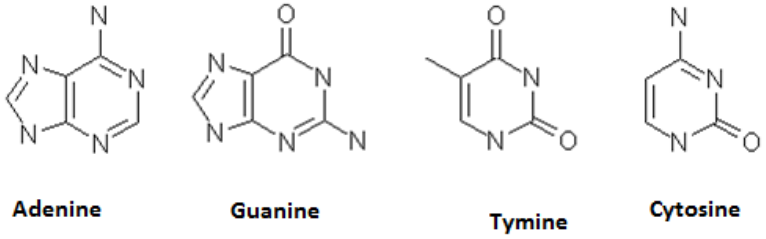

Figure 1.1 Chemical structures of the nitrogen bases (purine; adenine and guanine/pyrimidine; thymine and cytosine) that symbolize the DNA backbone units. The structures were drawn using ISIS/Draw.

The building block of the DNA chemical structure is the sequences of nitrogen bases. In the structure there are only four nitrogen bases; Guanine (G), Adenine (A), Thymine (T) and Cytosine(C). The two single strands of the DNA double helix run in an anti-parallel direction to each other. The sugar - phosphate back bone of each strand is on the outside of the double helix, whereas the nitrogen bases face inwards. The double helix is held together by hydrogen bounds between each pair of nitrogen bases, as shown in Figure 1.2. The significance in this connection, which is called Watson-Crick base pair, is that thymine (T) is always paired with adenine (A) while guanine is always paired with cytosine(C).

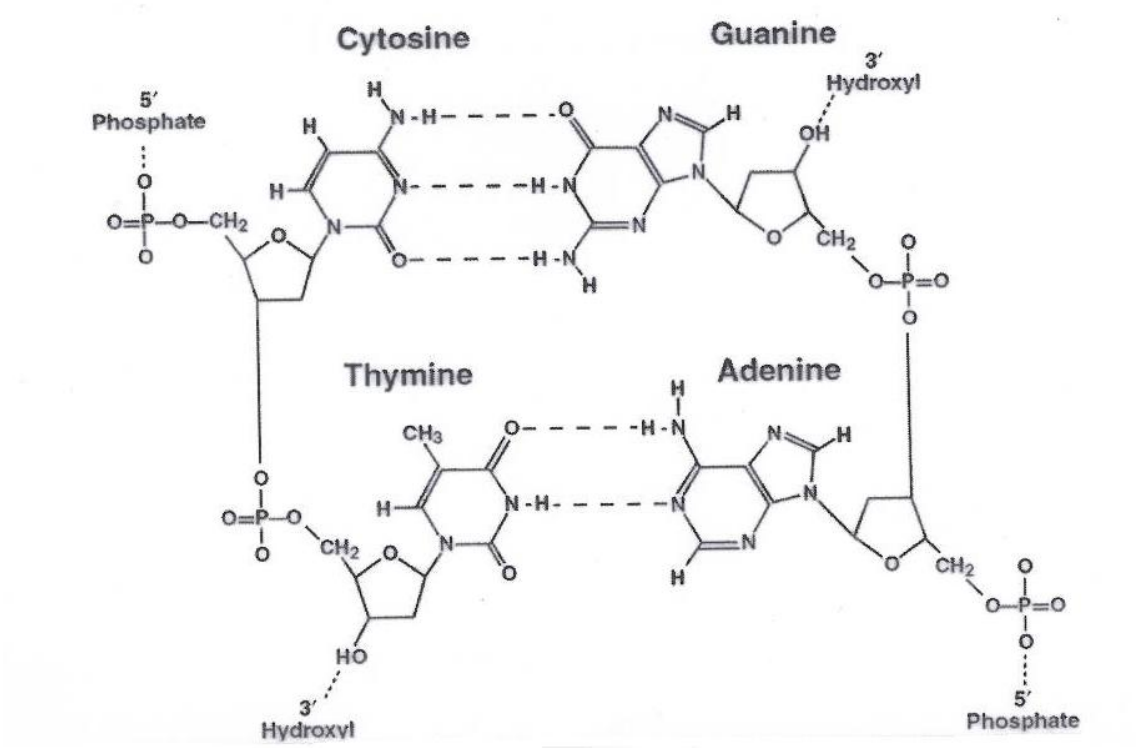

Figure 1.2 Chemical structure of double strand DNA molecule illustrating that the main structure is repeating units called nucleotides. Each nucleotide consists of one nitrogen base, one deoxyribose sugar and one phosphate molecule. The base pairs are connected by Watson-Crick base pair links adenine (A) is always paired with thymine (T) and cytosine (C) with guanine (G) in double strand DNA molecules. Phosphate-bond molecules link to deoxyribose sugar molecules to form the main stricture of the strand. The structure also illustrates that as one strand follows the sequence down the left-hand strand (C to T), the corresponding strand is also following the carbons of the deoxyribose ring, going from the 5′ carbon to the 3′ carbon. This is the basis for the 5′ to 3′ directionality of DNA. The 1′ carbon of each deoxyribose is substituted with a purine or pyrimidine base. In double-stranded DNA, bases face each other in the center of the molecule and base-pair via hydrogen bonds (dotted lines).

However, the nucleotides of the RNA contain Guanine (G), Cytosine(C), Adenine (A) and Uracil (U). The sugar molecule in the RNA is Ribose.

1.1.1 Principles of PCR technique

Enzymatic *in-vitro* amplification of nucleic acids has revolutionised the life science research and prompted numerous advances in biotechnology and analytical applications. Currently, nucleic acid amplification methods include, but are not limited to, polymerase chain reaction (PCR), single strand-displacement amplification (SSDA), nucleic acid sequence-based amplification (NASBA), rolling-circle amplification (RCA) and the Q_β replicas reaction. For example, single strand displacement amplification (SSDA) is an isothermal technique first introduced by Walker *et al,* in (1992) This method allows exponential amplification of double-stranded DNA. The

multiple strand displacement amplification (MSDA) technique is similar to SSDA, with the only difference being that during extension of the complementary strand; new annealing sites are generated for the first primer. Nucleic acid sequence base amplification (NASBA) was first initiated in 1991 by J. Compton. This method involves the simultaneous action of three enzymes that produce more than 10^9 copies of DNA under isothermal temperature (41 °C) conditions in 90 minutes. However, all of these methods have not yet replaced PCR because most of these methods are highly expensive and involve complex enzymatic processes in comparison with PCR (Auroux *et al*, 2004). PCR has been the most popular due to its simplicity and low cost. PCR is a three-step amplification process first introduced by Mullis and co-workers in 1986 (Mullis *et al*, 1986) It is a molecular biological method for amplifying DNA without using a living organism. It is, also a highly sensitive and specific methodology for the detection of nucleic acids and a useful tool for quantification of the amount of specific nucleic acid present in a target sample. The key component of the PCR process is the enzyme DNA polymerase, which occurs naturally in living organisms, where it functions to duplicate DNA when cells divide (Larrick, 1997).

PCR works by binding to a single DNA strand and creating the complementary strand. In Mullis's original PCR process, the enzyme was used *in vitro*. The double-stranded DNA was separated into two single strands by heating it to ~94°C. At this temperature, however, DNA-Polymerase was destroyed so that the enzyme had to be reloaded after the heating stage of each cycle. Mullis's original PCR process was very inefficient as it required a great deal of time, enormous amounts of DNA-Polymerase and regular attention throughout the PCR process. Mullis *et al*, (1986) discovered that the reciprocal interaction of two oligonucleutides and the DNA polymerase extension synthesise new DNA fragments, when they are hybridised to different strands of DNA template. These oligonucleutides are now termed “primers”. The primers are short segments of nucleotides, which complement a region of the DNA to be amplified, i.e. the structures of primers are copied from the original DNA template. They are the key components of the PCR amplification because they define the region of DNA to be amplified.

Basically, the PCR process consists of a series of thirty to forty cycles. Each cycle consists of three steps which can be described as the following:

1) The goal of this stage in PCR process is to breakdown the hydrogen bonds, which connect the double strand DNA (dsDNA), in order to provide single-stranded DNA molecules. The double-stranded DNA has to be heated to 94-96 °C in order to separate the strands. This step is called *melting;* it breaks apart the hydrogen bonds that connect the two DNA strands. This step must be accomplished in each PCR cycle. It was found that the versatile approach to ensure complete denaturation of dsDNA is to raise the temperature of the PCR mixture to a deflated degree ~94 °C. However, the optimal denaturation temperature and the optimal time required to achieve this goal still needs to be validated according to application and thermal-cycler efficiency. The DNA templates that are GC-rich in sequence may require a higher temperature, although the best denaturation is to be as low as possible for the shortest effective time that will maintain the highest DNA polymerase activity in the reaction (Bustin, 2010). Prior to the first cycle, the DNA is often melted for an extended time to ensure that both the template DNA and the primers have completely separated. This cycle requires, 1-2 minutes in conventional thermal cyclers. However, the minimum time for the denaturation step during thermal cycles is theoretically less than one second (Wittwer, *at el*, 1990)
2) After separating the DNA strands, the temperature is lowered so the primers can attach themselves to the single DNA strands. This step is called *annealing.* The primary annealing step is a sensitive and a specific step, which characterizes the success of the reaction. In the optimum annealing, the single-stranded primer molecules are annealed only to the target sequence on the single-stranded DNA template. However, several competing reactions also come about, such as, when the single-stranded DNAs are annealed with each other or the primers also anneal with each other to form a primer dimers. The optimum annealing temperature (T_a) depends upon the primer's melt temperature (T_m), which eventually depends upon the base sequence of the primers. The temperature of this stage depends on the primers and is usually 5°C below their melting temperature between 45-60°C. A wrong temperature during the annealing step will result in primers not binding to the template DNA at all, or binding at random. The time required for this step is between 1 to 2 minutes in conventional PCR machines. The temperature and time needed for annealing depend on the composition of the base, target DNA length

and concentration of the primers. Theoretically, duration of less than 1 second, could be used here like the denaturation time (Wittwer, *at el,* 1990).

3) The DNA-Polymerase has to fill in the missing strands. It starts at the annealed primer and works its way along the DNA strands. This step is called *elongation.* The elongation temperature depends on the DNA-Polymerase. This step takes much longer than the other two and the dwell time depends on the temperature, concentration, and the length of the target DNA segments. Longer extension times for early thermal cycles are helpful for complete amplification because more templates are made in the early thermal cycles, resulting in higher amplification rates and greater specificity (Wittwer, *at el,* 1990). The typical extension temperature is ~72 °C because the extension process is carried out using a thermo-stable DNA polymerase enzyme. The DNA polymerase in this step synthesise the target single strand DNA copy using the pooled dNTPs as a building blocks. The mechanism of the process is an enzyme polymerisation reaction. All four dNTPs are substrates, pyrophosphate (PP) is released, and the deoxynucleoside monophosphate (dNMP) is linked to the 3'-OH of the primer chain through formation of a phosphodiester bond. The deoxynucleoside monophosphate to be incorporated is chosen through its geometric fit with the template base to form a Watson-Crick base pair (A-T and G-C) see Figure 1.3.

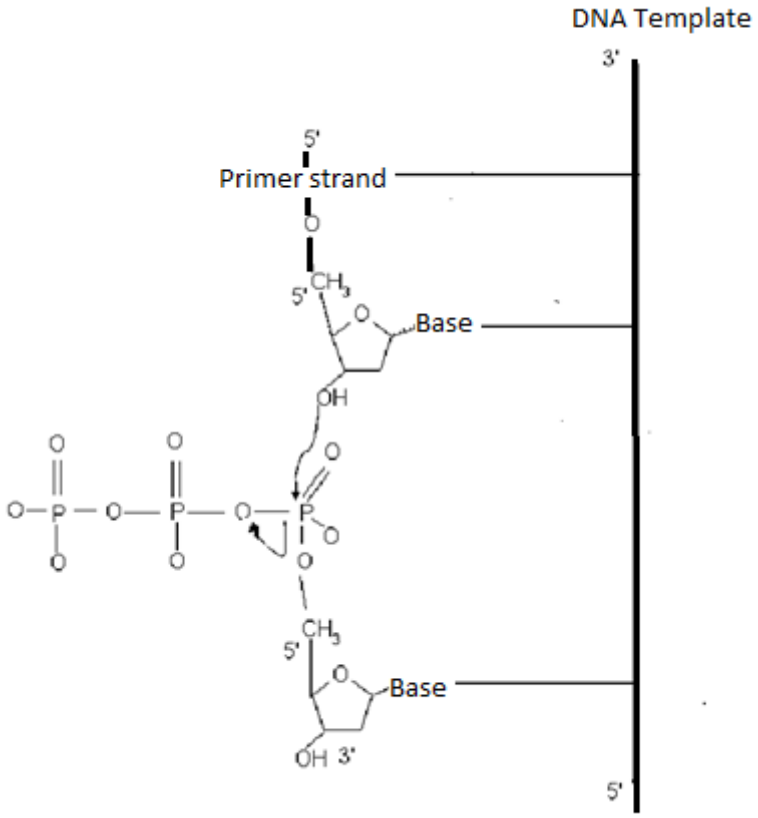

Figure 1.3 The mechanism of phosphodiester bond to attached to the 5`-deoxyribose of an oligonucleotide.

The first cycle, the dNTPs incorporate beyond the sequence complementary to the primer to form undefined DNA fragments, see Figure 1.3. However, from the second cycle, both primers (forward and reverse primer) flank the elongation and after that, the process exponentially increased to accumulate the target products (Harris and Jones, 1997).

In summary Figure 1.4, the first cycle of PCR progress, sample DNA is heated in a vial to 94 °C to separate the strands. The primers, free nucleotides, and a heat-stable DNA polymerase are present in the vial as the temperature is lowered to ~60 °C. At this temperature, the primers attach to the sample DNA sequences that match them. The primers contain a sequence that signals the polymerase to begin replicating DNA at that location. If the primers do not match any of the DNA in the sample, the DNA will not be replicated. However, if they do match, the polymerase starts to copy the matching piece of the DNA strand. As the next temperature cycle begins, the DNA is heated and the newly synthesized strands separate from the original strands. The enzymes start the

copying process all over again, doubling the number of DNA copies with each pass. After 30 cycles, the desired DNA fragment may be multiplied more than 1 million-fold (Brown, 2001).

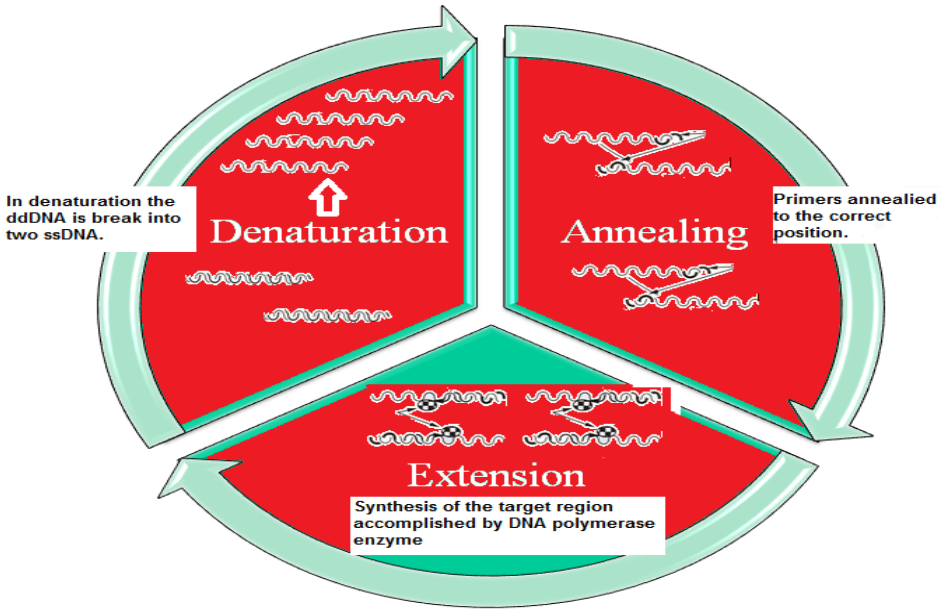

Figure 1.4 Schematic diagrams describing the three processing steps of PCR technique.

In chapter two of this thesis the kinetic of PCR will be discussed in more details. The mathematical model of heat transfer in response to PCR systems will also be described.

1.2 Current PCR applications

The area of PCR applications has extended across the range from genomic and developmental biology to medical diagnostics, forensic investigation and environmental analysis. It provides a predominantly flexible tool for the research scientist and clinical laboratories, due to the simplicity in implementation and reliability of the PCR. The main applications in medical diagnostic laboratories include the diagnosis of certain genetic diseases and the detection of pathogens, mutation detection and cancer diagnostics. The analysis and exploitation of genome sequencing information is mainly depending on PCR results for interpretation. Furthermore, quantitative real-time PCR technology has recently reached a level of sensitivity and accuracy also supports its use as a routine bio-technique for gene phase measurement. Cancer research has already

been implemented in real time PCR analysis and others are being validated, showing that this molecular biology tool can provide both researchers and clinicians with valuable information concerning the behaviour of tumours. DNA fingerprinting has been implemented worldwide for forensic investigation. This application revolutionised forensic science and established a new field of science called "forensic biology", which mainly exploited PCR technique as a powerful tool for detecting evidence.

Detection of genetically modified food (GM food) and the authenticity of food product are the main useful applications of PCR technique in food analysis. Detection of genetically modified food is accomplished using either a by PCR method or a protein based method. Both techniques are efficient and commonly applied methods. In the PCR method, the technique does not target the regulator genes but focuses on the artificially introduced DNA sequences. Semi-quantitative tests will detect GM food and compare the results to external reference standards of known GM food concentration, with a detection limit of 0.1%. Real-time (PCR) is used for greater accuracy in quantization and has a detection limit of 0.01%. The diversity of genetically altered crops most certainly will increase and, therefore, analytical demands will continue to increase as well (Meyer, 1999)

PCR is the best tool to detect pathogen viruses, which are currently the most public concern problem, especially the communicable diseases, such as influenza viruses or swine flu (H1N1) and sexual diseases, such as the human immunodeficiency virus (HIV).

1.3 PCR mathematical model

Polymerase chain reaction is the name of an enzymatic process related to three terms: "Polymerase" because the only enzyme involved in this reaction is DNA polymerase; "chain" because the products of the first reaction become substrates of the following one, and so on; "reaction" because the method progress depends upon enzyme synthetic reaction. The method, as described by Mullis *et al,* (1986) consists of "repetitive cycles of denaturation, hybridization and polymerase extension" and is known as PCR. Therefore, the PCR is a technique capable of specifically amplifying a single nucleic acid molecule into billions of copies (Mullis *et al* 1986).

In this chapter, the mathematical model of the PCR process will be described, in order to define the major factors which govern the efficiency, the specificity and quality of PCR as an analytical technique. In order to simplify the mathematical description, all the discussion will describe the DNA reaction process as a model.

1.3.1 PCR amplification process

The PCR process is started by one molecule of chromosomal double strand DNA (ds DNA) called the template. As this DNA molecule typically consists of millions of base pairs, the amplification process targets only a specific part of this template; then after one cycle of PCR amplification, the process generates two new DNA strands initiated from the primers, in addition to the original dsDNA template (Figure. 1.5). The new double strand DNA is shorter than the original DNA template but longer than the target region to be amplified. This is because the cycle is only defined at one end of the targeted region and the elongation takes place along the DNA template (Figure. 1.5). In the second cycle the primers anneal to the new single strands of DNA synthesized from the first cycle. The elongation of this cycle will produce two double DNA strands identified from both sides by the primers, which mark the target region to be amplified. In the further cycles this double stranded DNA will be amplified exponentially until the PCR reagents are exploited. However, the primers are not only annealed to the new DNA strand but also to the original DNA template and this generates double strands DNA elongated by primers on one side.

Theoretically, the number of templates should double after each cycle. In practice, the DNA increases by a factor of (1+ x) where (x) is the cycle efficiency. The number of target products are simultaneously increased by the increasing the cycle number (Saiki *et al*, 1985). The PCR efficiency was first calculated according to the formula:

$$Y = (X+1) \qquad \textbf{Equation 1.1}$$

Where (X) is the main efficiency per cycle, (n) is the number of cycles and (Y) is the yield of amplification. This relationship became the standard way to express the overall efficiency of PCR processes. According to this formula, the PCR amplification at 100 % efficiency should be able to generate in a quantity of more than 10^6 product molecules per original template molecule after 20 cycles, as described in Figure 1.6**.**

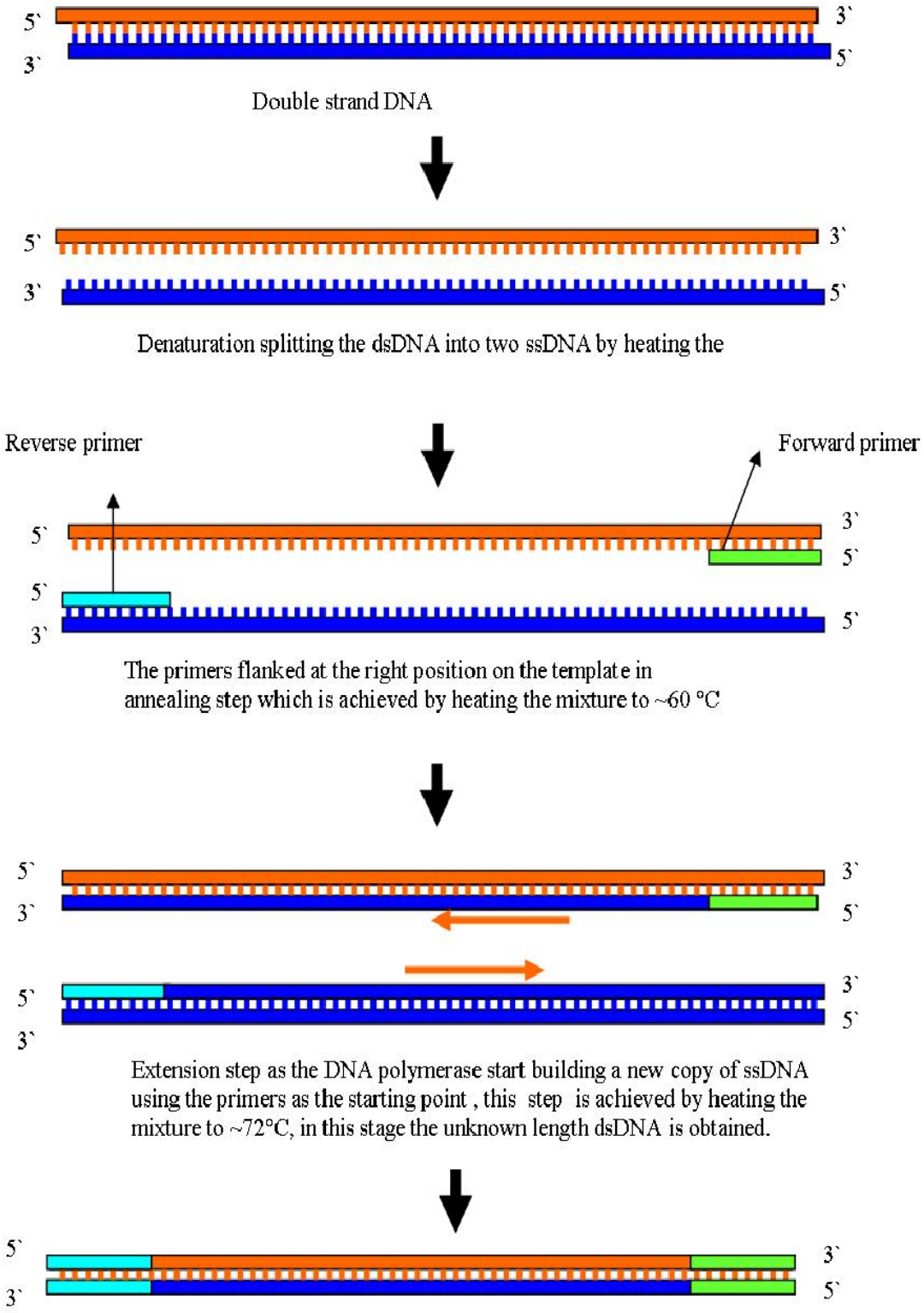

Figure 1.5 Sequence steps of PCR process: the steps show how the primers flank to the targeted region on the DNA template and then these new DNA fragments are amplified in further cycles.

However, the actual efficiency of the PCR process always varies depending on the reactant's concentrations and the thermal-cycler conditions. It has been experimentally observed that yields can vary from cycle to cycle. There is a general decreasing trend with the increasing cycle number. Typically, the reaction takes place in a vial situated at the thermal cycler when all the reactants and the polymerase enzyme are added. In the early cycles, the ratio between the concentration of the target DNA and the concentration of the primers and the enzyme will be in ratio of (0/100). At the mid stage of the reaction, the ratio between the concentrations of the target DNA and the reactants becomes more comparable (50/50), because the reactants are being consumed and the target DNA increased exponentially. In mean time, the behaviour of the thermal cycler and the rate of heating and cooling affect the efficiency of reaction. In standard thermal-cyclers, the absolute amount of the synthesized product does not always stand at a constant relationship to the initial target amount; this is because the efficiency of the amplification is sensitive to several variables that even include variations from one well to another (Mehra ,2005).

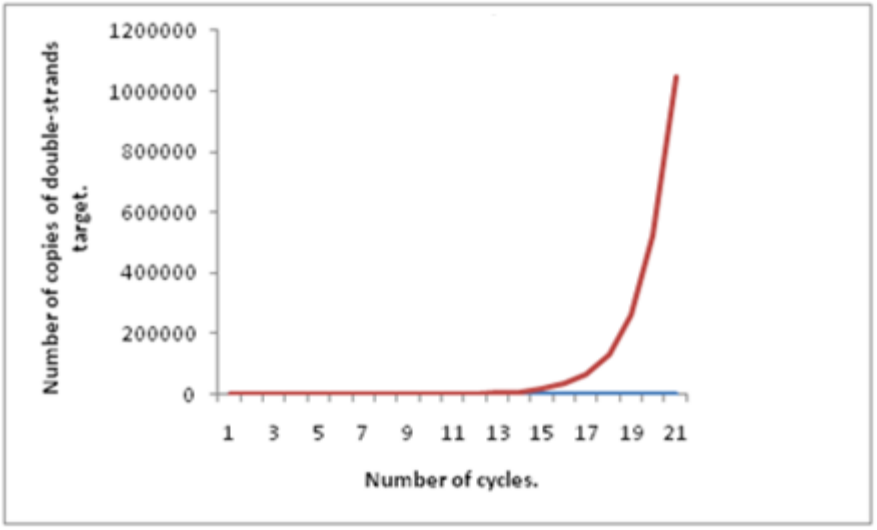

Figure 1.6 This curve illustrates the amplification expected from 100 % efficiency of the PCR process. As, can be seen blue line showed the base line and there is an exponential growth in the number of the target region to be amplified after cycle number 14 (red line) to cycle number 21.

1.3.2 PCR Kinetics

Enzymes are high molecular weight proteins and their reactions are particularly characterized because of their selectivity and specificity. This property is useful in terms

of analytical techniques, as "they are widely used in the determination of molecules (substrates) with which they combine when acting as catalysts" (Skoog *et al*, 2004). Generally, the mechanism of enzymes reactions are governed by the law of Michaelis-Menten kinetics (1913). The Michaelis- Menten equation is an empirical model used to characterize the ideal response of the enzyme initial reaction rate to the increasing concentration of substrate in solution. The accuracy of this model relies upon conditions of uniformly distributed substrate molecules in solution, each in motion with a random probability of collision with an enzyme molecule determined by the concentration of substrate and of the enzyme. Typical application of this model holds the enzyme concentration constant and varies the substrate concentration, over a range from zero to 10 times the expected substrate concentration K_m that produces one-half of the maximum reaction velocity (Jackson and MacCluer, 2010)

The Equation 1.2 describes the reaction mechanism.

$$E + S \underset{k-1}{\overset{k1}{\leftrightharpoons}} ES \xrightarrow{k2} E + P \qquad \textbf{Equation 1.2}$$

Where, (E) is the enzyme, (S) is the free substrate, (ES) is the enzyme-substrate complex, (P) is the product. As can be seen from the equation, it is divided into two steps: in the first step the enzyme (E) reacts reversibly with the substrate (S) to form an enzyme–substrate complex (ES), then dissociated irreversibly to produce the product (P) and the regenerated enzyme in the second step. Equation (1.2) is derived from the steady-state approximation, in which the concentration of the complex (ES) is assumed to be small and relatively constant throughout of the reaction. The rate constant of the (ES) complex is (k_1); the reverse of the first step rate is given by (k -1) and the rate of the second step is (k_2), by assuming that the concentration of [ES] is constant, which means that the rate of change $\frac{d\mathcal{X}\,[ES]}{dt}$ is Zero, where (t) is the time of the reaction (Skoog, *et al*, 2004).

By rearrangement of this equation, the rate of change then will be in this form:

$$\frac{d\mathcal{X}\,[\mathrm{ES}]}{d\mathrm{t}} = \mathrm{k}_1[\mathrm{E}][\mathrm{S}] - \mathrm{k}_{-1}[\mathrm{ES}] - \mathrm{k}_2[\mathrm{ES}] = 0 \qquad \textbf{Equation 1.3}$$

Equation (1.3) can be solved to magnitude [ES] at this arrangement:

$$[\mathrm{ES}] = \frac{\mathrm{k}_1[\mathrm{E}][\mathrm{S}]}{\mathrm{k}_{-1}+\mathrm{k}_2} \qquad \textbf{Equation 1.4}$$

However, if we want to express the rate low in terms of enzyme the total enzyme concentration that is known, then according to the mass balance the initial enzyme concentration will be:

$$[\mathrm{E}]_0 = [\mathrm{E}] + [\mathrm{ES}] \qquad \textbf{Equation 1.5}$$

Then, from Equation (1.4), and (1.5):

$$[\mathrm{ES}] = \frac{\mathrm{k}_1[\mathrm{E}][\mathrm{S}]}{\mathrm{k}_{-1}+\mathrm{k}_2+\mathrm{k}_1\,[\mathrm{S}]} \qquad \textbf{Equation 1.6}$$

Accordingly, the rate of product formation is:

$$\frac{d[\mathrm{P}]}{d\mathrm{t}} = \mathrm{k}_2[\mathrm{ES}] \qquad \textbf{Equation 1.7}$$

If the value of [ES] is replaced by equation (1.6), the formula will be rearranged the following form:

$$\frac{\mathrm{d}[\mathrm{P}]}{\mathrm{dt}} = \frac{\mathrm{k}_2\,[\mathrm{E}]_0[\mathrm{S}]}{\frac{\mathrm{k}_{-1}+\mathrm{k}_2}{\mathrm{k}_1}+[\mathrm{S}]} = \frac{\mathrm{k}_2[\mathrm{E}]_0[\mathrm{S}]}{\mathrm{K}_\mathrm{m}+[\mathrm{S}]} \qquad \textbf{Equation 1.8}$$

Where (K_m) is the Michaelis-Menten constant of the enzyme, which can be defined as the substrate concentration at 1/2 the maximum velocity as can be seen in Figure 1.7.

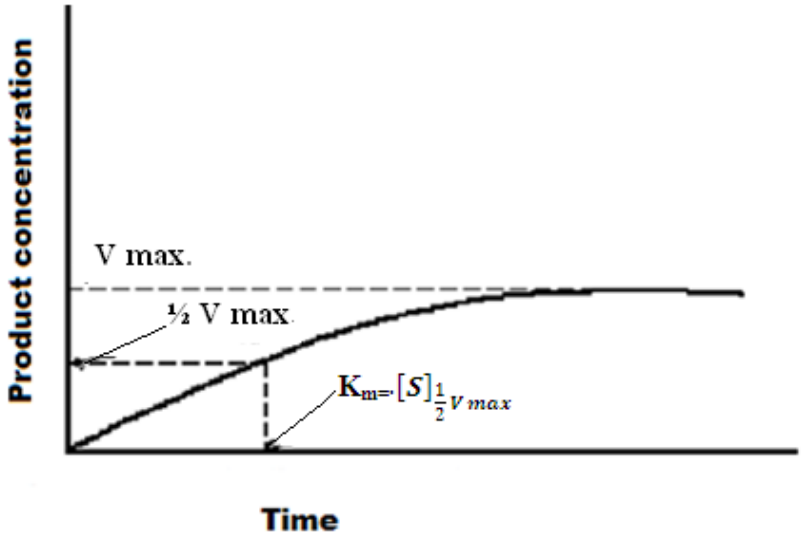

Figure 1.7 Michaelis-Menten kinetics for product concentration (Breathier and Silberzen, 2006).

Therefore, the Michaelis-Menten (K_m) will be:

$$K_m = \frac{k_{-1}+k_2}{k_1} = \frac{[E][S]}{[ES]} \qquad \textbf{Equation 1.9}$$

The PCR process is related to the concentration of free enzyme [E], which is DNA polymerase; the free substrate [S] is related to the primer-template complex; and the enzyme-substrate complex [ES] is related to the primer-template-polymerase complex. The Michaelis-Menten constant for nucleotide addition is 4 µM (Schnell and Mendoza, 1997)

The maximum velocity of reaction is described by (Equation 1.10):

$$V_{maxi} = k_2 [E_1] \qquad \textbf{Equation 1.10}$$

From equations 1.9 and 1.10, it can be elucidated that the rate of product formation in each PCR cycle as in Equation 1.11**:**

$$V = \frac{v_{maxi[S]}}{[S]+k_M}$$ **Equation 1.11**

Therefore, the rate of product formation after n cycles will be:

$$V_n = \sum_{i=0}^{n-1} V_{i=} \sum_{i=0}^{n-1} \frac{v_{maxi[T_i]}}{[T_i]+K_M}$$ **Equation 1.12**

Where, (i) is a specific cycle number, and (T_i) is the template concentration.

According to Equation 1.6 the rate of the product, formation is not exactly the same in each PCR cycle. Moreover, the "hyperbolic saturation", which typically effects the enzymes reaction, clearly happens during later cycles when the reaction reaches the maximum velocity (v_{maxi}) (Schnell and Mendoza, 1997) as described in Figure 1.8.

As has been explained in [1.1], each PCR cycle consists of three stages: denaturing of the DNA, annealing of primers to single strand DNA (ss DNA) and enzymatic elongation of the complementary strand by the DNA polymerase. The start of the cycle is defined as the beginning of the denaturing step.

As PCR is an enzymatic-based method, the Michaelis–Menten mechanism can be applied to evaluate the efficiency of the process. The mechanism calculates the enzyme characteristics; synthesis of products; and the analysis of enzyme completion and inhibition.

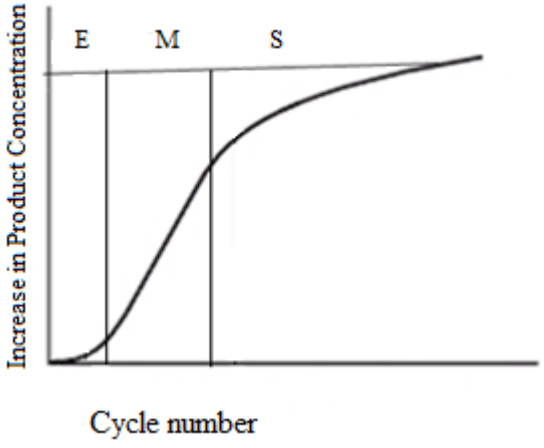

Figure 1.8 Kinetic accumulation of the target product during the PCR, (E) is the initial reaction phase where the product concentration is low, (M) is the exponential phase where the product is exponentially amplified and (S) is the saturation point or the plateau of the reaction (Schnell and Mendoza, 1997).

As can be seen in Figure 1.8 the amplification rate in the early phase of the reaction is slow as the primers at this phase are searching for the correct complementary position on the DNA template and producing non-specific DNA fragments, as has been described [1.1.1]. The following phase of the PCR reaction is the actual amplification process because the target molecules (the products) start doubling or are exponentially increased and the numbers of non-specific DNA fragments are decreased. This is because in this phase the target molecules are abundant and the concentration of the original template is small. The late phase is a saturation stage of the enzyme reaction because the velocity of the reaction reaches the maximum and the concentration of the products is high. Therefore, the polymerase concentration will not be enough to process a further exponential amplification reaction and, therefore, later cycles will produce fewer products.

1.3.2 PCR reaction and efficiency

1.3.2.1 Introduction

PCR efficiency is the ability of the system to duplicate the specific product in particular PCR cycle. As has been described [1.1], the PCR mixture contains: buffer (includes salt ions), dNTPs and polymerase enzyme at a concentration that allows addition of DNA template and primers to produce the final reaction volume. The primers concentration that should be used in a PCR depends upon the experiment, because the primer/template ratio is a vital concern. The scientists found that high concentration of primers in the PCR reaction could generate primer-dimer formation and mispriming on non-target sequence (McPherson and Moller, 2006).

Booth et al, (2010) found that the overall efficiency of PCR process depends on the efficiency of the denaturation step, the efficiency changes from cycle to cycle and different mechanisms may control the system over the whole cycles.

However, if the efficiency of the PCR is mostly determined by the ratio of the free total enzyme concentration during a particular PCR cycle (i), then the PCR efficiency (Εi) is:

$$\epsilon_i = 1 - \frac{[ET_i]}{[E_i]+[ET_i]} \qquad \textbf{Equation 1.13}$$

The following sections will describe systematic PCR reaction and the factors affecting its efficiency.

1.3.2.2 Optimisation of PCR reaction

In spite of PCR's power and flexibility, a PCR method must be carefully designed and applied only after correct validation. The efficiency of and results from DNA amplification are easily affected by controlled variations in reaction conditions, which may lead to significant difference in results due to the exponentially amplifying nature of PCR . Therefore, major factors affecting the reproducibility and comparability of PCR must be considered and controlled to set up reliable PCR based assays. These factors include quality and quantity of components such as DNA template, polymerase enzyme, and various chemical components, as well as the performance of thermal-cyclers conditions (Young *et al*, 2008)

In regard to PCR buffer ingredients, concentrations and, increasingly, PCR pre-mixture are commercially available. The companies such as: Promega, Alfa DNA, Bio-synthesis and Invitrogen are now providing PCR pre-mixture. These mixtures include buffer dNTPs and thermo stable Taq DNA polymerase at appropriate concentrations allowing the users addition of template DNA, primers and biological water to obtain the final reaction volume. Optimising the constituents' concentration is essential to achieve the best amplification because inappropriate concentration could inhibit the reaction (McPherson and Moller, 2006).

The suppliers of thermo- stable DNA polymerase provide 10 time concentrated reaction buffer with the enzyme. This buffer usually contains the constituents listed in Table 1.1.

Table 1.1 this table is an example of commercially available PCR buffer ingredients**. (**Promega ,USA)

#	Ingredient	Concentration in 10 X buffer	Function of the ingredient
1	Tris-HCl (*p*H at 25 °C)	100 mM	Regulate the *p*H of the reaction at different temperature, to be in between 6.8 to 8.3.
2	Potassium chloride (KCl)	500 mM	Ionic salt assist primer-template annealing.
3	Magnesium chloride ($MgCl_2$)	1.5 mM	Enhance polymerase activity.
4	Gelatine	1 mg / ml	Stabilise polymerase.
5	Tween-20	0.1 %	Prevent aggregation of DNA polymerase.
6	*NP-40	0.1 %	Prevent aggregation of DNA polymerase.
7	Bovine serum albumin (BSA)	500 µg / ml	Binds many PCR inhibiters in the reaction vial.

* NP-40 is a non-ionic detergent polyoxyethylene surfactant that is most frequently used as a component of cell lyses buffers or other solutions intended to extract DNA and proteins.

1.3.2.3 PCR primers

The purity and the specificity of primers are essential to ensure the perfect PCR amplification. Primers are annealed to the single strand DNA (ssDNA), that is, denatured dsDNA, to provide an initiation site for the extension of the target DNA molecule. The 3´-end of the primer must match the 3´- end in the target region to ensure correct polymerase extension. The 5´-end of the primers is less important in determining the target region and this depends on application. Primers can either be specific or non-specific. The specific primers are designed to be complementary to a known sequence gene. However, the non-specific primers, which are called "universal", are complementary to nucleotide sequences, which are very common in a particular set of DNA template i.e. can be found in many types and many species (McPherson and Moller, 2006; Bustin, 2004).

The primer's melting temperature (T_m) is used to indicate the annealing temperature setup and can be defined as the temperature at which half the primers are annealed to the target region. Many calculation methods can be used to estimate the primers melting

temperatures. The simplest method is Equation (1.14), which used to calculate the melting temperature of primers of (20) base pair or less. This equation depends on the fact that G/C base pairs are more stable than A/T base pairs; due to stronger hydrogen bonding (McPherson and Moller, 2006).

$$T_m = (\text{Number of G+C}) \times 4°C + (\text{Number of A + T}) \times 2\ °C \qquad \textbf{Equation 1.14}$$

However, if the primers have between 15 and 70 base pairs, equation (1.14) can be used to calculate melting temperature.

$$T_m = 81.5 + 16.6(\log_{10}(I) + 0.41\ (\%\ G + C) - (600/N) \qquad \textbf{Equation 1.15}$$

Where, (I) is the concentration of monovalent cations and (N) is the length of the primer (McPherson and Moller, 2006).

The melting temperature can be estimated using the melting curve, which can be accomplished by real time PCR thermal-cyclers as these machines are usually supplied with a fluorescence detection unit. The PCR mixture, which contains a fluorophore, is placed in the thermal-cycler and the temperature is gradually ramped from ~40 °C to ~90 °C while continuously taking a collection of fluorescence readout. As the fluorophore is brighter while binding with dsDNA, the fluorescence intensity drops down after all the dsDNA is denatured to ssDNA. The melting curve Figure 1.9 is then constructed by plotting the first negative derivative of the fluorescence as a function of the temperature ($\frac{dF}{dT}$) to obtain a peak of melting. Consequently, the annealing temperature can be estimated to be about 5 degree below the melting temperature (T_m) (Bustin, 2004).

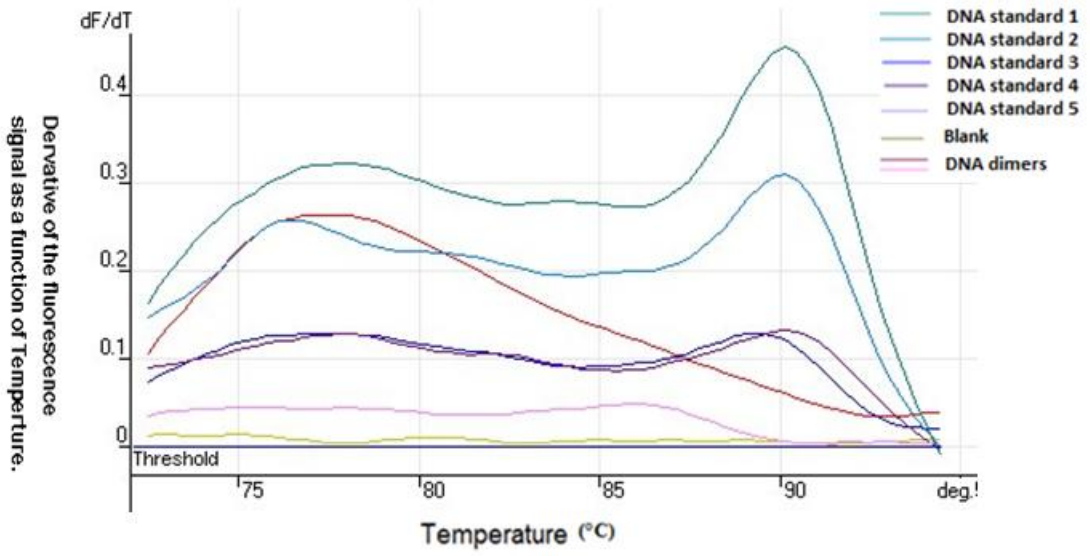

Figure 1.9 Typical melting curves, which indicate the melt peak of the PCR reaction mixture, these measurements can be measured using a real time thermal-cycler. (dF/dT is derivative of the fluorescence as a function of the temperature)

Primer concentration is also essential to optimise the PCR process. In any PCR experiments the forward and reverse primers are in equal concentrations. The common method used to estimate the appropriate primer concentrations is by determining the molar excitation coefficient of the primer aliquot and the absorbance of the solution at 260 nm, then applying the following equation (McPherson and Moller, 2006):

$$A_{260} = \varepsilon c I \qquad \textbf{Equation 1.16}$$

Where, A_{260} is the absorbance at 260 nm of the aliquot of the primer and (ε) is the molar excitation coefficient of the individual nucleotide ($M^{-1}cm^{-1}$). It is the extinction coefficient, which allows for estimation of the molar concentration of a solution from its measured absorbance and can be calculated by summing up the (ε) of each four nucleotides in the primer sequence multiplied by number of each individual nucleotide. The (ε) of each nucleotide in DNA is as follows (McPherson and Moller, 2006)

Adenine (A) = 15200 $M^{-1}cm^{-1}$× number of A in the primer sequence.

Guanine (G) = 12010 $M^{-1}cm^{-1}$× number of G in the primer sequence

Cytosine (C) = 7050 $M^{-1}cm^{-1}$× number of C in the primer sequence.

Thiamine (T) = 8400 $M^{-1}cm^{-1}$× number of T in the primer sequence.

(I) is the width of the absorption cell.

(c) is the primer concentration need to be estimated.

Accordingly the primer concentration will be:

$$c = \frac{A_{260}}{\varepsilon I} \qquad \textbf{Equation 1.17}$$

1.3.2.4 DNA polymerase enzyme

Optimising the PCR reaction and maximising amplification yield throughout can be achieved by improving the activity of DNA polymerase. A thermo-stable enzyme, *Taq*, which had been extracted from the bacterium *Thermus aquaticus* was the first remarkable step in PCR development (Saiki *et al*, 1988). In the early stages, the enzyme was heated in the denaturation step and lost its activity after each denaturation step. Consequently, the polymerase had to be reloaded after each cycle, which was arduous and, importantly, increased the risks of contamination during PCR as the sample vial had to be re-opened. This made optimisation almost impossible to achieve. Saiki *et al*, (1988) found that *Thermus aquaticus* is a heat-resistant enzyme and it is relatively unaffected by the denaturation step, "it does not need to be replenished at each cycle". Therefore, the introduction of a thermo-stable enzyme prevented this cumbersome procedure and also enabled the automation of the process.

Other enzymes, such as Pfu, KlenTaq, Vent or Tfi, have been applied to PCR later on. Significantly, some enzymes are nowadays modified to block their activity until they are heat activated. This is, for example, the case with PfuUltra hot-start DNA polymerase. In this instance, heat labile antibodies neutralise the enzyme activity until they are denaturised during the initial PCR denaturation step. Such a procedure limits the formation of non-specific products, as it damages the enzyme activity until thermo-cycling temperatures are reached.

1.3.2.5 Optimisation of the thermal-cycler condition

As has been mentioned [1.1.1], the PCR process is a complex of three reactions, each usually occurring consecutively at specific temperatures. In current thermal-cycler machines, a large fraction of time is needed to heat and cool the reaction mixture due to the need for bringing the large metal block to the cycle equilibrium temperature and to

transfer heat to the reaction mixture through the reaction tubes. Therefore, the cycle time is set by the thermal capacitance of the metal block and the heat transfer through the reaction tubes (Bustin, 2010, pp 48-50).

Optimal temperature and the time required to achieve it depends upon many factors including: melting temperature of the primers; the concentration of the primers; the length and the melting temperature of the product; the activity and stability of the DNA polymerase at different temperature and the thermal-cycler capacity.

1.3.2.6 Rapid thermo-cycling

The optimum time of PCR protocol depends mainly upon the instrumentation limitation. The laboratory based study of Young *et al.* (2008) investigated the effect of thermal cyclers on PCR performance. They measured inter-block reproducibility and intra-block repeatability showed that temperature-calibrated instruments consistently generated more repeatable rapid data than non calibrated instruments, regardless of the make and model of a thermal cycler.

However, the minimum time required to accomplish each PCR step depends upon the melting temperature (T_m), concentration of the primers and the stability of the DNA polymerase (Wittwer *et al,* 1990). Consequently, the thermal cycler's correct temperature setup is a vital factor of the PCR results and the attainment of one block for heating and cooling between the PCR steps. Ideally, the reaction temperature should change in a linear manner until it reaches a specific step in the PCR and remain constant during the step, as can be seen in the Figure 1.10.

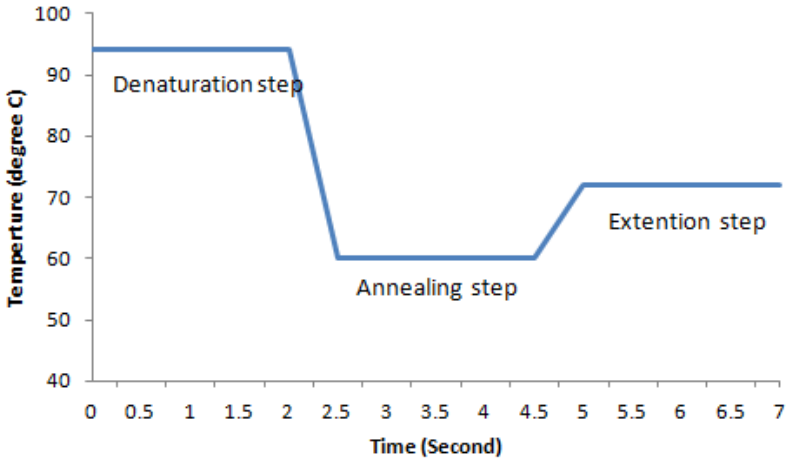

Figure 1.10 Diagram of conventional PCR cycles which focuses on three reactions (denaturation, annealing and extension). As can be seen during each PCR cycle, each reaction step occurs at certain temperature over a certain time span.

This type of cycle has generally occurred in the typical thermal-cyclers machine, as the time required for the temperature transition between steps is taking a longer time than the actual process. However, as the cycling speed increased in modern machines which applied advanced technology, such as Peltier technology, the proportion of time spent in temperature transition between the steps decreased and temperature ramping changed, as in Figure 1.11.

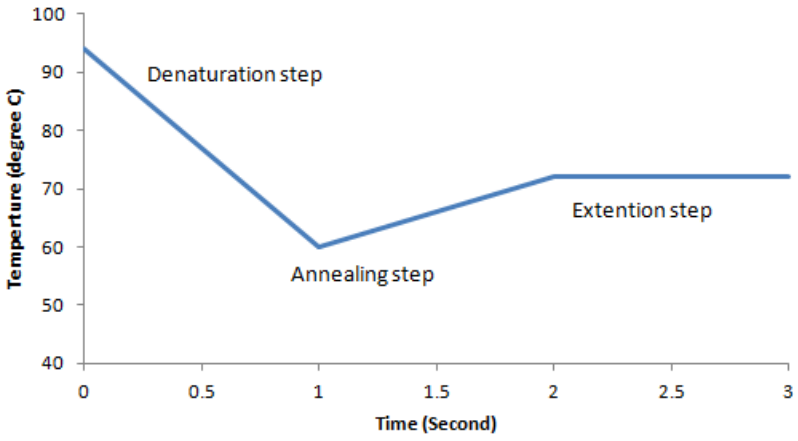

Figure 1.11 Diagram of rapid PCR cycles focused on three reactions (denaturation, annealing and extension). In this process the cycle time is less and the holding time depends upon the application.

During the rapid PCR, the hold time required for each step is adjusted according to the size of target region. If the target region is, for example, less than a 100 base pairs, no holding time is necessary to accomplish an efficient PCR reaction (Wittwer *et al,* 1990).

The number of cycles required to accomplish optimum amplification is mainly dependent on the efficiency of each reaction step and the concentration of the DNA template. The number of cycles also affects the specificity of reaction because the extra cycles may enhance the primers to anneal with non specific regions on the template. Generally, the ideal amplification can be managed in between 25 to 40 cycles (Harris and Jones, 1997): However, a more sensitive PCR-reaction can be achieved using a nested PCR, which usually amplifies the PCR product from the first process with more specific sets of primers.

1.4 Lab-on-a-Chip

1.4.1 Introduction

The key function of the microfluidic system is the manipulation and analysis of fluids within micrometre sized channels or chambers. Fabrication of these small components and networks has been mastered Figure 1.12 by micro-fabrication techniques adapted from semi conductor and plastics industries, such as photolithography, micromachining, replica moulding, hot embossing and injection moulding. Introducing miniaturised systems into analytical and bio-analytical laboratories could improve the analytical techniques by reducing the size of equipment, reducing the time of the analysis and automating the systems. Lab-on-a-chip devices are generally miniaturised versions of current lab processes, which have been scaled down onto a microchip format, where as Micro Total Analysis Systems are generally devices which have all process steps, integrated onto one device. Lab-on-a-chip (LOC) and Micro Total Analysis Systems (μTAS) are becoming of great interest amongst research groups. There are a wide range of applications for these lab-on-a-chip and μTAS devices, such as point of care diagnostics, chemical analysis, environmental monitoring, and forensic testing.

Figure 1.12 The picture summarises the concept of Lab-on-a-chip which is intended to scale down the all the laboratory activities in one chip. (Lab-on-chip.Gene-quantification.info, 2010).

The area of µTAS has rapidly grown during the last decade and there has been a steady expansion in the number of publications associated with this research field. Moreover, advanced research institutions invested greatly in nanotechnology research centres in order to develop cutting edge technology. This led to an obvious increase in the overall quality of the study performances. A search in PubMed database shows that there was a 30-fold increase in the number of publications within the last decade (Becker and Gärtner, 2008). In the mean time, the number of miniaturised devices patented has also increased. The main targeted market is medical and biomedical applications. The applications include: production of small devices for catheter tips, single cell diagnostics, combined drug delivery and monitoring devices, synthetics of replaced organs (e.g. eye) and biochemical laboratory testing at the point of care (POC). Therefore, there is s demand for cutting edge technology in this field.

The opportunity for microfluidic research in this field is to fabricate the implementation and integration of a complete analytical device in one chip. The process involves various fluid manipulation components (e.g. pumps, valves, filters and mixers) and analytical separation and detection techniques (e.g. chromatography, spectroscopy, electrochemistry and thermal analysis techniques) (Fiorini and Chiu, 2005)

1.4.2 Benefits of creating PCR-on-a-chip

The concept of lab on-a-chip has shown the possibility of performing all the steps of the PCR amplification and detection on a single chip leading to significant advantages in terms of speed, cost and automation, along with very high sensitivity. However, PCR on-a-chip systems, which have been reported in the literature, have not yet replaced the current systems due to weaknesses in their designs. For these systems to become commercialised they need to meet several requirements, including low-cost, easy to use with fast analysis times, and the ability to manipulate small volumes from crude samples.

In regards to commercially available thermal-cyclers, the study carried out by Young *et al.* (2008) on different types of thermal-cyclers shows that a majority of the tested conventional PCR instruments having a significant curving and overshooting in their temperature profiles, which substantially influenced the results of the temperature-sensitive multiplex PCR. Also there is a variation between wells in the same instrument. PCR technique devices in many application fields demand many improvements, mainly including decreased cost of production and use, decreased time of nucleic acid amplification and reduced consumption of biological samples necessary for PCR. Furthermore, there is a requirement for portability, integrity of the PCR device with a detection unit and acceptable disposal of the PCR reaction vessel. Single molecule PCR can easily be performed by PCR microfluidics, starting with a single-copy sequence in the PCR mixture. In addition, rapid heat transfer from the heating block to the in-tube sample liquid ensures high efficiency of amplicon multiplication; for that reason, a thermal processor should guarantee temperature uniformity for all samples within an individual run as well as run-to-run repeatability (Easley *et al.* 2006)

1.5 Preview of the investigation

It is thought that the PCR technique is the best tool available but not the perfect tool for all applications due to many technical reasons (Bustin, 2010 pp 189-200). DNA must be extracted and purified from samples such as blood or tissues through a variety of lyses, protocols and purification techniques. Therefore, direct specimen testing, without a need for additional handling, would be useful to avoid any cross contamination or PCR inhibitors occurring in the DNA extraction process. Furthermore, there is a demand for the development of a device that is portable and can perform the necessary operations for DNA analysis. However, researchers have faced three key difficulties in developing a point of care device for DNA analysis. These are the size, the complexity and the noise sensitivity of the device (Lagally, Medintz, and Mathies, 2001)

In this project, the proposed device is portable and allows automated operation for a variety of applications. Varieties of polymer materials have been investigated for optimal manufacture and application properties. Consequently, high replication approaches have been used to allow the manufacture of the device at low cost. Particularly, the application has been focused on the rapid detection of infectious diseases with the potential for a cheap and portable device for use in developing countries.

1.6 Project Objectives

The project aims to build on previous designs and knowledge of portable PCR devices by investigating a tape system for amplification and detection of DNA sequences using thermo-cycling conditions (Figure 1.13). The proposed tape design will be advantageous, as it will lower the risk of cross-contamination of PCR samples by implementing the use of individually sealed plastic chambers of fluid that moves rapidly between different constant-temperature zones. This design is promising to be advantageous over current rapid/micro- PCR designs for the following reasons:

1) Moving the chamber between zones would eliminate the need to heat or cool one zone of the device, thereby creating a more rapid reaction that is not limited by

long thermal time constants. Cycling should be achieved in seconds rather than minutes.

2) The material selected for the chamber will be optimal for heat transfer to the liquid, and potentially be much thinner than conventional PCR tubes as it does not need to be rigid.
3) The material will be selected for optimal optical properties to allow 'in reaction' detection and quantification of the PCR product.
4) The system will comprise the encapsulation of all PCR components (enzyme, nucleotides, buffer and primers) in a sealed and sterile environment, which only needs to be penetrated once for the injection of template DNA. One injection will avoid the requirement to perform multiple transfers of liquid to assemble a PCR mix. The advantage of the device is the possibility of using it in locations where a sterile environment is not available.

With a relatively low-cost, mechanically simple and small instrument, there is a potential for much wider application than analysis in centralised laboratories.

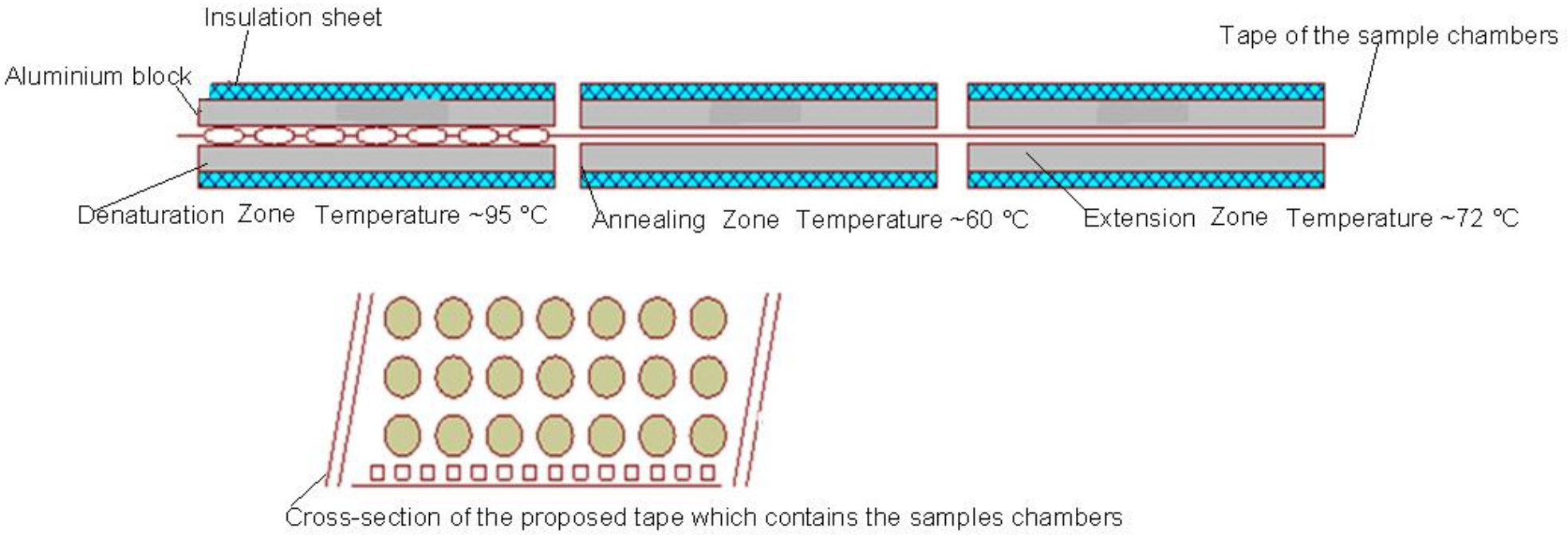

Figure 1.13 Schematic diagram of the proposed PCR system using automation to move tape between stationary heaters.

Chapter 2 Literature review

2.1 Introduction

Robust portable PCR systems for point-of-care applications and pathogen detection in the field could supplement or replace expensive bench top laboratory apparatus. Besides, the ability to achieve a disposable, reliable PCR on a chip will facilitate its use in applications such as pathogen detection, forensic investigations and food control testing (Christensen, 2007). Moreover, scaling-up of pre-existing procedures for higher throughput would not suit continuous environmental monitoring and on-site studies. Miniaturisation of PCR integrated bioassays potentially possesses all of the desired qualities and comes with additional benefits relating to sample tracking, contamination, and savings in cost and time. Most developments in miniaturisation have stemmed from institutes with strong analytical, engineering and fabrication expertise.

Since the year 1993, many miniaturisation methods have been investigated and many miniaturising techniques have been applied. As can be seen in Figure 2.1**,** according to a search in Scopus web search, the number of articles describing PCR-on-a-chip significantly increased this decade.

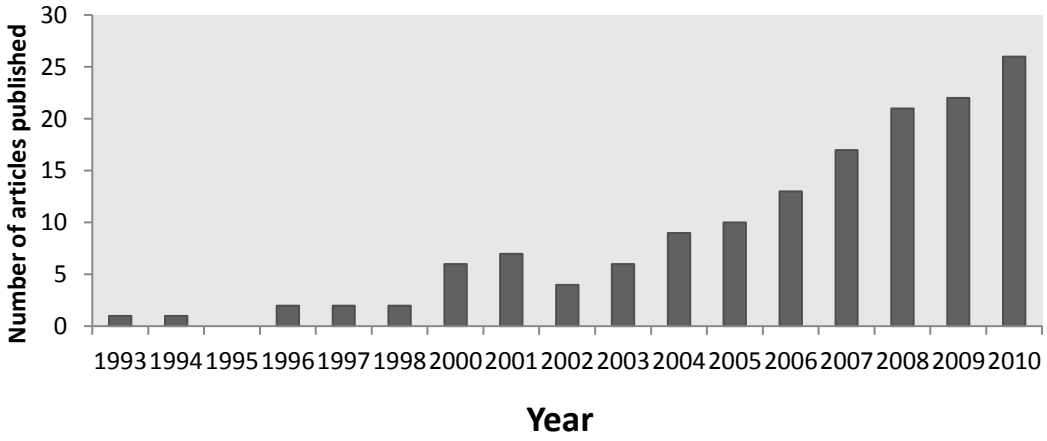

Figure 2.1 The column chart shows the number of articles describing microfluidic PCR systems from the year 1993 until the year 2010. The chart shows the developing in the number of publications after year 1993.

Researchers have been using different microfabrication methods to achieve a suitable microchip-PCR system. Different types of thermal-cycler design have been demonstrated and many detection techniques have been used. However, none of these attempts, yet, replace the bench-top systems. In this review, the significant prototypes of miniaturised PCR, since 1993 until year 2010 are highlighted. The argument focuses on the advantages and disadvantages of the models produced and the materials used to establish the devices, in addition to comparing different types of detection units. This discussion will assess the role of the researcher in choosing the best way of initiating a sensible and a practical model of PCR on-a-chip, which will resolve most of the limitation in the prior models

2.2 Fabrication materials

Basically, the three main aspects of guided materials selection are: material properties, feasibility of fabrication method and device functions. A huge amount of fabrication materials are available with a broad range of chemical, mechanical, electrical and optical properties. These materials could be classified into two main categories: silicon/glass-based and polymer-based. The correct choice of microfabrication materials for almost any given application is a challenge due to the huge diversity in the materials properties. In the first years of microfabrication research, glass/silicon or quartz based devices were dominant. This is because micro-scale structures in glass, silicon or quartz are easier to fabricate and have a more stable shape. However, applications demanding disposable devices are better suited to polymer-based fabrication materials owing to the low cost of the materials, low cost of fabrication and compatibility with applications. Polymers are macromolecular substrates composed of many repeating units with a high molecular mass. The repeating units are called monomers and they classify the polymers into two main groups. The chemical structures of the monomers are identical in the case of the homopolymers group and various in the case of the heteropolymers group (Soane, 1992)

Polymers can be classified into three groups according to their physical parameter: thermoplastic, elastomeric and thermosetting. Elastomeric polymers are very weakly

cross-linked polymer chains. Thermoplastics are those, which soften and flow upon heating, typical examples of thermoplastic polymers being polyethylene (PE), polypropylene (PP), nylon, polymethyl methacrylate (PMMA), polystyrene (PS) polycarbonate (PC) polyvinylchloride (PVC), polyethylenetetraphthalate glycol (PETG), cycloolefin copolymer (COC) and polyimide.

Polymers could be also classified into three groups according to the position of glass transition temperature (Tg). This classification is more likely to define the feasibility of the microfabrication process:

1) *Thermoset:* it is a kind of resinous material used commercially in liquid or solid form (at room temperature) and can be activated by a process called curing. During this process the polymer chains start to cross-link. The curing process could be accomplished by either exposing the material to a high dose of radiation, such as Ultra Violet light (UV), or heating the polymer to a defined temperature (Tg). The typical example of this kind of polymer is SU-8, which could be a cured by (UV). Polyimide also belongs to this class of polymer and could be cured by heating the polymer above 300 °C. These polymers are appropriate for lithography fabrication method.
2) *Thermoplastic*: a chemical reaction intrinsically makes *thermoplastics* more usable because they can be simply shaped and reshaped by heating to the glass transition temperature (Tg) and cooling down to room temperature. These kinds of polymers are commercially available in the form of ready to use sheets, rods, tubing and films .They are commonly fabricated by methods like hot embossing and injection moulding. The most popular examples of *thermoplastics* are: poly (methy methylacrylate) (PMMA), polycarbonate (PC), poly olefin copolymers (COC) and poly olefin polymer (COP).
3) *Elastomers*: the molecular chains are in this class of polymer typically do not show a chemical interaction but are physically entangled. The polymer chains untangle if any external force is acting on the polymer and allow the polymer to stretch elastically. This gives the elastomers a more flexible nature and easy handling. Poly (dimethysiloxane)(PDMS) is the most popular example of elastomeric polymers. This class of polymers can be used to develop fine

replicates of microsystems replicas using moulding techniques. They are also suitable for the lithography method (Becker and Gärtner, 2008).

A compilation of physical and chemical properties of the most widely used polymers for microfluidic applications is illustrated in Table 2.1.

Table 2.1 This table summarizes the physical and chemical properties of commonly used polymers in addition to the current applications in biotechnology and medical field.

Material	Abbe number*	Glass transition temperature (Tg°C)	Heat distortion temperature (HDT °C)	Water absorption (%)	Optical quality	Biocompatibility and applications	Other applications
Poly(methyl methacralate) (PMMA)	57.2	110	90	2	Excellent transparent in visible region	Electrophoresis separation of ds-DNA and RNA fragments and PCR-on-a-chip. Ref. Lee *et al.*2004	Packaging for tablets, pills, capsules, suppositories, urine containers, sterilisable equipment.
Poly carbonate (PC)	29.8	148	125	0.3	Excellent transparent in visible region	DNA preparation and PCR, DNA detection. Ref.) Yang *et al*., 2002; Liu *et al*., 2004.	Laboratory safety shields, vacuum desiccators and centrifuge tubes
Polystyrene (PS)	30.9	100	70	<0.4	Good		
Polyethylene (PE)		110/-140	80/100	<0.015	Fair	Affinity assays, electrochemical and biochemical analysis. Ref. Rossir *et al.* 2002.	
Polypropylene (PP)		0-10	100-110	0.01-0.1	Good	Affinity assays, electrochemical and biochemical analysis. Ref. Rossir *et al.* 2002.	Suitable for items such as trays, funnels, pails, bottles, carboys and instrument jars that have to be sterilized frequently for use in a clinical environment.
Cycloolefine /copolymer (COC)	56.4	140	170	0.01	Excellent transparent in visible region	PCR-on-a-chip. Ref. Koh *et al.*, 2003; Fan *et al.*, 2003.	A new pharmaceutical and medical packaging product. Very good blood compatibility, excellent biocompatibility.
Cycloolefine/polymer (COP)		138	140	0.01	Excellent transparent in visible region	PCR-on-a-chip. Ref. Koh *et al.*, 2003; Fan *et al.*, 2003.	
Polyetheretherketone (PEEK)		143	250	0.5	Good	PCR-on-a-chip. Zou *et al*., 2002	
Poly(dimethylsiloxane) PDMS	40.4	120	200	0.1	Excellent transparent in visible region	PCR-on-a-chip. Ref. (Cady *et al*. 2005)Cady *et al*., 2005;	Widely used to built microfluidic devices
SU-8		210			Excellent transparent in visible region	PCR-on-a-chip. Ref. El-Ali *et al*., 2004;;	The photoresist SU-8 is a common material for the fabrication of polymer microfluidic systems
Polyimide (Pl)		285	400	2.9-4		Affinity assays, electrochemical and biochemical analysis. Ref. Rossir *et al.* 2002.	Low outgassing and non-contaminating

*Abbe number is a measure of optical disoperation in relation to the refractive index (variation of refractive index with wavelength).

The fabrication materials used for PCR microfluidics can be classified into two main materials: silicon/glass-based and polymer-based, based on the micro-fabrication methods. The microfabrication methods applied to accomplish PCR devices include silicon wafer etching to photolithography printing techniques, thermal growth of silicon oxide, chemical and electrochemical etching, ion etching, chemical vapour deposition (CVD), physical vapour deposition, epitaxy and anodic bonding, which have all been applied to microfabricate silicon-based PCR microfluidics.

Polymers tend to be favourable in DNA application. Polymer materials can be fabricated easy and quickly in a low cost technique as: injection moulding, casting, or hot embossing. The specification of the polymers must have a low thermal mass, efficient heat transfer and be inert to PCR reaction in order to manage a PCR vessel with rapid temperature transition whilst retaining high thermal homogeneity in the PCR mixture (Becker and Gärtner, 2008).

2.3 Fabrication Method

A variety of methods exist for the fabrication of microfluidic devices. These methods include: silicon wafer etching, photolithography printing techniques, thermal growth of silicon oxide, chemical and electrochemical etching, ion etching, chemical vapour deposition (CVD), physical vapour deposition, epitaxy and anodic bonding, which have all been applied to microfabricate silicon-based devices.

2.3.1 Photolithography

Photolithography is a top-down microfabrication technique in which geometric shapes on a photomask are transferred to a thin layer of UV sensitive material known as a photoresist. Photolithography was originally developed to reproduce engravings and photographs as well as making printing plates it was then found as an ideal process in order to mass produce integrated circuits in the 1960s (Madou 2002)

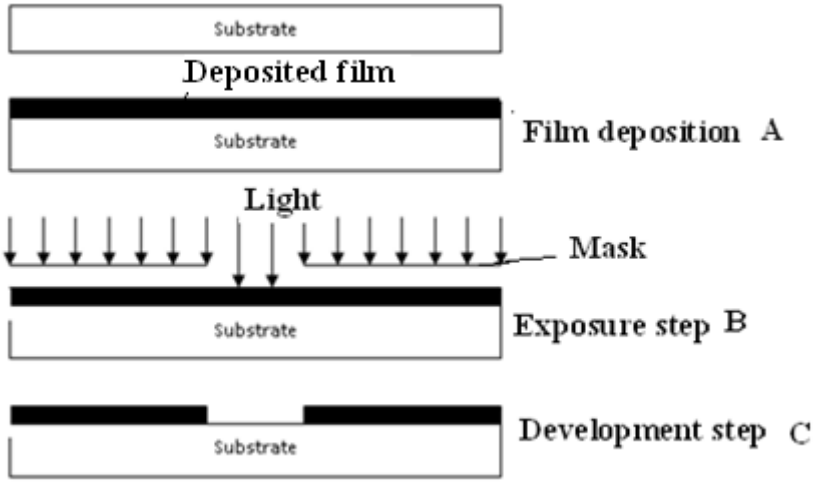

Figure 2.2 This figure described the basic Photolithographic Processes steps.

The basic photolithographic process is shown in Figure 2.2. The first step of this process is to spin coat a thin layer of the UV sensitive photoresist, (Photoresists are polymeric compounds which are sensitive to UV light causing the structure of the polymer to change through UV exposure), (A). The substrate and photoresist are then exposed to UV light through a photomask which contains the desired pattern, which is to be transferred (B). Once the photoresist has been exposed to UV light it is then developed in a developer solution removing certain parts of the photoresist (exposed or unexposed), forming the desired pattern (C). Afterwards the substrate can be further processed by either etching (wet or dry etching), or by deposition of materials such as metals. After further processing of the substrate, by either etching or deposition the remaining photoresist is removed.

2.3.2 Etching

The etching process removes any areas of the substrate that is not protected by a photoresist layer. This can be done by either wet chemical etching or dry etching and can be either isotropic (all directions at once at the same rate) or anisotropic (in one direction). Dry etching covers a wide range of techniques but the three main types of dry etching are; plasma etching, reactive ion etching (RIE) and deep reactive ion etching (DRIE). In dry etching, the surface of the exposed substrate is etched away either through ion bombardment or by chemical reaction (Madou, 2002).

2.3.3 Metal Deposition

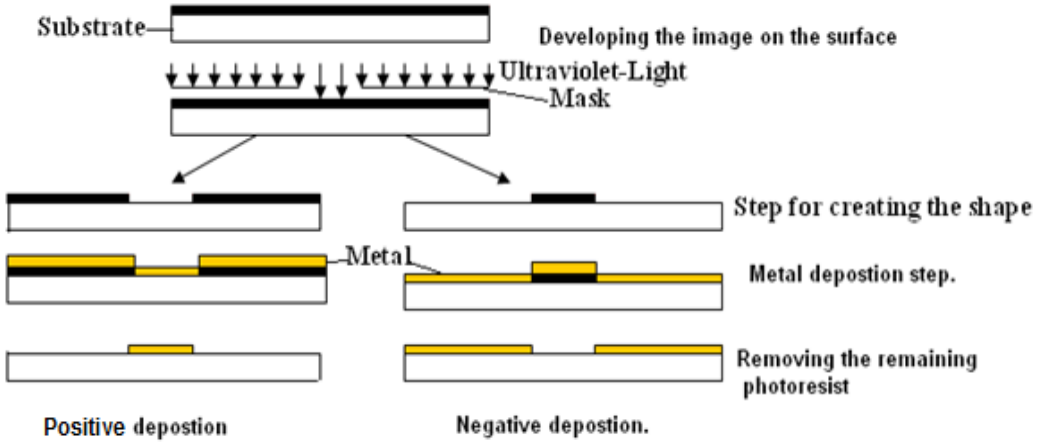

Figure 2.3 Diagram showing the lift-off process for positive and negative photo-resists process.

The deposition of metals is a very useful and important step in the photolithography lift-off technique. The lift-off process follows the same process steps as standard photolithography, except after the image has been developed a metal is deposited onto the surface; then the remaining resist is stripped away leaving a metal layer on the areas of the substrate that weren't covered with photoresist (Figure. 2.3).

Deposition techniques allow for materials, such as metals, to be deposited onto the surface of the substrate; this can be done instead of or after the etching process.Metals can be deposited onto a substrate through either physical or chemical layer deposition techniques. There are two main physical vapour deposition (PVD) techniques; evaporation and sputtering. The evaporation method involves heating the required material that is to be deposited onto the substrate in a vacuum chamber to high temperatures, usually by passing a high current through the substance. The evaporated material then condenses onto the surface of the substrate. Although this is a conventional and well understood method, it is very rarely used due to poor layer adhesion (Fatikow and Rembold, 1997).

2.3.4 Hot Embossing

The process of hot embossing involves pressing a master dye into a polymer at a temperature above the glass transition temperature (Tg) of the polymer. In the hot

embosser the master dye and the substrate are heated separately under a vacuum. Once the polymer and dye have reached the desired temperature, the dye is then pressed into the polymer with a controlled force, (typically in the order of several Kilo-Newtons (KN)) for several seconds, and then cooled to below the glass transition temperature. Figure 2.4 is describing the process.

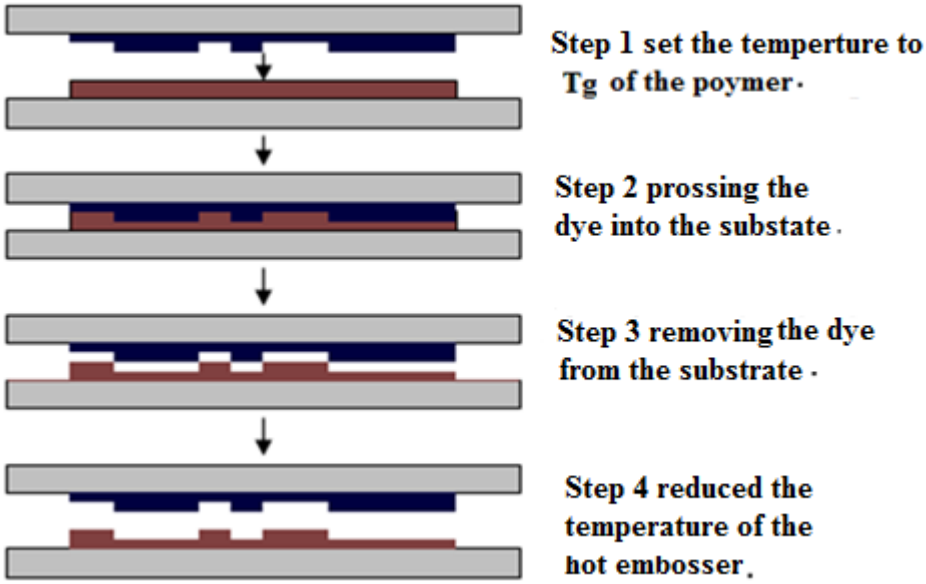

Figure 2.4 Diagram showing the hot embossing process steps. Tg is the glass temperature of the polymer.

After cooling, the dye and the polymer were separated, leaving the desired pattern in the polymer substrate. In order to minimize thermal induced stress and replication errors caused by the different thermal expansion coefficients of the dye and polymer substrate, the thermal cycle should be as low as possible (Becker *et al*, 1998). There are three major issues in the hot embossing process: the filling of structures by the polymer, reproduction fidelity, and master separation during de-embossing (Franssila, 2004). Structures created through the hot-embossing process can vary from 150 nm to 150 µm; however, the limiting factor of the hot embossing process is making the master dye.

2.3.5 Micro-milling

Micro-milling is a mechanical process that is capable of producing microstructures in materials such as polymers; this is achieved by using a small revolving cutting

tool which then removes areas of the polymer to create the structures in the polymer. In the micro milling system a computer is used to position and move the cutting piece and is often referred to as computer numerical control or CNC milling (Geschke *et al*, 2004).

2.3.6 Micro Injection Moulding

Micro injection moulding is similar to hot embossing, resulting in an inverted copy of the mould; however, unlike hot embossing the mould is not pressed into a polymer at its glass transition temperature, and instead the molten polymer material is injected into the mould cavity at pressures between 500-2000 bars. For the micro injection moulding technique it is important that the mould is heated to the softening temperature of the polymer before the polymer is injected in; this is done in order to prevent hardening of the injected polymer (Rotting *et al*, 2002). Once the molten polymer has been injected into the mould, the mould is then slowly cooled to harden the polymer. When the polymer has hardened, it can then be removed from the mould (Geschke *et al*, 2004). Micro injection moulding is capable of producing microstructures as small as several nanometres but is also capable of producing more replicates, when compared to hot embossing, owing to the shorter cycling times needed for this process.

2.3.7 Laser Ablation

Laser ablation is a non contact fabrication technique which does not produce any internal stress on the material that is being processed. This technique can be used for a number of different things, such as drilling, patterning, cutting, as well as annealing of materials such as metals, plastics, ceramics, semiconductors and glass. This technique works on the basis of using intense UV or infra-red radiation from a laser in order to remove the polymer. The removal mechanisms of the polymer are dependent on the radiation wavelength used. When an infrared laser is used the irradiated material is heated and decomposes; when UV radiation is used the irradiated polymer decomposes by a combination of thermal (caused by heat) and direct bond breaking caused by direct absorption of UV photons (Geschke *et al*, 2004). There are two types of laser systems that can be used; the choice of system to

be used is dependent on the application, when using an infrared laser the direct writing systems is normally employed, where as when using a UV laser a mask projection system is usually used.

2.4 The problems associated with PCR-on-a-chip

The main benefit of miniaturisation is the increased surface to volume ratio. However, this physical phenomenon has two effects on PCR on-a-chip. On the one hand, it decreases the process timing, which takes place by a rapid temperature transition from the heat source to the reaction chamber and, also, improves temperature uniformity. On the other hand, this increases the interactions between the biochemical components of the PCR mixture and the chip surface because the PCR-mixture consists of a mixture of biochemical compounds mixed in a buffer. This mixture includes DNA-polymerase enzyme, DNA oligonucleotides and DNA template in addition to magnesium salt. The concentration of each constituent in the mixture is optimised and any change in the concentration of any constituent will have a negative effect on the whole process. Therefore, this can have a detrimental effect on the PCR performance because a binding of the PCR components to the chamber surface will disrupt the often delicate and optimized concentration of the PCR components (Christensen *et al*, 2007). Consequently, selection of material and fabrication methods is critical and has to be done with consideration of the biochemical assay being conducted.

2.4.1 Evaporation and its Inhibition Measures

Sample evaporation is often problematic because PCR volumes are usually very small. Typically, as denaturation temperatures approach 100 °C, the sample evaporation is so rapid that the sample dries up quickly under standard atmospheric pressure. To avoid such evaporation, a number of methods are applied, but all have their relevant advantages and disadvantages. A mineral oil cover layer is frequently used as a vapour barrier to prevent evaporation. Mineral oil is a suitable liquid cover because it has a boiling point well above 100 °C and a density slightly below 1.0 g/cm3. However, its applicability is questionable for highly integrated PCR systems because mineral oil could inhibit DNA extraction. Another approach uses a solid

cover or valve to resist the internal pressure generated during PCR. It is known that the evaporation rate decreases with the increase gas pressure around a liquid. Chen *et al*, 2005)

Chen *et al,* (2005) extended this concept to the oscillating-flow chip. In their approach, a single opening serves equally as sample loader and syringe pump port. When the sample plug is pumped to high-temperature zones, the internal pressure increases six times and thus the sample evaporation is greatly reduced. Remarkably, within the continuous-flow PCR chip, the relative sample evaporation loss can be decreased because of the reduction in the free surface area of the liquid. In addition, sample evaporation is also affected by the PCR chip substrates. For example, the water diffusion/ vapour loss property of PDMS could lead to sample evaporation and thus special approaches such as vapour barrier should be considered to reduce the sample loss at elevated temperatures.

2.4.2 Formation of gas bubbles and Inhibition Measures

Biochips, in general, consist of reaction chambers and fluid-flow systems. The fluid-flow system includes transport and separation channels for easy loading samples and reagents. The PCR system involves liquid handling of master-mix and DNA template solutions including measurement and mixing of PCR component solutions. As described earlier, PCR component concentrations are critical to the success of the amplification. Therefore, the successful PCR reaction in the biochip depends on a complete loading of the PCR solution in a micro-chamber. However, an important drawback of the PCR chip micro-system is the generation of air bubbles, which not only causes large temperature variation in the sample but can also expel the sample from the PCR chamber.

Gong *et al*, (2006) studied the effect of micro-chamber design on the PCR reaction process and air bubble formation. The study evaluated the effect of chamber inlet and outlet channels on PCR reaction and also studied the effect of chamber depth. The researchers revealed that the surface wetting property of the micro-chamber was the main reason for the formation of the air bubbles inside the chamber during the loading of the PCR solution in the reaction chamber. It was found that the deeper the

micro-chamber, the more difficult it was for the PCR solution to flow into the chamber without trapping air bubbles. Therefore, a thinner sample chamber would avoid trapping air bubbles. Furthermore, once the micro-chambers and the inlet bridge channels were made highly hydrophilic, the trapped air bubbles could be avoided or minimized during the loading of the PCR solution, as can be seen in Figure 2.5.

Several methods have been used to avoid the prerequisites and inhibit the bubble generation (Zhang and Xing , 2007)

1) The structural design of the PCR chamber, a diamond-shaped or rhomboidal chamber is superior to a circular chamber in preventing bubble formation. Recently; Gong *et al*. (2006) reported that the deeper the PCR chamber, the more difficult it is for the PCR solution to flow into the chamber without trapping bubbles. However, the size of the chamber or the shape and size of the inlet and outlet have little or no influence on bubble formation, see Figure 2.5.
2) The surface treatment of the PCR chamber. In general, the wetting properties of the PCR chamber and its inlet/outlet have an obvious effect on bubble formation.
3) When the chamber surface is highly hydrophilic, the PCR sample can flow into the chamber smoothly and rapidly without creating an air bubble.
4) The sealing pressurization of the PCR chamber, nder pressurization and high-temperature, gas solubility will increase and the dissolved gases and micro-bubbles in the PCR sample cannot rise in volume, thus preventing air bubble formation.
5) Degasification of the PCR sample. This process can eliminate non-condensable gases in the PCR sample before loading and consequently decrease the risk of bubble formation.
6) The addition of high boiling-point biocompatible reagents to the PCR sample. When a solvent with a boiling point above 100C (e.g. glycol, glycerol or poly ethylene glycol is included in the PCR sample, the boiling point of the resulting sample is increased, and thus prevents bubble formation at high temperatures.

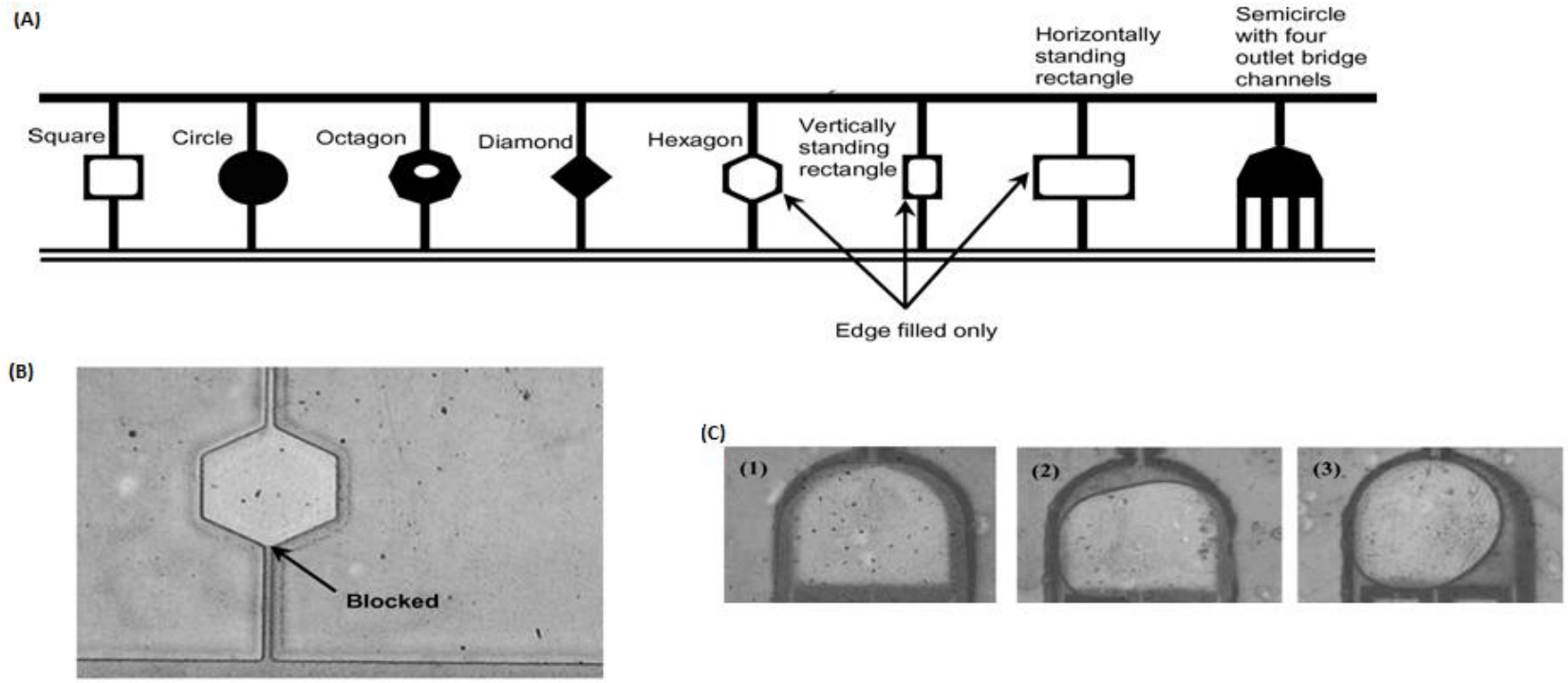

Figure 2.5 A selected sample loading failure modes. (**A**) A diagram shows effect of the shape of the microchamber on the loading of the PCR solution, where the black portion indicates the area filled with PCR solution. The sample loading failed for certain chamber geometries. The microchambers with shapes like square, hexagon, vertically standing rectangle, and horizontally standing rectangle were only filled in the area near the chamber sidewall. The off-sidewall area were not filled because of the air trapping caused by the blockage of the microchamber air venting exit by the fast moving liquid along the sidewall. (B) The picture shows how a sample loading was failed when the sample stopped at the exit of the inlet bridge channel and failed to flow into the microchamber. This failure is contributed by both narrow inlet channel and lack of high hydrophilicity of the glass surface of the microchamber. (C) Video snapshots of a liquid loading sequence in a semicircle microchamber entrapping air in the central portion of the microchamber due to non-uniform hydrophilicity on the surface of the microchamber (Gong *et al*, 2006).

2.5 Integrating system for nucleic acid analysis on-a-chip

The achievement of a fully integrated system for nucleic acids analysis is the vision of many micro-Total analysis system (μTAS) researchers. However, a substantial challenge still prevents the production of one. As described earlier, nucleic acid molecules are a part of the biological context. Most of the biological samples contain a complicated mixture of compounds. Part of these compounds may inhibit or promote the nucleic acid amplification process in *vitro* e.g. polysaccharides and proteins. The conventional nucleic acid extraction protocols generally include processes such as sample filtration, centrifugation, dilution and extraction. Some of these steps require treatment of the sample contexts with chemicals. These chemicals would inhibit the PCR process, if not separated during the extraction (Li *et al*, 2009). Therefore, miniaturising the nucleic acid extraction step is the most difficult part of the entire DNA analysis process on- a-chip-scale.

Many methods based on miniaturisation concepts and physicochemical mechanisms have been implemented to achieve chip-scale DNA extraction along with amplification and detection. However, none of the designs produced could be efficient for all kinds of samples. For example, in using nucleic acid purification through solid-phase extraction (SPE) from blood samples, the major challenge associated with integrating sample treatment steps into a microfluidic design is the incompatibility of SPE reagents (guanidine and iso-proponal) with the PCR process . This problem was resolved by applying elastomeric valves and laminar flow, which were used to isolate SPE solvents from the other domains without compromising DNA extraction.

However, an important issue associated with this model is cross-contamination, because the chip was not disposable and it was made from glass and fabricated by high cost technology. The researchers suggested a cleaning step prior to use. The cleaning step suggested was as follows: the glass-chip should be exposed to a 1:1 methanol: hydrochloric acid (HCl) solution for 30 min, rinsed with distilled water, and exposed to concentrated sulphuric acid (H_2SO_4) for 30 min. The SPE domain was cleaned with 2 M hydrochloric acid (HCl) for a total of 1 h. The entire device

was then rinsed thoroughly with distilled water and the PCR and SPE fields dried with nitrogen (Easley *et al*, 2006).

Lee *et al*, (2006) demonstrated a rapid DNA extraction and real-time detection of pathogens in a single chamber of a microchip within 32 minutes without channels, pumps or valves. The pathogen detection system focused mainly on the detection of the pathogen genome. They had developed a unique sample preparation method using Laser-Irradiated Magnetic Bead System (LIMBS) for efficient cell lyses and DNA isolation from various pathogens. LIMBS as single step cell and DNA isolation method provides rapid DNA release and the removal of denatured proteins from pathogens at the same time. A micro device with a chip size of 7.5 mm ×15 mm and 10 ml sample volume was fabricated using silicon, glass, polycarbonate film, and double-coated tape. The fabrication technique used to produce this chip is photolithography in two steps and then polycarbonate film was bounded using double-coated tape. The chip, as can be seen in Figure 2.6, body was made from silicon wafer with a thickness of 680 µm sandwiched between Pyrex cover and PC film with a thickness of 100 mm. The silicon wafer was bonded with the glass substrate using an anodic bonding technique. Polycarbonate film was bonded to the silicon wafer using double-coated tape with a thickness of 150 mm.

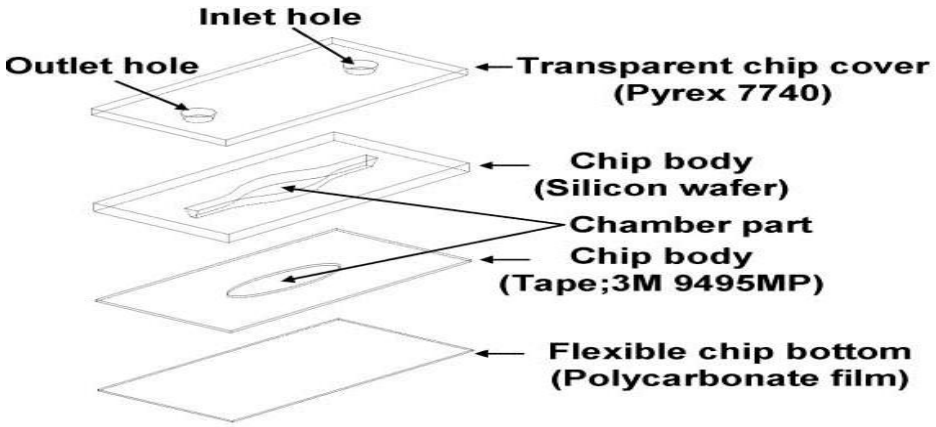

Figure 2.6 Schematic diagram of silicon glass, single chamber microchip for real time PCR (Lee *et al*, 2006)

When the nucleic acids extraction method is applied it provides efficient cell lyses and nucleic acid isolation for various pathogen detections. However, this intelligent microchip method is not useful in the extraction of nucleic acid from animal or plant tissues because the tissues matrix is more complicated than bacterial culture, which is used in this method and requires extra purification steps.

The most distinctive integrated design is the one produced by Baier *et al.* (2009) The researchers had demonstrated a lab-on-a-chip system capable of hands free automatic sample preparation and nucleic acid extraction from complex samples. The necessary steps of cell pre-concentration; cell lyses and nucleic acid concentration are performed by solid phase extraction within a disposable chip. The chip is connected with amplification and detection units. The amplification technique applied is NASBA (Nucleic Acid Sequence Based Amplification) and subsequent fluorescence detection is readily integrated into a chip format. Nucleic acid sequence-based amplification (NASBA) is a primer-dependent technology that can be used for the continuous amplification of nucleic acids in a single mixture at one temperature. The amplification methodology involves the use of three enzymes, reverse transcriptase, T7 RNA polymerase, and RNase H; and the final amplification product is single-stranded RNA with a polarity opposite that of the target**.** The sample preparation system made of a disposable chip is shown in Figure 2.7A and Figure 2.7B.

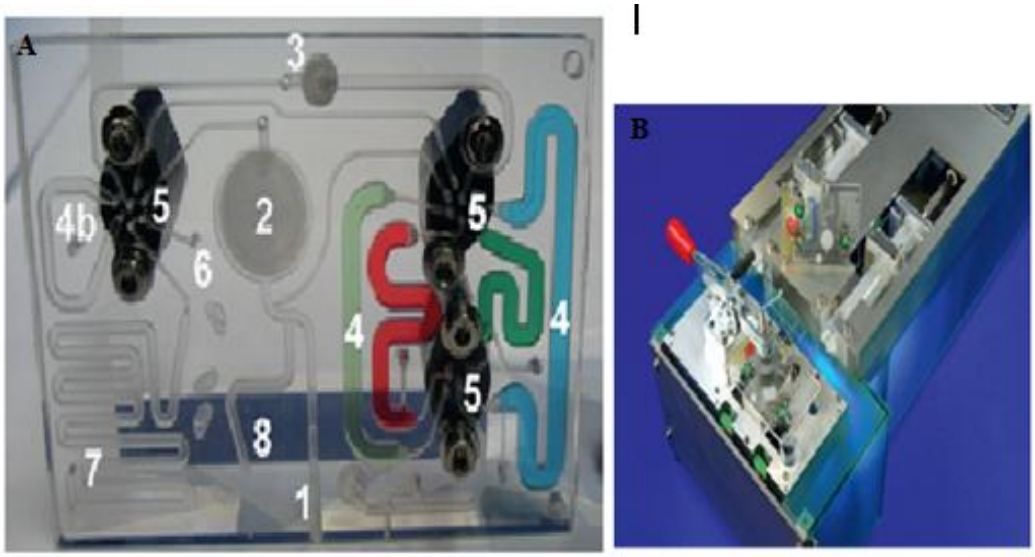

Figure 2.7 (A) Pre-filled sample preparation chip showing (1) sample inlet, (2) cell filter, (3) SPE chamber, (4) reagent storage, (4b) storage DMSO/ sorbitol, (5) turning valves, (6) waste outlet, (7) sample outlet, (8) pressure sensor. For demonstration reasons only. (Baier *et al*, 2009). **(B)** Instrument for the sample preparation chip. (Baier *et al*, 2009).

The chip material is COC (cyclic olefin copolymer; Ticona, COC-5013) sealed with COP (cyclic olefin polymer; Zeon, Zeonor 1420R). All chips were fabricated by milling into blank injection moulded chips with a size of 64 ×43 ×3 mm^3. The instrument produced was efficiently used to amplify and detect mRNA from viruses. The researchers claim that the system can be readily integrated with further downstream operations such as RT-PCR amplification instead of NASBA. As a consequence, it is possible to adapt the system to the most appropriate nucleic acid analysis for a targeted application. The range of possible applications for such a system could encompass foodstuff analysis, animal feed control, personalised medicine, Point-Of-Care, forensics, security application and others. The system is reasonably designed but, inevitably, it is also complicated; and it would have been more complicated if it had been combined with the PCR system.

Budge *et al*, (2009) introduce an integrated microchip system for DNA analysis from bacteria. The system performs bacterial lyses, nucleic acid isolation and concentration, nucleic acid amplification and end-point fluorescent detection. The chip includes a channel filled with a porous polymer monolith (PPM) embedded with silica particles for the lyses of bacteria and the isolation of the released nucleic acids. The PPM channel acts as an on-chip solid phase extraction (SPE) column. The

chip includes zigzag mixers to mix reagents, fluid reservoirs to allow different fluid velocities through various regions of the chip, a PCR chamber and an optical detection well for an end-point fluorescence measurement. The chip was made from Cyclo-Olefin Polymer (COP) as it has a high glass transition temperature to sustain the temperature range required by PCR, has a good UV transmissibility to allow in *situ* UV-curing of the PPM and low auto-fluorescence to allow on-chip fluorescence-based detection of amplicons. The chip was designed to be manufactured *via* injection moulding, as can be seen in Figure 2.8.

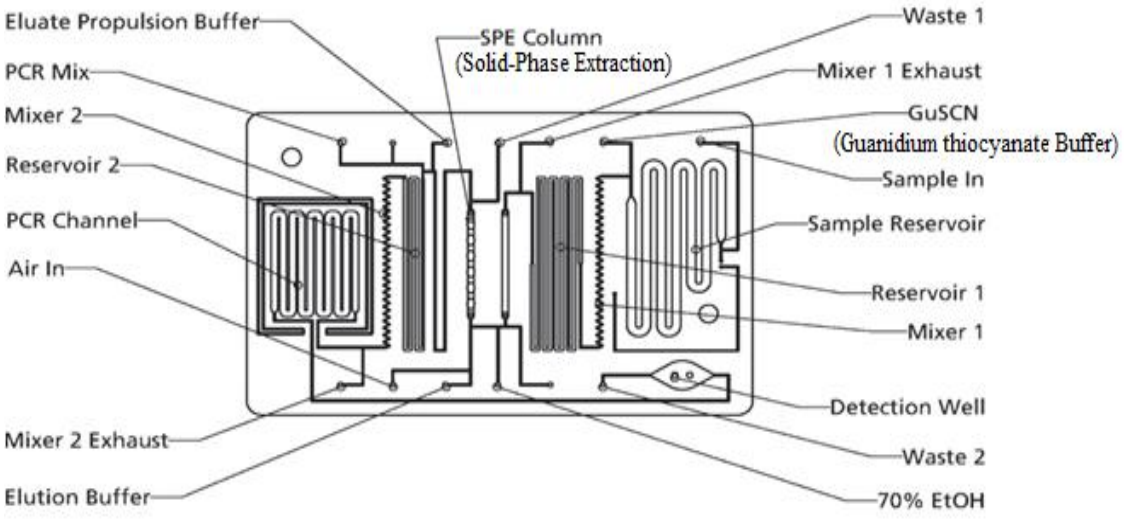

Figure 2.8: Final chip design with fluid inputs and outputs and functional regions labelled (Budge *et al*, 2009).

The valves and mixers established in this chip were enough to exemplify the completions required to create nucleic acid extraction process in the chip. Consequently, the nucleic acids extraction systems are sufficiently complex without adding the complexity of the analysis systems, such as PCR and a detection unit. Moreover, the fabrication techniques available for the extraction, lyses and analysis components are not always compatible, so substantial design and manufacturing work has to be completed to make these components combinable. Therefore, a production of an integrated analysis system requires additional expertise and the technology must be developed before true nucleic acid lab-on-a-chip systems, which can handle a wide range of samples, are routinely generated and become commercially available (Li, Xing, and Zhang, 2009).

Kim *et al.* (2009) demonstrated a pathogen detection technique from whole blood using an integrated single micro-chip. The microchip was fabricated from silicon wafers using standard MEMS techniques. It was designed to have PCR volume of 3 µl, pillar interspacing of 15 µl, and each pillar has the size of 25 µm × 25 µm × 100 µm. The chip size was 7.5 µm × 15 µm, which was compatible with the package for mounting on a conventional PCR thermal-cycler as described in Figure 2.9.

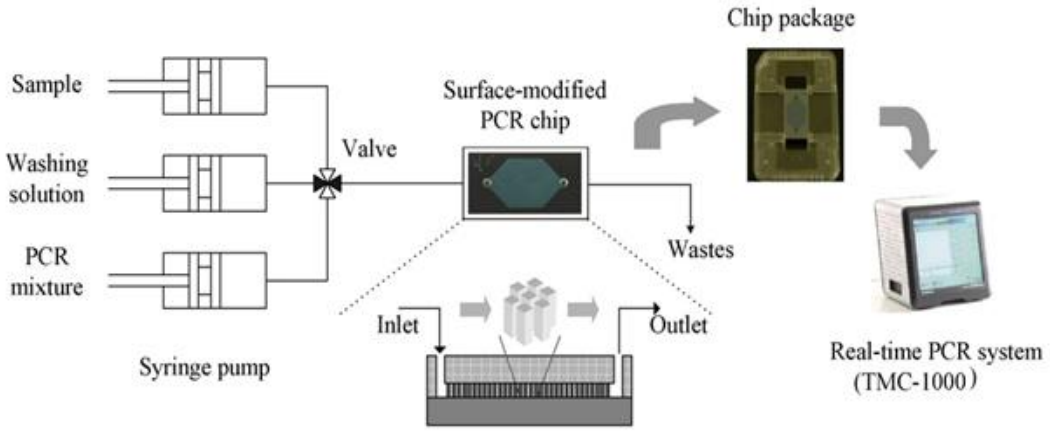

Figure 2.9 Experimental setup for real-time PCR along with detection unit, which were investigated for detection of bacterial cells from whole blood in a single micro-PCR chip. (Kim *et al.* 2009).

Florescence detection was tested in this system. The researchers also reported the effect of BSA and polyethylene glycol (PEG), as PCR passivity agents, on florescence intensity and they found that As PEG content increased, the threshold of the template value decreased and started to saturate at 5% (v/v). However, fluorescence intensity significantly decreased when PEG concentration increased from 5% (v/v) to 10% (v/v). As regards to BSA, the optimum concentration found was 0.62 mg/ml.

2.6 PCR Microchip Designs

Three types of PCR–on-a-chip have been produced: continuous flow-through PCR model; stationary-based chamber PCR model and shunting PCR model. All of these types have been designed to achieve faster thermal cycling and reduce sample/reagent consumption. Most of the models produced have facilitated DNA amplification by much faster rates, as the result of smaller thermal capacity and a

larger heat transfer rate between the PCR sample and temperature-controlled components. The main advantage of the flow-through PCR is its ability to reduce the heating and cooling time and thus shorten the total time of the PCR reaction. However, it is difficult to separate the different temperature zones, to examine the PCR results or to collect the PCR product for further analysis (Easley, Karlinsey, and Landers, 2006) The shunting-PCR model combines the advantages of both previous models, as the sample chamber is cycled between the three temperatures zones, allowing the sample to stay at a specific temperature zone for known residence time according to the program. Fast temperature ramping was achieved in this model (Bustin, 2010).

In this review, three models were discussed to evaluate the best practical model with a reasonable cycling rate, in addition to finding out the suitable detection technique. In addition, it should be pointed out that flow-through PCR chip microfluidics has generated a great deal of interest from researchers and is demonstrating rapid development, in competition with stationary chamber PCR microfluidics, since it was introduced for the first time by (Kopp, De Mello, and Manz,1998). Therefore, the challenge is to achieve a practical low cost design of a thermal cycler and compatible detection mode.

Table 2.2 summarizes the different types of thermal-cyclers designs that have been published and shows the variations between models in terms of: the heating and cooling rates, sample sizes and the materials used to create the devices.

Table 2.2 The PCR-on-chip models categorised according to the thermal-cycler type used and the chamber model. Details of fabricating materials are also incorporated. The table shows the sample volume used in addition to a comparison between the models in terms of heating /cooling rates.

Thermal-cycler model	Model category	Heating andcooling rate	Sample volume	Reference (s)
One zone heater model in chip **All are (stationary model)**	Chamber made from Cycloolefine /copolymer (COC).	Heating rate 12 ºC / S and cooling rate is ~2 ºC / S.	4 µl.	Fan *et al*. 2003.
	Chamber made from silica and glass.	Heating rate 6 ºC / S and cooling rate is 3.5 ºC / S.	2.5 µl.	Zou *et al*.2005.
	Poly(dimethylsiloxane) (PDMS) chamber.	3.1/3.1 (35 min for 40 cycles).	*12 µl.*	*Cady et al. 2005*
	Polyethylene terephthalate (PET) chamber made by thermal foaming.	*Heating rate 34-50 °C / S* *Cooling 23- 31 °C / S*	*20 µl*	*Zou et al. 2002.*
Three zone heater in chip	made from Poly(methyl methacralate) (PMMA) **(continuous flow model (CF)**	~80 ºC /S - ~60 ºC / S (~7 min for 30 Cycles).	~200 nl	*Lee et al. 2004*
		Spiral channel with 50 µm wide and 150 µm Deep 20 cycles in 5.3 minutes.		*Hupert et al, 2003*
	CF channel made from Poly carbonate (PC**)** by hot embossing **continuous flow model (CF)**	9 minutes *Pumping rate between the three chambers is 6.4 µl/s.*	*25 µl*	Li *et al*,.2009. Wang *et al*, 2009
	Tube made from Polytetrafluoroethylene (PTFE)	20 minutes for whole amplification process.	40 µl	Frey *et al.* 2007.
	Three zone chambers made from PDMS by casting technique.**(continuous flow model CF)**	Sample shuttled between three temperature zones.	~ 100 nl	
	Thermosiphone effect chip PDMS casting. **(shanting model)**			
Micro-heater	Chamber made from Silica.**(stationary model)**	Heating rate is 10 ºC/ S Cooling rate 2.5 ºC / S	25 µl	Woolley *et al.* 1996.
	Micro-chamber made from SU-8, silica and glass..**(stationary model)**	Heating rate is 16 °C / S Cooling rate is 9.6 °C / S	20 µl	El-Ali *et al.* 2004
Microwave heater	Poyamide chamber fabricated by laser ablation. **(stationary model)**	Heating rate 10 °C/ S Cooling rate 10 °C/ S	1.7 µl	Giordano *et al.* 2001
	Polycarbonate (PC) chamber. **(stationary model)**	Heating rate is ~ 24 ºC/ S	4 µl	Garg *et al.* 2008

2.6.1 Model one Continuous-flow- PCR

The continuous-flow model is a dynamic thermal-cycling solution for microfluidic PCR system. As, the PCR mixture is flow through the three temperature zones required to complete PCR amplification.

Nakano *et al*. in year 1994 was first introduced this model and after that several attractive models were presented. As illustrated in Figure 2.10, a thermal cycler builds on three separated heating zones. Each single zone has a unique temperature. The temperatures in each zone represents the three different PCR cycling stages, DNA denaturation at ~ 94 °C , DNA annealing at ~45- 60 °C and DNA extension at ~72 °C.

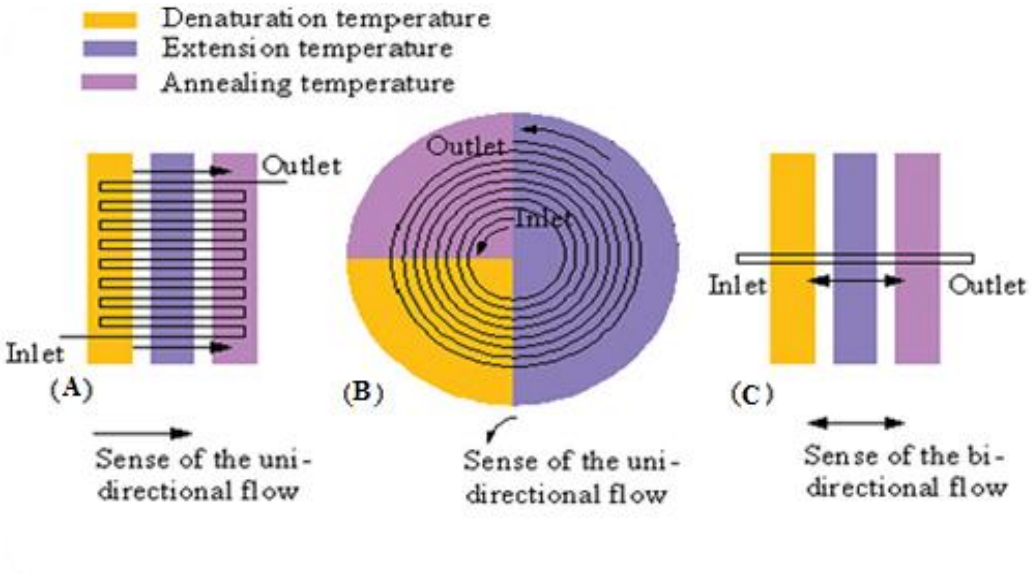

Figure 2.10 Three types of continuous flow PCR thermal cycling system, (**A)**; twisting channel continuous-flow, (**B)**; coiled channel continuous flow. (**C)**; strait channel continuous flow. (Zhang, Xing and Xu , 2007).

The sample is pumped through a micro-channel tube cycled in the region of the three zones. This system can realize high-throughput PCR amplification, due to the significant features as follows:

(1) Heating /cooling speed and high thermal cycling allowing for the achievement of total run times of the order of minutes because the heating and cooling rates are confined by the flow rate of the sample in a micro-channel.
(2) High potential for further development of μ-TAS by incorporating much functionality.
(3) Ability to integrate with the diversity of microfluidical liquid transport such as magneto-hydrodynamic (MHD) actuation.

Three different models were produced by the researchers in the last few years:
(1) The twisting channel continuous-flow, figure 11, A.
(2) The coiled channel continuous flow, figure11, B.
(3) The strait channel continuous flow, figure11, C.

Hashimoto *et al,* (2004) reported the development of a flow –through biochip capable of amplification and detection of DNA. The thermal-cycling channel produced is a model of a spiral channel continuous flow PCR. The miniaturised reaction channel is fabricated in polycarbonate (PC) and the detection unit is fabricated in PMMA.The micro-channel pattern for the array chip, which is made from PC, is hot-embossed into a PMMA plate. Drilling of interconnecting micro-channels is achieved using a laser micro-milling.

Zhang, Xing and Xu (2007) presented a thermal cycler with cylindrical structure without detection method in a chip. They have developed a compact capillary-based continuous-flow PCR microfluidics, in which the three temperature zones are constructed by using the flexible thin film heaters with low thermal mass, thus resulting in the decreased energy consumption. These thin film heaters are evenly arranged on an insulating plastic core in an order of denaturation, annealing, and extension so as to form a thermal cycler with cylindrical structure.

A significant design of this type is the model produced by (Li, Xing, and Zhang, 2009). This model is basically a 4-cm diameter and 10-cm length copper cylinder segmented into three pieces; each single piece represents a temperature bath in PCR process; denaturation at ~ 94 °C , annealing at ~45- 60 °C and extension at ~72 °C. The extension region in this model is double the size of the other two zones. Two

sheets of thickness (3 mm) insulating sheets were used to separates the three temperature zones from each other. A polytetrafluoroethylene (PTFE) capillary tube was used to pump the sample around the thermal cycler. The length of this tube is varied according to the number of cycles required; the range is between 35 to 65 cycles depending upon the application.

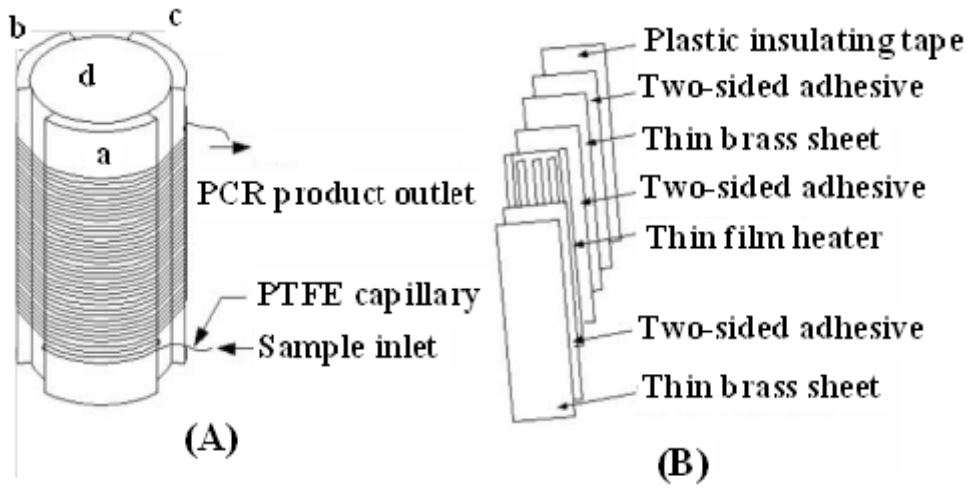

Figure 2.11 (A) Schematic diagram of the continuous-flow PCR device: the thin film heaters (a), (b), and (c) for denaturation (94 °C), annealing (54 °C), and extension (72 °C), respectively, and (d) the thermally insulated plastic core. PTFE is polytetrafluoroethylene . (**B)** Schematic diagram of laboratory-made micro-heater using flexible thin film heater (Li, Xing, and Zhang (2009).

However, continuous-flow PCR poses several problems. During thermal cycling:

(1) Gas bubbles are easily generated in the micro-channels, which adversely affect PCR amplification.

(2) Pressure-driven flow easily produces a hyperbolic flow profile that may lead to progressive sample dispersion. Also, it often requires an external bulky syringe pump which adversely affects the development of compact, portable and integrated continuous-flow PCR chips.

(3) The rate at which the PCR solution travels between different temperature zones are difficult to regulate, and thus most of the continuous-flow PCR systems lack the flexibility to regionally control fluid flow velocity to meet different PCR requirements.

(4) Highly integrated continuous-flow PCR chips are rarely reported due to high fabrication cost and difficulties in controlling the continuous liquid flow.

(5) A limitation of this approach is the fixed cycle number which is dictated by the channel layout.

(6) Integrating a real time PCR detection system cooperative with this kind of design is not easy to achieve due to distribution of the sample along the tube.

2.6.2 Model two: stationary chamber-based PCR

Chamber-based stationary PCR is a miniaturised version of the conventional thermo-cycler machines, where the PCR mixture is kept stationary and the temperature of the system is heated and cooled according to the desired programme. Figure 2.12 below describes an example of this kind of PCR in a chip. Generally, two types of stationary PCR chamber prototypes produce a single PCR chamber chip and a multi PCR stationary chamber chip see Figure 2.12 A, B and C.

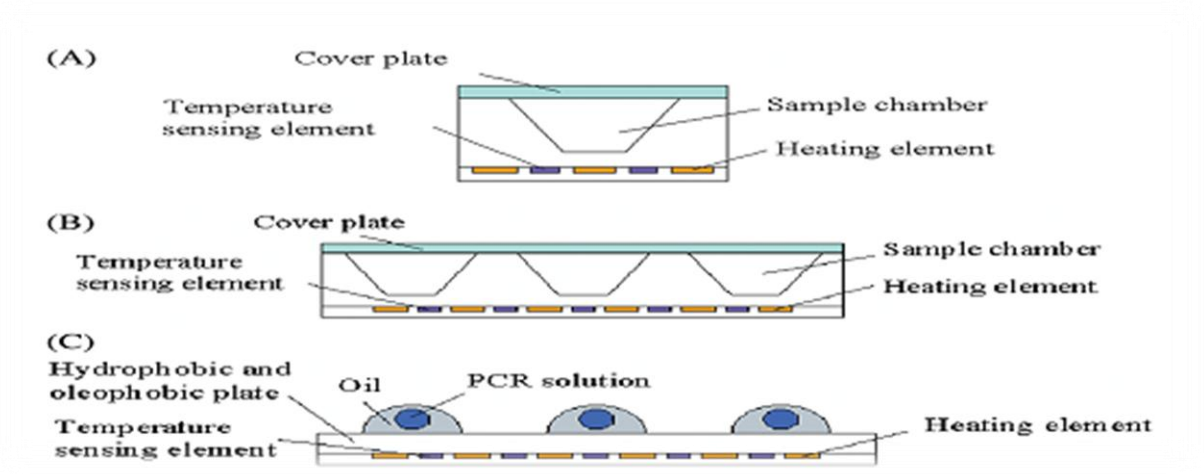

Figure 2.12 The first Stationary chamber based PCR chip. **(A)** Single chamber PCR chip **(B)** Multi chamber PCR chip. **(C)** VRC PCR. The PCR sample is introduced into the single/multiple/virtual chamber(s). The chip is then heated and cooled to provide thermocycling conditions (Zhang, Xing and Xu, 2007).

The single chamber performs very well in terms of fluidic and thermal controls and offers beneficial properties such as reduced thermal and fluidic crosstalk between chambers. However, it is not suited to high throughput and cannot readily be used for special purposes, such as single cell gene expression analysis. In order to

overcome these issues, great efforts have been made to develop a multi-chamber stationary PCR. However, special care must be taken to achieve the thermal optimization of a chamber array in order to obtain homogeneous temperature fields between chambers. In addition, precise handling and processing of a sample of microfluidics on such PCR chips still face challenges (Ji *et al*, 2007)

Northrup *et al*, (1993) introduced the first type of miniaturised PCR in a chip. Fabricated reaction silicon chambers are inserted into a pressure-fit electrical control holder to control a thermal cycler heater. This design can be recognized as the first stationery based chamber PCR in a chip. Since then, this format has been widely replicated and improved.

There are two reasons motivating the researchers to prefer this model of PCR-on-a-chip:

(1) The ability to accomplish thermal cycling in a clean separated sample chamber.
(2) The possibility of producing a disposable chamber.

However, special care must be taken in the thermal design of a chamber array in order to obtain temperature uniformity between chambers. Without a careful design to administrate temperature uniformity and the elimination of any possible differences in amplification, the reliability, repeatability, sensitivity, efficiency and specificity of PCR amplification across the different chambers may be compromised. In addition, handling and processing of small sample volumes in the case of the increasing number of PCR reaction chambers on a single chip create some potential challenges. The resulting issues are loss of a sample on the walls of transferring devices, loss by evaporation, loss of components from the sample during manipulation, possible loss of a sample resulting from the immediate contact of the PCR solution with chamber walls (Ji *et al*, 2007)

Chamber-based PCR chips are constructed as closed systems where the reaction Chamber (s) is actually microfabricated on the chip. Their design does not differ significantly from the model presented by Northrup *et al*, (1993). Woolley *et al*,(1996) presented a successful model of a stationary PCR chamber as they

produced a microchip based on a reaction chamber and a capillary electrophoresis detection unit. The reaction chamber is made from double-sided polished silicon wafer. The improvement in this model is the speed of the DNA amplification and detection because the whole process can be accomplished in 45 minutes. However, the model is made by an expensive technology and using the chip is likely to enhance cross-contamination, because it is not disposable and has to be well-cleaned in between the samples.

Giordano *et al*, (2001) presented a PCR microchip used in conjunction with IR-mediated thermo-cycling. Polyimide was used to fabricate the PCR chamber in this microchip. This material represents a possible substrate for use in microchips with a more complex architecture. Some of the properties that make it desirable as a material for integrated microchips for DNA analyses include high breakdown voltage (> 4 kV/mm or 1500 kV/cm), optical transmission in the useful IR range in which the IR mediated thermo-cycling was done and a high glass transition temperature (350°C). The PCR chambers were formed by laser ablation of a single layer (150 mm thick) of polyimide. This layer was sandwiched between two additional layers of polyimide (125 mm thick), one of which contains two laser-ablated ports producing a 150-mm-deep chamber. The total thickness of the microchip was 400 mm with a chamber volume of 1.65 µl as can be seen in seen Figure 2.13.

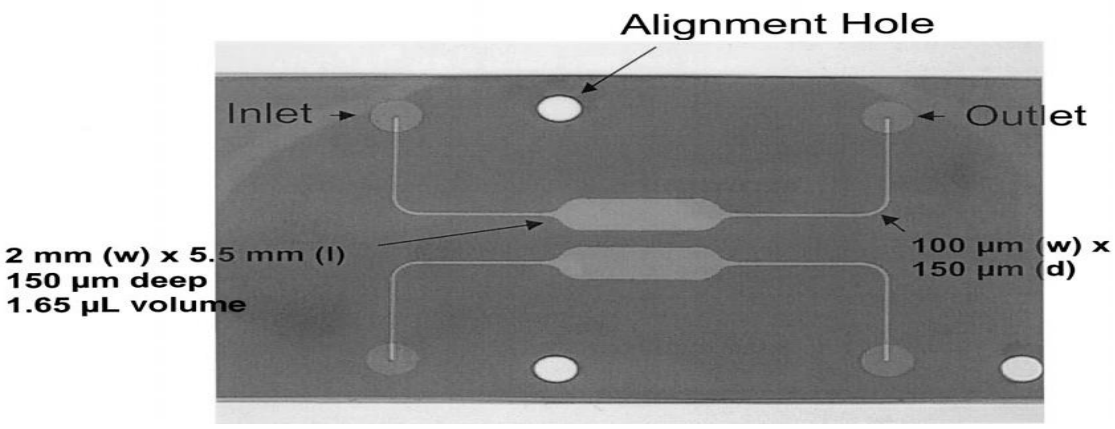

Figure 2.13 The figure shown the shape and the size of the PCR chambers and channels connected the outlet and outlet of the system. The system made by laser ablation on single layer (150 mm thick) of polyimide sheet. The alignment hole used to aligned the system as the polyamide sheet was sandwiched between two additional layers of polyimide (125 mm thick**)** to close the system (Giordano *et al*, 2001).

Guttenberg *et al,* (2005) proposed a completely different approach to handling a small-scale sample. They used a hydrophobic/oleophobic surface to provide effective fluid captivity. However, having to implement a stationary heater that requires heating and cooling on the same heating block is time consuming and very difficult to control. This design basically replicates the disadvantages of conventional PCR machines but on a small scale. The system suffers from problems such as overshooting and undershooting in the temperature profile. As well as this, the design lacks the flexibility to modify the reaction rate, resulting in more cycling and heating time.

Jia *et al.* (2007) designed a low cost disposable card PCR chamber. The reactor consists of a reaction chamber (volume 25 µl), inlet/outlet/ice valves (1 mm circles) and connecting channels (0.3 mm wide). Four reactors are arranged in a plainer format on a foot print area of 78 mm × 36 mm × 0.25 mm (the thickness of the PC sheet is 0.25 mm). The PCR card contains three layers: a structured polycarbonate (PC) film in the middle, a polypropylene (PP) and an Aluminium (Al) foil on the top and bottom side of the PC film, respectively. The top and middle films are aligned and laminated using a custom made assembling jig, followed by sealing AlumaSeal II foils. The three layers are bound together by taking advantage of adhesives on the thermal seal film and AlumaSeal II foils as can be seen in Figure 2.14.

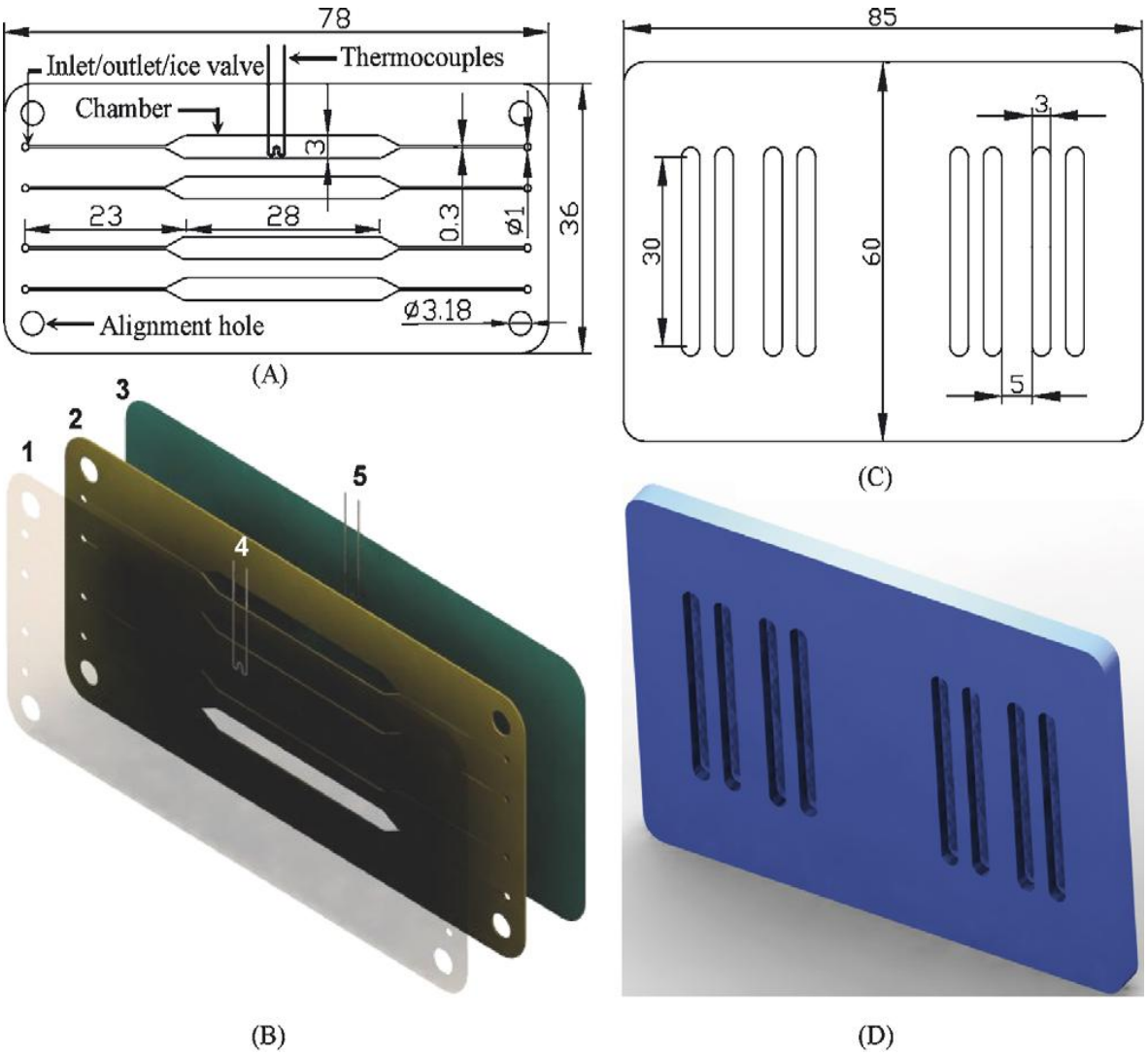

Figure 2.14 Design of PCR card and top plate. (A) Layout of PCR card with thermocouples. (B) Rendering of PCR card assembly: (1) PP film; (2) structured PC sheet; (3) Al foil; (4) thermocouple, top; (5) thermocouple, bottom. (C) Layout of top plate. (D) Rendering of top plate. (Jia *et al*, 2007).

Xiang, Xu, and Li (2007) reported a new chip-based real-time PCR system. It consists of a PDMS reactor chip, miniaturized thermal cycler and a fibre- optic fluorescence excitation and detection module. The fabrication techniques applied are soft photolithography and replica processes. The miniature thermal cycler is built with a thin film heater for heating and a fan for rapid cooling. The PCR chip is composed of two layers of 0.15 mm glass with a layer of PDMS in between, as shown in Figure 2.15.

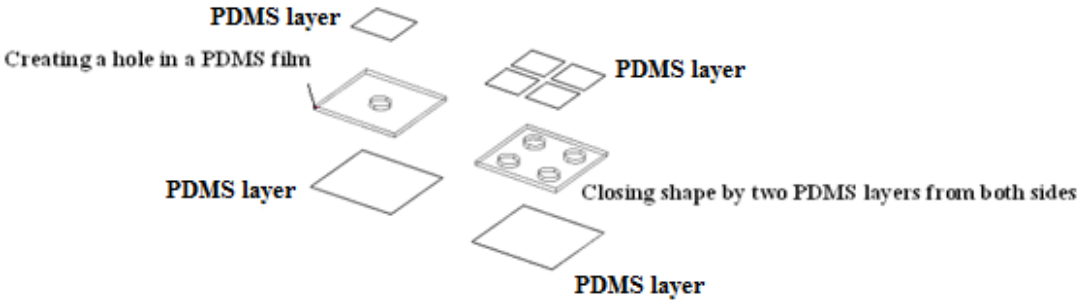

Figure 2.15 Schematic diagrams of the one well and four well PCR chip design. They are composed of two layers of thin glass (0.15 mm) and a layer of PDMS. The PDMS is a 0.5 mm thick square-shaped sheet with 4 mm holes in diameter to form either one well or four wells of the containment of reagents. The smaller glass cover is placed onto the chip to seal PCR reagent (Xiang, Xu and Li, 2007).

The PDMS is a 0.5 mm thick square-shaped sheet. It has 4 mm holes in diameter punched through on the stage to form either one well or four wells for holding the reagents. The PDMS layer and the glass base are permanently bonded by bringing both surfaces together after plasma treatment.

Liao *et al*, (2005) demonstrated a portable RT–PCR system. The device is a model of miniaturized PCR system for amplifying RNA-based molecules such as RNA virus or mRNA. The system consists of two major components, namely a micro temperature control module and a microfluidic control module. In the micro temperature control system, the heating and temperature sensing elements are fabricated of the same material platinum (Pt) and are located within the reaction chambers to ensure a uniform temperature distribution, low power consumption and high heating and temperature sensing rates as can be seen in Figure 2.16. This system is capable of providing a rapid and precise temperature control. PDMS are used to produce a microfluidic control module that operates the movement of individual membranes to realize micro pumps and micro valves with which to control the fluid flow within the device. The total time for the PCR test in this work was accomplished in 55 min and the total sample volume consumed was 15 μ.

Giese *et al*, (2009) demonstrated a short tandem repeat (STR) PCR amplification system, which can be used for forensic analysis. The biochip has been designed and custom built by Network Biosystem (Netbio). This system consists of a high output

thermoelectric cooler/heater mounted to a high efficiency heat sink. The biochip in Figure 2.17 contains 16 PCR reaction chambers, which are coupled to a heat pump by applying a compressive pressure with a clamping mechanism. Each reaction chamber is 500 µm deep and 1 mm wide and holds 7 µl of PCR reaction solution.

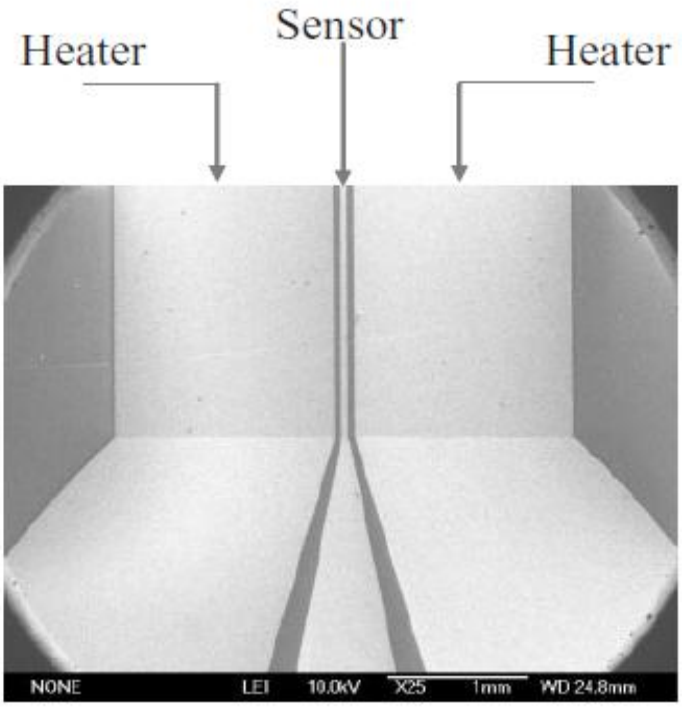

Figure 2.16 The two micro heaters are located within the reaction chamber in order to improve the uniformity of the temperature field (Liao *et al*, 2005).

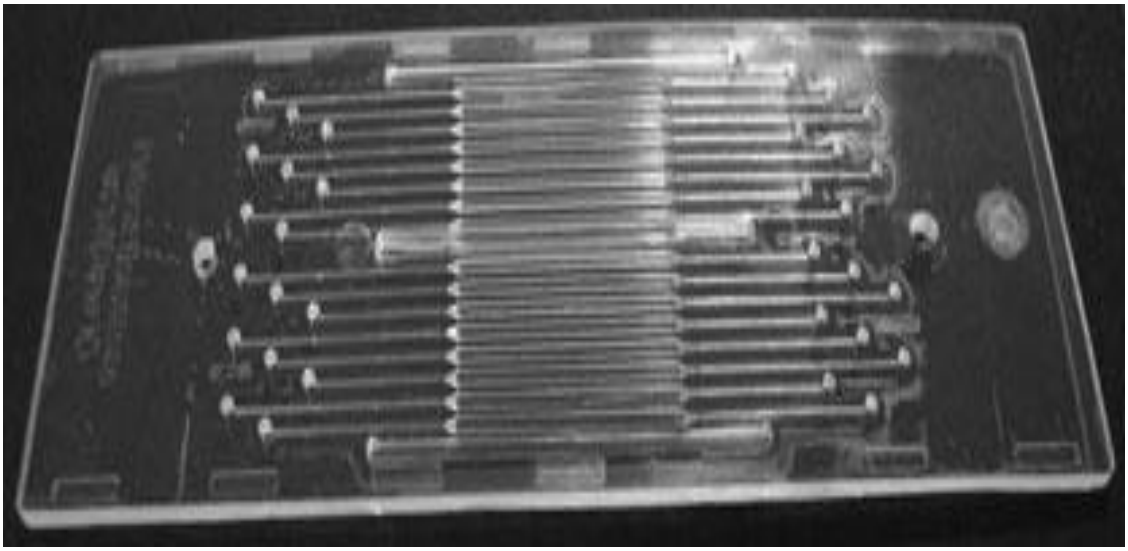

Figure 2.17 A photograph of 16 lane microfluidic bio-chip designed by Giese *et al*, (2009); each lane volume is 7 µl of PCR sample.

2.6.3 Model three shunting PCR system

This model of miniaturised PCR combines the advantages of the previous models as the sample chamber is transferred back and forth along three different temperature zones. The attractiveness of this model is that the sample settles at a defined temperature for the known resident's time (Bustin, 2010). The difference between this model and the continuous-flow model is that in this model the liquid sample or sample chamber is circulated between the three constant temperature zones for a pre-determined number of cycles (e.g. 35) meaning that the number of cycles is not variable. However, in the continuous-flow model the liquid sample is cycled through a micro-channel and the number of micro-channel cycles represents the number of cycles. This model is the most practical miniaturised PCR for three reasons. The first reason is that the sample in this model is amplified in a clean disposeable chamber and this prevents any cross-contamination. The second reason is related to the mechanism of heat transfer because the sample in the light chamber possesses an elevated ramping rate for heating and cooling. The third reason is related to PCR kinetics as the sample attains the targeted temperature in each step of the PCR process without over-shooting, which affects the PCR amplification. The researchers produced many types of this model.

Wang *et al,* (2009) presented a micro PCR chip system incorporated with a fluorescence detection module for on-line detection of infectious diseases. The system proposed was developed to reduce cooling and heating times for a PCR process. In this system, a pneumatic micro-pump is adopted to precisely drive the sample flowing through three reaction chambers. It is made of two polydimethylsiloxane (PDMS) layers and a glass substrate. The top PDMS layer is for serpentine-shape (S-shape) pneumatic micro-channels and reaction chambers. The bottom PDMS layer is for liquid micro-channels. The glass substrate is then used for depositing micro-heaters and micro temperature sensing resistors. The full microfabrication steps are described in Figure 2.18.

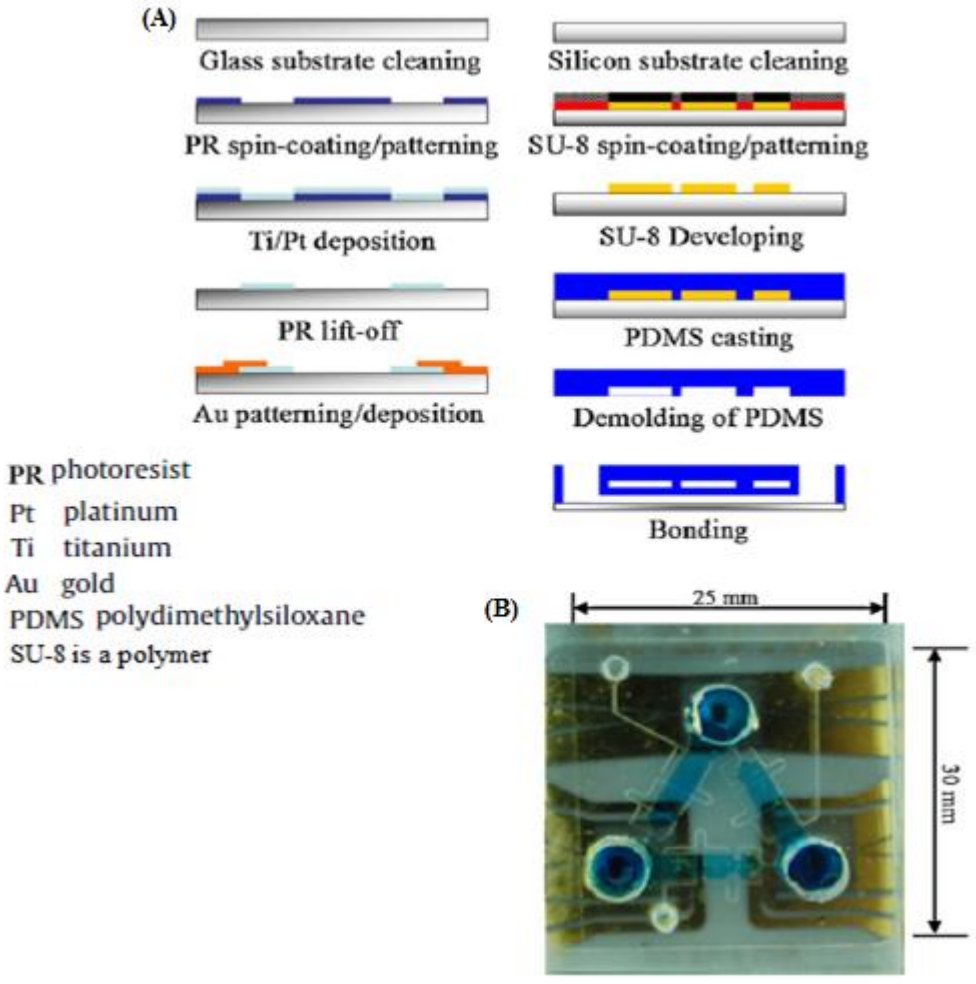

Figure 2.18 (A) Overview of fabrication process used to manufacture micro PCR chips. (B) Photograph of the flow-through PCR chips with microthermal and microfluidic control modules.(Wang *et al*, 2009).

The light source and spectrometer are employed to provide excitation and fluorescence spectral dispersion for DNA binding dye detection (SYBR Green1). A blue-light LED is employed as the excitation light source, with a peak emission at a wave length of 470 nm. The spectrometer is used to detect fluorescence accumulation in the PCR reaction chamber.

Recently, several studies have proposed microfluidic PCR utilizing a thermal convection. These models possess the merits of both static chamber and continuous-flow PCR devices. In the convection PCR devices, PCR samples are shunted and circulated using the buoyant force (called thermosiphon effect) generated by the thermal energy of the PCR reaction itself. As the PCR system requires three different temperature zones, the temperature differences within the closed loop give rise to buoyancy differences and the liquid reactant continuously circulates along the closed loop by the thermosiphon effect (Chung *et al*, 2010).

Chung, Park, and Choi (2010) proposed impressive convection-based PCR systems see Figure 2.19. The system proposed consists of triangular closed-loop disposable polymer channels, a heating block unit and a temperature controller. The whole polymer chip was made from polycarbonate and fabricated using injection moulding technique. A PCR reagent mixture is introduced into a polymer chip by dropping it onto the inlet of the polymer chip Then, the chip is inserted vertically into a slot of the preheated blocks and the three zones of the loop channel in the polymer chip are heated to three different temperatures for PCR. Buoyant convection is generated by the density differences among the heated zones, and a continuous circulatory flow is formed along the loop channel in the polymer chip.

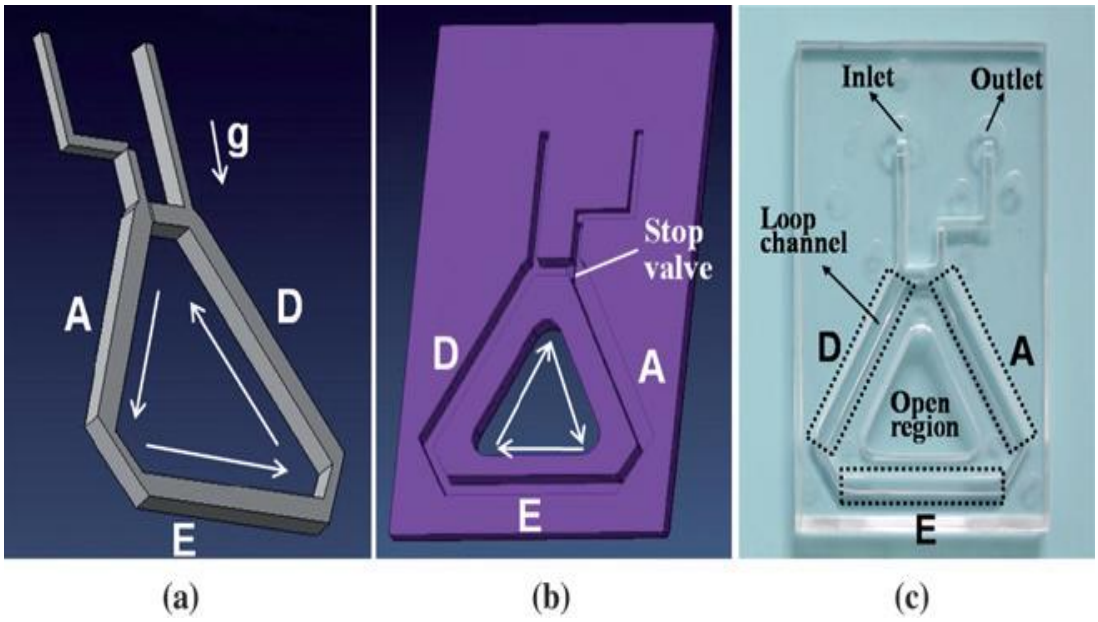

Figure 2.19 The picture illustrates the PCR-thermal cycler model, which works by thermosiphon effect. (a) The geometry of the channel in the polymer chip. (b) The design of substrate with three channels represents three PCR-zones. (c) The actual chip produced. AS can be seen in (a) g is the gravitational acceleration area. D represent denaturation zone, A represent annealing zone and E represent extension zone (Chung *et al*, 2010).

Sun, Kwok, and Nguyen (2007) also demonstrated a significant model of continuous-flow PCR on-a-chip. They produced a close-loop circular ferrofluid driven microchip for rapid PCR. An external magnet is used to drive a small ferrofluidic plug inside the circular microchannel, Figure 2.20, which in turn pushes the PCR reaction mixture to move around the circular microchannel and to travel through the three temperature zones. The number of thermal cycles can be varied by controlling the number of rotation cycles of the magnet. Cycle time of the PCR mixture is adjusted by changing the rotation speed of the magnet. The PCR chip was fabricated in PMMA substrate by laser ablation.

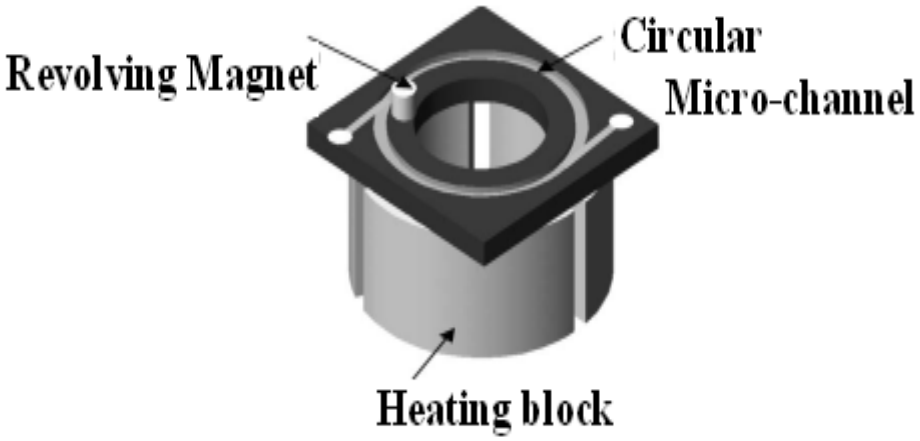

Figure 2.20 Schematic drawing of the PCR microchip with heating blocks and magnetic source (Sun, Kwok, and Nguyen , 2007).

Fery *et al,* (2007) described a shunting design of a polymer-based, multichannel device for PCR. In this system, the shuttling sub microliter sample of the PCR mixture moves back and forth over three constant temperature zones by pneumatic actuation with integrated system. The actuated pneumatic pump and microfluidic components in the channels allow for a robust and autonomous sample manipulation as can be seen in Figure 2.21.

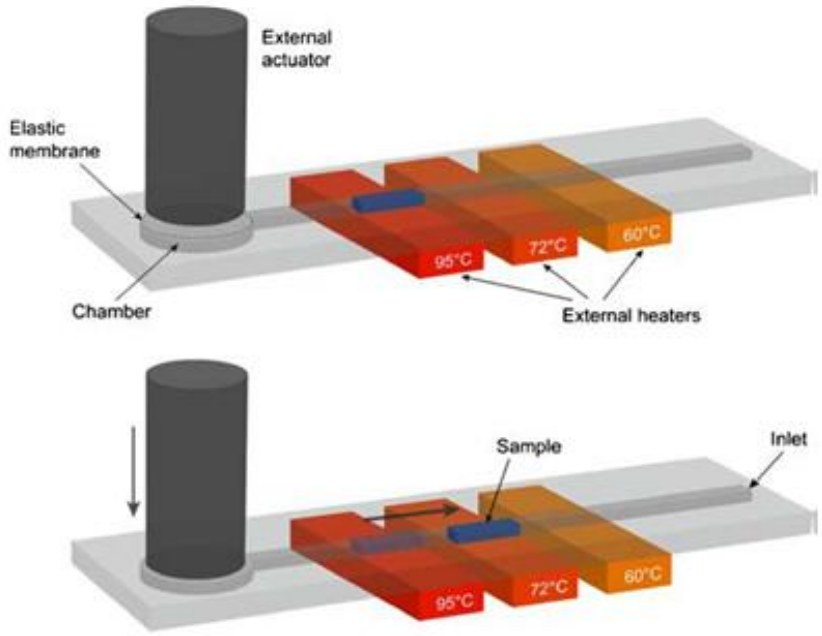

Figure 2.21 Principle of sample shuttling: The PCR reaction is performed inside a straight channel ending in a chamber with a membrane which is deflected to move the liquid sample back and forth over three constantly heated regions. Actuation and heating is done externally so that the chip can be kept as simple as possible. (Fery *et al*, 2007).

The system proposed in this project is similar to the model described by Fery *et al*, (2007). However, this system is different as the sample handling technique utilizes a pneumatic actuation system to move the sample over the three zones. The sample chamber in this system was a channel and the liquid sample was shunted back and forth over the three heaters. Whereas in our proposed system the sample chamber (which contains the PCR mixture), is mechanically shunted in between the three heaters. Moreover, the heaters are double plates in order to sandwich the sample chamber, as will be discussed in chapter three of this thesis.

2.7 Detection method

One of the major challenges associated with the development of a nucleic acid analyzer on a chip is to meet the physical limitations required by a portable detection module for on-line PCR detection and quantization. In order to integrate PCR system

on a chip, selection of an appropriate detection method is essential. The same detection methods used in conventional PCR have been miniaturised with different microfluidic techniques. Agarose gel electrophoresis with ethidium bromide staining is simple and inexpensive but suffers from a lack of sensitivity and specificity. Often, PCR products appear on the gel as a number of bands or as a smear. In these cases, it is difficult to determine whether the correct size band has been generated. This method had been applied on-chip by many researchers. Capillary electrophoresis (CE) is another group of modern chemical analysis methods, where measurements are carried out most commonly in conditions of the solution flow through the measuring system. The fundamental nature of this technique is movement of ions, or charged particles in the solution in the electric field, which is most commonly associated in the capillary system with electro-osmotic flow of the whole solution volume in the capillary. CE in its various forms is treated, from the analytical point of view, as a high performance separation method because of differentiated electrophoretic migration of ions and electrically charged particles depending on their size and charge. Woolley *et al*, (1996) published the first PCR amplification and detection chip applied CE method to separate amplified PCR products. They described methods that permit direct integration of micro-fabricated PCR thermal-cycler and CE components on a single micro-device. The PCR reactor is fabricated from polished silicon wafer using photolithography technique and CE is fabricated from glass using photolithography and etching techniques. The disadvantage of this technique is as described earlier, in that the PCR chamber is not disposable and the CE detection method may complicate the design of the device.

Lagally, Medintz, and Mathies (2001) also produced PCR-CE system on-a-chip with high sensitivity. The system could detect up to 20 DNA copies /µl . The CE separation medium consist of 0.75 % (w/v) hydroxyl-ethyl cellulose in 1× Tris acetate EDTA (TAE) buffer with 1 µM thiazole orange. Electrophoretic separations were detected using a laser-excited confocal fluorescence detection system. The chip was placed on a stage and the 488-nm line from the argon ion laser was focused on one of the separation channels at a position 4.6 cm from the injection cross. Fluorescence was collected by a 32× (0.4 NA) objective, spatially filtered by a 160-

μm pinhole, spectrally filtered by a 515-nm band-pass dichroic filter (30-nm band width), and detected by a photomultiplier.

Electrochemistry-based detection method is an alternative method of choice for hand-held instruments. Some researchers claim that the sensitivity and selectivity of the electrochemical detection are comparable to that of the laser-induced fluorescence detection. The advantages of the electrochemical detection over the optical techniques include not only the inherent miniaturisation and portability, but also independence from the optical path length, sample turbidity, extremely low-cost, low-power requirements and compatibility with micro fabrication (Fang *et al*, 2009).

For quantitative PCR detection, Electrochemiluminescence can also present an alternative detection method. Electrochemiluminescence is the ability of the substance to emit light when stimulated by an electric field. This method requires amplification of PCR with two types of primers; one primer is biotinylated and the other one unmodified primer. After amplification, the PCR products are hybridized to oligonucleotide probes containing the electrochemiluminescencent label. The commonly used reagent is TBR (Tris-2, 2' –bipyridine ruthenium (II) chelate). After hybridization, the reaction mixture is mixed with streptavidine-coated magnetic beads that bind the biotin-labeled hybrids. The magnetic beads are then loaded into the fluorescence spectrometer which contains an electrochemiluminescent detection chamber. The magnetic beads are bound magnetically to the electrode and are washed to remove any unbound materials and non-hybridized TBR-labelled probes. Ultimately, the electrode supplies an electric field to the bound material and the electric field and produces light stimulate the TBR-labelled probe, which has hybridized to capture PCR products. In this case the intensity of the light is proportional to the concentration of the PCR products Duan, Zhou, and Xing (2010)

This detection system has gained much attention as an option for miniaturized bio-sensing platforms, as it provides higher sensitivity and requires less instrumentation than fluorescence methods. The background signal in chemiluminescence detection is extremely low, but the generated signal is also very low, compared with fluorescence signals (Hatakeyama *et al*, 2009). The most common on-line detection

scheme for micro PCR amplification is based on fluorescence techniques. Fluorescence detection has been reported, using of miniaturised excitation and emission sources for microchip devices. Most devices investigated were utilise bulky bench-top excitation sources, including lasers and mercury lamps. Moreover, fluorescence detection has commonly been accomplished with microscope-based CCD cameras or other large instruments that systematically inhibit portability In contrast to these larger systems, light emitting diodes (LEDs) have been used as excitation sources, combined with miniaturized detectors such as photodiodes and miniaturised photomultiplier tubes (Banerjee *et al,* 2010).

A number of investigators have attempted to integrate fluorescence detection with microfluidic chips. Edel *et al*, (2004) demonstrated the use of a poly fluorine based LED (polymer LED) as light source, an avalanche photodiode as a detector with limit of detection(LOD) of 1 mM for fluorescein dye. Yao *et al*, (2005) fabricated a microfluidic device with an integrated organic LED (OLED) excitation source and a photomultiplier tube (PMT) as detector for on-chip fluorescence detection using a pinhole and interference filter for masking the excitation light. A LOD of 3 mM was achieved for Alexa 532 dye using this method. Kim *et al*, (2006) demonstrated a compact device using an OLED as light source and an integrated photodiode as detector, with an interference filter to mask the excitation light and secured a LOD of10 mM of TAMRA dye.

Wang *et al*, (2009) demonstrated a fluorescence detection system in the chip capable of detecting 10 copies of hepatitis B virus. The on-line fluorescence detection system is shown in Figure 2.22.

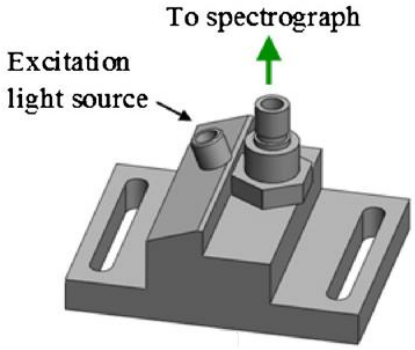

Figure 2.22 Wang *et al*, (2009), demonstrated a fluorescence detection setup based on geometry of 20 degree of excitation source and 90 degree of a detector.

A diameter of 5 mm was used in this study to allow access of fluorescence detection. A blue-light LED was employed as the excitation light source, with a peak emission at a wavelength of 470 nm. The spectrometer is used to detect fluorescence accumulation in the PCR reaction chamber.

2.8 Summary of literature review and conclusion

All PCR systems comprise of three components: a reaction chamber, a thermal cycler, and a PCR product detector. Both static chamber-chips (Lin *et al*, 2000; Giordano *et al*, 2001; Nagai *et al*, 2001; Lagally *et al*, 2001; Yang *et al*, 2002; Lee *et al*, 2003) and continuous-flow PCR chips (Kopp, De Mello, and Manz 1998; Obeid *et al*, 2003; Hashimoto *et al*, 2004; Liu, Enzelberger, and Quake, 2002**)** had been reported. PCR chips have been made by various materials such as silicon (Nagai *et al.*, 2001; Matsubara *et al.*, 2005; Lin *et al*, 2000), glass (Lagally, Medintz, and Mathies, 2001), polycarbonate (Yang *et al*, 2002) and polyamide (Giordano *et al*, 2001 and PMMA (Lee *et al*, 2004). Nagai *et al*. (2001) and Matsubara *et al*. (2005) reported a single-well PCR chip and a multiple-well PCR chip. A contact and non-contact heating system (Giordano *et al*, 2001) as well as Joule heating system (Hu *et al*, 2006) were used to power the thermal cycling. The analysis methods of the amplified PCR products include gel electrophoresis (Obeid *et al*, 2003; Lin *et al*, 2000; Lee *et al*, 2004). Fluorescence scan after PCR test were used by Matsubara *et al*. (2005) and Yang *et al*. (2002);real time fluorescence intensity detection by

fluorescence microscope were used by Nagai *et al* (2001) and Lee *e*t *al.* (2004). Cady *et al,* (2005) reported a prototyped fluorescence detection module. Table 2.3 summarises the comparison aspects between the most important models.

It can be deduced from the previous discussion that published PCR-on-a-chip devices can be classified in three main groups: chamber-based stationary PCR, continuous-flow PCR and shunting PCR. All types had been designed to achieve faster thermal cycling and reduce sample/reagent consumption. The main advantage of the continuous-flow PCR is its ability to reduce heating and cooling time and thus shorten the total time of the PCR reaction. However, it is difficult to isolate the different temperature zones, to examine the PCR results and to collect the PCR product for further analysis; whereas, shunting PCR module combines the advantages of both stationary-based chamber and continuous-flow PCR modules.

The ideal material to fabricate the PCR chamber must be chemically, electrically and mechanically robust enough for the PCR reaction and the thermal cycler design. It is also important that the design is economical allowing disposable cartridges to be fabricated whilst avoiding cross contamination during the process. Most of the early miniaturized PCR devices were fabricated in silicon or glass by taking advantage of well-established micro-fabrication technologies. However, glass and silicon are known to be a source of PCR inhibition. Also, polymeric materials have been explored as more flexible alternatives for fabrication of microfluidic PCR chambers, especially polycarbonate, which has already been adapted for PCR reactions, as it is used to generate the conventional Eppendorf tubes (Becker and Gartner 2008). However, there are complications related with the fabrication of thin film chambers and their performance in the PCR process. There are two main problems in thin film encapsulation. These include a suitable method of encapsulation and the method of sample introduction. It appears that no microfabricated PCR device has successfully amplified long or complex DNA targets while simultaneously reducing the required time, volume and quantity of starting material, compared with what is required by a standard thermal cycler. The duration of a PCR can only be shortened by decreasing the thermal mass, which will increase the heating and cooling rate (Zhang *et al.* 2006).

Most of the models produced have facilitated DNA amplification at much faster rates, as the result of smaller thermal capacity and a larger heat transfer rate between the PCR sample and temperature-controlled components.

Subsequently, it can be concluded that the shunting model is the best for PCR application due to the following reasons:

(1) Shunting the PCR mixture in a chamber is essential to prevent any cross contamination especially for designing a portable device, as this device can be used in a non-decontaminated environment.

(2) This model is more practical to scale-down or scale-up the sample size because the sample-chamber can be fabricated according to the requested sample volume.

(3) Multiplication of a simple disposable polymer sample-chamber is more affordable than producing more complicated chambers, such as the model that includes a heater or a model that replaces the capillary tube, as in the continues-flow model.

(4) Fluorescence detection is more flexible so it can be used for either endpoint detection or real-time PCR.

Table 2.3 The most important models of PCR-on-a-chip, which have been produced and highlight on the model type; the materials used to fabricate the chips and detection technique applied. The last column outlines the articles that described the models.

Fabrication technique used	Material used	Model type	Detection unit	Reference (s)
Hot embossing	PMMA	Chamber	Fluorescence.	Lee *et al.* 2004
	PC	CF	End point detection	Hashimoto *et al.* 2004; Chen *et al.* 2005..
Injection moulding	COC	Chamber	Electrophoresis	Fan *et al.* 2003
	Zeonex 690R	Chamber	End point detection	Sauer-Budge *et al.* 2009
	PC	**Shunting siphon**	fluorescence	Chung, Park, and Choi , 2010
Adhesive bounding	PC, PP and Al	Chamber	End point detection	Jia *et al.* 2007
Soft lithography	PDMS	Chamber	Fluorescence.	Cady *et al.* 2005
	Glass &PDMS	Chamber	Fluorescence.	Xiang & Li 2007
	Silica	Chamber	Electrophoresis	Burns *et al.* 1996.
	PDMS	**Shunting chamber**	Fluorescence	Wang *et al,* 2009
Multilayer soft lithography.	PDMS	CF	End point detection	Liu *et al.* 2002
	PDMS	CF	Electrochemical	Fang *et al.* 2009.
(Applied filip-chip bounding)	Silica & glass	Chamber	detection. End point detection	Zou *et al.*2005.
Moulding technique	PDMS	Chamber	Hybridization	Peytavi *et al.*2005
	PDMS	Chamber	Fluorescence	Gong *et al.* 2010.
	PDMS	**Shunting chamber**	Fluorescence	Fry *et al,* 2007
Micro machining	SU-8 & glass	Chamber	End point detection	Christensen *et al.*2008
	Silica& glass (ICP-DRIE technique).	Chamber	Electrochemical detection. Fluorescence	Yeung *et al.* 2008.
	Silica (DRIE)			
	Silica	Micro-pillar	Fluorescence	Kim *et al.* 2009.
	PTFE*	CF	Fluorescence	Li *et al,* 2009
Thermal foaming	PET	Chamber	End point detection	Zou *et al.* 2002
Drilling & micro milling	Silica	Chamber	Fluorescence.	Neuzil *et al.* 2006
Laser appellation	Polyamide	Chamber	Capillary Electrophoresis	Giordano *et al.* 2001
	PC			Yang *et al.* 2002
Wet chemical etching & photolithography	Glass	Chamber	Capillary Electrophoresis	Khandurina *et al.* 2000; Toriello *et al.* 2006
	Silica wafer	Chamber	Capillary Electrophoresis	Lagally *et al.* 2001

* Poly(methyl methacralate) (PMMA)
* Polycarbonate (PC)
* Poly Tetrafluoroethlene (PTFE)
* Polyethylene terephthalate (PET)
* Cycloolefine /copolymer (COC)
* Polypropylene (PP)
* Poly(dimethylsiloxane) **(**PDMS)

Chapter 3 Thermal-cycler and chip fabrication

3.0 Introduction

Based on the discussion in chapter two, a critical challenge to the establishment of a thermo-cycling instrument is the ability to fabricate a relatively fast and low cost configuration to perform efficient repeating heating and cooling steps. In this project an innovative thermo-cycling design has been introduced. A key element of this design is an architecture of double-sided heaters that allows the entire thermo-cycling process to be actuated pseudo-isothermally by simply maintaining each heater at constant temperature. The sample holder, which contains the sample reaction chamber, was fabricated to smoothly shunt between different temperature zones, allowing the sample to stay at each temperature for known residence times i.e. the temperature required for denaturation step, temperature required for annealing step and temperature required for extension step. The design was redeveloped three times during the assessment scheme; that is, three different prototypes thermal-cyclers design were constructed and tested in this project. All types produced were based on the original proposed design shown in section [1.1.6] Figure 1.13

This chapter will explain all the engineering work that had been completed in this project. The first section will describe the method used to measure the temperature profile in conventional thermal-cycler systems and discuss the temperature profile for selected types of thermal-cyclers. This is followed by sections providing details of the configuration of the proposed thermal-cycler design and fabrication. The last sections will describe and discuss the materials and method used for chip fabrication

3.1 Materials and methods

3.1.1 Temperature profile measurements

This test was performed in order to assess the temperature profile of different types of conventional thermal cyclers and determine the efficiency of each system to raise or decrease the temperature between the PCR steps. The results will be compared with the suggested device temperature profile in a later study. This study will prove the influence of the thermal cycler design on temperature control efficiency. The

machines selected to perform this test are: Progene model (model No. 1294), Gene AMP (model No.9700) and Rotorgene (model No.3000). Both Progene and Gene AMP use one block heated and cooled to reach the PCR temperature step.The Rotorgene uses an air heating and cooling technique and the samples are subjected to the air stream of the step temperature.

The experiment was performed by using ultra thin close tolerance thermistor (Farnell-UK) and data was collected by data-logger from Pico Technology (UK) (device type is ADC-24). The calculation of the connection between the thermistor and the data-logger is described in details in Appendix 1. The equation created was used as the basic equation to operate the thermistor before it had been calibrated.

For calibration, the thermistor was placed in the water bath at room temperature along with the two thermometers. Then, the temperature controller of the water bath was raised to 100 °C and left steadily elevated. The thermistor measured the temperature every minute and at the same time the temperature readings were recorded manually from both thermometers.

3.1.2 Thermal-cyclers temperature profile measurements

The thermister was inserted inside a polypropylene 0.2 ml Eppendorf PCR tube. Specifically, the Eppendorf tube was altered in the following manner: the locked-cap was removed and replaced by an adhesive sealed film (PCR adhesive film from (Thermo-Scientific-UK). Then the altered tube with thermister was placed in the thermal cycler block. 25 µl of biological water (Promega grade water) was then added to the tube and the thermal cycler was secured as a normal run (as can be seen the, Fig.ure 3.1A and B. Temperature data was recorded every one second for 1200 second using the data logger. All measurements were repeated three times.

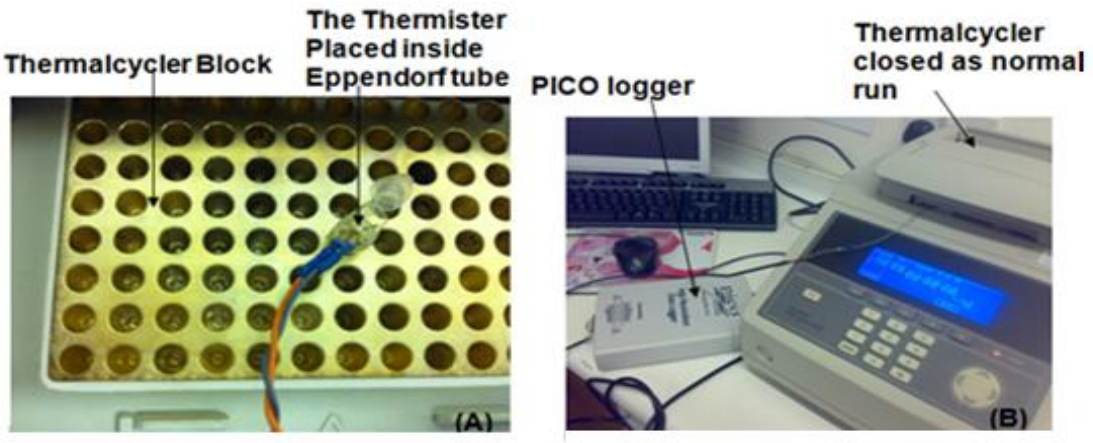

Figure 3.1 picture **(A)** illustrate how the thermister was inserted into the tube positioned inside the thermal-cycler block during the temperature profile test. Picture **(B)** temperature measurement process.

Table 3.1 List contains the parameters of the thermal-cycler program, which used for temperature measurements.

Thermal-cycler step	Temperature of the step	Time of the step
Denaturation step	95 °C	30 second
Annealing step	55 °C	30 second
Extension step	72 °C	30 second

3.2.3. Construction of the first prototype device

The first prototype model presented in schematic diagram is illustrated in Figure 3.3. The main purpose of constructing this design was to enhance heat transfer from the blocks to the sample chamber. The system consisted of three parts: six heating blocks (2 × 2 × 3 inch), a controlled power supply unit and a temperature-monitoring unit. The heating blocks were made from highly thermally conductive metal (Aluminium) to ensure uniform temperature around each block. The six blocks were ordered from left to right to accomplish the three PCR thermal cycler periods; denaturising, annealing and extension phases. An insulation foam layer to isolate the blocks from the ambient temperature and from the adjacent blocks covered the paired blocks. Each pair of blocks exemplified one thermal cycler phase, as can be seen in Figure 3.2. Each pair of blocks were attached together to form a double side temperature zone and soft spring flaps were placed on the other side to in order to slot in the sample chamber between the heaters .The sample chamber was inserted horizontally between each pair of blocks at each thermal-cycle step. This foam-

insulated model also compressed flexibly, squeezing the sample chamber while it was cycled between the blocks, as can be seen Figure 3.3.

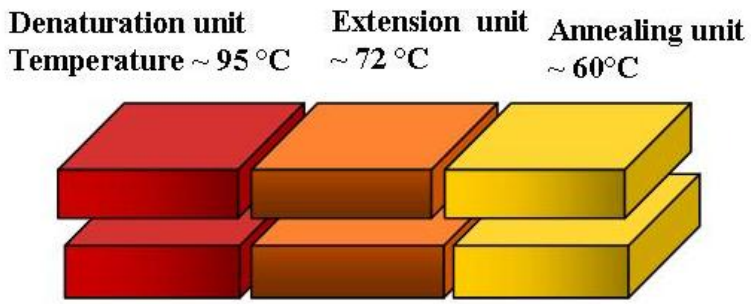

Figure 3.2 Schematic diagram shows the prototype thermal-cycler system, which consists of 6 aluminium blocks arranged in three units (representing the three PCR steps: denaturation, annealing and extension). Each unit consists of two aluminium blocks and each block (Depth ×Width ×Length) 5.1×5.1×7.6 cm.

The electronic parts are as described in Figure 3.3. Each block contained a heating element (Farnell, brand Duratool, electric iron power of 48 watt) and a platinum resistance thermometer type (PT100, from Farnell). The thermometer was connected with a relay switch to control the temperature in the blocks. The temperature sensing probe used was (Thermocouple Type: K from Farnell), temperature measuring range of the sensor from - 50°C to 350°C. The temperature profiling of the system was then tested using the pre-calibrated temperature sensor.

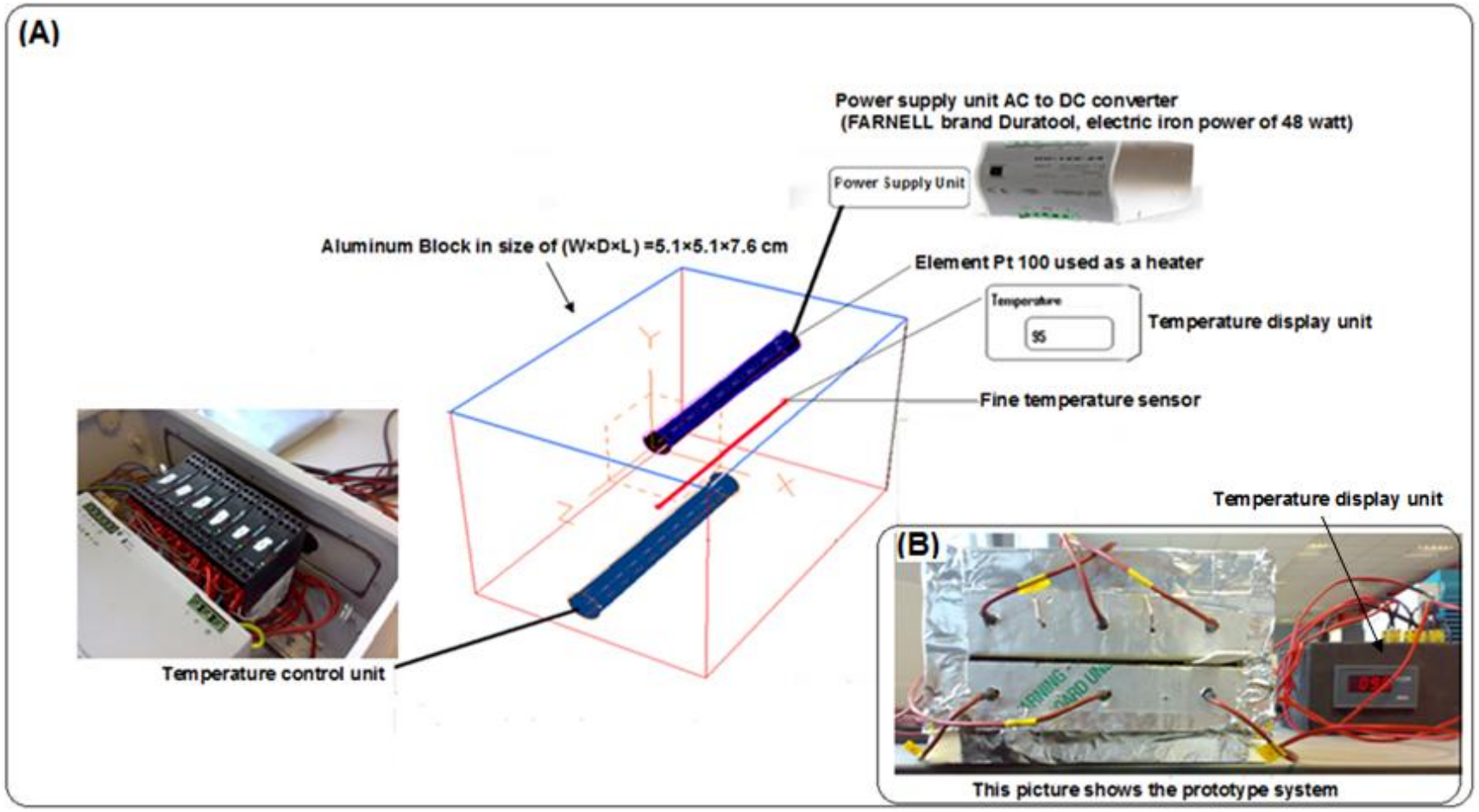

Figure 3.3 (A) Schematic diagram of the prototype of the thermal cycler illustrating the electrical parts inside of each block. **(B)** a picture shows the final shape of the thermal-cycler system fully covered by heat insulation and the temperature display unit.

3.1.3 Altering the system design

Using the previous system created many problems related to scaling down the system. Accordingly, the thermal-cycler system was altered to achieve a better quality designed more efficient automatic system. The system required a mechanical actuator unit but it was thought that the best way to implement more efficiency was by utilising a rotating element. The PCR process required cycling the reaction chamber in between three temperature zones. Therefore, arranging the three zones in a circular shape could generate an efficient practical thermal cycler system.

Subsequently, a lightweight heating element was proposed to control the temperature of disc-mounted chambers in the miniaturised PCR system. Various flat heating elements could have been selected, for instance an etched foil element type, which is created by etching using strong acid to form a circuit in resistant alloy foil. These heaters have been commercially available on the market in three types: silicone, rubber, Kapton (a polyamide thin light organic polymer) and polyester type. The heated sections would be surrounded by insulation as the system had been fixed in place. The main requirement of this is to maintain the temperature constant within about -0.5 to +0.5 °C at all times. If the samples were rapidly transferred from the 95 ºC to the 60ºC zone, the hotter zone tends to cool slightly, which could be prevented by predictive control. The temperature may be measured by thermistors, PT100 sensors, or possibly by monitoring the resistance of the heating element itself if the aluminium plates are very thin. The project required building, characterising, modelling, simulating and controlling a prototype heater.

The system proposed to be fabricated in a disc format and the samples were thermo-cycled between three pairs of heating systems, each of these pairs representing one zone of PCR. However, as the sample chamber transported between heating zones, high thermal inertia elements were used to induce rapid temperature change, in both heating and cooling phases. Flat plate heater elements were available as ceramic/cermet, and as metal film on silicone or Kapton. Temperature was regulated by thermistor or by monitoring the temperature-dependant resistance of the heating element itself. The detection unit was assembled after the extension stage and the sample automatically detected after each cycle. Finally, the system was connected

with the Labview software to formulate all the calculation required and to display the results.

3.1.4 The second prototype thermal-cycler design and fabrication

The previous design was a proposal, but the actual circular design was built from segments as described below. The thermal-cycling device was constricted using three pairs of heating plates. Each pair was assembled by 18.9 Ω flexible silicon Kapton resistive heating element in contact with an aluminium plate on the opposite side of which a thermal conductive silicon pad was mounted, as can be seen in Figure.3.5. The complete form of the thermal-cycler consists of two identical plates connected by an angle hinge as in Figure 3.5. Each plate contains three segments arranged in the circular form, as illustrated in Figure 3.4, to achieve consecutive three PCR thermal cycler periods; denaturising, annealing and extension phases Figure 3.5. Each heating zone contains a heating element (Farnell, brand Duratool, electric iron power 48 watt), a temperature sensor (Farnell PT100, 2X2.3mm). The sensor was connected with an electronic controller to control the temperature in the zone. The disc, which contained the sample chambers, was sandwiched between the two thermal-cycling plates.

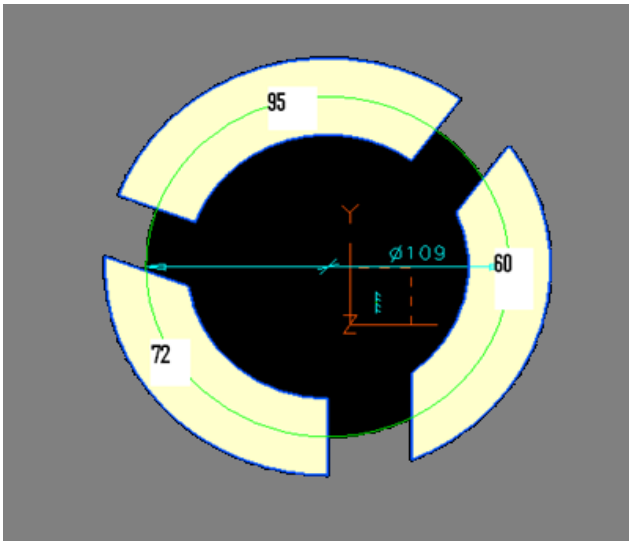

Figure 3.4 Schematic diagram of the device in final form.

Insulation foam was placed in between and outside the heating segments in order to isolate the temperature segments from each other. In addition, an insulating foam layer to isolate the system from the ambient temperature covered the blocks.

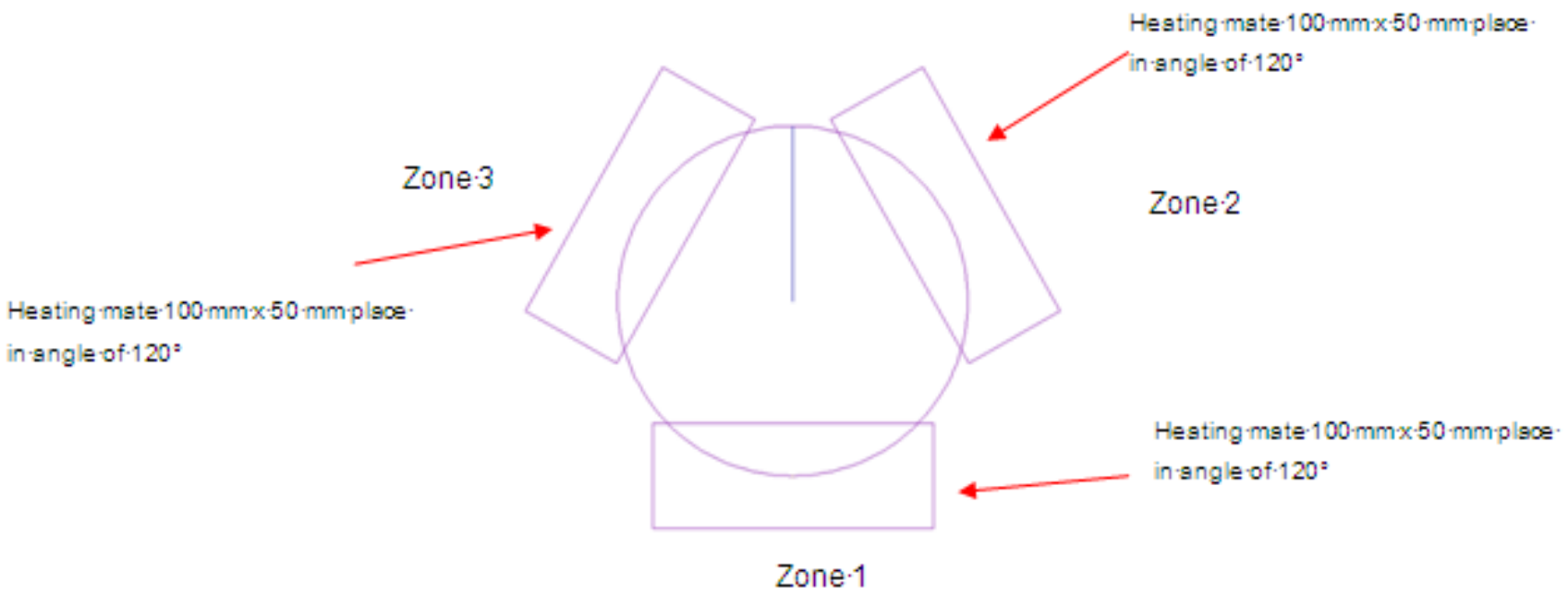

Figure 3.5 Schematic diagram crated in AutoCAD illustrates the arrangement of the proposed thermal-cycler zones.

3.1.5 The third prototype design and fabrication

As a proof of concept, the second prototype thermal-cycler system was working as a PCR thermal-cycler. However, the system was creating problem related with temperature control and unit. The system performance was tested and the result obtained can be seen in Figure 3.6. As can be seen in the image of the agarose gel, the sample amplified in the second prototype thermal cycler was faint band. The result reveal that the system is poorly amplified the DNA fragment. Accordingly, the system was improved to produce the third prototype thermal-cycler system.

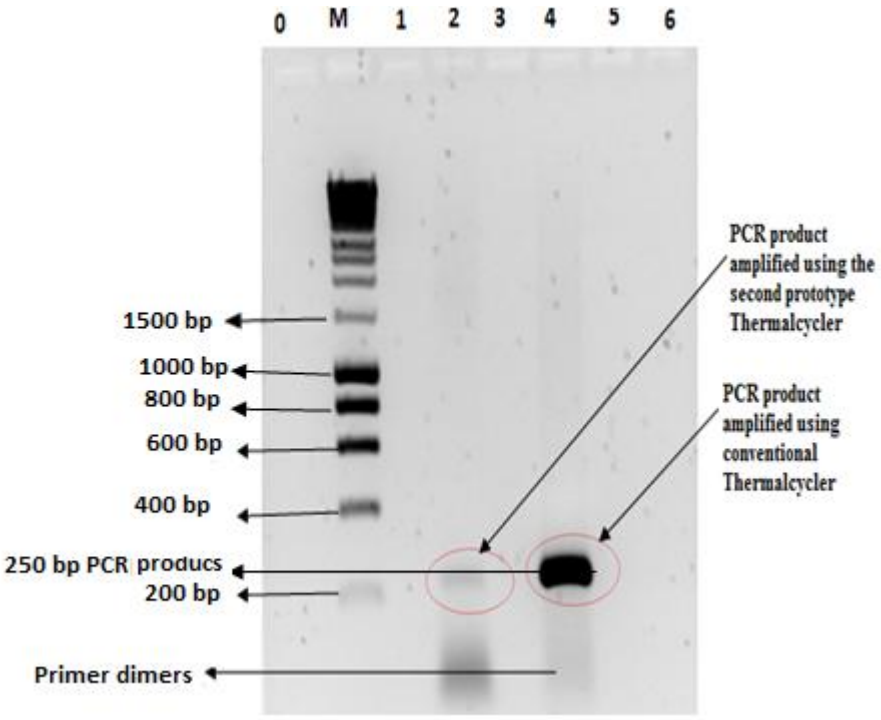

Figure 3.6 The image shows sample resolutions on 1.5 % (w/v) of agarose gel electrophoresis at 90 V for 80 minutes. Agarose gel electrophoresis of the DNA fragment from *E .coli* was amplified by PCR using AS_530R and GC338F primers; the amplicon size is 250 bp. Lane 0: empty, Lane M: DNA Hyperladder 1 (Bioline) marker, Lane 1: blank , Lane 2: PCR product amplified using prototype thermal-cycler (amplicon size is 250 bp), Lane 3: empty, Lane 4: PCR product amplified using conventional thermal-cycler GeneAMP 9700 (Applied Biosystems, UK) (,amplicon size is 250 bp), Lane 5 and 6 are empty. This is the first experiment on the second prototype thermal-cycler, as can be seen the sample amplified in the prototype thermal-cycler was demonstrating a faint band, as this sample was amplified using second prototype thermal-cycler.

In order to achieve high temperature uniformity within a reaction chamber, GHD heaters were used to prototype the thermal-cycler system. The heaters were a simple way of getting smooth, well-finished temperature controlled plates with rounded edges so that the 'chip' would slide through them. Temperature was controlled by a thermistor embedded in the aluminium plate and there was a microcontroller-basedheat control circuit that maintains a steady temperature. As the required temperature was much lower than the standard or 450 deg, F (190 deg C) the element heaters were wired in series rather than parallel, reducing the maximum power by a factor of 4, as the GHD heaters have already built in precise temperature sensor. Besides, the air bubbles problem is common in PCR-on-a-chip system, as has been discussed [2.4.2]. The air bubbles also inhibit the fluorescence measurements within the chip by creating an interference signal and this leads to unreliable measurements. In this system, the built-in wave's generator is working as a degassing component in the system. This feature is an improvement to our previous prototype system. Figure 3.7 shows the diagram of the temperature measurement of the system. The improved PCR results will be discussed in chapter five of this thesis.

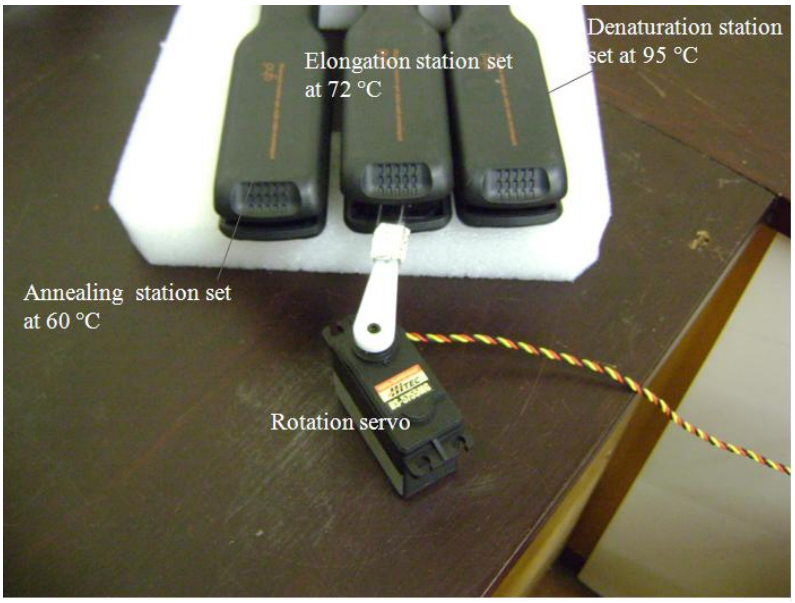

Figure 3.7 This picture illustrates the GHD arrangement needed to build the prototype thermal-cycler, as can be seen by the position of the rotation servo used to transfer the sample chip in between the three temperature zones.

The three thermally isolated reaction zones can be achieved by using three sets of GHD heaters. With this approach, the temperature sensors of the GHD heaters have been altered to attain the desired temperature for each zone. The layout of the thermal-cycler was adapted to perform the PCR procedure. However, the number of thermal cycles and the duration of the annealing, extension and denaturation processes are determined by mechanically transferring (back and forth) the chip in between the three temperature zones. Thus, these chips can only perform three thermal steps with a constant time ratio. Since the dimensions of the three heating regions and chips are fixed, the PCR processes are optimised by adjusting the time ratios of the three-temperature process. A new design of array-type GHD heaters and polycarbonate chip were adopted to improve the thermal uniformity in the PCR chambers and to facilitate the operation for temperature calibration. The thermal cycler system was then incorporated with a fluorescence detection module for DNA amplification and end-point detection and potentially improved for DNA quantification. The polycarbonate chip that contains the sample chamber is automatically transferred between the three PCR temperatures and resides in each zone for a specified period of time. A rotational servo (HS-5755MG, digital quarter scale, from Hitec, UK.) served as an actuator to transfer the chip between the thermal-cycler zones, as can be seen in Figure 3.10. The servo was controlled by data acquisition software programmed using (C#) language (ISO/IEC 23270, 2006) to trigger the position of the chip in the thermo-cycler for a defined period.

3.2 Results and discussion

3.2.1 Thermistors calibration method

The objective of this experiment is to ensure the reliability and accuracy of the thermistor temperature measurements. The test was carried out on the thermistor before being used in the temperature profile measurements. Comparative temperature measurements between two calibrated thermometers and the thermistor reading were made at the same time in identical conditions. Before starting the calibration of thermistor, the thermometers were calibrated.

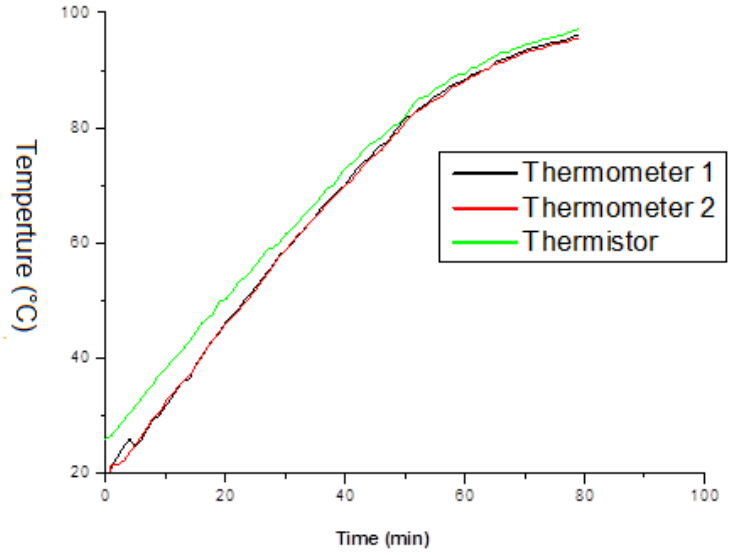

Figure 3.8 The first attempt of thermistor calibration.

At temperature 100 °C the measurements were stopped and a graph of measurements was sketched, as shown in Figure 3.8.This test was repeated three times and in each attempt, the thermistor equation was changed according to values obtained from appropriate temperature ranges. The best three different temperature ranges were at 50 ºC, 70 ºC and 90 ºC, then the equation was developed and the calibration achieved is illustrated in Figure 3.9. The detail of the equation was described in Appendix 1.

According to Figure 3.9 and Figure 3.10, the thermistor temperature measurements were improved in agreement with the thermometer temperature measurements in most of the measured readings. Therefore, it was safe to use the thermistor to measure the temperature in the chambers because the temperature needed to be measured in a range between 55 °C to 95 °C

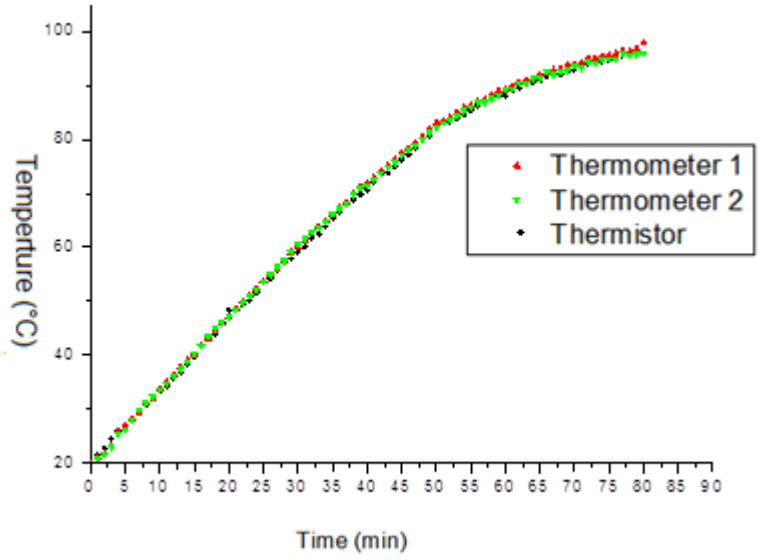

Figure 3.9 Dots plot shows the temperature measurements that exhibit that the thermister temperature measurements are identical to the conventional thermometer measurements.

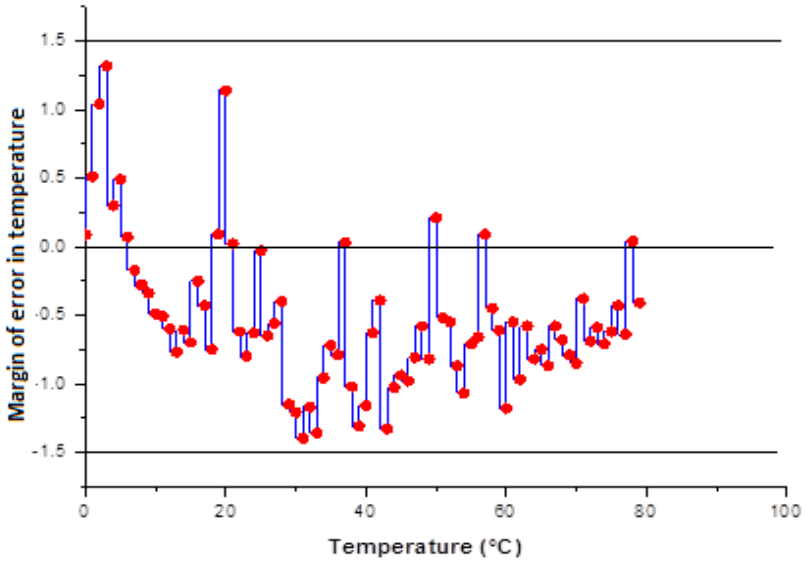

Figure 3.10 The plot indicates the error in the temperature measurement of the thermistor in comparison with the calibrated thermometers. The error is in the range between 1.32 to -1.4 for the all measured points.

3.2.2 Thermal-cycler temperature profile

Thermal cyclers are the programmable heating blocks that control and maintain the temperature of the sample through three temperature-dependent stages that constitute the single cycle of PCR: template denaturation (95 °C); primer annealing (50–65 °C); and primer extension (72 °C). These temperatures are cycled up to 40 times to obtain amplification of the DNA target (Zhang and Xing, 2007).

As the PCR process is a temperature dependant, the optimization of the PCR thermal cycler at three temperature steps is a crucial factor in DNA analysis. During denaturation step at 95 °C, double stranded DNA melts open to single stranded DNA, and the enzymatic extension from the previous cycle (72 °C) is reduced to a minimum. The polymerase enzyme is a heat stable enzyme, and the denaturation temperature is partially inactivated by the polymerase enzyme and then a fine balance between enzyme inactivation and template denaturation is established. Consequently, batch-to-batch variation of the polymerase enzyme is a substantial factor in this process. The highest activity of these enzymes should be present during the last cycles of the reaction process, as the largest amount of template is present at this stage of the PCR process, but the enzyme in this stage is already losing activity, which may lead to enzyme depletion and a considerable decrease in or even lack of yield. The annealing step is also a heat sensitive process, as the time and temperature are important to optimizing the signal to minimize non-specific binding of primers to the template (Zhang *et al*, 2006)

A major factor inhibiting the reproducibility and comparability of PCR results is a temperature control over the PCR phases. The PCR system must be designed carefully and applied only after correct validation at the desired temperatures. However, the results of temperature performance tests for several brands of thermal cyclers show that most cyclers do not perform within the manufacturers` specifications (Xiang, Xu, and Li, 2007).

The laboratory-based study of Saunders *et al.* (2001) investigates the effect of thermal cyclers on PCR performance. The measured inter block reproducibility and intra block repeatability shows that temperature-calibrated instruments consistently

generated more repeatable rapid data than non-calibrated instruments, regardless of the make and model of a thermal cycler. Consequently, the thermal cycler's correct temperature setup is a vital factor in the PCR results and the use of one block for heating and cooling between the PCR steps. The overview of our results shows that the given cycling speed of the tested thermal cyclers presented some distortion in their temperature profiles. Ideally, the reaction temperature should change in a linear manner until it reaches a specific step in the PCR and remain constant during the step, as has been described [1.3.1].

As can be seen in the curve Figure 3.11 of the Rotorgene thermal cycler, the system was agitated to 120.7 °C before reaching stability at 95 °C. In addition, it is not stabilised at this point for 10 seconds, as was programmed, but there was a clear variation in range between 95.4 °C to 97 °C. In the extension step the target temperature is 72 °C, but in the measured profile the temperature was raised to 88.1 °C before it started to stabilise in a range between 73.9 °C to 71.8 °C. Therefore, effective step lengths were substantially shorter than the programmed value in the rapid cycling mode. As can be seen from the graphs the GeneAMP thermal cycler, the temperature profile was more stable than the other thermal cyclers. This system was calibrated last July 2009; however, it seems to be increasing or decreasing towards the target temperature as it takes 46.5 second to cool from 96.51 °C to 61 °C and 12.5 seconds to raise the temperature from 61.1 °C to 72.9 °C.

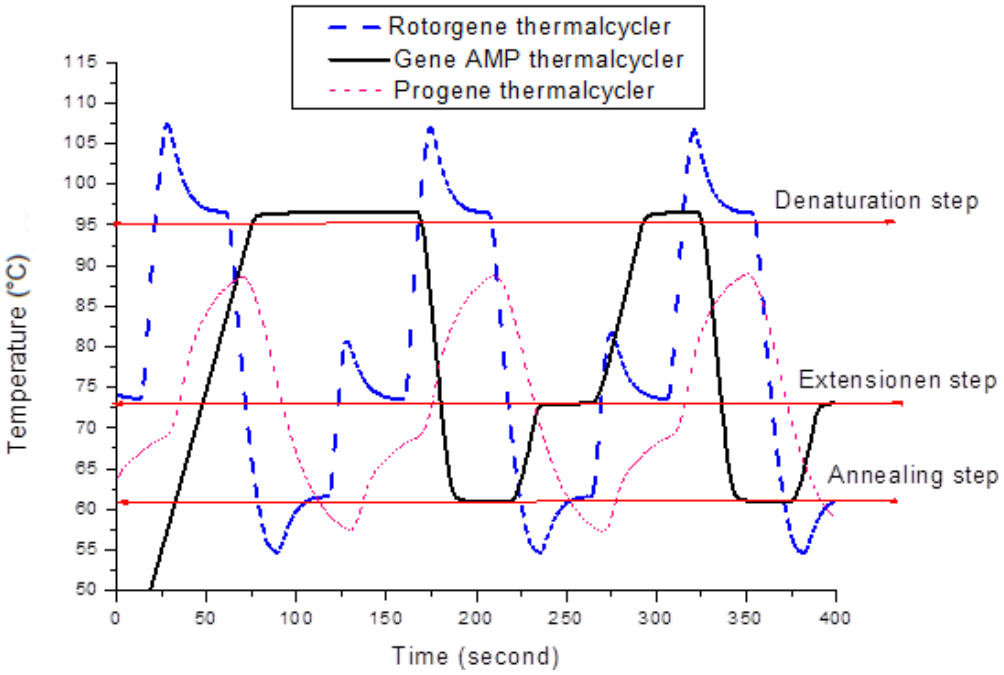

Figure 3.11 Comparison graphs obtained from the study of the different types of thermal cyclers.

The optimum temperature profile for the models with relatively slow ramping rates i.e. the heating and cooling rate of the system slowed the reaction process, as the block needed time to reach the target temperature, as in (GeneAMP), whereas the models of fast ramping rates in the Rotorgene model tended to produce overshooting Figure 3.11.

3.2.3 Thermal-cycler prototype design

According to the classification of microfluidics-PCR models, a shunting-PCR model is the most similar model to the proposed design, as it has been discussed [2.2] , Table 2.1. Hence, the discussion here will be focused on the comparison between the proposed design and shunting PCR-on-a-chip models.

Cheng *et al*, (2005) developed a temperature cycling method for performing temperature cycling reactions in laser-etched in poly (methylmethacrylate) (PMMA) microfluidic chips, as can be seen in Figure 3.12. The developed microfluidic chip is circular in shape and is clamped in contact with a circular heater chip of an equivalent diameter. The heater is fabricated from transparent indium tin oxide coated glass (ITO).In this study the PCR reagents shunted in between the three temperature zones by a syringe plug, which could be positioned in the desired temperature zone of the microchannel by controlling the position of the syringe piston. The plug could then be shuttled back and forth between the desired temperature locations by varying the syringe pressure appropriately.

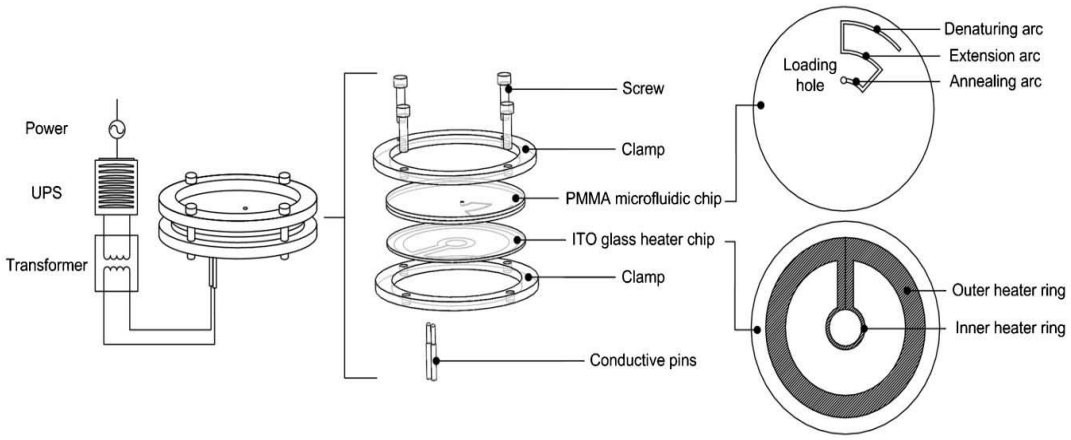

Figure 3.12 Microfluidic system setup showing assembly of microfluidic chip and heater chip. The two chips are clamped together and secured by screws. All components other than the glass chip and the conductive pins are made of plastic. The heater chip is fabricated from ITO-coated glass.The shaded area denotes the energized strips used for heating. The microfluidic chip is fabricated from PMMA. Note that only one opening exists. The radius for both chips is 85 mm **(**Cheng *et al*, 2005).

This model exhibits rapid temperature ramping rate ~4.5 °C/second. However, the challenge in this model is automation because the heater must be a multiple in similar numbers to the sample channel. Moreover, the sample in this model is pumped through a fine channel in size of ~80 mm. These processes cannot guarantee the shuttling of the whole sample amount to the right desired temperature range. This problem is inherited from the continuous-flow model, which has been discussed [2.5.1]. If this model is compared with the proposed model, the proposed design is better in terms of multiplication of sample chamber and device handling. This is because the samples are introduced in individual chambers and cycled in between stationary temperature zones. In addition, potentially, the samples can be automated by a centrifugal disc, which can be used to measure and distribute the liquid from a main reservoir Kong and Salin (2010).

As it has been discussed [2.5.2] (Giordano *et al*, 2001) miniaturised a thermal-cycler using an infrared-mediated (IR) temperature controller and a PCR reaction chamber in a microchip fabricated from polyimide. This chamber was formed by laser ablation technique. A 150 µm thick sheet of polyimide is sandwiched between two additional layers of (125 µm thick), one of which contains two laser-ablated ports, to produce a 150 µm deep chamber with total chamber volume of 1.7 µL. The most important development in this model is applying IR thermal-cycler design. The IR enhances temperature reproducibility and this generates an efficient DNA amplification within 15 cycles only compared to 35 cycles in the conventional method. The model demonstrates a x lack of portability and further problems related with the sample accommodation inside the sample chamber. Furthermore, the system is not suitable for online detection or real-time PCR as the use of IR interferes with online fluorescence detection. The proposed design is made from low cost materials so refining this design potentially improves the efficiency of the amplification process because if the sample chamber is cycled in precise temperature zones, the DNA amplification will be improved.

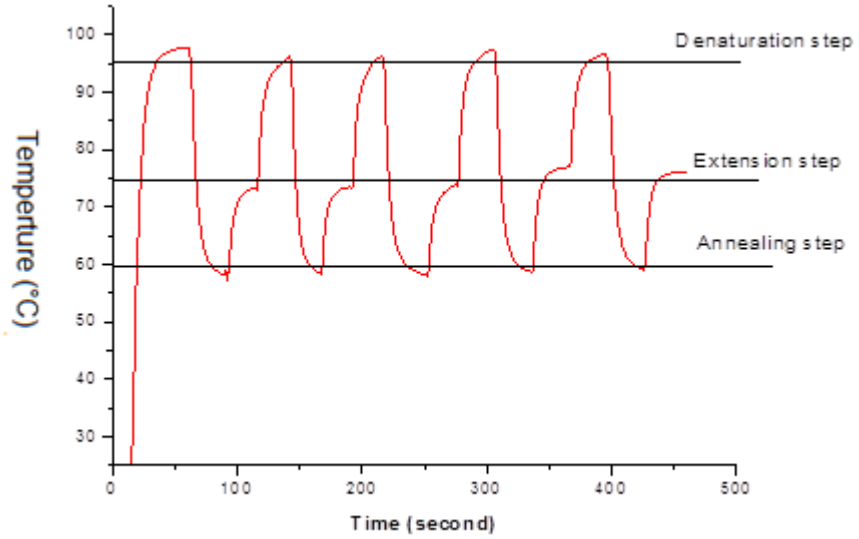

Figure 3.13 View of three amplification cycles on the second prototype thermal-cycler device. Thermal cycling profile demonstrates excellent heating and cooling rates Each cycle of PCR can be completed in 60 second (10 sec denature, 20 sec anneal, 30 sec extend) **.**The temperature inside the reaction chamber were measured using a sensing probe, ultra thin high tolerance thermister (Rapid Electronics) and data were collected by data-logger (Pico Technology ADC-24). The results obtained are demonstrated in the graph.

As has been discussed [2.5], Fery *et al*, (2007); Wang *et al*, (2009) and Chung, Park, and Choi (2010) presented the most impressive models of shunting PCR-on-a-chip. The thermal-cyclers of these models were constructed in a similar way as the proposed design. However, the proposed model improved in slotting the sample chamber in between two identical temperatures control plates, which boosted the temperature ramping rate and reproducibility of the temperature-working zone.

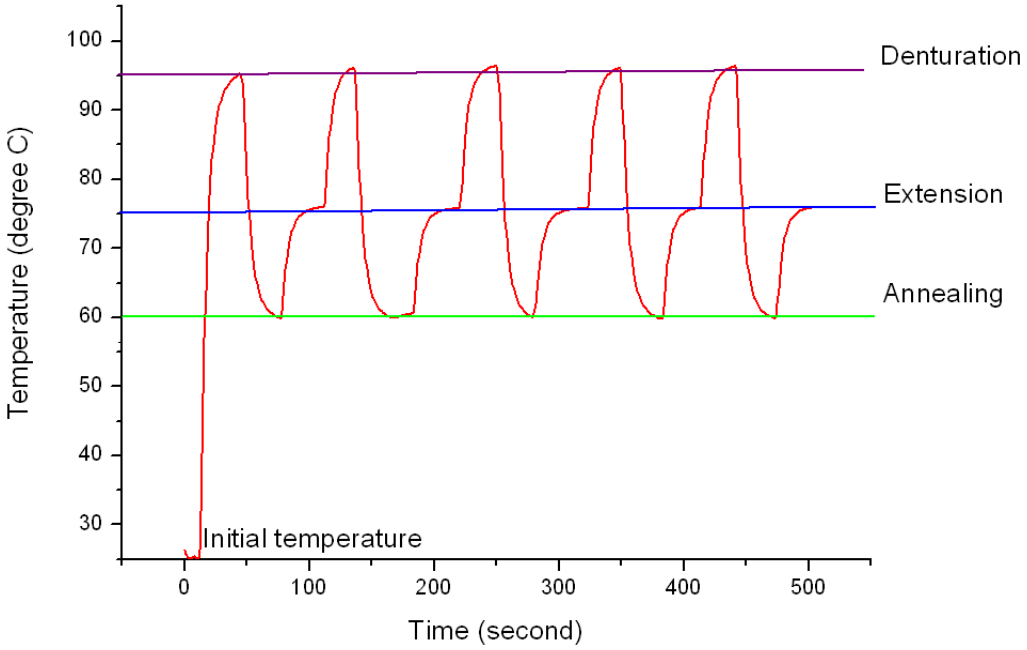

Figure 3.14 View of three amplification cycles on the third prototype thermal-cycler device. Thermal cycling profile demonstrates excellent heating and cooling rates and great uniformity. Each cycle of PCR can be completed in 60 second (10 sec denature, 20 sec anneal, 30 sec extend) .The temperature inside the reaction chamber were measured using a sensing probe, ultra thin high tolerance thermister (Rapid Electronics) and data were collected by data-logger (Pico Technology ADC-24). The results obtained are demonstrated in the graph.

Table 3.2 summarize the similarity and the differences between the proposed design and the other published designs.

#	Description of the design	The Similarity	The difference
1	Reagents shuttling in micro-channel along temperature gradient (Cheng *et al*, 2005)	The system compressed three temperature zones.	The PCR reagents pumped in "S" shape loop of microchannel and cycled back and forth using syringe control.
2	Autonomous microfluidic multi-channel chip for re-l time PCR (Frey *et al*, 2007)	Three constant heaters allocated for three temperature zones.	-The whole device is disposable. -The sample is shuttled inside a micro-channel by pneumatic actuation system.
3	A circular ferrofluid driven micro-chip (Sun, Kwok, and Nguyen ,2007)	Three temperature zones are arranged in circular shape.	The sample is placed in circular micro-channel and travelled through three temperature zones by an external magnet, which was used to drive a small ferrofluid plug inside the circular micro-channel.
4	PCR system operated using thermosiphon effect (Cheng *et al.* 2005)	The system compressed three temperature zones.	The PCR reagents are cycled using conviction effect along a triangular closed loop channel.
5	The flow-through PCR chip (Wang *et al*, 2009)	Three zones micro-chambers.	A pneumatic micropump was used to precisely drive the sample flowing through three reaction chambers.

3.3 Chip fabrication

3.3.1 Materials and method

As has been discussed [2.2], Polycarbonate is a thermoplastic polymer with features such as temperature resistance, impact resistance and optical clarity. Its physical properties includes a melting temperature of 267 °C, glass transition temperature of 150 °C and a molecular weight of 254.3 g/mol. The optical response of PC in the IR spectral region provides information about the bonding structure, as can be seen in Figure 3.15, the electric field of the infrared (IR) beam causes the excitation of the bonding vibrations. It has a high glass transition temperature (Tg ~148.8 C) and can withstand the sustained high temperatures associated with PCR.

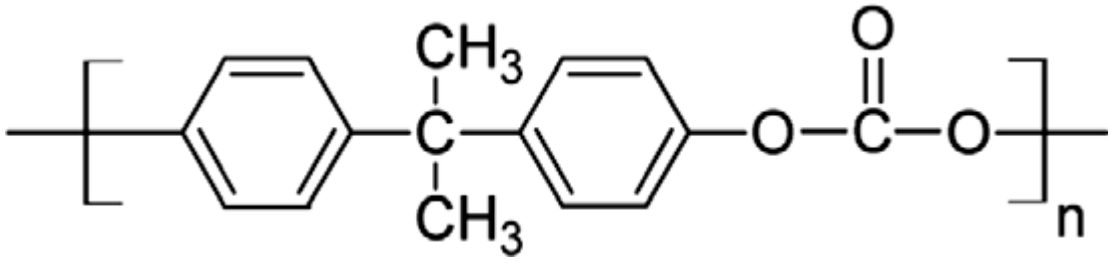

Figure 3.15 The chemical stricture of PC shows the unit molecule of PC that contains two benzene rings and one CO carbonyl group(the structure build on ISIS software and modify by Microsoft paint)

.

In this project a clear polycarbonate sheet of 1 mm thickness and clear 127 μm thickness PC film (The supplier was Professional Plastics, USA) were used for the chip fabrication. The proposed chip mainly consisted of two chambers connected by a channel; the design is illustrated in Figure 3.16. The first chamber opened from one side and worked as a supplier cavity. The channel served as a two-way pressure control valve, which connected the supplier cavity with an individual sample chamber as can be seen in Figure. 3.16**.** The first chamber contained an injection port and was called a reservoir chamber, whereas the second chamber was a sample chamber.

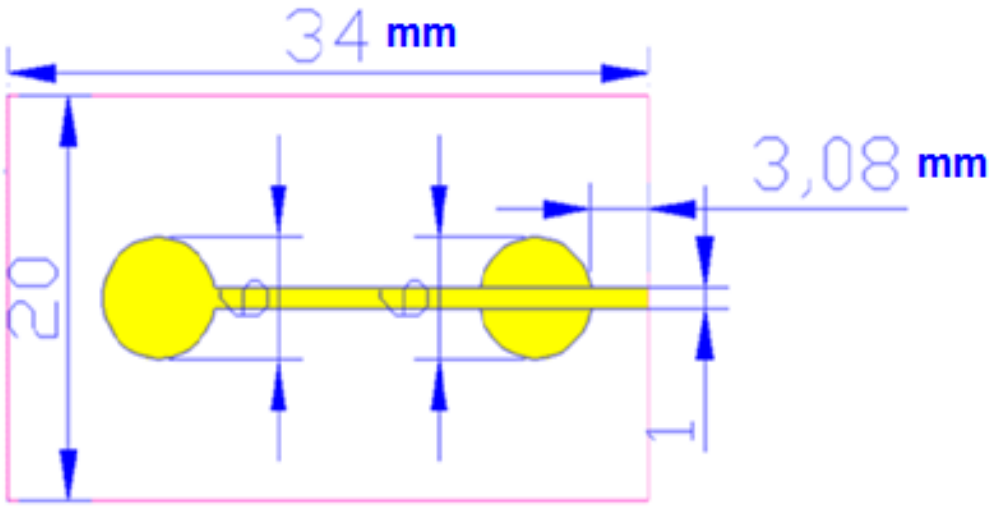

Figure 3.16 AutoCAD diagram illustrates the chip design and all the dimensions of the chip features, unit measurement is millimetre for all. All measurements unit used in millimetres (mm).

The PCR chip consisted of three layers: two polycarbonate films, thickness 127 µm (0.127 mm) sandwiched a polycarbonate slide, thickness 1000 µm (1 mm). The PC slide contained a pattern of wells and channel Figure 3.17 and 3.18, and the wells and channel held the samples in close proximity while preventing cross contamination. The PC parts were well cleaned, prior to use, by soaking them with decon 90. Then they were rinsed by distilled water before being sonicated in distilled water for 10 minutes to remove any decon 90 residues, which inhibit bonding.

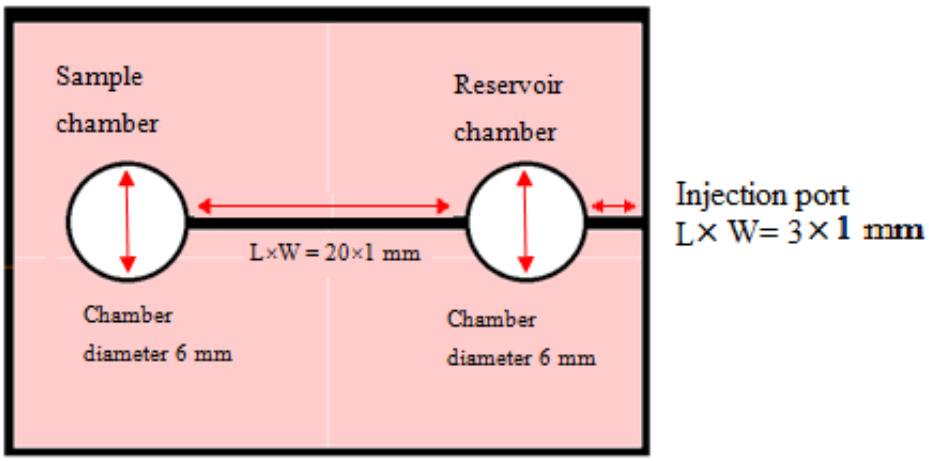

Figure 3.17 Schematic diagram of the proposed chip made from polycarbonate sheet of 1.0 mm thickness covered by thin polycarbonate film of 127 µm thickness.

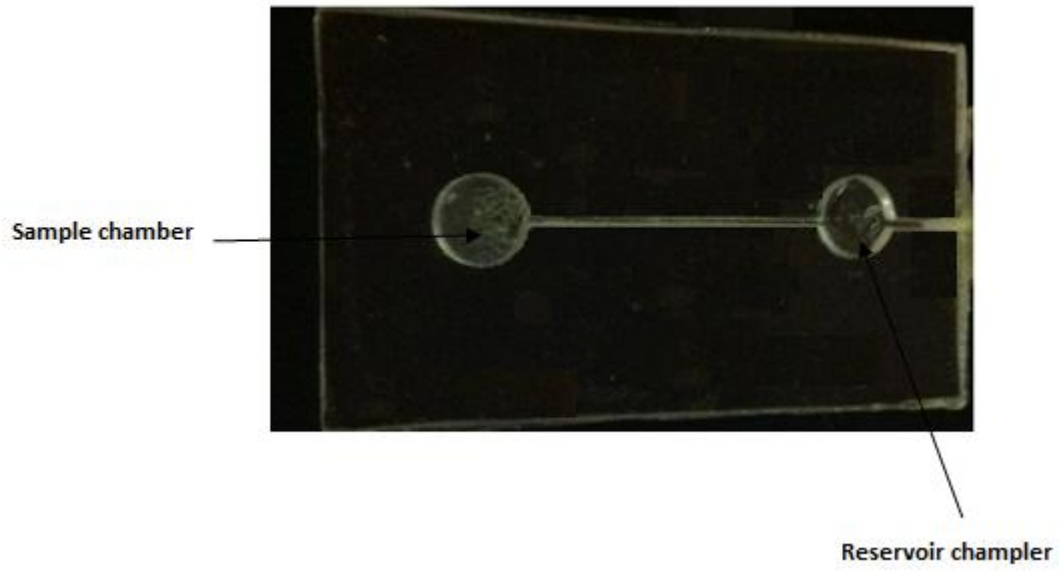

Figure 3.18 The chip being used in the final shape

Finally, the pieces were soaked by isopropan-2-ol (Analar grade, BDH) to ensure clear surfaces. Then the parts were placed in the oven at 105 °C for at least 2 hours to dry. The three pieces were placed in the oven at 165 °C for two hours under pressure of 12.5 kg weight, which apply a pressure of 245 Pascal .This temperature is over the transition temperature of polycarbonate (148 °C) and the pressure is enough to increase bonding strength and conserve the structure of the chip. After two hours, the temperature diminished by 10 degree centigrade gradually every 15 minutes in anticipation of room temperature. The bonding steps are lustrated in the schematic chart Figure 3.19.

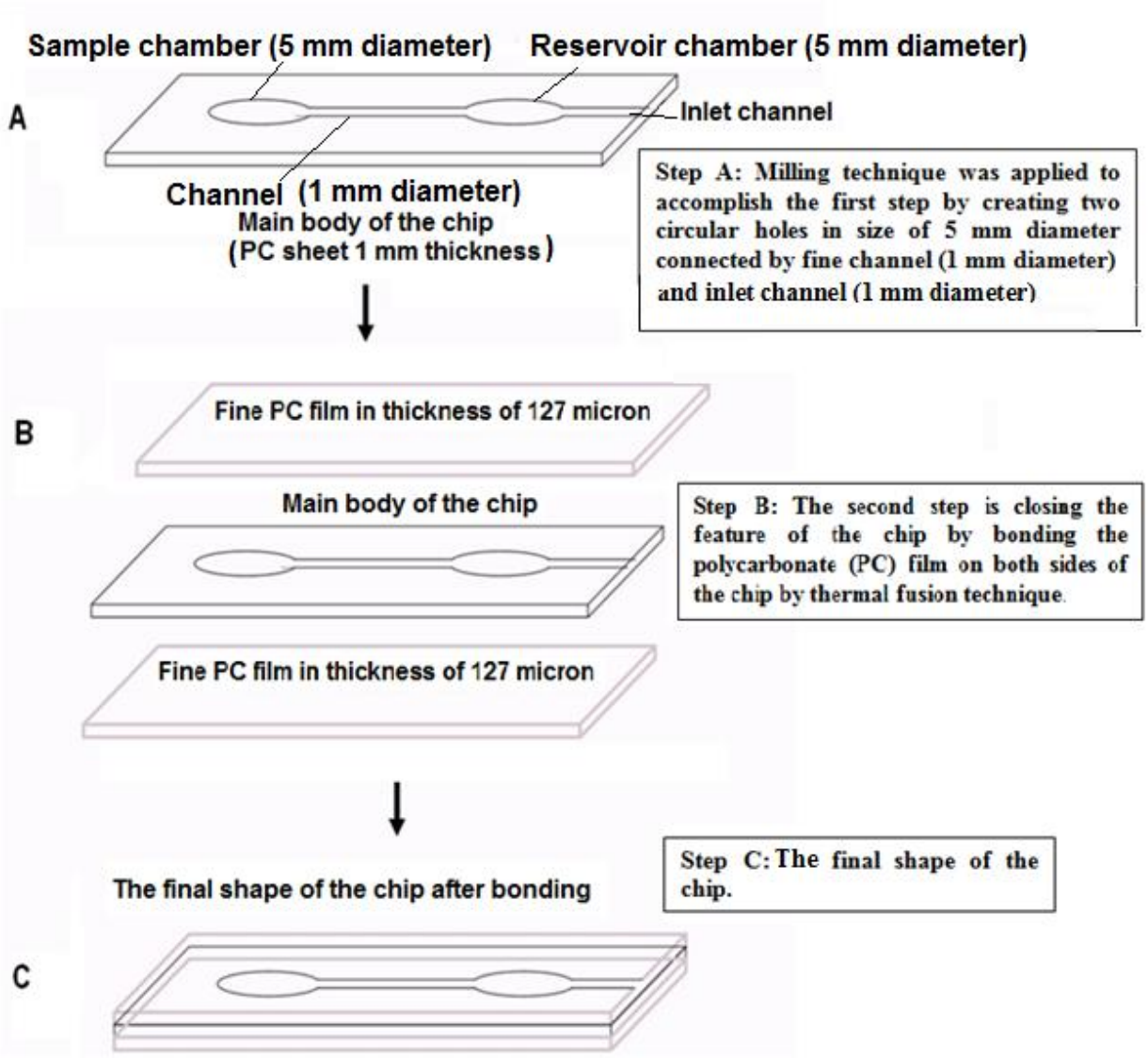

Figure 3.19 Schematic of fabrication process for thermal-fusion bonding method (A) 1 mm thick PC slide contains the chambers and channel as in (B) The stricture slide placed in between two thin PC film. (C) the shape of the chip after bonding**.**

3.3.2 Results and discussion

Increasing surface to volume ratio (SVR) is an important physical phenomenon in microfluidic devices, which is an advantage in many cases due to rapid heat transport and faster reactions related to surface chemistry. In the PCR process, the reaction is restricted to the bulk liquid and a high SVR will be a challenge due to an increased probability of interaction between the biochemical components and the surrounding surfaces. The complex nature of a PCR mixture enhances the possibility of interaction between the surface of the reaction chamber and at least one of the PCR components. This process has a detrimental effect on PCR performance because binding of PCR components to the surface will alter the optimized concentrations of the PCR components. An interaction with the surface can impede the biochemical components and slow down or inhibit the reaction (Christensen *et al,* 2007).

The reaction chamber made by Jia *et al* (2007) was fabricated in a planar format. He formulated a PCR card that contains three layers of saturated polycarbonate (PC) film in between a polypropylene (PP) film and aluminium foil. This model shows a potential attainment in terms of a heat transfer study. An aluminium film chamber is a high-quality option in term of heat transfer but it is not inert to PCR reactions. The main factors controlling the temperature ramping rate, according to the heat transfer law, are chamber size, surface area and a thermal conductivity of the chamber materials

The heat conduction transfer rate per unit area is proportional to the normal temperature gradient:

$$\frac{q}{A} \propto \frac{dT}{dX}$$ **Equation 3.1**

When the proportionality constant is inserted then: (*Fourier's law*)

$$q = -kA \frac{dT}{dX}$$ **Equation 3.2**

Whereas:

Q= the heat transfer rate.

$\frac{dT}{dX}$= the temperature gradient in the direction of the heat flow.

K= the thermal conductivity of the materials the units of watts per meter per degree.

Table 3.3 Outlines the temperature capacity of different types of the proposed materials, which could be used to create the sample chamber.

Material name and Chemical Formula	Molecular mass (g/Mole)	Thermal conductivity (w/mk)	Specific heat capacity(kJ/kg k)
Silicon (Si)	28.0855	83.6073	0.703
Aluminium(Al)	26.98154	220	0.897
PET $C_{10}H_8O_4$	192.17112	0.15-0.4	1
PDMS $Sio(CH_3)_2$	74.15446	0.15	1.46

Different types of chambers have been tested on the device to detect the heating and cooling rate of each chamber. The results will be used as a pilot study to demonstrate the thermal-cycler ability to progress the PCR test profile.

In testing the models of reaction chambers, the thermistor was inserted inside the chamber and the chamber was shunted back and forth between the three temperature zones. The reaction chamber, which made from a fine film of Polyethylene terephthalate (PET) in a thickness of (10 µm), was presented the results shown in Figure 3.20. The results shows that the chamber required 10 seconds to rise from ~40 °C to ~83 °C , 30 seconds to cool from 97 °C to 61 °C and 15 seconds to rise from 60 °C to ~72 °C. However, it takes only 15 seconds to rise from ~72 °C to~ 92 °C. Therefore, the PCR programme being used should accommodate the time difference before the system reaches the desired temperature. For example, a sample should

stay at the denaturising stage for not less than 20 seconds, at the annealing stage for not less than 45 seconds and at the extension stage for not less than 30 seconds. This to in order to guarantee that the sample achieves the correct temperature for at least 15 seconds, which is the absolute best reaction time possible in many PCR applications.

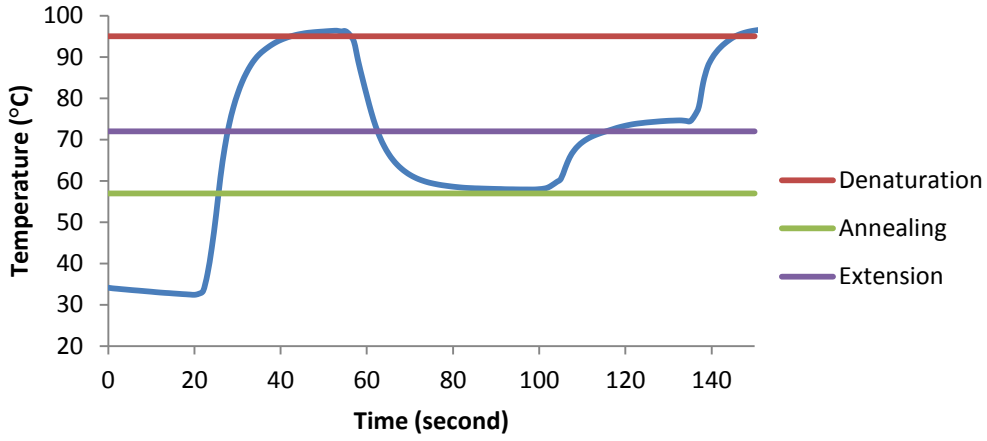

Figure 3.20 Temperature profile of film chamber achieved by our thermal cycler system.

The aluminium chamber as can be seen in Figure 3.21 takes ~9 seconds to rise from ~30 °C to ~90 °C, ~6 seconds to cool from 93 °C to 61 °C and 4 seconds to rise from 60 °C to ~72 °C. However, it expends only ~5 seconds to rise from ~72 °C to~ 92 °C. Therefore, the PCR programme will be shorter in this form of sample chamber.

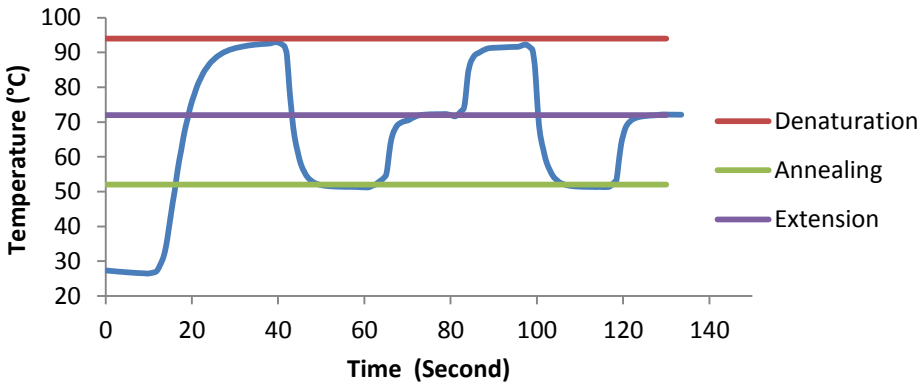

Figure 3.21 Temperature profile of Al and film chamber achieved by our thermal cycler system.

Therefore, the ideal material used to fabricate the PCR chamber must be chemically, mechanically and optically suited to the PCR reaction and the thermal cycler design. Most of the early-miniaturized PCR devices were fabricated in silicon or glass by taking advantage of well-established micro-fabrication technologies. However, glass and silicon is known to be a source of PCR inhibition. Polymeric materials have been explored as more flexible alternatives for the fabrication of microfluidic PCR chambers, especially as the polycarbonate polymer is already adapted to PCR, for example; it is used to generate the conventional Eppendorf tubes. Despite the low thermal diffusivities of polymers, a thin film polymer is promising (Becker and Gartner, 2008). Two researchers have used PET film to produce PCR chambers, as can be deduced from Table 3.2 Zou *et al.*, (2002) and Giordano *et al*, (2001).The complication is related with the fabrication of thin film capsules and using it to perform the PCR process. There are two main problems associated with using the thin films, namely, disclosing the chambers and sample accommodation.

Temperature cycling protocol for DNA amplification can be divided into six segments: three end point temperatures and three temperature transitions. Time spent in transitions is usually wasted, although theoretically a slow transition between annealing and extension may be useful for a poorly annealing primer. The transition time from denaturation to annealing and from extension to denaturation has no function i.e. the faster the better (Wittwer *et al*, 1990).

Denaturation temperature is very important to achieve a successful PCR process as inadequate heating leads to failure in the complete separation of the DNA strands. Moreover, a too high or too low denaturation temperature may lead to an obvious loss of polymerase enzyme activity, which can also reduce the yield of amplified product. The optimum denaturation temperature depends upon the base sequence of the target DNA. If the DNA template is rich in G and C bases, it would require higher temperatures than those having a balanced mix of bases. This is because the hydrogen bonding between G and C bases is stronger than the hydrogen bounding between A and T bases (Harris and Jones, 1997). Typically, an initial denaturation is carried out at 94 °C for 5 minutes and the denaturation step at 94 °C for 45 seconds. This time is not including the heating or cooling time.

At this stage of PCR, the primers anneal to their complementary sequences on target DNA. The optimum annealing temperature depends upon the melt temperature and the base sequence of each primer. It is important that both primers have similar annealing temperatures. The functional annealing temperature is 5 degrees below the melt temperature of the primers used. Theoretically, as in Equation1:

$$\mathrm{T} = \mathrm{Tm} - 5 \ = 2(\mathrm{A} + \mathrm{T}) + 4(\mathrm{G} + \mathrm{C}) - 5 \qquad \textbf{Equation 3.3}$$

Extension of primers on the DNA template is carried out using a thermo stable DNA polymerase enzyme, which is able to synthesis a complimentary copy of the initial stDNA by incorporating of dNTPs available in the reaction. The optimum extension temperature is 72 °C, which seems to be suitable for most applications.

The number of cycles required for best possible amplification depends upon two main factors: the initial concentration of the PCR constituents and the efficiency of each amplification step. In conventional PCR machines, no amplified products are seen when fewer than 20 cycles are performed. The most effective amplification had been seen at 40 cycles. However, increasing the number of cycles to 50 or 60 cycles could lead to amplification of specific and nonspecific products (Harris and Jones, 1997).

Therefore, decreasing the heat competence of the cycling system can clearly decrease the total time required for PCR. Furthermore, decreasing the denaturation and annealing steps should theoretically reduce nonspecific amplification and polymerase inactivation. Fast DNA amplification is achieved by the system produced because it significantly improves the ramping rate of heating and cooling the PCR mixture.

The temperature increased from ~47 °C to ~92 °C in the rate of 1.0 degree per second and decreased from ~92 °C to 60 °C in the rate of ~1.8 degree per second. The temperature rose from 60 °C to 72 °C and from 72 °C to 92 °C in the rate of 2.0

degree per second Figure 3.22. Consequently, initial denaturation stage required at least 2 minutes to ensure complete denaturation of dsDNA and adding10 seconds in each step would be enough for the PCR mixture to attain the desire temperature.

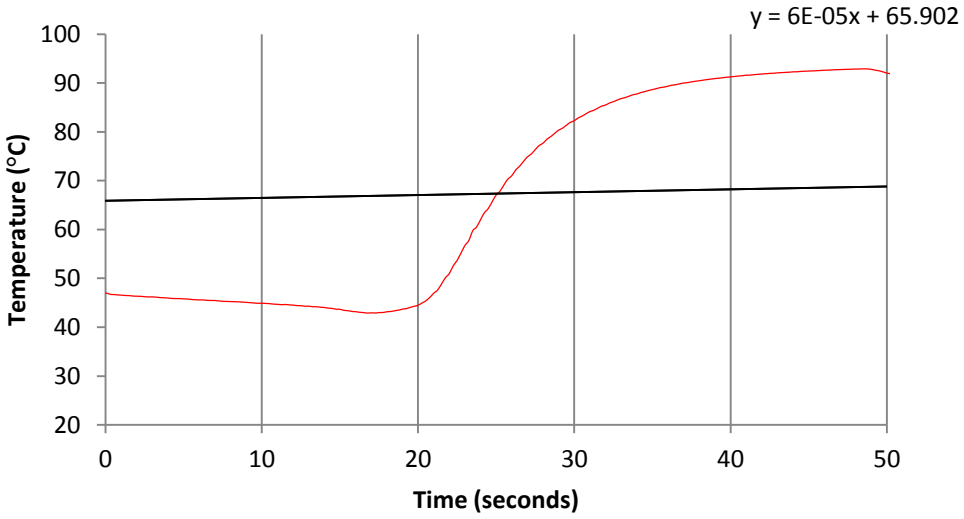

Figure 3.22 This illustrates the progress of temperature heated in denturation step inside the chip.

In reference to the discussion in the literature review (chapter two), the comparison between the prototype sample-chamber and other sample-chamber already published summarized in Table 3.4:

Table 3.4 Comparison between the features of the prototype chip and the other micro-chips models published.

Chamber-body materials	Fabrication method	Sample volume	Chamber size	Heating rate and Cooling rate (°C/ second)	Reference
Glass	Wet etching.	200 n L	36 µm depth	20 °C/s	Lagally *et al*, 2001
Teflon tube.	Custom-made tube.	24 µL	0.8 mm internal diameter.	Heating rate 3 °C/s Cooling rate 1.6 ° C/s.	Bruckner *et al*, 2002
Silicon/PET	Silicon moulding bounded with PET using thermal forming.	20 µL	400 µm depth.	Heating rate 34-50 °C/s Cooling rate 23-31 °C/s.	*Zou et al*, 2002
Glass/PDMS	soft-lithography	1.75 µL	L×W×D 10 mm× 20 µm × 50µm	4.5 °C/s	Prakash *et al*, 2007.(Cheng *et al*. 2005)
PMMA	laser ablation	4.5 µL	Capillary loop of 70 mm , 1.2 mm width and 0.6 mm depth.	~ 10 °C/s	Cheng *et al*, 2005
Glass/Teflon	Photolithography	15 µL	Droplet	Heating rate 38 °C/s Cooling rate 7.9 °C/s	Chang *et al*, 2006
PC/PP and Al	Thermal sealing	25 µL	28 mm × 3mm × 0.25 mm	10 °C/s.	Jia *et al*, 2007
PDMS	Casting and oxygen-plasma bounding	125 nL	50 µm	0.1 s required to transfer the sample from one zone to another.	Frey *et al*, 2007
PMMA	laser ablation	2 µL	62.8 mm length channel with a diameter of 20 mm	~ 12 °C/s (PCR achieved in 9 second for each zone)	Sun *et al*, 2007
Polymer microchip.	Custom-made chip.	7 µL	500 µm depth and 1 mm width.	Heating rate 14.8 °C/s Cooling rate 15.4 °C/s.	Giese *et al*, 2009
PDMS	Casting	22 µL	A diameter of 5 mm	Inevitable	Wang *et al*, 2009
Polycarbonate(PC)	Injection moulding	40 µL	10 mm length of each zone and the loop diameter is 1 mm.	8.7 °C/s.	Chung *et al*, 2010
Polycarbonate(PC)	Thermal forming	25 µL	Circular chamber with a diameter of 6 mm	Heating rate of 1.8 °C/s Cooling rate of 2 °C/s	Prototype chamber

* Poly(methyl methacralate) (PMMA)
* Polycarbonate (PC)
* Poly Tetrafluoroethlene (PTFE)
* Polyethylene terephthalate (PET)
* Cycloolefine /copolymer (COC)
* Polypropylene (PP)
* Poly(dimethylsiloxane) (PDMS

3.4 Conclusion

The driving force behind the increasing development of miniaturized PCR thermal cycler system is certainly due to their potential commercialization, but the challenge is the production of practical higher performance and throughput design. In this project a novel thermal-cycler design of double-sides, heaters were investigated. The proposed design based on constructing three thermal isolated zones to regulate the heat transfer across the sample chamber. In progress of the proposed design, three formats of double-sides heaters were constructed and tested. Compared with the conventional gradient PCR machine, the proposed system has several obvious advantages including, simple, inexpensive, faster amplification rate, easy operation and portable. Along with the thermal-cycler structure, a fine polycarbonate chip was fabricated. A fine disposable PCR chip was developed in this work for rapid DNA amplification. The fabricated chip, which includes the sample chamber, was used to perform thermal cycling. The body of the chip was built using polycarbonate (PC) sheet (1-mm thickness) and film (127-micron thickness). The polycarbonate film was laminated with a structured card (made from 1 mm thick polycarbonate sheet) by taking advantage of the thermal binding between the PC of the sheet PC film. The PCR reactor was experimentally characterized by using thin thermistor. The time consumption for amplification is low and the temperature-increased rate is 1.0 degree per second and decreased in the rate of ~2.0 degree per second. In addition, power consumption of the proposed thermal-cycler is small, and the device is capable of being integrated in battery supplied portable compact analysis or diagnostic systems. The device is practically portable and affordable for pathogen diagnostics.The proposed device will be integrated real time PCR system with florescence detection.

Chapter 4 Detection system

4.0 Introduction

In this chapter, the prototype fluorescence detection unit used for DNA detection will be described and discussed based on the experiments carried out on the system. The prototype design and the optimisation steps of the detection system will be discussed. A spectrometer (HR4000, ocean optics, USA) was used as control spectrometer to evaluate the efficiency of the prototype photo-detector. Finally, the DNA and PCR measurements on the system will be examined by verifying the results with available standard fluorescence technique.

4.1 Theoretical background

4.1.1 Fluorescence spectroscopy

Fluorescence spectroscopy is a highly sensitive technique for the quantitative detection of suitable species, with limits of detection in the parts per trillion (ppt) being reported for state of the art measurements. For this reason, fluorescence is widely used in many applications, such as: immunodiagnostics, optical microscopy, chromatography, electrophoresis, real time PCR and DNA sequencing. In chemical molecules, each electronic state has several associated vibration states. In the ground electronic state, almost all electrons occupy the lowest electronic state. However, if the molecules were excited by a particular light source or temperature, the electrons were promoted to the higher electronic shell or vibration state (Schulman, 1985).

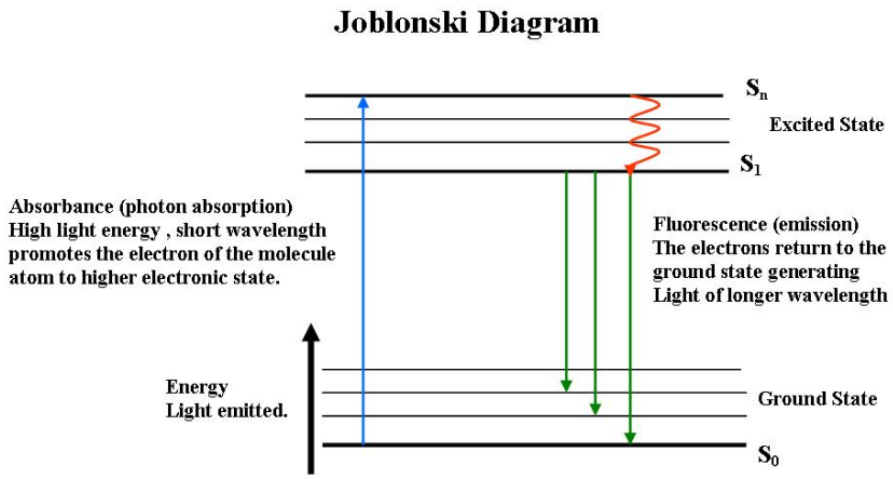

Figure 4.1 Jablonski diagram illustrating the excitation and emission is taken place inside the nucleus of the fluorophore molecule. Fluorescence results from the absorption of light energy by fluorophore molecule at a specific wavelength and re-emitted at longer wavelength and lower energy. The difference in wavelength is called stokes shift. This process occur at time between ($1^{-1}0x10^{-8}$ second) and is called fluorophore lifetime.

Fluorescence is the emission, which results from the return of the electron to the singlet ground state. This phenomenon is known as "chemiluminescence" and the chemical compounds emitting fluorescence known as "fluorophores". The benefit of fluorescence is that can be used to quantify chemical compounds. Fundamentally, the absorption of light by the fluorophores excites electrons to the higher energy level (higher unstable state). The electron then remains in this level for a very short time, 10^{-8} to 10^{-7} seconds. Eventually the fluorophore molecule returns to the ground state following the emission of a photon with lower energy level hence longer wavelength. The wavelength and the amount of light absorbed and emitted are known as the fluorescence signature. The difference in the light wavelength between the absorption and emission is termed the Stokes shift. The fluorescence analysis can be quantified by defining the amount of energy falling upon a defined area (measured in square metre m^2) within a defined wavelength region, which can be measured in nano-meter (nm) (Bustin, 2004).

Molecules of certain compounds known as fluorophores can absorb light at a defined wavelength and almost instantaneously re-emit the light at a longer wavelength or lower energy.

However, as in any optical measurements, the fluorescence detection signals are not steady. This is due to low frequency optical interference and low frequency noise.

The problem is solved by using an intensity modulated optical source and a lock-in detection system. Modulating the source shifts the measuring signal up the frequency spectrum and away from the low frequency noise. A lock-in amplifier is then used to recover the signal while removing the noise and interference.

Lock-in measurements require a frequency reference. Typically, an experiment is done by exciting the light at a fixed frequency (from an oscillator or function generator) and the lock-in detects the response from the experiment at the reference frequency (Dorrington and Künnemeyer, 2002).

The temperature of the experiment can affect the fluorescence efficiency of the fluorophore because a raised temperature can increase the collision relaxation of the molecules (Skoog *et al*, 2004).

4.1.2 Fluorescence and DNA detection

DNA binding dyes, such as SYBR Green I, are fluorophore compounds. They are, in general, heterocyclic or polyaromatic hydrocarbons, characterised by conjugated double bounds and rigid in their structure, as can be seen in the structure of SYBR Green I (Figure 4.2).

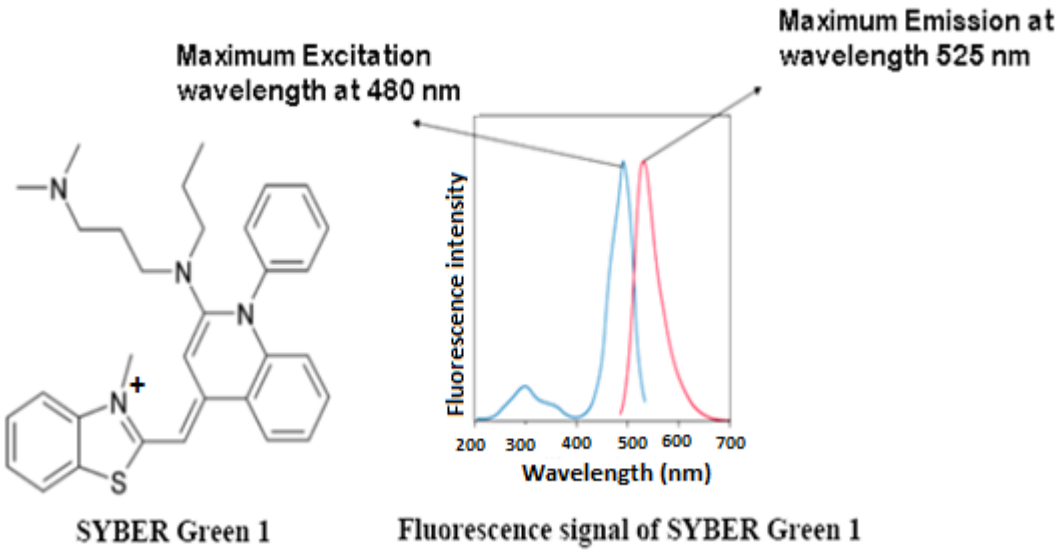

Figure 4.2 The left side of the picture illustrates the chemical structure SYBR Green 1 (Draw using ISIS software).and the right side illustrates the excitation peak (blue) of SYBR Green 1 at 480 nm and the emission peak (red) at 525 nm (Bustin, 2004).

The fluorescence efficiency of these compounds depends on their ability to absorb and emit photons. The absorption efficiency of the fluorophores, expressed as an extinction coefficient (e), represents the energy captured by one mole of the dye. The range of most available dyes is in between 10,000 to 250,000 $cm^{-1}M^{-1}$. The emission efficiency is expressed by the quantum yield (Φ) which is defined as the ratio of the number of photons emitted to the number of photons absorbed by the dye (Bustin, 2004).

The fluorophore in free buffer solutions, such as SYBR Green 1, displays relatively low fluorescence but when bound to dsDNA its fluorescence increases over 1000-fold (Bustin, 2004). The more dsDNA present, the more binding sites there are for the dye, so fluorescence increases proportionately to DNA concentration. This property of the dye provides the mechanism that allows it to be used to determine the nucleic acids concentrations and to track the accumulation of PCR product. As the target is amplified, the increasing concentration of double stranded DNA in the solution can be directly measured by the increase in the fluorescence signal (Figure 4.3). Compared to probe-based methods, SYBR Green I assays are relatively easy to design and optimize (Bustin, 2004). All the previous aspects are necessary to design a set of primers, optimize the amplification efficiency and specificity. These factors makes SYBR Green I a common choice for optimizing.

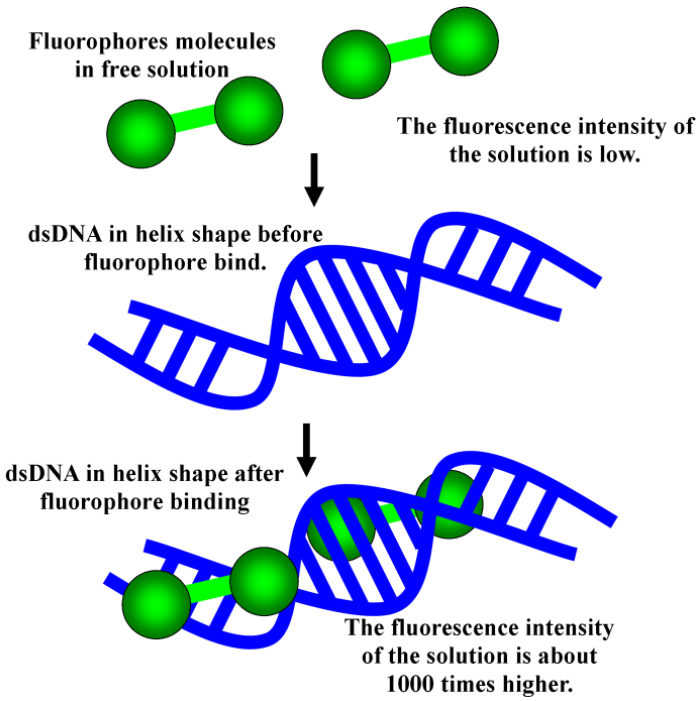

Figure 4.3 Mechanism of fluorophore reaction to the dsDNA molecules. The binding of the fluorophore molecules to dsDNA enhance the fluorescence intensity of the solution and can be easily detected by the fluorometers.

Absolute real-time PCR is a quantitative PCR method for the determination of concentration of PCR templates such as DNA in a PCR reaction. The key aspect of this technique, in particular, is a determination of the reaction cycle that gives a significant fluorescence signal called the cycle threshold (CT). The signal intersects with all the PCR amplification curves during their exponential phases. This signal is proportional to the concentration of amplified nucleic acid as can be seen Figure 4.4. This information can be used to quantify initial copy number based on threshold cycle (Ct) i.e. the fluorescence signal is proportional to the concentration of amplified nucleic acid (Higuchi *et al*, 1993)**.**

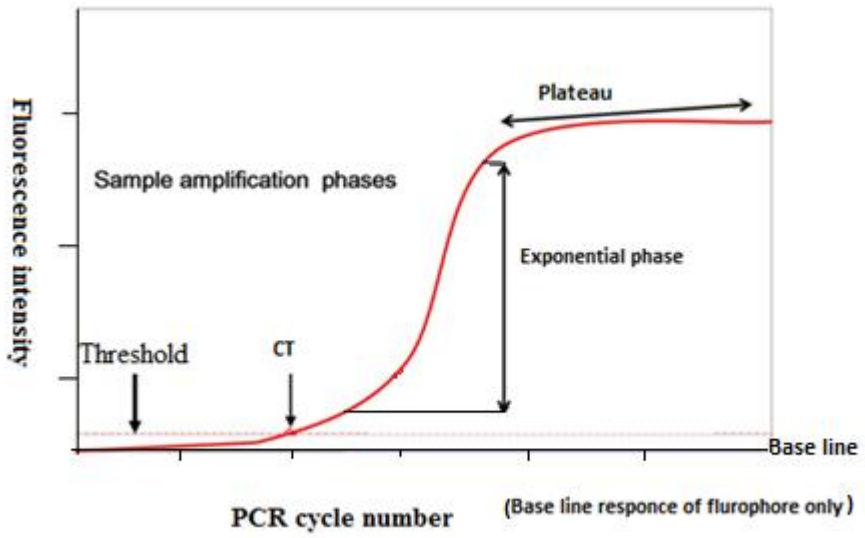

Figure 4.4 The graph shows the ideal progress of real time PCR detection expressed by fluorescence data when fluorophore was used. As can be seen the significant amplification is started at the threshold point and then the exponential phase proceeding until plateau phase, which indicate the enzyme exploding in this phase of process.

The technique depends upon the incubation of a suitable fluorophore compound in a PCR reaction mixture that was cycled between three temperatures. During each thermal cycle, the amount of targeted DNA fragment is approximately doubled. The fluorescence probe is used to monitor the reaction and each amplified strand causes a fluorescence probe to increase its fluorescence output. After several cycles, a sample-containing target DNA will produce a florescence signal that can be distinguished from a base line signal. There are two types of real-time-PCR: probe-based and intercalation-based. Both methods require a special thermocycler equipped with a sensitive camera that monitors the fluorescence in each well at frequent intervals during the PCR Reaction (Bustin, 2004).

For most miniaturized quantitative-PCR detection systems with stationary or flow-through chips, bench-top light sources including large lasers and mercury lamps were commonly adopted to excite the labelling dyes or probes. In addition, microscope-based charge-coupled-device (CCD) cameras or other optical sensing instruments were used to accomplish the fluorescence detections. Compared to these large systems with high power requirements, compact excitation sources (light emitting diodes, LED) and optical sensors (photodiodes and photomultiplier tubes) have been used to perform the fluorescence detection. For instance, a fluorescence detection system was incorporated with a capillary PCR system for on-line detection

of PCR products (Lee *et al*, 2004). Even though these micro systems can perform nucleic acid amplification and detection on a single chip, it still requires a relatively complicated process to integrate these devices.

4.2 Materials and methods

4.2.1 Design of the system

The optical system (Figure 4.5) has three functions: focusing the incoming excitation beam onto the reaction chamber, filtering of the excitation light and collection of fluorescent light.

1) Excitation

The goal is to direct (focussing needs a lens) the excitation light by means of a cylindrical tube onto a small vertical line in the centre of the reaction chamber (Figure 4.5). The excitation light, with a wavelength of 480 nm, is directly brought to the reaction chamber, which is placed as close as possible to the excitation unit. The incoming light is propagated through the 1 mm side of the reaction chamber at the position of the centre of the reaction chamber. As mentioned before, the reaction chamber substrate is made from 1 mm transparency polycarbonate. The blue LED used was type LUMILEDS - LXHL-NB98 Farnell -UK)

2) Fluorescence

The setup implemented for fluorescence was an orthogonal setup, as can be seen in the Figure 4.5, meaning that the direction in which fluorescence is collected and the direction of the light path of the excitation are perpendicular to each other. At the surface of the chip, light rays will be reflected by means of total internal reflection and they will propagate back through the reaction chamber, while the fluorescence will be collected by the fibre optic toward the detector. Stray excitation rays are reduced by means of the dichroic filter, which is situated on the top face of the reaction chamber. The distance between the fibre optic connector and the surface of the chip is fixed at 2 mm; this is to ensure easy access to the chips for the measurements and to minimise the interference of the excitation rays. A black hard paper was placed underneath the chip in order to minimise the effect of the excitation

light. This arrangement guarantees that the detector will collect most of the emitted light.

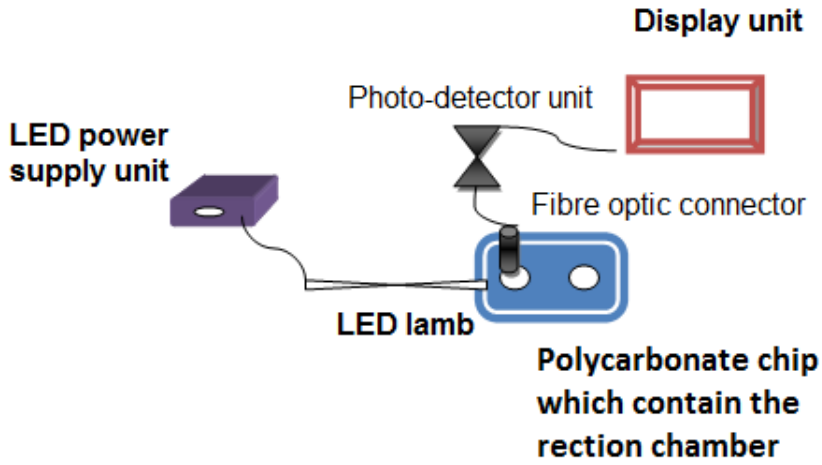

Figure 4.5 A schematic diagram illustrating the experimental setup to measure the fluorescence intensity in the prototype chip. The diagram shows the orthogonal fluorescence detection setup, which provides a geometrical separation of excitation light and fluorescence emission.

The system is controlled by the following options:

1) Light Source Power: the LED power supply unit controls the excitation intensity, which will grow with increasing power. Excitation light intensity will increase with the rating of the LED power. In addition, emission light intensity will be increased by increasing the power.
2) Light Source Focus: excitation intensity will increase with optimized focus of the position of the LED lamp.
3) Alignment: the light path within the chip can be optimized and fixed at the optimum position for the following measurements.
4) Optical Integrity: optical filters become cloudy with use so their replacement may improve excitation intensity.

4.2.2 *In-situ* Photo-detector

The photo-detectors work by converting the light energy to an electrical signal. A selective photodiode detector and a dichroic filter help to detect only the desired wavelength of light. The prototype photo-detector as illustrated in Figure 4.6 is a lock-in system which consists of three main parts: an analogue to digital converter

(ADC) DDC112 (Texas Instruments Inc., Dallas TX, USA); photodiode detector (ODD-525W (OPTO Diode Corp., California, USA) and blue LED as a fluorescence excitation source (DS23) from (Lumileds Lighting, U.S.A). This ADC has a current integrating input capable of single bit resolution as low as 94 fA which is ideal for sampling low level photo-detector outputs, and automatically provides the accumulation process. It also has a 20 bit resolution providing a wide dynamic range useful for sampling low level optical signals in the presence of relatively high ambient light levels. Charge integration is continuous as each input uses two integrators; while one is being digitised, the other is integrating. For each of its two inputs, the DDC112 combines current-to voltage conversion, continuous integration, programmable full-scale range, A/D conversion, and digital filtering to achieve a precision, wide dynamic range digital result. In addition to the internal programmable full-scale ranges, external integrating capacitors allow an additional user-settable full-scale range of up to 1000pC (data sheet from Texas Instruments).

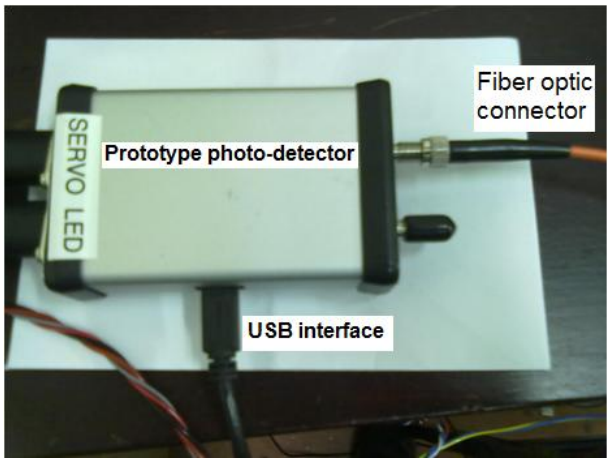

Figure 4.6 This picture illustrates the actual prototype photo-detector which had been designed by Dr. Simon Bateson. It is a small box, the dimensions of the box are: L x W x H: 9 x 5 x 2 cm. It contains the microprocessor, photodiode and A/D convertor. This device can integrate the LED lamp and can be connected to a fibre optic connector to pick up the fluorescence signal

4.2.3 Data acquisition unit

The photo-detector has a universal serial bus (USB) interface, which can be connected to any personal computer (PC) to control all the photo-detector functions.

The software was programmed using the C# programme language (ISO/IEC 23270, 2006). This software controls the photo-detector device functions and the servo movement. The microcontroller device has a number of output interfaces, the first one controlled the photo-detector and the other one controlled the automation of the servo, as has been described [3.4], the device controller was also established to power the LED lamp, which could be switched on only if the PC was powered. Furthermore, the excitation light integration time is fully controlled by the software programme. The photodiode used for fluorescence detection was coupled to a lock-in amplifier so that the detection of noise signals in the system and its surroundings was minimized.

The results, illustrated in Figure 4.7, show clearly identifiable recovered fluorescence signals obtained in the display unit. This signal can be saved as an excel sheet. The plot obtained is fluorescence intensity against time in seconds. This plot is further processed by means of an excel sheet to attain a numerical value signifying the signal.

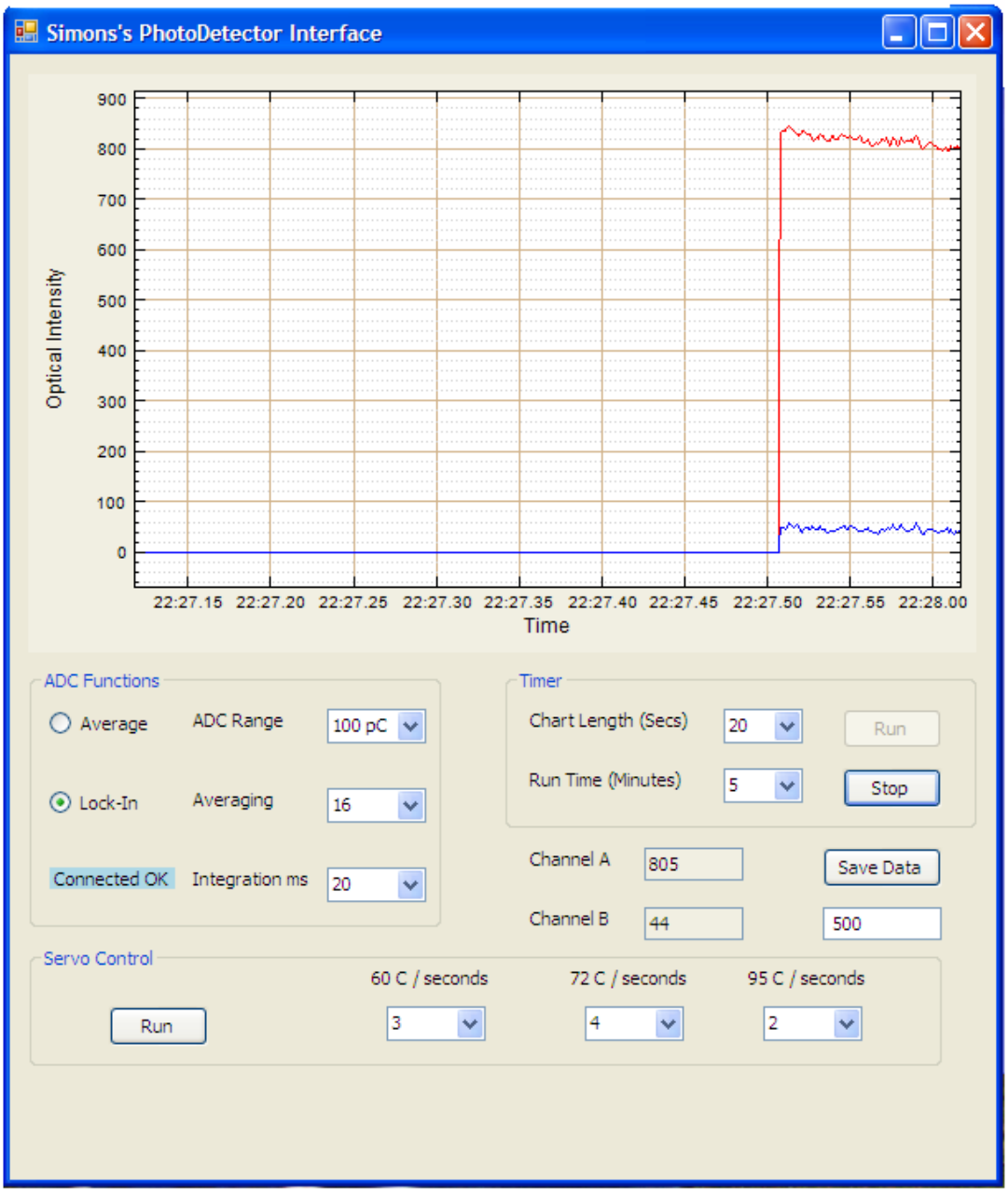

Figure 4.7 This picture shows the photo-detector interface in the display. The interface gives the user full control of the sensitivity of the detector. The parameter controls are: integration time (in second in the range between 2 to 250) locked in average in the range between (2 to 64), ADC in the range (between 50 to 880) and the ability to save the signal as a numerical unit on an Excel sheet, the signal then processed for calibration. Other parameters can be controlled in the programme as chart length.

4.2.4 Proof of Concept Demonstration

4.2.4.1 Geometric Placement of the Detector

To excite the molecules in the sample chamber, an LED is used to excite the light at 480 nm. The blue LED (LUMILEDS - LXHL-NB98 - LED, LUXEON, STAR, W OPTIC, BLUE, Farnell -UK) was used. According to the LED data sheet, the luminous flux will vary from a minimum of 6.3 lm at 460 nm to a typical of 20 lm at 480 nm due to this effect. Although the luminous power efficiency is lower in the short blue wavelength range, radiometric power efficiency increases as wavelength decreases. The light is directly coupled into the system, which is optimized for use close to the chip. As such, it is automatically aligned with the rest of the system. The LED lamp was fixed inside an aluminium cavity and the beam path is defined through a 2 mm diameter tube from the side of the cavity. The light from the LED uniformly illuminates the detection region from the side of the chip on the chip while the photo-detector detects the fluorescent emission at 90 degree, i.e. from the surface of the chip. The setting was verified using a spectrometer (HR4000, ocean optics, USA) as control spectrometer to evaluate the prototype photo-detector results.

4.2.4.2 Optimization of Fluorescence Detection: System Calibration

The fluorescence light is transferred by means of the optical fibre to the detection unit. This orthogonal fluorescence detection setup provides a geometrical separation of excitation light and fluorescence emission. In theory a filter is not necessary, yet, in practice, scattering of the excitation light will occur so additional spectral filtering of the fluorescence emission is needed as can be seen Figure 4.8.

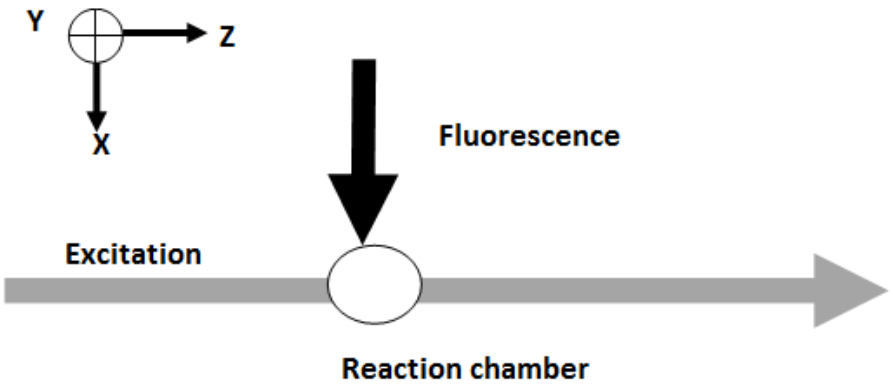

Figure 4.8 Schematic diagram of the ray tracing of the experimental setup for the fluorescence detection unit; the diagram shows the 90 degree position of the chip between the light source and fluorescence collection.

An optic fibre length of 45 centimetres and diameter 600 µm (MM Patch Cables, Thorlab, USA) was used to convey emitted light from the detection microchip through the emission filter as the emission filter was sited directly on the objective chip. The clear aperture for imaging the reaction chamber is 5 mm in diameter which is 100 % of the area of the 19.65 mm^2 square chamber. This translates into 500 µm spot size at the entrance and exit of the optic fibre.

The resulting fluorescence is filtered by dichroic filter (Filter Wratten, Edmund optics, from Kodak, USA) to maximize transmission of the emission signal and eliminate excitation signal and coherent interference artefacts emission. The photo-detector is provided by photodiode 520-525nm from 525NM TH, from Opto Diode Corp. UK). The light from the LED uniformly illuminates the detection region from the side of the chip on the chip while the photo-detector detects the fluorescent emission at 90 degree, i.e. from the surface of the chip.

4.2.4.3 Optimisation of Fluorescence Detection: Limit of Detection using FITC

Finally, the photo-detector component is used and its performance is characterized in a proof-of-concept demonstration setup. The complete setup (Figure 4.9) is consists of the following main parts: the source and the coupling of the excitation light in a

10 mm tube, the chip base part to position the sample chip between the excitation and beneath the emission detection unit. An optic fibre cable situated on the top of the chip to transfer the fluorescence signal to the detection unit and the fluorescence detection part. As the fluorescence signal should be verified by a standard detection system, the optical fibre cable was a flexible part in this setup so that the connection was easily switched between the photo-detector unit and HR 4000 ocean optic (Ocean Optics, Inc. World, USA) unit without altering the system setup. Fluorescein isothiocyanate (FITC) Figure 4.9 from (Thermo scientific, UK) was used to detect the limit of detection of the photo-detector. The protocol followed was as described from the supplier. According to the data sheet the excitation coefficient is > 70,000/M cm.

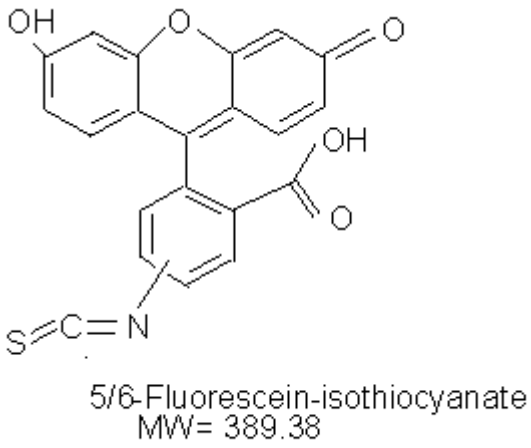

Figure 4.9 chemical strcture of FITC is showing the stracture of rich conjugated double-bond ,which inhances the Fluorescence propertiy of the compound (Draw using ISIS software).

4.2.6.4 Optimisation of Fluorescence Detection: Limit of Detection using dsDNA Kits

Two types of dsDNA fluorescence quantification kits were used to perform these experiments. The first kit was Quant-iT dsDNA kit (Invitrogen, UK) which was used as a reference standard method to demonstrate DNA quantification in the system. The Quant-iT™ dsDNA is a high-Sensitivity and accurate assay used for DNA

quantification. The Quant-iT™ dsDNA (Invitrogen, UK) is highly selective for double-stranded. The kit was provided with concentrated assay reagent, dilution buffer, and pre-diluted DNA standards. The assay is performed at room temperature, and the signal is stable for 3 hours. The kit is designed for assaying samples containing 2–1000 ng of DNA.

The protocol in brief as described by the supplier is as follows:

1) The fluorophore reagent was diluted 1:200 using the supplied 1XPBS buffer.
2) Then, 200 µl of buffer was loaded into the wells of micro-plate, after mixing well, at least 3 blank wells were used.
3) 10 µl standards volumes (the concentration of the DNA standards in the range between 0.5 to 10 ng μl^{-1}) were added to the wells in triplicate.
4) The mix standards were loaded into the sample chip and then the fluorescence measurements were carried out on the system.

The microplate reader used for fluorescence measurements comparison was Synergy HT Multi-Mode Microplate Reader, (Bio Tek,UK).This system was used to test the kit performance.

The second kit was QuantiFluor^{TM} dsDNA kit (Promega, UK) which was also used to detect the limit of detection of photo-detector. The advantage of this kit compared with Quant-iT dsDNA kit that this kit was supplied with stock dsDNA and the user can prepare his appropriate dsDNA concentration according to his test. The QuantiFluor™ dsDNA kit contains a fluorescent dsDNA-binding dye (504nmExitation /531nm Emission) that enables sensitive quantization of small amounts of dsDNA.The protocol followed was as described from the supplier. After each measurement the chip chamber was purged by passing biologically pure water (DNAse/RNAse free) through the chamber for 3 times which caused the detector output to return to baseline levels. HR 4000 ocean optic (Ocean Optics, Inc. World, USA) was operated in all experiments as follows: Integration time (msecond) is 300, spectral average is 1, boxcar smoothing is 0 and spectral type S4000 and ADC type is HR4000. The LED lamp power supply unit was fixed on 4.50 volts and 150 milliamperes for all measurements. The photo-detector was also fixed on the

following conditions: the integration time (msecond) is 250 ms and ADC range is fixed on 50 and locked in average at 16.

4.3 Results and discussion

4.3.1 Optimisation of the Fluorescence Detection system: System Calibration

The quantum efficiency (Φ_f) is define "as the fraction of the incident radiation, which is re-emitted as a fluorescence at longer wavelength" (Vogel's, 2000)

$$\emptyset_f = \frac{\text{number of photons emitted}}{\text{number of photons absorbed}} = \frac{\text{quantity of light emitted}}{\text{quantity of light absorbed}} \leq 1 \qquad \textbf{Equation 4.1}$$

The total fluorescence intensity (F) is quantified by the equation:

$$F = I_a \emptyset_f \qquad \textbf{Equation 4.2}$$

Where (I_a) represents the intensity of light absorption and (Φf) is the quantum efficiency of the fluorophore compound.

Since

$$I_0 = I_a + I_t \qquad \textbf{Equation 4.3}$$

Where I_0 the intensity of the incident is light and I_t is the intensity of the transmitted light, then

$$F = (I_0 - I_t)\, \emptyset_f \qquad \textbf{Equation 4.4}$$

Therefore, the total fluorescence intensity is proportional to the concentration of the chemical compound in the specific sample chamber. The excitation light source and spectrometer are employed to provide excitation and fluorescence spectral

desperation for DNA binding dye (fluorophore) detection. The surface area of the chamber is 28.3 mm^2 and it was made from polycarbonate film in a thickness of 127 µm to allow access of fluorescence detection. The volume of the sample is 28.3 millimetre. A blue-light LED, which was used as an excitation source has peak emission at a wavelength of 480 nm. The Fluorescence intensity is defined from the chemical properties of FITC which absorbs the light at 480 nm and emits at 520 nm.

The signals processing was designed, an initial test of the fluorescence detection capability. The experiment was performed to determine if the concept of the optical device should be pursued further and to define the smallest emission signal which could be detected by the photo-detector. The fluorescence intensity of the FITC solution in the chip-reaction chamber was monitored over different experimental setups before defining the described setup. To avoid measuring the incident light, the fluorescence emission was measured at right angles to the incident beam, as illustrated in Figure 4.10.

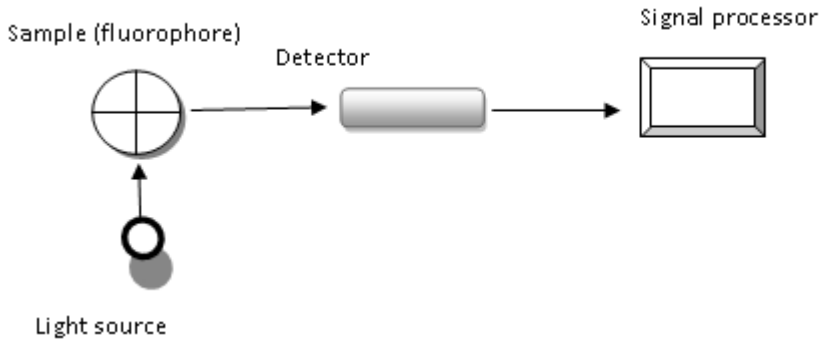

Figure 4.10 schematic diagrams illustrating the normal method used for fluorescence measurements.

In order to define the optimum setup of our experiment, the previous setup was tested in different ways. The first plan was a front-face arrangement, which was applied by directing the light source through a fibre optic at geometry of 20 degrees and by collecting the signal at 90 degrees. This setup was useful but the signal obtained was poor, as can be seen in Figure 4.11.

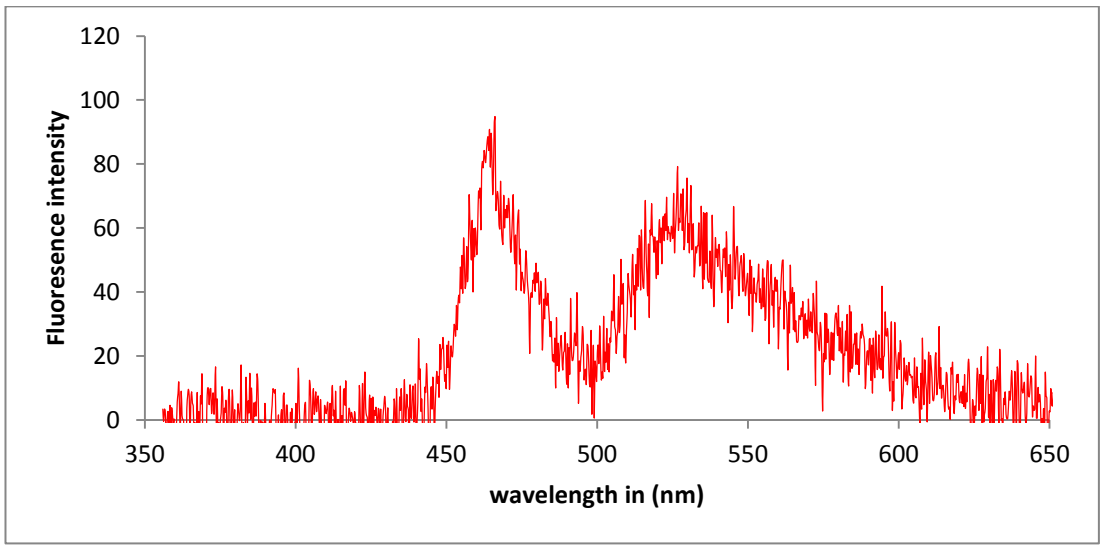

Figure 4.11 This graph shows the poor signal of fluorescence measurements of FITC were done in the chip using an Ocean Optic spectrometer before the optimisation the fluorescence signal. The geometry of measurements was done using fibre optics. The excitation was fixed at 20 degrees and the emission at 90 degrees.

The low sensitivity is due to two factors. The first factor is the fibre optic, which decreased the incident light from the LED, and the second factor, typical in this arrangement, is that a large fraction of incident light reflected off the surface of the chip (Lakowicz, 1983)

This plan was applied in different methods, such as avoiding using fibre optic and collecting the signal by the detector. However, this method also presented a high noise detection signal. Ultimately, the system was optimized using the setup described [4.2.4].

A solution of fluorescence dye FITC was prepared in concentration of 0.5 ng ml^{-1} (1.28 nM) and used to determine the fluorescence signal achieved from dye in the chip -reaction chamber. This experiment was carried out in order to establish the optimum fluorescence signal could be obtained from the system and to ensure the system reliability. The fluorescence signal was first optimized using ocean optic HR4000, which had been measured before and after the filter; the signal obtained is illustrated in Figure 4.12 and Figure 4.13. The fluorescence intensity was observed on exposure of the dye solution to different concentration of FITC before system calibration.

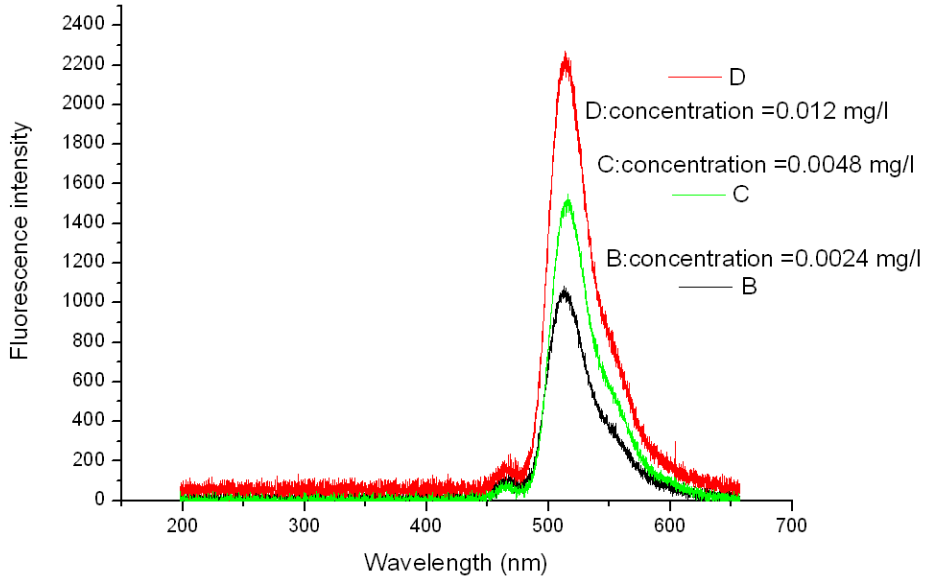

Figure 4.12 Intial test optimization of the fluorescence detection using HR4000 optic fibre spectrometer. The test was accomplished using FITC florophore in concentration of 4.8 × 10-2 mg/L, dissolved in 1 % phosphate buffer. The excitation angle was fixed at 90 ° and the emission at 25 °.

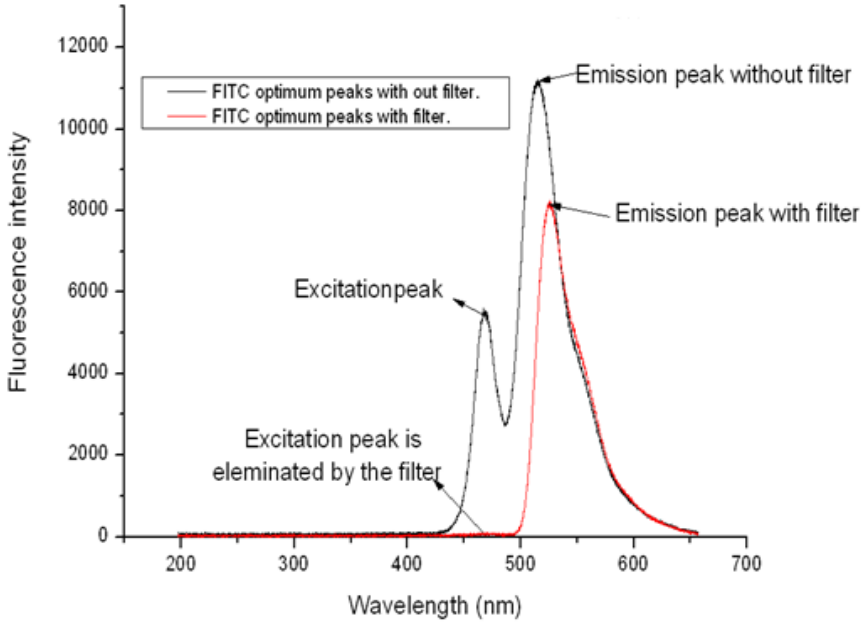

Figure 4.13 The graph illustrates the optimum fluorescence signal obtained from the FITC as a Fluorescence dye in the chip-reaction chamber, as the excitation signal is lower than the emission signal. The orthogonal fluorescence detection setup applied is the best setup position to obtain the maximum fluorescence signal from the chip-reaction chamber. The experiment was carried out on lower LED power (9 watt) in order to minimise the excitation signal. However, the excitation signal is eliminated after a dichroic filter is employed.The red peak is illustrating the emission signal obtained from dye in the chip-reaction chamber. The measurements were taken by HR4000 ocean optic spectrometer.

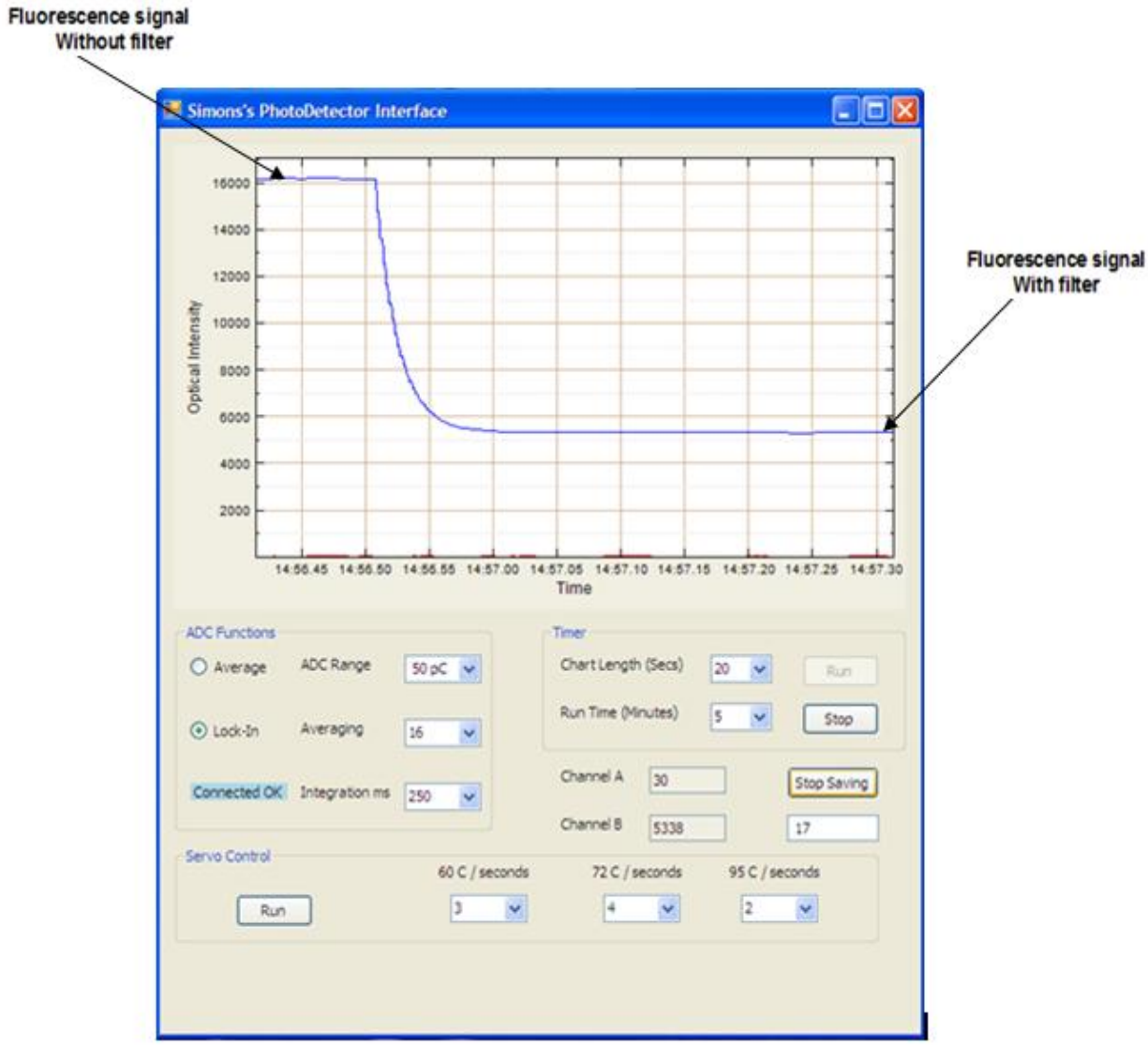

Figure 4.14 The peak in a signal of 16000 illustrates the optimum fluorescence signal obtained from the FITC as a Fluorescence dye in the chip-reaction chamber, as the excitation signal is lowe than the emission signal. The orthogonal fluorescence detection setup applied is the best setup position to obtain the maximum fluorescence signal from the chip-reaction chamber. The experiment was carried out on lower LED power (9 watt) in order to minimise the excitation signal. However, the excitation signal is eliminated after a dichroic filter is employed. The peak in a signal of 5800 is illustrating the emission signal obtained from dye in the chip-reaction chamber. The measurements were taken by the prototype photo-detector.

As can be seen in Figure 4.14, the system is efficient enough to determine the fluorescence signal from the prototype chip and the experimental setup is an effective unit for this size of chemical sample in the chip. The following experiments will be focused on defining the sensitivity of the system and the investigation of the unit for PCR detection.

4.3.2 Optimisation of Fluorescence Detection System: Limit of Detection Using FITC

The performance of a detection system is typically defined by means of the limit of detection (LOD). The detection limit is defined as "the smallest concentration that can be reported with a certain level of confidence" i.e., the smallest concentration of an analyte for which we can decide whether that analyte is present or not in the sample under test. As a result, although the detection system will sometimes detect smaller concentrations of that analyte than the LOD, the LOD represents the smallest concentration that indicates the "true" detection proficiency of the system (Vogel's 2000). The LOD is mathematically expressed as a concentration and will be derived from the fluorescence signal generated by the photo-detector, which converts optical power into a voltage signal.

The calculation of LOD required the calibration of the measurement system and determination of the background level. The background level is defined as the concentration above which the decision 'detected' is made. This level corresponds to the minimal significant signal that can be distinguished from the noisy background signal. In this system, the background was measured by injecting a PBS buffer *p*H 7.4 in the sample chamber, as the PBS buffer is the sample matrix of fluorophore dye (FITC). The signal illustrated in Figure 4.15**.**

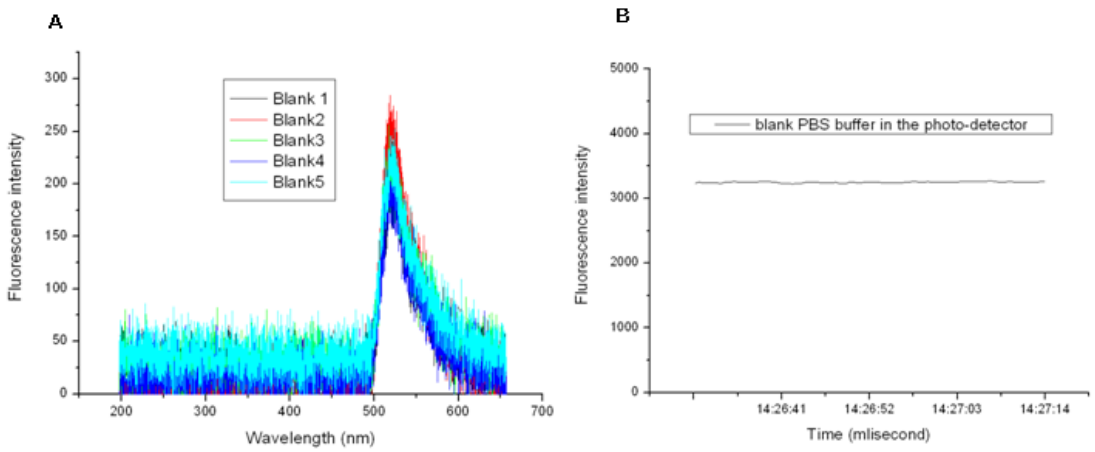

Figure 4.15 Graph (a) illustrating the background signal measured by HR4000 ocean optic spectrometer; graph (b) illustrating the background signal measured using the prototype photodetector. Both signals were detected by injecting PBS buffer into the chip reaction chamber and detection followed the experimental setup described in section 4.2.1

The detection limit was investigated for both the FITC and the dsDNA standards solutions. Large sample plugs were injected for these sensitivity measurements, so that the dispersion effects did not cause dilution of the maximum achievable sample fluorescence. A calibration curve was finally constructed and by analyzing the background noise distribution obtained for methanol without FITC in the reaction chamber, detection limits were estimated for each serious of measurements.

For the FITC calibration stock solutions of FITC solution were prepared fresh by dissolving 1 mg of FITC dye in 20 ml of phosphate buffer saline (PBS) to obtain a standard solution in concentration of 0.05 µg ml^{-1} or (128.41 nM) . A middle dilution of 0.5 ng ml^{-1} (1.28 nM) was then used to prepare serial working standard solutions listed in Table 4.1:

Table 4.1 The different concentrations of FITC used for system calibration.

	Concentration in ng ml^{-1}	Concentration in nM(10^{-9}M)
1	0.50	1.284
2	0.25	0.640
3	0.20	0.512
4	0.15	0.385
5	0.10	0.265
6	0.05	0.128

For every concentration prepared, three consecutive measurements were performed using the photo-detector and ocean optic HR4000. In calibration measurements a 28 µl of each standards were injected into the chip reaction chamber and spectra were taken of each concentration using ocean optic spectrometer and the prototype photo-detector. The fluorescence signals obtained from each system were illustrated in Figure 4.16 (a) and (b).

Accordingly, calibration graphs were plotted for each system depending upon the experimental setup [4.2.4], as can be seen from the graphs in Figure 4.17 and Figure 4.18 the correlation coefficient (R^2) was 0.9968 and 0.9978 respectively. The values obtained are within the accepted limit.

The lowest limit of quantification and detection were (LOD) of the chip reaction chamber by ocean optic spectrometer and prototype photo-detector are 0.036265 ng/ml (36.265 pg/ml) and 0.040596 ng/ml (40.596 pg/ml) respectively.

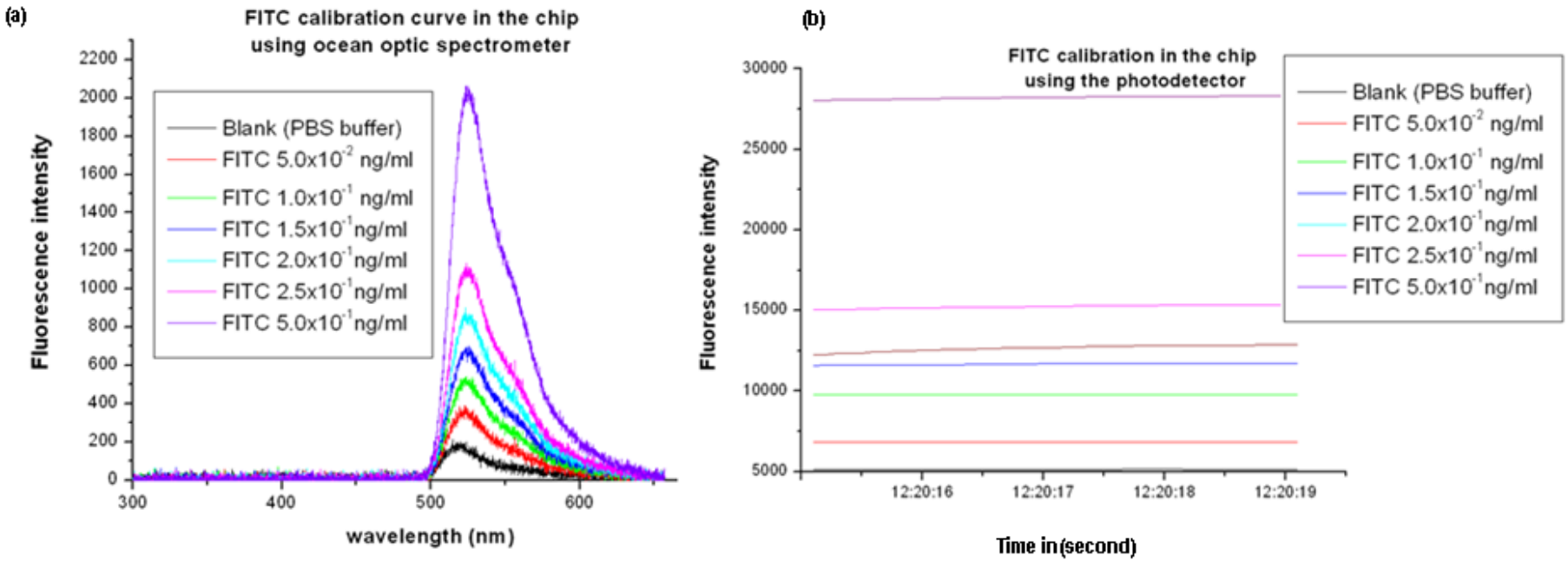

Figure 4.16 (a) Emission peaks of different concentrations of FITC in the range (0 to 0.5) ng ml^{-1} (0- 1.28x10-9 M). The measurements were taken using an HR4000 ocean optic spectrometer. It can be seen that there is a significant signal development at wavelength 520 nm.
(b) Fluorescence intensity of different concentrations of FITC in the range (0 to 0.5) ng ml^{-1} (0- 1.28x10-9 M), the measurements taken using the prototype photo-detector.

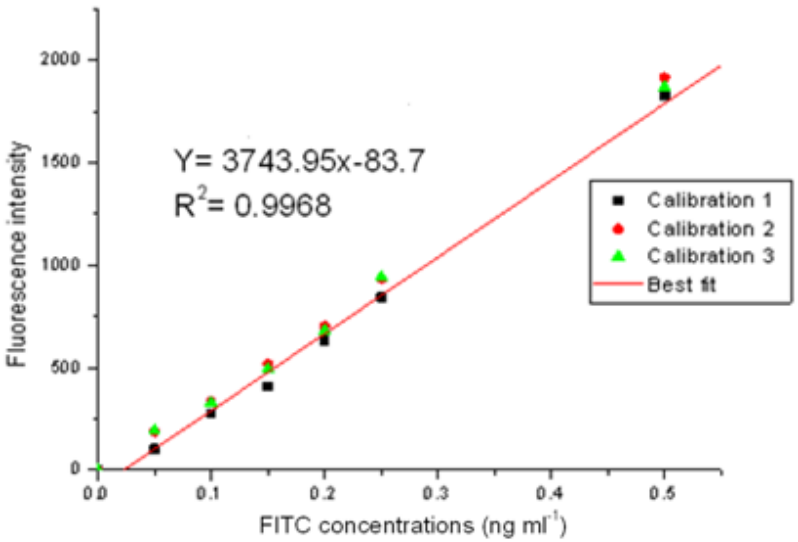

Figure 4.17 Based on data shown in Figure 4.16a: calibration plots of three measurements on HR-4000 ocean optic spectrometer for fluorescence signal against FITC concentrations. The R^2 value of the plot is 0.9968 and the plot equation as indicated in the graph.

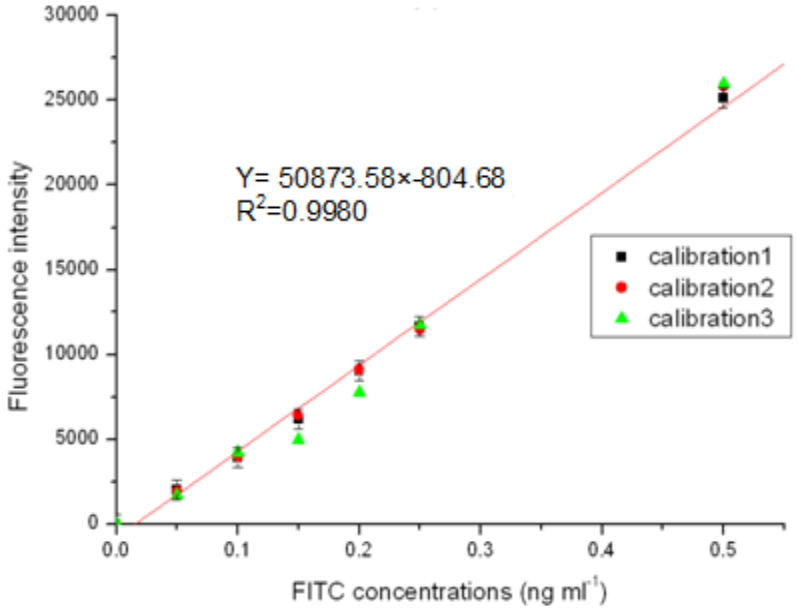

Figure 4.18 Based on data shown in Figure 4.1**6**b calibration plots of three measurements on prototype photo-detector show fluorescence intensity against FITC concentration. The R value of this plot is R^2= 0.9980.the plot equation as indicated in the graph.

Experimentally, the LOD was also detected by preparing low concentrations of FITC in a range of ($1.25x10^{-3}$ to $15.0x10^{-3}$ ng ml^{-1}) as can be seen in Table 4.2 and the calibration graph shown in Figure 4.18.

Table 4.2 The FITC concentrations were prepared for LOD detection experimentally in the chip system for Ocean optic spectrophotometer**.**

	Concentration in ng ml^{-1}	**Concentration in nM(10^{-9}M)**
1	0.0125 ($1.2x10^{-3}$)	0.032 (32 pmole)
2	0.025($2.5x10^{-3}$)	0.064(64 pmole)
3	0.050($5.0x10^{-3}$)	0.128(128 pmole)
4	0.075($7.5x10^{-3}$)	0.193(193 pmole)
5	0.10($10x10^{-3}$)	0.257(257 pmole)
6	0.05($15x10^{-3}$)	0.385(385 pmole)

The fluorescence peak maximum was estimated for each concentration using HR4000 ocean optic spectrometer, as can be seen in Figure 4.19. Then a calibration curve was plotted Figure 4.20. Good linearity was observed with $R^2 = 0.9917$

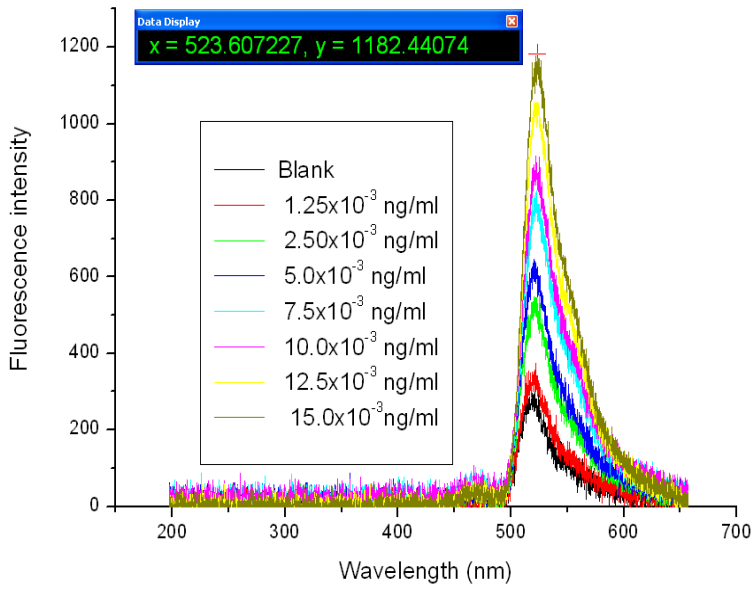

Figure 4.19 Emission spectrophotmetric peaks of different concentrations of FITC in the range 0 – $15x10^{-3}$ ng ml^{-1}. The measurements were taken using HR4000 ocean optic spectrometer; it is clear that there is a significant signal development at wavelength 523 nm.

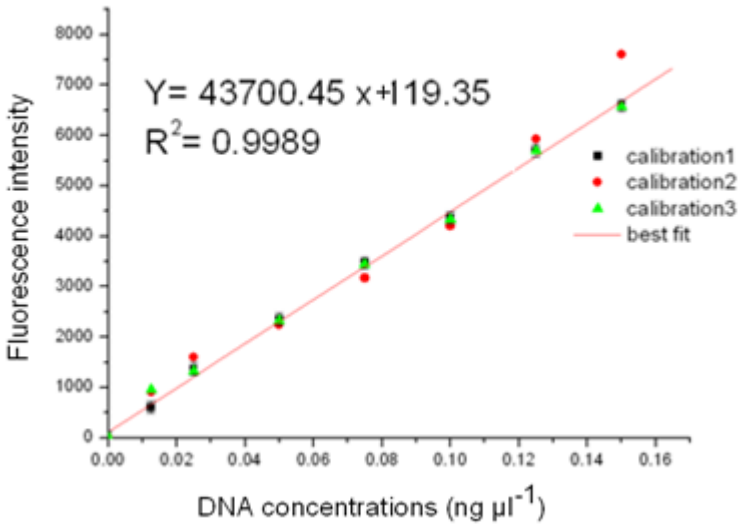

Figure 4.20 Based on data in Figure 4.19: calibration plot for the fluorescence signal of FITC standards were obtained from chip measurements using an ocean optic spectrometer. FITC concentration X axis against fluorescence intensity y axis: the R^2 value of this plot is R= 0.9989; the plot equation as indicated in the graph.

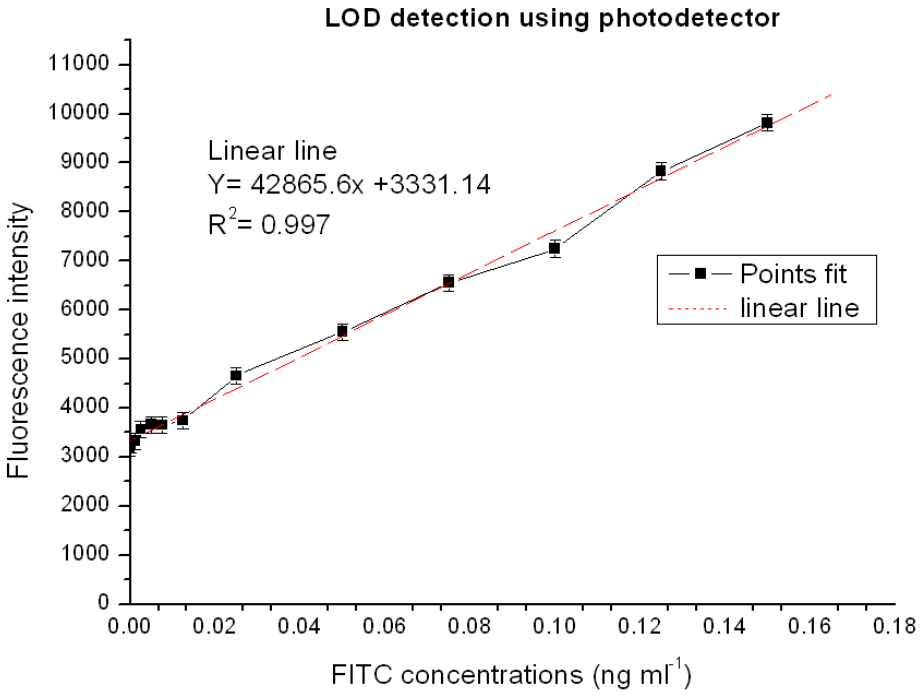

Figure 4.21 This graph was plotted using spectrophotmetric data used to define experimentally the LOD of the prototype photo-detector. Serial low concentrations of FITC were prepared and fluorescence measurements were taken using the chip. As can be seen from the black display, the lower significant signal was above the concentration of 1.0 x10-3ng ml-1FITC.

However, in order to estimate the LOD detection using prototype photo-detector, serial low concentrations of FITC solutions were prepared. The lower FITC standards solutions prepared are shown in Table 4.3. The low concentration solutions were incorporated with the standard solutions in Table 4.3 to establish the LOD detection graph shown in Figure 4.21.

Table 4.3 The FITC concentrations prepared for practically detecting LOD in the chip system for photo-detector.

	Concentration in ng ml^{-1}	**Concentration in nM(10^{-9}M)**
1	0.00025 ($2.5x10^{-4}$)	$0.064x10^{-4}$ (0.64 pmole)
2	0.00125($1.25x10^{-3}$)	$3.2x10^{-3}$ (3.2 pmole)
3	0.0025($2.5x10^{-3}$)	$6.4x10^{-3}$ (6.4pmole)
4	0.005($5.0x10^{-3}$)	0.0128 (12.8 pmole)
5	0.0075($7.5x10^{-3}$)	0.0256 (25.6 pmole)
6	0.0125($1.25x10^{-2}$)	0.032 (32 pmole)

The fluorescence intensities for the FITC standards solutions were also measured using the prototype photo-detector and then a calibration curve was plotted. The calibration curve obtained is shown in Figure 4.21. The linearity of the curve in accepted limit as the correlation coefficient is (R^2) is 0.9989. The results deduced are that, experimentally, the lower concentration (LOD) of FITC detected was $1.0x10^{-3}$ ng ml^{-1} (10.0 pg ml^{-1}) in both systems. This value of LOD is near the theoretical LOD estimated in plots Figure 4.20 and Figure 4.21, which were 0.032 ng ml^{-1} (32.3 pg ml^{-1}) in the in ocean optic spectrophotometer.

However, in the prototype-photo-detector the LOD evaluated was 0.0078 ng ml^{-1} (7.8 pg ml^{-1}), which clearly indicated that the prototype photo-detector was more sensitive. This method was repeated in different atmospheric conditions although no significant variation in the results was found. Therefore, it shows good robustness and. Robustness. A summary of the data regression analysis and LOD is shown in Table 4.3.

In comparison of this system with number of investigators work, there has been many attempted to integrate fluorescence detection with microfluidic chips. Edel *et*

al, (2004) have demonstrated the use of polyfluorine based (polymer LED) as light source, avalanche photodiode as a detector with limit of detection (LOD) of 1 µM for fluorescein dye. Yao *et al*, (2005) fabricated a microfluidic device with an integrated OLED excitation source and a PMT as detector for on-chip fluorescence detection using a pinhole and interference filter for masking the excitation light. A LOD of 3 µM was achieved for Alexa 532 dye.Kim *et al*, (2006) demonstrated a compact device using an OLED a slight source and an integrated p-i-n photodiode as a detector, with interference filter to mask the excitation light and secured a LOD of 10 µM of TAMRA dye. Pagliari *et al*. 2009 recently demonstrated apromising new light source technology –an inherently polarized light source using electro- spun light-emitting-polymer nano-fibres. Banerjee *et al*, (2010) had been able to successfully measure Rhodamine 6G down to 10 nM by means of a thin microfluidic chamber that used organic devices both as optical sources (organic light emitting device) and detectors (organic photodiode). A cross-polarization scheme, placed on the both side of the chamber, was used to mask the pump light from the signal detector. However, the photo-detector system has successfully secured a LOD of 19.7 pM of FITC.

4.3.3 Optimisation of Fluorescence Detection: Limit of Detection using dsDNA Kits

The Quan-iT dsDNA high sensitivity kit assay was used as an application kit to control DNA detection in the detection unit. The assay works by binding a supplied fluorophore (HS-reagent) with dsDNA. This process as has been described [4.1.2]. The reaction basically depended upon the fact that the fluorescence intensity was proportional to the concentration of dsDNA in the reaction. Therefore, calibrating the system by this assay endorsed the ability of the system for DNA detection and PCR progress measurements.

This assay was designed for fluorometers that apply micro-plate readers. The kit was supplied with a series of dsDNA standards in concentrations between 0.5 to 10 ng μl^{-1}. The reaction assay for DNA standards were performed as normal in micro titre plates and the fluorescence measurements were taken using microplate reader (Synergy HT Multi-Mode Microplate Reader, BioTek,UK). The quantification of fluorescence signals from the experiments was calculated by conducting the four independent experiments and the mean were taken for calculation. The calibration curve obtained is shown in Figure 4.22.

Table 4.4 Comparison between fluorescence signals for the same standards of the Quant-iT dsDNA kit (Invitrogen, UK) measured by three detectors; micro-plate-reader, HR4000 ocean optic spectrometer and prototype photo-detector. The table shows the difference between the fluorescence signals of each detector for the same DNA concentrations.

concentration of DNA standard ($ng\ \mu l^{-1}$)	**Fluorescence signal (mean of three measurements)**		
	Microplate reader R^2**= 0.9947**	**Ocean optic** R^2**=0.9939**	**Photo-detector** R^2**=0.9908**
0.5	3	18	217
1.0	7	43	898.4
2.0	17	61	1553.8
4.0	38	212	3424.8
6.0	55	333	4990.4
8.0	74	435	6322
10.0	81	491	6810

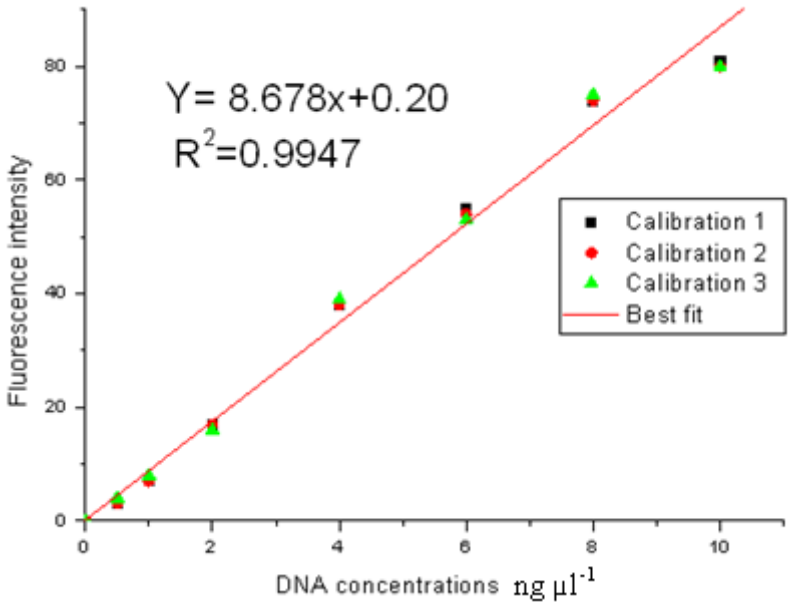

Figure 4.22 Calibration plots of DNA standards on Micro-plate reader. The plot illustrates the DNA concentrations vs. fluorescence intensity. The R^2value of the best fit is = 0.994.

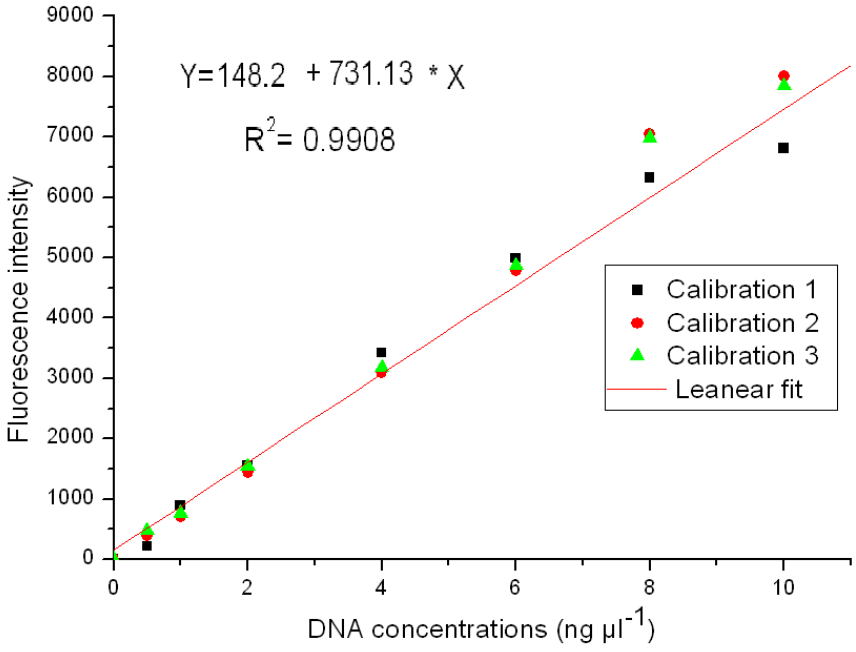

Figure 4.23 Based on data in Table 4.5 of fluorescence intensity obtained from the photo-detector, a plot of DNA standards concentrations vs. fluorescence intensity.

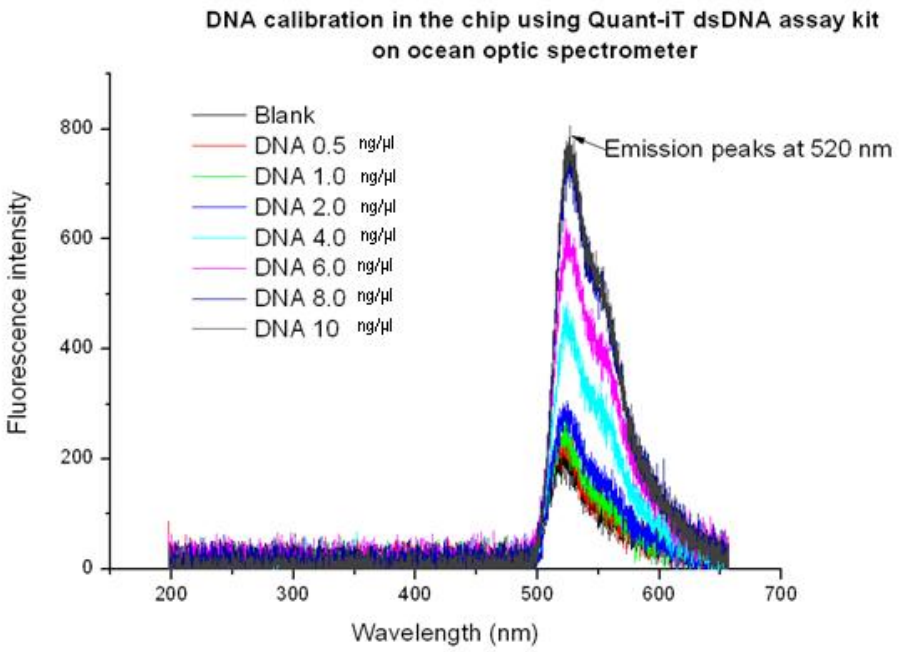

Figure 4.24 Maximum emission peaks of serial dilutions of DNA concentrations in the range 0 – 10 ng µl-1, the measurements taken using HR4000 ocean optic spectrometer. It is clear that there is a significant signal development at wavelength 523 nm. The measurements were taken using the system set-up described in section [4.2.1].

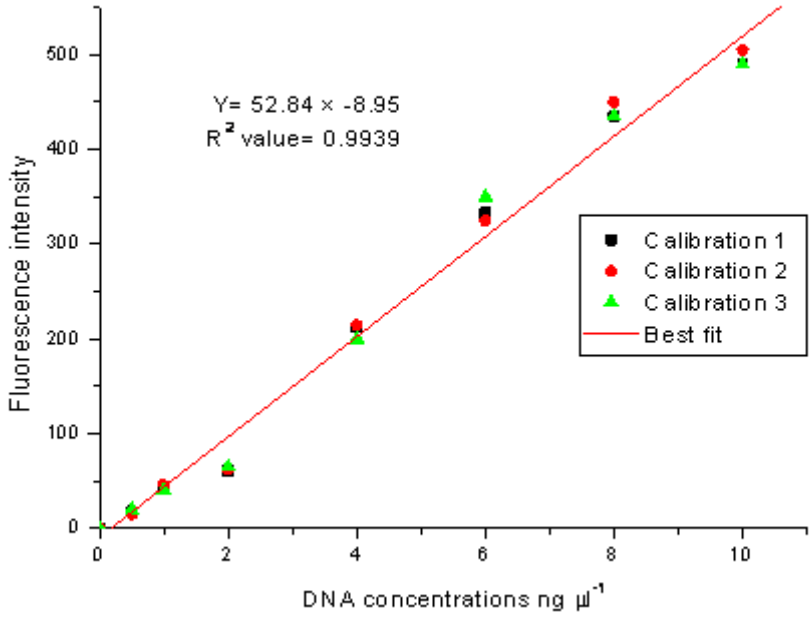

Figure 4.25 Based on data in Figure 4.24 of fluorescence intensity obtained from HR 4000 ocean optic spectrometer, a plot of DNA standards concentrations vs. fluorescence intensity.

The same set of reactions, using the assay kit, was also carried out in the micro titre plate but the reaction mixture was individually injected into the chip reaction chamber. The fluorescence signals in the first experiments were measured using HR 4000 ocean optic spectrometer and on the prototype photo-detector, the fluorescence signals obtained on ocean optic are shown in Figure 4.24. Calibration plots were constructed and regression analysis was carried out to estimate the LOD. The graph obtained is illustrated in Figure 4.25. As can be seen from the fluorescence signals obtained from venous systems, the prototype photo-detector was more sensitive than the Ocean Optic spectrometer and microplatereader.

The LOD, estimated according to the microplate reader measurements, which had been measured in standard microplate cells, not in the prototype chip, was: 1.31 ng μl^{-1}(131 ng ml^{-1}). However, the HR 4000 ocean optic spectrometer fluorescence measurements, which had been carried out using the prototype microfluidic chip, presented LOD of 1.42 ng μl^{-1}(142 ng ml^{-1}). LOD of the photo-detector fluorescence measurements, which had been measured using the prototype chip was 1.8 ng μl^{-1}(180 ng ml^{-1}).

The LOD obtained was 103 ng ml^{-1}. However, as can be seen in Figure 4.26 and Table 4.6, there was a significant signal obtained from standard 1, which had a concentration of 100 ng ml^{-1}. Therefore, experimentally the lower detection of the dsDNA estimated on the photo-detector was 100 ng ml^{-1}.

Table 4.5 The table shows the dsDNA standards from kit QuantiFluor™ dsDNA kit (Promega, UK) which was used for calibration curve and the output signal of each standard, the measurements were taken using the prototype photo-detector.

Volume of TE (µl)	Volume (µl) of Diluted Standard (2µg/ml).	Volume of (µl) QuantiFluor™ dsDNA	Final concentration of dsDNA (ng ml^{-1})	Fluorescence signal On photo-detector ($\bar{x}$)
100	0	100	0	2829.2
90	10	100	100	4599.6
80	20	100	200	6074.2
70	30	100	300	7489.6
60	40	100	400	8431
50	50	100	500	11383.5
40	60	100	600	13849.75
30	70	100	700	15875.8
0	100	100	1000	20857.4

The calibration curve was plotted according to the fluorescence measurements taken on the prototype photo-detector Figure 4.26 based on the fluorescence signal obtain from HR 4000 spectrophotometer.

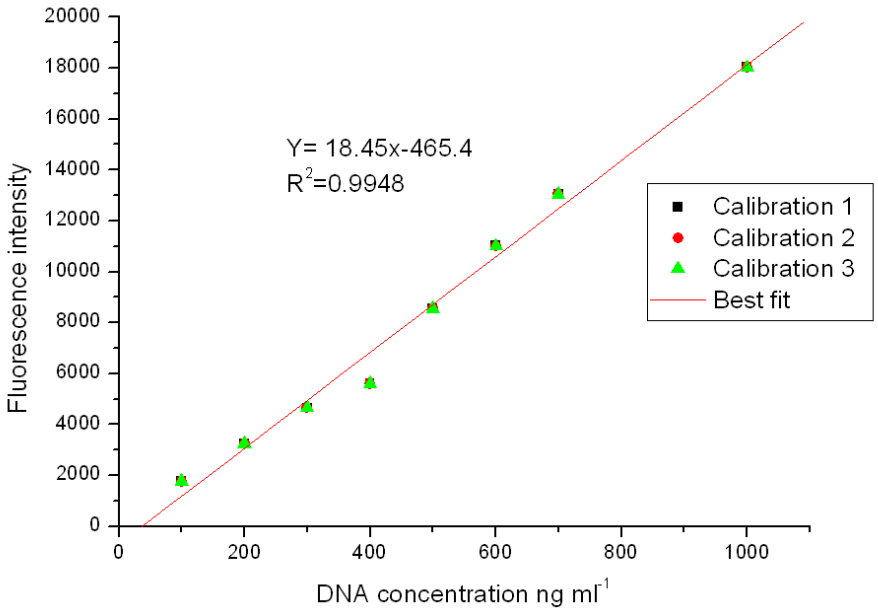

Figure 4.26 Calibration curve based on data of three fluorescence measurements on the photo-detector. The plot shows dsDNA standards concentrations vs. fluorescence intensity. The line fit (red line) shows the best linear fit between the points at least 8 points fit with line.

4.3.4 Statistical Analysis of Detector Systems

The measurements were taken for 10 consecutive injections and the resulting signals for the background were distributed about the mean value ($\bar{x}$), with a standard deviation (SD). A common method for stating precision, evaluated in terms of relative standard deviation (RSD), is calculated as follows:

$$\text{Standard deviation (SD)} = \sqrt{\frac{(x_1-\tilde{x})+(x_2-\tilde{x})+(x_3-\tilde{x})+(x_4-\tilde{x})\ldots}{n-1}} \qquad \textbf{Equation 4.5}$$

Where (n) is the number of data points

RSD % = 100 × Standard Deviation / mean.

To indicate the inherent "true" detection capability of the detection system, the distribution of the measurements of the signal level corresponding to the detection limit concentration (mean value of LOD and standard deviation SD) should also take into consideration. LOD should be sufficiently larger than the background signal to have a significant certainty that concentration LOD will be detected and, therefore, to define it as the detection limit.

The calibration procedure was then carried out to define the sensitivity and reliability of the fluorescence measurements. The goal was to focus on the advantage of using the micro-fabricated chip to directly integrate and align both the DNA amplification and fluorescence detection system. Accordingly, the correlation coefficient was calculated to establish whether there is a linear relationship between series concentration of the fluorescence dye and the fluorescence signal obtained from the photo-detector or not.

The correlation between concentrations (x-axis) and the corresponding fluorescence intensity signal levels (y-axis*)* were estimated experimentally by injecting a series of FITC standards with different concentrations dissolved in the PBS buffer *p*H 7.4. The signal for each concentration was measured by using the same chip and these results were to obtain a calibration curve.

The Pearson's correlation coefficient or coefficient of determination (R^2) is estimated for each calibration standards to find out the reliability of the linear calibration. It is also possible to determine the correlation coefficient, *r*, which gives us a measure of the reliability of the linear relationship between the *x* and *y* values. A value of (R^2) indicates an exact linear relationship between (x) and (y).The Values of *r* close to 1 indicate excellent linear reliability. If the correlation coefficient is relatively far away from 1, the predictions will be based on the linear relationship.

Values of (R^2) of (1) and (-1) indicate perfect positive and negative correlation. An *r* value of (0) indicates that there is no linear correlation, it is important to stress that this does not imply that there is no correlation.

$$R^2 = \frac{\sum_i \left\{ \left(x_i - \bar{x}\right)\left(y_i - \bar{y}\right) \right\}}{\left\{ \left[\sum_i \left(x_i - \bar{x}\right)^2 \right] \left[\sum_i \left(y_i - \bar{y}\right)^2 \right] \right\}^{1/2}} \qquad \textbf{Equation 4.6}$$

If it is assumed that there is a linear relationship between the analytical signal (y) and the concentration (x), it is possible to calculate the best straight line through the calibration points using the method of least squares. Since it is assumed that all the errors are in (y) this is done to minimize the deviations in the y-direction. Since some of these deviations (known as residuals) will be positive and negative, the aim is to minimize the sum of the residuals. The line is required to pass through the centre line of the points (Miller and Miller, 1993).

The line of regression calculated can be used to estimate the concentrations of test samples by interpolation and can also be used to determine the limit of detection. (LOD). The calculation of LOD using regression analysis depends upon calculation of the statistic (S_y/x). S_y/x is given by: the equation below:

$$s_{y/x} = \left\{ \frac{\sum_i (y_i - \hat{y}_i)^2}{N-2} \right\}^{1/2}$$ **Equation 4.7**

We can calculate (S_b), the standard deviation for the slope (b) and and (S_a) which is the intercept (a) using the following equations

$$s_b = \frac{s_{y/x}}{\left\{ \sum_i \left(x_i - \bar{x} \right)^2 \right\}^{1/2}}$$ **Equation 4.8**

$$s_a = s_{y/x} \left\{ \frac{\sum_i x_i^2}{n \sum_i \left(x_i - \bar{x} \right)^2} \right\}^{1/2}$$ **Equation 4.9**

The values of (S_b) and (S_a) can be used to estimate the confidence limits for the slope and intercept. The confidence limits for the slope and intercept are given by:

$$b \pm t \times S_b$$

$$a \pm t \times S_a,$$

Where, the t-value is taken at the desired confidence level and (n-2) degrees of freedom.

A commonly used definition of the limit of detection is the analyte concentration giving a signal equal to the blank signal, where (S_B) is the standard deviation of the blank

$$y - y_B = 3s_B \qquad \textbf{Equation 4.10}$$

However,

$$a = (y - y_B,)$$

$$S_B = (S_y / x).$$

Then,

$$LOD = \frac{3S_B}{a} \qquad \textbf{Equation 4.11}$$

Table 4.6 Summery of statistical analysis of DNA calibration using the two dsDNA kits in the chip for the measurements performed on different fluorescence detectors, the table also shows comparison of LOD in different systems.

FITC calibration	Standard error (S_y/x)	R square (R^2)	Intercept (a)	P-value*	Confident level	LOD
Calibration 1(high concentrations) on ocean optic	63.27	0.9968	$5.4x10^4$	0.000119	95 %	0.034 ng ml^{-1}
Calibration 3 (high concentration) on photo-detector	420.13	0.9979	$1.6x10^4$	$9.2x10^{-8}$	95 %	0.040 ng ml^{-1}
Calibration 4 (low concentration) on ocean optic	58.51	0.9736	$5.3x10^2$	$8.5x10^{-7}$	95 %	0.032 ng ml^{-1}
Calibration 4 (low concentration) on photo-detector	112.8	0.9989	$4.3x10^4$	$7.43x10^{-8}$	95 %	0.0078ng ml^{-1}

*P-value is a value range between (0 to 1) used to measure the correlation between the population having means overall the smaller P-value, the stronger evidence of results (Miller and Miller, 1993)

Table 4.7 Summery of statistical analysis of FITC calibration in the chip and comparison between LOD figured in photo-detector and ocean optic spectrometer.

DNA calibration	Standard error (S_y/x)	R square (R^2)	Intercept (a)	P-value*	Confident level	LOD (ng ml^{-1})
Calibration on microplatereader (standard cells)	3.78	0.9947	8.63	$4.33x10^{-8}$	95 %	131.0
Calibration on ocean optic spectrometer(prototype chip)	25.37	0.9939	53.35	$7.95x10^{-6}$	95 %	142.0
Calibration on photo-detector (prototype chip).	433.95	0.9980	722.74	$2.51x10^{-5}$	95 %	180.0
Lambda dsDNA calibration on Photo-detector	703.6	0.9944	15.66	$5.1x10^{-7}$	95%	103.0

*P-value is a value range between (0 to 1) used to measure the correlation between the population having means overall the smaller P-value, the stronger evidence of results (Miller and Miller, 1993)

4.4 Conclusion

An optical system for the end point detection of PCR was developed in several stages. The operation of the sensor depended on the fluorescence binding dye. Initial optimization of the system setup was performed using FITC and the results were verified using HR 4000 Ocean Optic spectrometer. The tested prototype photo-detector was suitable for the development of portable, robust, and detection device. The detection system was implemented with a fibre optic to collect the fluorescence signal, which was directly aligned onto the microfluidic reaction chamber. A Dichroic filter, an LED excitation source, and a photo-detector detector completed the detection unit. FITC dye was used in a proof-of concept demonstration setup, where the detection limit for fluorescence detection was investigated.

Samples with various concentrations of FITC dye were injected in a prototype polycarbonate reaction chamber in a thickness of 1 mm and a calibration curve was constructed giving the correlation between the concentration of the sample and the resulting photo-detector signal. The detection limit was estimated both theoretically by means of the regression analysis, and experimentally. The smallest concentration detectable experimentally by HR4000 Ocean Optic spectrometer and prototype photo-detector in the chip was 12.5pg ml^{-1} FITC (32 pmol FITC). However, the smallest concentration measurable by the prototype photo-detector measurements was 7.8pg ml^{-1} (19.7 pmol FITC).

As a result, the proof-of-concept of the proposed detection configuration was tested using a prototype disposable polycarbonate chip that could be easily replaced, but ultimately, the future goal would be to adapt this detection approach for online detection of PCR. The application of this photo-detector unit could also be extended for DNA quantization or real time PCR detection. The future enhancement of the system would be focussed on increasing its performance by:

1) Lowering background noise to reach lower LODs;
2) Enhancing the detector sensitivity for an excitation source with optimal properties;
3) Improving the collection of light in the microfabricated system;

The system will be adapted with thermal-cycler unit for online real time PCR detection.

Chapter 5 Device Application

5.0 Device application

5.1 Introduction

As discussed in Chapter (1), the polymerase chain reaction (PCR) is a powerful molecular diagnostic tool for identifying and monitoring the source of infectious diseases or genetic disorders in patients, in addition to its forensic and environmental application. The time and cost required for the analysis of PCR results was reduced by the development of a post–PCR device that addresses the point-of-care (POC) demand. The prototyped device is a POC-PCR device utilises fluorescent dye molecules in a reaction mixture to monitor the amount of PCR products at the end of the thermal cycling process. Therefore, it does not require time consuming post-PCR manipulations, such as staining gel electrophoresis, and visualization with a fluorescence setup. The labour-intensive and time consuming sample preparation processes have been a limiting factor for the actual application of PCR outside of the research facilities (Auroux *et al*, 2004; Zhang and Xing, 2007). In contrast, our prototype device is convenient in using as portable instrument for PCR application on the field.

This project investigated a prototype PCR-based diagnostic device consisting mainly of three parts: thermal–cycler unit for nucleic acid amplification, polycarbonate fabricated chip and fluorescence detection unit. The thermal-cycler design is categorized as a shunting type, which is based on the fact that PCR reaction is accomplished in three stages, each having a different temperature action. All the processes from DNA amplification and PCR based detection were carried out in a disposable prototype polycarbonate reaction-chamber. In order to eliminate potential cross-contamination between samples and to simplify device operations, several disposable identical sizes and shapes of chips were used to carry out the analysis. The chips were micro-fabricated as it has been discussed [3.3.4]. The study target DNA was extracted from *E. Coli* (strain K-12). In this chapter the investigation of PCR tests, amplification efficiency and PCR product detection will be described and

discussed. The prototype device performance was confirmed by testing PCR amplification targeting the 16S rRNA gene to acquire three sizes of PCR amplicon 250, 512 and 1500 bp respectively. In general, this system provides a cost-effective solution to a simple and efficient PCR analysis and it could have wide applications in the field of point-of-care (POC) for the diagnosis of infectious diseases.

5.1.2 System assembling

The prototype thermal-cycler and the detection unit were assembled and controlled fully by a data acquisition system through a personal computer with the control program based on C# programming language (ISO/IES 23270, 2006) as it described in section [4.2.3]. The thermal-cycler system was incorporated with the prototype photo-detector module for DNA amplification and end point detection. The system is potentially improved for DNA quantification.

The prototype thermal-cycler device is intended to create uniform heating and fast thermal response times while minimizing the energy inputrequired operating the device. The heaters were segmented into three temperature zones to allow for standardized temperature, reducing the chances for over-shooting. The greater thickness of the sample reaction chamber and the double-side heater are necessary to reduce the power and to achieve uniformity in the temperature. Figure 5.1 presents the temperature profile as a function of time for thermal cycling conducted using the thermistor-controlled heater. It was necessary to maintain the temperature at the heater to achieve the correct temperature within the chamber.

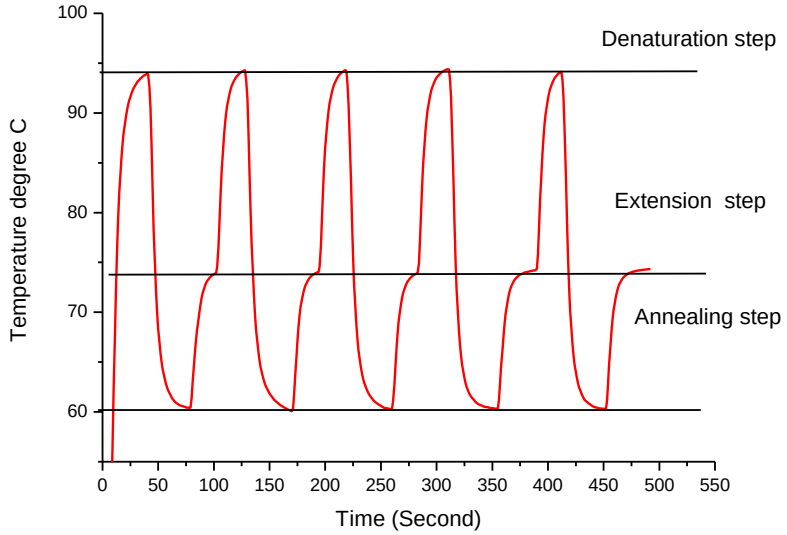

Figure 5.1 The temperature profile of the polycarbonate-chip is shown for the standard cycling parameters used on the prototype thermal-cycler. The average cycling time is less than 60 seconds and typical 40 cycles PCR reactions could be performed in 35 minutes

When differences in product yield were seen for two PCR fragments that differ only in size, the observed results can only be explained by the residence time in the extension zone approaching the kinetic limit for the PCR unless the primers differ in annealing specificity since thermal equilibration effects on product yield are unaffected by product size. In addition, since the annealing temperatures of the primer sets used for each PCR product were comparable, the denaturation/annealing kinetics cannot be used to explain the product yield differences between these two fragments. As extension times are decreased below the kinetic limit for fully extending the fragment length defined by the forward and reverse primer pair, a failed PCR reaction will result. Therefore, it is clear that under favourable thermal conditions, the fundamental limit on PCR time is highly dependent on the length of the product required.

As described in chapter four of this thesis, a blue light emitting diode (LED) (480nm, 80mW) was used as a fluorescence excitation source. This was chosen based on its ability to excite the light at 480 nm because the fluorophore dye used is SYBR Green 1, which absorbs blue light at 485 nm, and emits at 520 nm. The fluorescence detection system both excites and detects fluorescence in PCR

microchips at the end of amplification reactions. The LED is filtered using an excitation filter and laterally excites the detection microchip through a chrome-coated glass-waveguide. The whole PCR prototype device is shown in Figure 5.2.

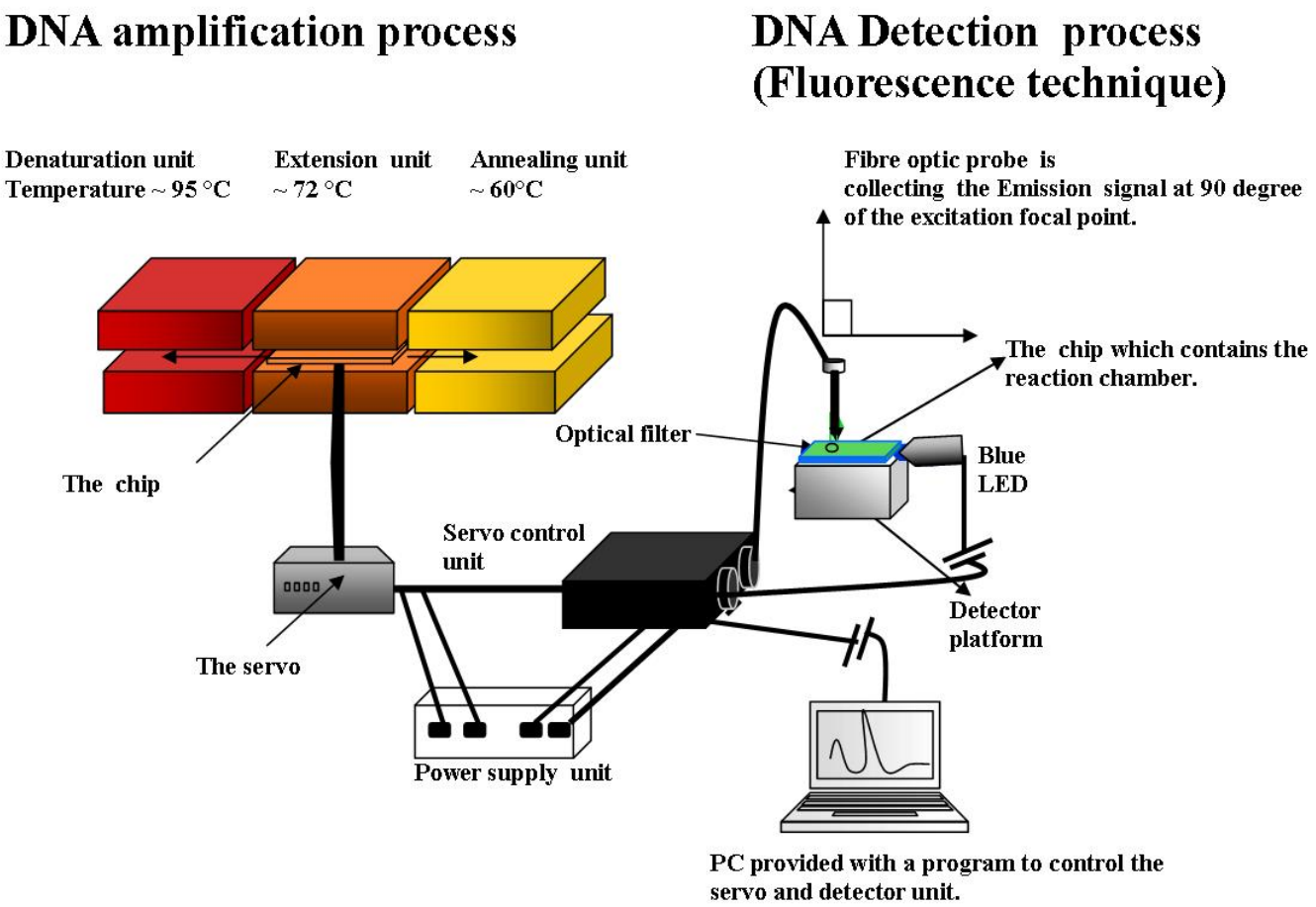

Figure 5.2 Schematic of the prototype device, the lift side shows the amplification unit which include three heaters, each heater has a constant temperature. The right side of the picture is a diagram represents the detection unit which include the excitation part (the LED lam) and the emission part (the prototype photo-detector). In addition to the data acquisition unit to control the whole device process (PC).

5.2 Materials and method

5.2.1 The Benchmark Test

In order to ensure the consistency in PCR tests, a non-pathogenic *E. coli* (K-12) culture was used to extract one lot of chromosomal DNA. This DNA was used to carry out all the PCR tests either in the conventional PCR machine or in the prototype device. The quality of the DNA was tested in the laboratory to ascertain the quality. Therefore, the DNA template utilized in the project investigation was carefully prepared and tested. As a result, a high biomass culture of *E. coli* (K12) with an optical density of 1.981 was used to extract high quality and high quantity DNA**.**

5.2.1.1 Bacterial Growth

Typically, the optical density measured in a spectrophotometer can be used as a measure of the concentration of bacteria in a suspension. As visible light passes through a cell suspension the light is scattered. Greater scatter indicates that more bacteria or other material is present. The amount of light scatter can be measured in a spectrophotometer at wavelength of 600 nm (OD_{600}). In this work, the non-pathogenic *E. coli* (K-12) culture was grown in nutrient broth medium (Oxide, UK) and incubated for 24 hours at 37°C with shaking at 120 rpm. The optical density (O.D) was then measured with a bench top spectrophotometer (Pharmacia-LKB Ultrospet III) at 600 nm.

5.2.1.2 Genomic DNA Extraction and Purity Testing

The *E. coli* (K-12) cultures were then distributed to 4 similar aliquots of 1.5 ml each and used for chromosomal DNA extraction using CTAB (Hexadecyl Trimethyl Ammonium Bromide) extraction method (Murray HG and Thompson, 1980). The protocol was as follows:

1) 15 mg of bacterial cells were collected from an agar plate and placed into a clean Eppendorf tube.
2) 500 µl of the lysis buffer were added to each tube containing 15 mg of cells and the cells resuspened carefully in the lysis buffer. In this protocol vortex never

used as it will damage the DNA and clean tubes tips were used between each tube to prevent cross contamination which will not only affect results but will contaminate the solutions used. Lysis buffer was prepared by dissolving 200 µg of proteinase K (Sigma Aldrich, UK) in 10 ml of 0.5 % Sodium dodecyl sulfate (SDS) (Sigma Aldrich, UK).

3) The tubes were placed in a float and incubated in the water bath at 55 ^{o}C for 30 minutes. During this incubation as the lysis of the cells is taking place the tubes were mixed by gently inverting them every 10 minutes.
4) The float was removed from the water bath and the tubes were opened, then 100 µl of the pre-warmed 5M Sodium chloride (NaCl) (Sigma Aldrich, UK) and 80 µl of pre-warmed CTAB (Sigma Aldrich, UK) solution were added to each tube. This step should be done as quickly as possible so that the solutions are still as close to 65 °C as possible. The lids of the tubes were closed and mixed by gentle inversion. This step can be done by holding the tubes in the float and inverting the float which therefore mixes all of the tubes at once.
5) The tubes were placed in the 65 °C water bath for 10 minutes.
6) After the 10 minute incubation time at 65 °C the tubes were removed and the lids were opened 680 µl isoamyl alcohol: chloroform (BDH, AR) (1: 24) were then added and the tubes were shaken well to form an emulsion but do not vortex.(an emulsion is achieved when the tube contents turn completely white and milky).
7) The tubes were centrifuged for 5 min at full speed (14000 rpm) to produce three distinct layers within the sample. Using a cut off tip remove the top aqueous layer into a clean Eppendorf tube. The easiest way to do this is to hold the tube at an angle and draw the aqueous layer into the tip slowly and gently. At least 600 µl of aqueous layer should be obtained.
8) The top aqueous layer removed and transferred into new clean Eppendorf tubes. This layer contains the DNA precipitate which, then washed out by adding 0.6 volumes of isopropanol (BDH, AR) (360 µl.) and mixed carefully by gently inverting the tubes.
9) The DNA precipitates were left in the tubes to completely precipitate at room temperature for 30 min.

10) The tubes were centrifuged at full speed (14000 rpm) for 10 min to pellet the DNA. Chilled centrifuge (4 °C) was used if possible as this will keep the DNA pellet on the side of the tube for longer.
11) The supernatant were pouring off gently and the tubes placed upside down on some absorbent paper to remove excess isopropanol.
12) The DNA pellets then washed by pre-chilled 70 % ethanol by gently adding 300 µl to each tube. Do not mix the tubes treat them with care – the ethanol will just wash over the pellet.
13) The tubes were centrifuged for a further 10 min at full speed (14000 rpm) using a chilled centrifuge.
14) The supernatants were pouring off gently and the tubes were placed upside down on some absorbent paper towel to remove excess ethanol.
15) The tubes were placed in a rack and the pellet allowed to air dry for 30 minutes to an hour before resuspending.
16) The DNA pellet were resuspended in 100 – 200 µl of TE (Tris with EDTA) or with RNAse water.
17) The DNA extracts from the four samples were then pooled in one tube and the purity and quantity was then tested.

In order to assess the purity of extracted DNA, the ratio of spectrophotometric absorbance of the sample at 260 nm to that of 280 nm was measured. This test was done to ensure that the DNA extracted was not contaminated with RNA or proteins. The absorption test was carried out at A_{260} and A_{280} using a Bio TEK, Synergy HT Multi-Mode Micro-plate Reader, (UK).

In order to measure the concentration of the DNA obtained, a fluorescent DNA-binding dye commercial kit was used (Quant-iT dsDNA High Sensitivity Assay Kit, Invitrogen-UK). The kit provides concentrated assay reagent (fluorophore dye), dilution buffer and pre-diluted DNA standards. This kit is easy to use and quantify dsDNA accurately. It is provided with a linear detection range between 0.2 ng and 100 ng dsDNA corresponding to initial experimental sample concentrations between 10 pg/µL and 100 ng/µL. Moreover, its fluorescence signal is unaffected by many common contaminants, including free nucleotides, salts, solvents and proteins. Due

to commercial proprietary nature of the kit, the exact compositions of the chemicals are not provided, with only commercial names being given to the components. The protocol used is as follows:

1) The assay HS reagent was diluted 1:200 times with the HS buffer provided by the supplier.
2) The diluted HS reagent (200 µl) was loaded into the first 3 wells of a fluorescence micro- well plate (Thermo Scientific, UK) and used as blanks.
3) Aliquots (5 µl) of the sevenHS DNA standards were loaded into the subsequent wells with 195 µl of diluted HS reagent. The HS DNA standards concentration used were as follows: 0.5, 1, 2, 4, 6, 8 and 10 ng/µl.
4) Triplicates of 5 µl of the unknown DNA solutions were also mixed with 195 µl diluted HS reagent and transferred to the subsequent wells.

The fluorescence measurements were taken using the Bio TEK, Synergy HT Multi-Mode Micro-plate Reader (UK).

5.2.2 PCR Primers Background Information

Three different sets of primers were used in PCR tests. The primers were selected to produce three different target sizes. Each set of primers was tested in the conventional PCR machine and in the prototype device. This experiment was performed to test the ability of the prototype device for use with differing sized amplicons across a range of 250 bp to 1500 bp. This experiment is also important to demonstrate the prototype device application. The primers sets used were as follows: PCR primer set 1 (250), PCR primer set 2 (512) and PCR primer set 3 (1500), Table 5.1 summarised the background information of the primer sets.

Table 5.1 A summary of the nucleotide sequences of the oligonucleotides used and their target genes.

Primer used	Nucleotide sequence	Target gene
Primer set 1:F AS_GC356	5`-CGCCCGCCGCGCCCCCGCCCCGG CCCGCCGCCCCCGCCCACTCCTACGGGA GGCAGC-3`	16S rRNA gene
R AS_519	5`-GTATTACCGCGGCTGCTG-3`	
Primer set 2:F	5`-AGCAACAGGCAGCAGAGGCG-3`	flavoprotein FixA
R	5`-GACGTTCGCGCTGTTTCGGC-3`	in *(E Coli*)
Primer set 3:F 11	5`GTTTGATCCTGGCTCAG-3`	Near complete
R 1512	5`GGTTACCTTGTTACGACTT-3`	16S rRNA. gene

The three sets of primers were used to perform the PCR tests on the prototype device and the results obtained were tested on agarose gel electrophoresis as a standard method to analysis the size of the DNA amplicons.

5.2.2.1 PCR Primer Set 1(250 bp)

The first primer set sequences were as follows: AS_519 as a reverse primer: (5`-GTATTACCGCGGCTGCTG-3`) and AS_GC356 as a forward primer: (5`CGCCCGCCGCGCCCCCGCCCCGGCCCGCCGCCCCCGCCCACTCCTACG GGAGGCAGC-3`). The primers were purchased from Sigma Aldrich, (UK). The master mix used was as in Table 5.2 and it was used to perform PCR tests in both conventional thermal-cycler and in prototype device.

Table 5.2 The optimum reaction mixture of 25 µl used to run the PCR for a universal primer set targeting the 16S rRNA gene at the V3 region (Ferguson *et al*, 2007).

Master Mixture	1X Reaction	Final concentration
AS_GC338F (10 µM / 100 ρmol)	2.5 µl	1 µM / 100 ρmol
AS_530R (10 µM / 100 ρmol)	2.5 µl	1 µM / 100 ρmol
Promega PCR master mix 2X	12.5 µl	1X
BSA	1 µl	0.4 mg/ml
PCR grade Water	4 µl	-
Template (240 ng/µl)	2.5 µl	24 ng/ µl

5.2.2.2 PCR Primer Set 2 (552 bp)

The second primer set was designed *de novo* to target a fragment of the putative electron transfer flavoprotein FixA as identified in the complete chromosomal genome of *Escherichia coli* K-12 substr. DH10B. The gene was adopted to obtain a PCR product length of 552 bp. The details of the primers are illustrated in Table 5.3**.**

Table 5.3 Characteristics of the primer set for flavoprotein Fix A of *E. coli* K12.

Sequence (5'->3')	Strand on template	Length	Start	Stop	Tm	GC%	MW
Forward primer	AGCAACAGGCAGCAGAGGCG	Plus	20	42548	72.3	59.97	6214
Reverse primer	GACGTTCGCGCTGTTTCGGC	Minus	20	43099	74.2	59.85	6119
Internal oligo		Plus					
Product length	552						

The primers were tested on a conventional thermal cycler (Gene AMP 9700, Applied Science, UK) in order to determine their optimal amplification conditions. The master mix used was as in Table 5.4 and it was used to perform PCR tests in both conventional thermal-cycler and in prototype device.

Table 5.4 The optimum reaction mixture of 25 µl used to run the PCR for the designed primer set.

Master Mixture	1X Reaction	Final concentration
Forward primer (10 µM / 100 ρmol)	2.5 µl	1 µM / 100 ρmol
Reverse primer (10 µM / 100 ρmol)	2.5 µl	1 µM / 100 ρmol
Promega PCR master mix 2X	12.5 µl	1X
BSA	1 µl	0.4 mg/ml
MQ Water	4 µl	-
Template (240 ng/µl)	2.5 µl	24 ng/ µl

5.2.2.3 PCR Primer Set 3 (1500 bp)

The third primer set is the bacterial universal primer described by Felske *et al* (1998). The primer sequences were as follows: 11F 5`GTTTGATCCTGGCTCAG-3`and 1512R 5`GGTTACCTTGTTACGACTT-3`. The primers were purchased from Sigma Aldrich, (UK). The master mix used was as in Table 5.5 and the same mixture was used to perform PCR tests in both conventional thermal-cycler and in prototype device.

Table 5.5 The optimum reaction mixture of 25 µl used to amplify 1500 bp of 16S .rRNA.mega gene.

Master Mixture	1X Reaction	Final concentration
11F (10 µM / 100 ρmol)	2.5 µl	1 µM / 100 ρmol
1512R (10 µM / 100 ρmol)	2.5 µl	1 µM / 100 ρmol
BSA (10 mg/ml)	1 µl	0.4 mg/ml
Promega PCR master mix 2X	12.5 µl	1X
$MgCl_2$ (25 mM) promega	1 µl	1mM
MQ Water	3 µl	-

5.2.3 PCR Reagent Preparation

The PCR experiments were categorised into three different segments based on the size of amplicons, which were amplified with three sets of primers. The 25 µl PCR reaction volumes were used in all PCR tests using Promega (USA) PCR Master Mix. Table 5.6 describes the components of the master mix.

Table 5.6 PCR Master Mix constituents were used (Promega, USA).

Master mix Constituents	Volume required in µl	Final concentration
PCR buffer 2x (*p*H 8.5) with	In 2X master Mix	1 X
$MgCl_2$ (15 mM) in the buffer		3 mM
dNTPs* (400 µM)	In 2X master Mix	0.3 mM each
Taq Polymerase (50 Unit/ml)	In 2X master Mix	2.5 U/ml

dNTPs: Deoxyribonucleotide phosphate includes: dATP (2'-Deoxyadenosine 5'-triphosphate), dGTP (2'-Deoxycytidine 5'-triphosphate , dCTP (2'-Deoxyguanosine 5'-triphosphate), dTTP (2'-Deoxythymidine 5'-triphosphate)*

5.2.4 Conventional Thermal Cycler PCR Tests/Experiments

The conventional PCR tests were performed using a Gene AMP 9700 manufactured by Applied Science, UK. The PCR master mix used in all experiments was as described in section [5.2.2 and 5.2.3].

For the primer set 1, the conventional thermal cycler was programmed as follows: holding step for 10 min at 94ºC, followed by 40 cycles with 30 second denaturation at 94º C, 1 min annealing at 60º C and 30 second extension at 72º C and a final holding step of 10 min at 72º C.

For the primer set 2, the conventional thermal cycler was programmed as follows: an initial denaturation step at 95°C for 5 minutes followed by 35 amplification cycles of 95°C for 30 seconds; 68°C for 30 seconds and 72°C for 20 seconds and final an extension step at 72°C for another 5 minutes.

For the primer set 3, the conventional thermal cycler was programmed as follows: an initial denaturation cycle 5 minutes at 94°C followed by 35 cycles of 20 seconds at 94°C, 20 seconds at 54°C, and 2 minutes at 68°C for the final extension cycle. This was followed by one 5-minutes cycle at 68°C.

All resulting PCR products were analysed on an agarose gel alongside the corresponding prototype device products.

5.2.5Prototype Device

5.2.5.1 PCR Experiments

The PCR polycarbonate chip was rinsed with sterile distilled water three times and then rinsed with analytical grade isopropanol (BDH, UK) to clean the chamber from any cross contaminants. The chip was then kept in the oven to dry at ~100°C for 30 minutes. The 25 µl of 1 µg/ml BSA (BioLabs, UK) was inserted into the reservoir chamber with micro syringe. The chip was then centrifuged for 5 seconds at 1400 rpm to transfer the BSA to the sample chamber. The chip was subsequently stored in the fridge at 4 °C overnight before it was used to perform the PCR test. The BSA

was taken out of the chamber the next day prior to PCR by spinning the chip in the centrifuge. The chip was then washed three times with PCR grade water to ensure that the chip was free of BSA.

In order to reduce or eliminate any cross contamination that may cause inhibition of the DNA amplification, the chambers were sterilised before use by incubating the chambers for 30 minutes in Ultra Violet (UV) cabinet for PCR (UV Sterilisation cabinet, Scie-Plas Ltd., UK)

The master mix used to perform the PCR tests for the three primer sets were described in Table 5.3, Table 5.4 and Table 5.5 respectively. Thus, 50 µl (or 2 reactions) were prepared in one standard Eppendorf tube (200 µl). The reaction mixture was divided into two portions, each 25 µl. The first aliquot was used as a control for comparison of PCR amplification between the conventional (Gene AMP 9700, Applied Science, UK) and prototype thermal cyclers. The control sample was run in parallel to the PCR amplification in the Perkin Elmer Gene AMP 9700 (Applied Science, UK) in order to ensure direct comparability with results obtained from the chip. The conventional thermal-cycler (Gene AMP 9700, Applied Science, UK) was programmed as described [5.2.4].

During the PCR process, 25 µl of the PCR mixture and 20 µl of mineral oil (Fisher Bio-reagent, UK) were loaded sequentially into the reservoir chamber of the prototype chip, as shown in Figure 5.3, and centrifuged for 5 second at 1400 rpm to displace the PCR mixture into the sample chamber. The mineral oil was used to avoid the formation of air bubbles during the process and also to prevent reagents from evaporating (McPherson and Moller, 2006).

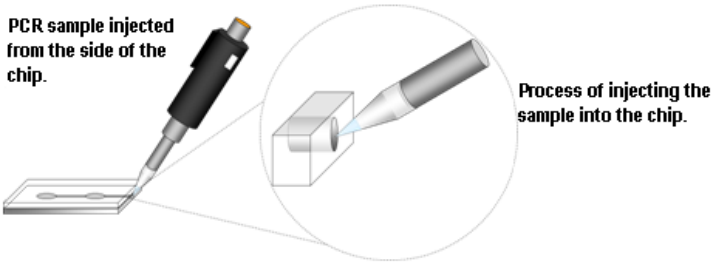

Figure 5.3 Schematic diagram illustrates how a sample is injected into the chip from the side 1 mm diameter hole using a micropipette

The chip which includes the sample chamber was shunted in between the three temperature zones of PCR process by means of a rotational servo, as has been discussed [3.3]. the device was subjected to three different cycling conditions depending on the primer set being amplified according to the tables below (Table 5.7, Table 5.8 and Table 5.9 respectively.

Table 5.7 Primer set 1 programme applied to amplify DNA fragments in size of 250 bp

Step #	Thermal cycler condition	Step description	Notes
1	Zone 1 temperature set at 95 °C for 30 seconds	Initial denaturation step.	
2	Zone 1 temperature set at 95 °C for 20 seconds	Denaturation step.	35 Cycles
3	Zone 2 temperature set at 60°C for 30 seconds	Annealing step	takes ~47
4	Zone 3 temperature set at 72 °C for 30 seconds	Extension step	minutes.
5	Zone 3 temperature set at 72 °C for 2 minuets	Final extension step.	

Table 5.8 Primer set 2 programme applied to amplify DNA fragments of size 552 bp.

Step #	Thermal cycler condition	Step description	Notes
1	Zone 1:temperature set at 94 °C for 30 seconds	Initial denaturation step.	
2	Zone 1 temperature set at 94 °C for 20 seconds	Denaturation step.	Total 35
3	Zone 2 temperature set at 68°C for 45 seconds	Annealing step	Cycles takes
4	Zone 3 temperature set at 72 °C for 45 seconds	Extension step	~63 minutes.
5	Zone 3 temperature set at 72 °C for 2 minuets	Final extension step.	

Table 5.9 Primer set 3 programme applied to amplify DNA fragments of size 1500 bp.

Step #	Thermal cycler condition	Step description	Notes
1	Zone 1:temperature set at 94 °C for 30 seconds	Initial denaturation step.	
2	Zone 1 temperature set at 94 °C for 20 seconds	Denaturation step.	35 Cycles takes ~100 minutes.
3	Zone 2 temperature set at 54°C for 30 seconds	Annealing step	
4	Zone 3 temperature set at 68 °C for 120 seconds	Extension step	
5	Zone 3 temperature set at 68 °C for 5 minuets	Final extension step.	

5.2.5.2 Agarose Gel Electrophoresis

PCR products from both devices (conventional and prototype) were ran on gel electrophoreses in a 1.5% (w/v) agarose gel (Fisher Bioreagents,UK) and visualized by staining with SYBR safe (Invitrogen, UK). The gels were stained with 3 µl of SYBR Safe per 30 ml buffer and the final concentration of SYBR safe in each gel was about 1 mg/l .The gels were then run on electrophoresis at 90V for 80 minutes. Hyper-Ladder 1 (Bioline , UK) was used as a marker for size determination of the products.

5.2.5.3 Fluorescence Test on the Prototype Device

The PCR tests on the prototype device were repeated using a commercial kit Quantification master mix (Q-PCR Master Mix) from (Promega, UK) This product contains SYBR Green1, as a fluorescence DNA-binding dye that exhibits fluorescence upon binding to dsDNA.Components of the product were as in Table 5.10.

Table 5.10 Components of 2x QuantiFast SYBR Green PCR Kit (Promega ,UK)*

Component	Features	Benefits
HotStarTaq *Plus* DNA Polymerase	5 min activation at 95ºC	Set-up of qPCR reactions at room temperature
QuantiFast SYBR Green PCR Buffer	Balanced combination of NH_4^+ and K^+ ions	Specific primer annealing ensures reliable PCR results
	Unique Q-Bond additive	Faster PCR run times, enabling faster results and more reactions per day
SYBR Green I dye	Yields a strong fluorescent signal upon binding to double-stranded DNA	Highly sensitive amplification
ROX dye	Normalizes fluorescent signals on Applied Biosystems and, optionally, Agilent instruments	Precise quantification on cyclers that require ROX dye. Does not interfere with PCR on any real-time cycler

** Also contains a dNTPs mix (dATP, dCTP, dGTP, dTTP).*

The sample chip with PCR mixture (including Q-master mix, primers and DNA template) was tested before and after completing the amplification reactions. The fluorescence measurements were taken using a spectrometer (HR4000, ocean optics, USA) spectrometer and the prototype photo-detector described in section [4.2.2].

5.3 Results and discussion

5.3.1 The Benchmark Test

The full functionality of the chip was demonstrated with DNA extracted from *Escherichia coli* as a model system. Pathogenic *E. coli* strains are responsible for infections of the enteric, urinary, pulmonary, and nervous systems. This strain was sequenced by Blattner *et al* (1997) because it approximates wild-type *E. coli* and has been maintained as a laboratory strain with minimal genetic manipulation. Blattner *et al* (1997) annotated 4288 protein-coding genes from 4,639,221-base pair sequence of *Escherichia coli* K-12.

All three primer sets utilised DNA extracted from *E. coli* to demonstrate that the system can successfully amplify and detect the nucleic acids and detect the presence of the amplicon via fluorescence optical measurements. Although the endpoint fluorescence data varies with the template concentration, the methodology is not strictly quantitative as the fluorescence measurement is not conducted concurrently with the thermal cycling.

As already discussed [1.2.3], the quality and quantity of DNA template is one of the most important factors affecting the reproducibility and comparability of PCR reaction and must be considered and controlled to set up a reliable PCR based assay. The presence of genomic DNA in the extracts was analyzed on 1.5 % (w/v) agarose gel electrophoresis and visualized with SYBR safe (Figure 5.4). All methods used to extract/purify the extracted DNA showed a good recovery of DNA.

The four vials used to collect the DNA extract then pooled in one vial to come up with homogeneous DNA quality in all investigation tests.

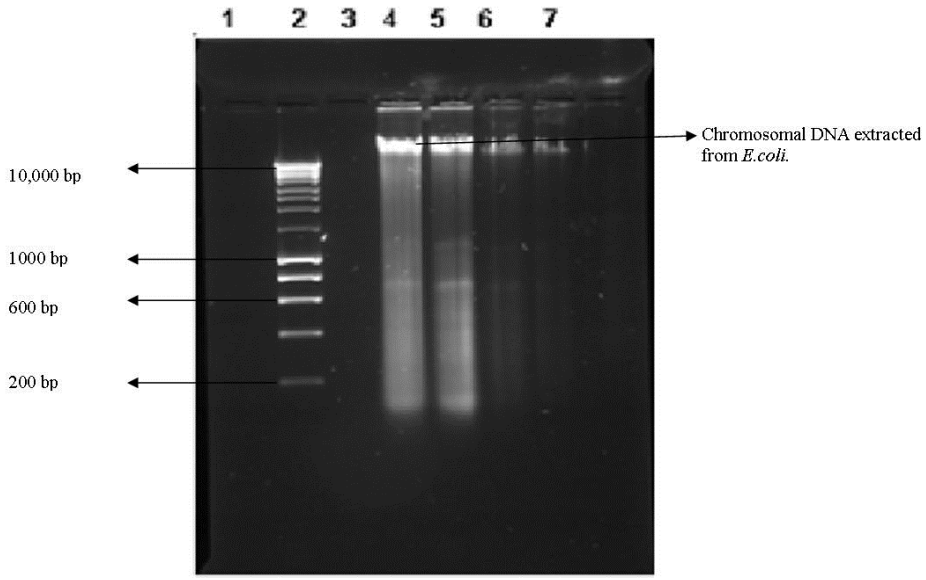

Figure 5.4 Chromosomal DNA resolutions on 1.5 % (w/v) agarose gel electrophoresis at 90V for 80 minutes. The DNA was extracted using CTAB extraction method. Lane 2: Hyperladder 1 (Bioline) marker, Lane 4: *E. coli* genomic DNA sample1, Lane 5: *E. coli* genomic DNA sample 2, Lane 6: *E. coli* genomic DNA sample 3 and, lane 7: *E. coli* genomic DNA sample 4.

The homogeneous DNA was then tested using fluorescent DNA-binding dyes (Quant-iT dsDNA High Sensitivity Assay Kit, Invitrogen-UK). The calibration plot is shown below (Figure 5.5), from this the average concentration of the DNA was calculated to be 245 ng μl^{-1}. The absorption test at ratio (A_{280}/A_{260}) of the DNA extract was 1.8 which indicates that the DNA yield is pure and free from RNA and proteins (McPherson and Muller, 2006).

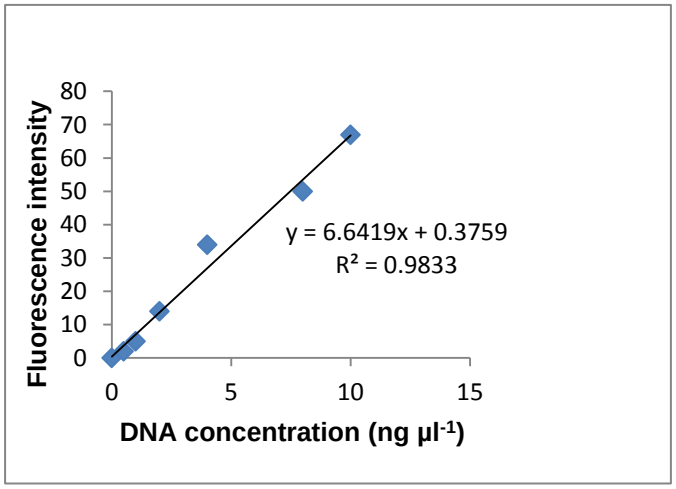

Figure 5.5 The standard curve constructed between standards dsDNA concentration and fluorescence intensity excitation at 480 nm and emission at 523 nm.

The DNA then used as template to perform the PCR using the three primer sets described in sub-sections [5.2.2.1], [5.2.2.2] and [5.2.2.3]. This experiment was carried out using conventional thermal-cycler (Gene AMP 9700, Applied Science, UK) described in section [5.2.4]. The results obtained shown in Figure 5.6 and indicate that the DNA was in high-quality to fulfil the investigations of the project.

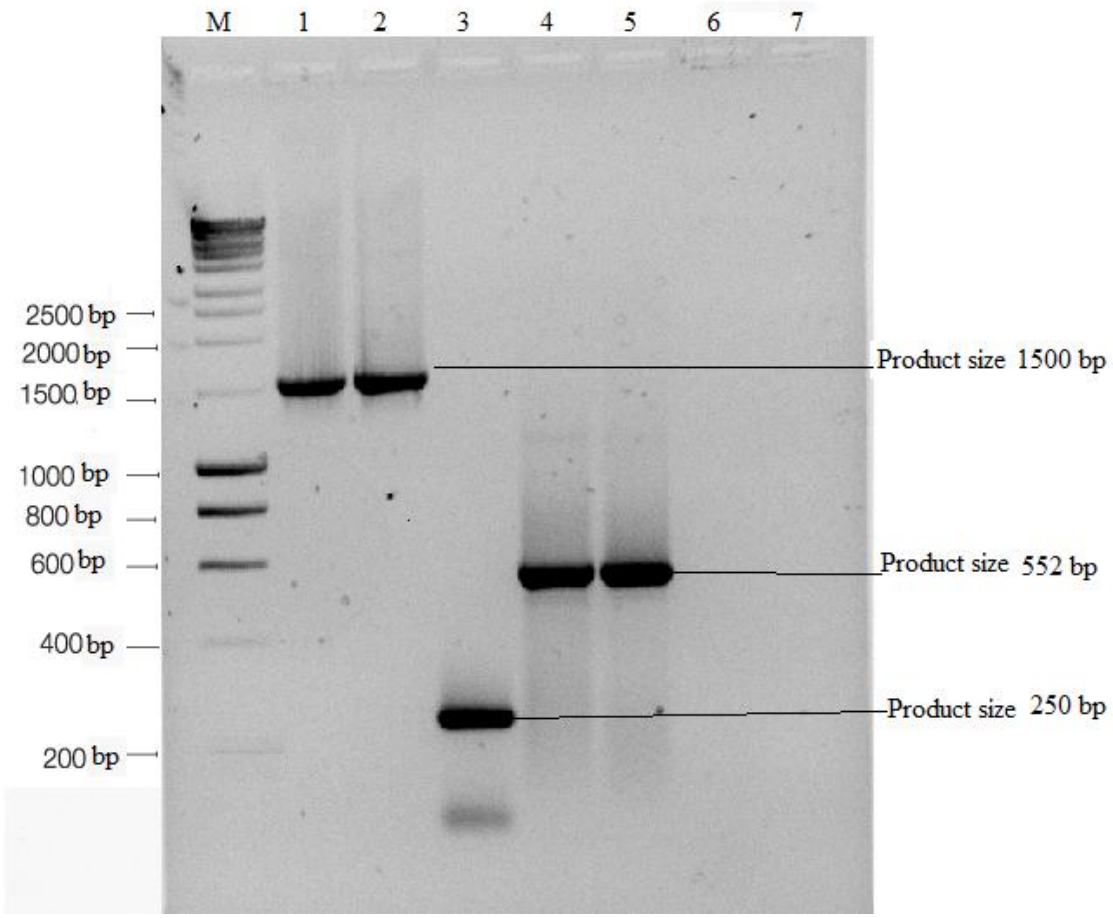

Figure 5.6 The PCR product resolutions under UV of 1.5 % (w/v) of agarose gel electrophoresis at 90V for 80 minutes. Agarose gel electrophoresis of the DNA fragments from *E .coli* was amplified on GeneAmp PCR system 9700 (Applied Biosystems) using the three primer sets. The sample arrangement was as follows: M: DNA hyper lather 1, 1 and 2: DNA fragments size 1500 bp of DNA from *E .coli* were amplified using near complete 16 S rDNA, primer set is 11F and 1512 R, lane 3: DNA fragments size 250 bp of DNA from *E .coli* were amplified using universal primers AS_530 and GC338, lane 4 and 5: DNA fragments size552 bp of DNA from *E .coli* were amplified using the designed primers set described in section 5.2.2, lane 6 and 7 Negative controls.

5.3.2 PCR Primer Set 1

5.3.2.1 Gel Electrophoresis Results

The microfluidic biochip design leverages the benefits of microfluidics including having a high surface to volume ratio and reduced diffusion times to maximize heat transfer, and uniform heating and cooling. The system proposed is based on plastic biochip as using of plastic biochips is critical in this regard as the relatively low cost of plastic manufacture allows the biochips to be disposable, eliminating the labour required to reuse the biochip and reducing the possibility of contamination. The repeatability and reproducibility of the system was evaluated by performing PCR test using primer set one to come up with a result identical to the PCR test on any conventional thermal-cycler.

In the first experiment on the prototype device, the optimized time and temperature set points for amplification of primer set 1 were shown in Table. 5.6, section [5.2.5]. The first PCR products generated from the prototype system are shown in Figure 5.7. The results demonstrate that the PCR products were obtained from thermal-cycling in the prototype polycarbonate chip using the device. The chip underwent a total of 35 thermal cycles by mechanically shunting the chip in between the thermal-cycler temperature zones for each step of the PCR process (denaturation, annealing, and extension), with the exact ratio depending on the location of each zone.

The first PCR products generated from the second prototype system as has been described in section [3.1.5] Figure 3.6. The device architecture was improved in order to rectify the temperature controller and get a precise temperature in each step of PCR cycle. Consequently, the system was produce better products and less primer dimers as can be seen in Figure 5.7, which presents the comparison between the amplicon of 250 bp that was amplified in the prototype thermal cycler and the one amplified in the Gene AMP (9700, Applied Science, UK) as a conventional thermal cycler. The tests were then repeated three times as can be seen in Figure 5.8 to confirm the ability of the prototype device in performing the PCR test on this set of primer to produce similar size of amplicons.

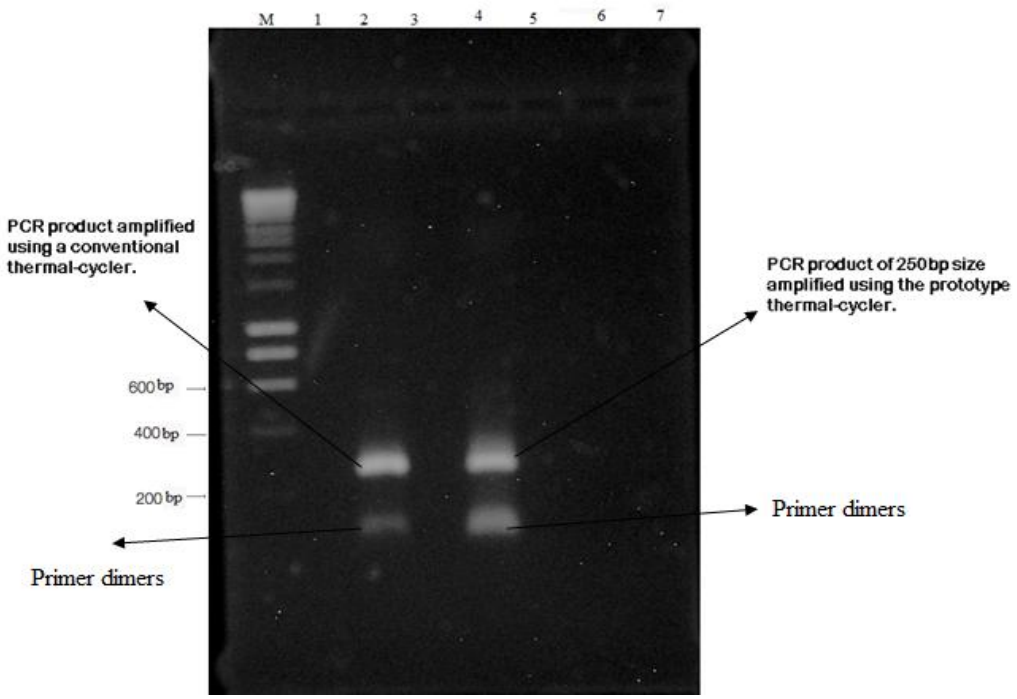

Figure 5.7 Sample resolutions on 1.5 % (w/v) of agarose gel electrophoresis at 90V for 80 minutes. Agarose gel electrophoresis of the DNA fragment from *E. coli* was amplified by PCR using AS_530R and GC338F primers. The Lane M contains Hyperladder 1 (Bioline, UK) and the Lane 3 amplicon size is 250bp amplified using Gene AMP (9700, Applied Science, UK), Lane 5 contains the amplicon amplified using the third prototype thermal-cycler.

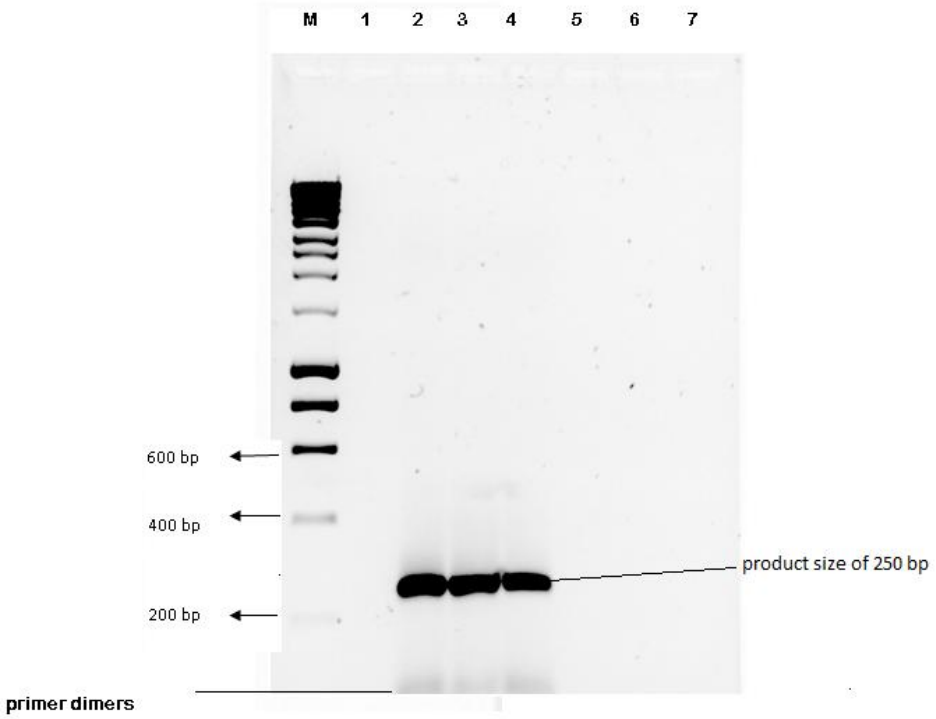

Figure 5.8 Sample resolutions on 1.5 % (w/v) of agarose gel electrophoresis at 90V for 80 minutes. Agarose gel electrophoresis of the DNA fragment from *E. coli* was amplified by PCR using AS_530R and GC338F primers. The Lane M contains Hyperladder 1 (Bioline, UK) and Lane 1 is negative sample, Lanes 2, 3, and 4 are three samples of the amplicon size is 250 bp had been amplified using the third prototype thermal-cycle**.**

The 35 cycles were completed in about 47 minutes as described in Table 5.6 and the product yield for the device was similar to that obtained using the conventional thermal cycler. The lower product yield was due to partial deactivation of the PCR mixture and/or insufficient residence time in each temperature zone in this investigation of prototype device (Wittwer *et al*, 1990).

The product yields from both devices were similar as can be seen in Figure 5.7 and Figure 5.8. The lower product yield could be due to partial deactivation of the PCR mixture and/or insufficient residence time in each temperature zone in this investigation of prototype device. Theoretically, as the system segmented into three reaction temperature zones, a 1 µg of DNA template will amplify by 20 cycles, as the 20 cycles will be enough to produce sufficient detectable PCR products as described by Saiki *et al*, (1985).

5.3.2.2 Fluorescence Results

The performance test of the device was done by fluorescence measurements for the sample chip before and after completing the amplification reactions as can be seen in Figure 5.9 and Figure 5.10.

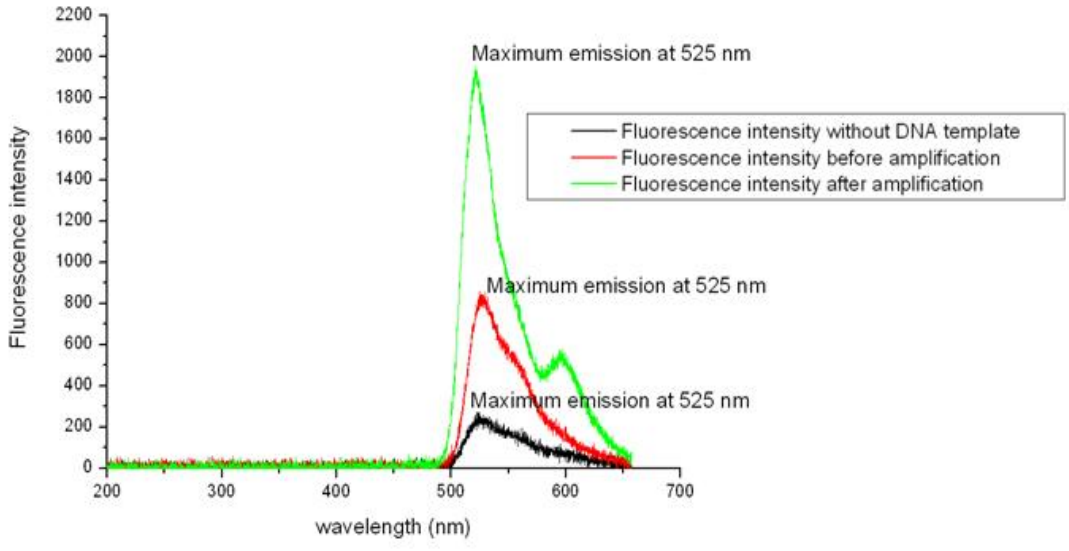

Figure 5.9 Fluorescence signal of the chip contains the PCR mix along with SYBR Green after the sample had been amplified in the device. The test performed using blue LED lamp and determined on (HR4000) spectrometer by means of 100 µm fibre optic

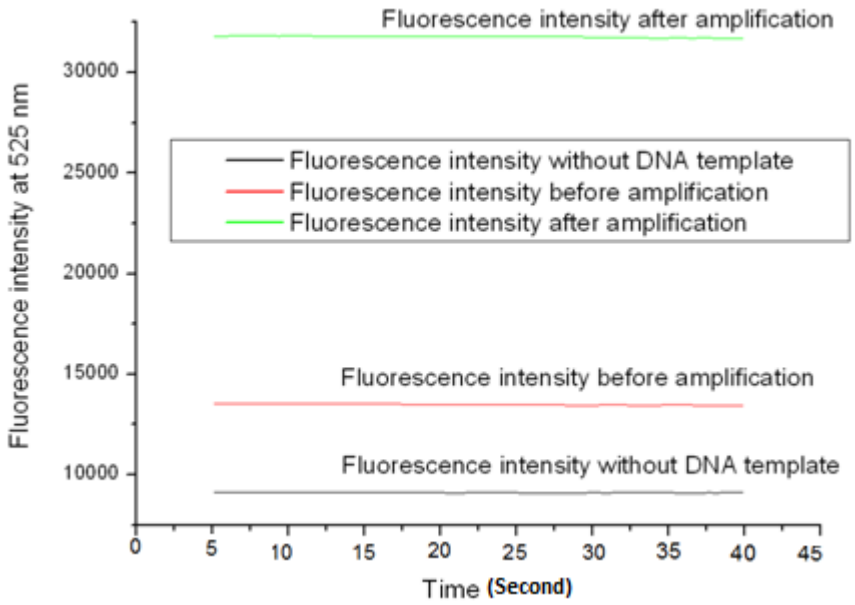

Figure 5.10 Fluorescence signal of the chip contains the PCR mix along with SYBR Green after the sample had been amplified in the device. The test performed using blue LED lamp and determined on the prototype photo-detector by means of 100 µm fibre optic.

The results reveal that there is a significant fluorescence signal produced after amplification of the sample in the prototype device and this can suggest that the target PCR amplicon has been amplified in the system.

5.3.3 PCR Primer Set 2

5.3.3.1 Gel Electrophoresis Results

The second test was performed on the primer set designed to produce DNA fragments in size of 552bp. Primer design is crucial in optimizing the polymerase chain reaction (PCR). A poorly designed primer can result in little or no target product (McPherson and Muller, 2006).

Numerous web-based or standard-alone programs for PCR primer design are available, but vary in quality and functionality. The primers chosen should be identical to specific portions of the template; this means that their sequences match the template at those places i.e. the forward primer have the same sequence of the first portion of single strand and the reverse primer has the same sequence of the last portion of the opposite single strand. The forward and reverse primers are each oriented towards the region being amplified, and thus towards each other.

In this project, the NCBI web site was used to design suitable primers to produce a ~500 bp size of PCR products. NCBI is the most popular non-commercial primer design software because of its capabilities and free accessibility. The NCBI has great flexibility to optimize a number of parameters such as product size, melting temperature (Tm), GC content, primer length, 3' end stability, self-complementarity, primer dimer possibility, position constraints and so forth to get the best primer pairs, and provides the potential to design different types of PCR primers to meet various needs. The primer set designed was selected to target a fragment of putative electron transfer flavoprotein FixA in *Escherichia coli* str. K-12 substr DH10B. In general, the putative electron transfer is a protein involved in the transport of electrons, a process by which electrons are transported through a series of reactions from the reductant, or electron donor, to the oxidant, or electron acceptor, with concomitant energy conversion. This process is necessary for both photosynthesis and aerobic respiration. The detail of the primer design was shown in Appendix 4.

The target locus is predicted to be the gene responsible for the synthesis of flavoprotein FixA in *Escherichia coli* str. K-12, which is an electron transfer flavoprotein subunit, required for anaerobic carnitine reduction. Electron transfer flavoproteins are present in eukaryotic mitochondria and serve as essential electron acceptors for at least nine dehydrogenase enzymes available in the matrix of mitochondria or peripherally associated with the matrix side of the inner mitochondrial membrane (Tsai and Saier, 1995).

The *E. coli* DNA template was amplified using the PCR protocol described in section 5.2.2 In first stage the conventional thermal-cycler (Gene AMP 9700, Applied Science, UK) programme was used to optimise the PCR reaction and the optimum conditions are described in Table 5.7. The same sample mixture was then introduced to the chip and PCR process was performed on the prototype thermal-cycler. The completed reactions (35 cycles of each process) were analyzed by gel electrophoresis to confirm amplification of the appropriately sized fragment Figure 5.11.

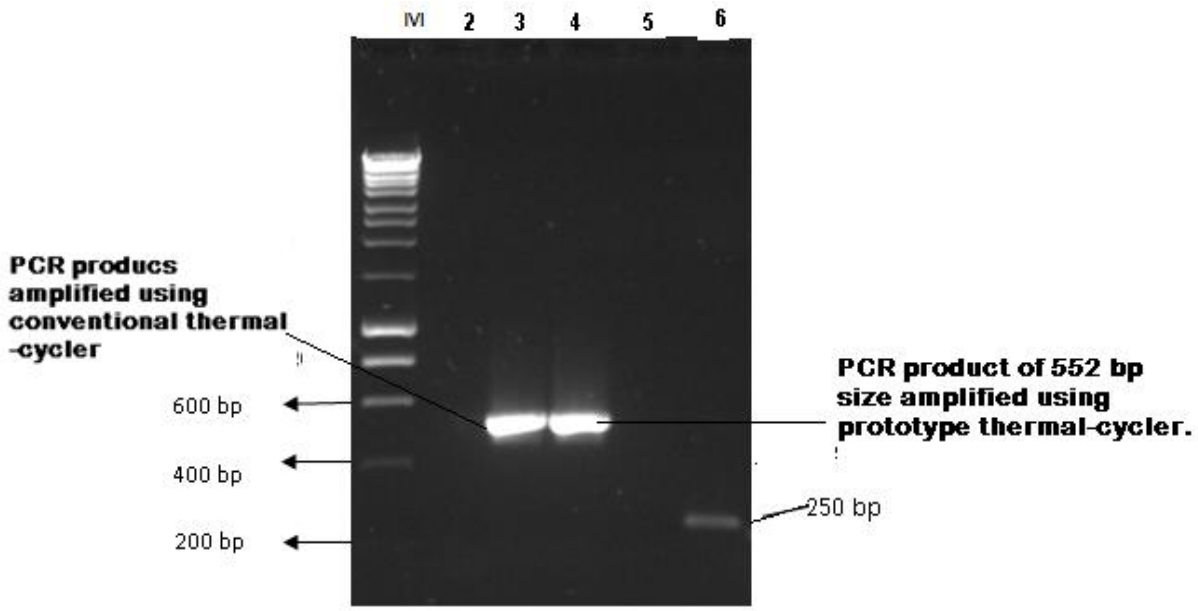

Figure 5.11 Sample resolutions on 1.5 % (w/v) agarose gel electrophoresis at 90 V for 80 minutes. The agarose gel electrophoresis of the DNA fragment from *E .coli* was amplified by PCR using designed primers, M contains Hyper ladder 1, Lane 2 negative control the amplicon size is 552 bp visualized in Lane 3 was amplified using GeneAmp PCR system GeneAMP 9700 (Applied Biosystems, UK) and lane 4 contains the sample which was amplified using the prototype thermal-cycler. Lane, Lane 6 empty and Lane 7 DNA amplicon size 250 bp for comparison amplified by the universal primer set described in section [5.2.2].

The results demonstrate the success of the primer design because the product attained is absolutely as predicted. The size of the amplified product was 552 base pair fragment. The amplification of 552 base pair fragments specific for *E. coli* K12 primers revealed positive amplification of 552 base fragments with DNA template extracted from *E. coli* K12. The PCR process then had been applied using the prototype thermal-cycler device, the protocol described in section 5.2.2, in order to demonstrate the ability of the prototype thermal-cycler to achieve the same fragments. The same PCR master mix and same primer concentrations were introduced in the prototype chip. The amplification process of the prototype thermal-cycler was tested on 1.5 % (w/v) agarose gel as normal PCR product. The result obtained is illustrated in Figure 5.12. Therefore, one of the objectives of this study was the use the prototype thermal-cycler to complete amplification of the DNA template and specific detection of specific DNA target is achieved.

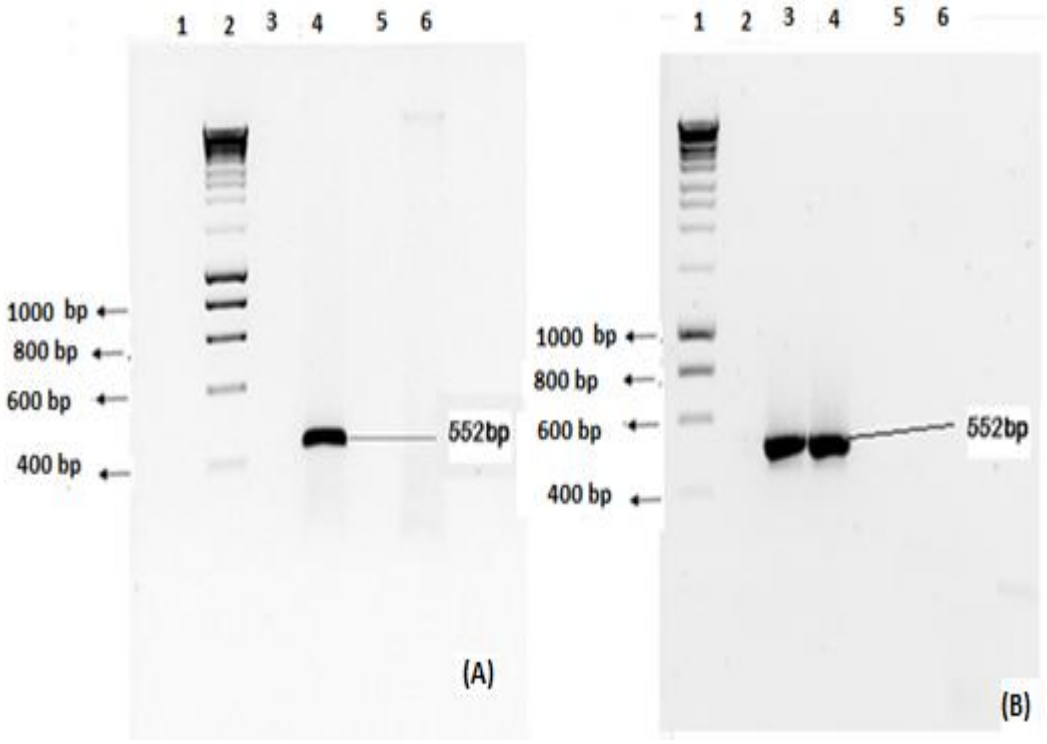

Figure 5.12 Two agarose gels for sample resolutions on 1.5 % (w/v) in 1× TBA of agarose gel electrophoresis at 90 V for 80 minutes. Agarose gel electrophoresis of the DNA fragment from *E .coli* was amplified by PCR using the designed primers, the amplicon size is 552 bp amplified in the prototype device. 12.5 µl of PCR product were placed in each lane.In **(A)** Lane 1,empty, Lane 2 contains Hyper ladder (Bioline, UK), Lane 3 empty and Lane 4 contains the target amplicon size is 552 bp amplified in the prototype device, Lane 5,6 sample empty. In **(B)** Lane 1empty, Lane 2 contains Hyper ladder (Bioline, UK), Lane 3 and Lane 4 contains the target amplicon size is 552 bp amplified in the prototype device Lane 5,6 sample empty

5.3.3.2 Fluorescence Results

The performance test of the device was done by fluorescence measurements for the sample chip before and after completing the amplification reactions as can be seen Figure 5.13 and Figure 5.14**.**

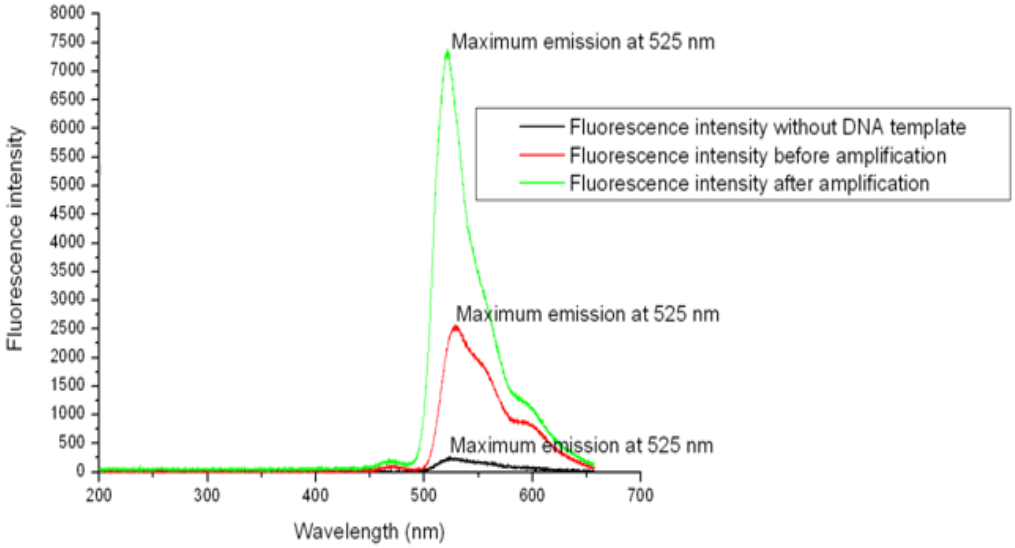

Figure 5.13 Fluorescence signal of the chip contains the PCR mix along with SYBR Green after the sample had been amplified in the device. The test performed using blue LED lamp and determined on (HR4000) spectrometer by means of 100 µm fibre optic

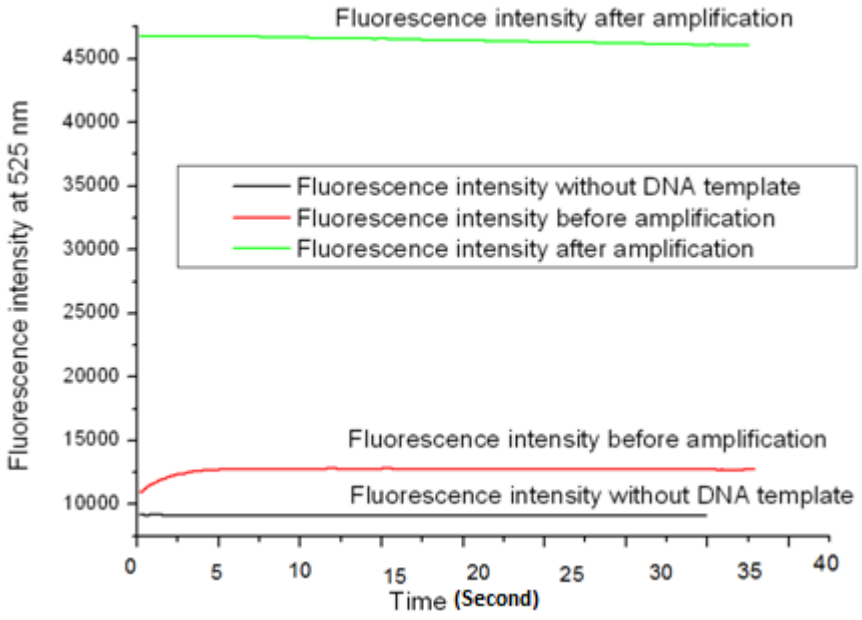

Figure 5.14 Fluorescence signal of the chip contains the PCR mix along with SYBR Green after the sample had been amplified in the device. The test performed using blue LED lamp and determined on the prototype photo-detector by means of 100 µm fibre optic.

The results reveal that there is a significant fluorescence signal produced after amplification of the sample in the prototype device and this can induce that the target PCR amplicon have been amplified in the system.

5.3.4 PCR Primer Set 3

5.3.4.1 Gel Electrophoresis Results

The 16S rRNA gene is common to all Bactria. This gene could be used as a genetic marker to detect bacteria phylogeny and taxonomy due to the following reasons:

1) It is a common gene in almost all bacteria, often existing as a multigene family, or operons.
2) The function of the 16S rRNA gene over time has not changed, suggesting that random sequence changes are a more accurate measure of time (evolution);
3) The near16S rRNA gene (1500 base pair) is large enough for informatics purposes.

The third primer set tested was near complete 16S rRNA. This gene was used as a feasibility tool to evaluate the ability of the prototype thermal-cycler to amplify a large size PCR product. This size of PCR product is a challenge for PCR-on-a-chip devices. For the first validation the PCR kit (Promega master mix and primers) was optimised on conventional thermal-cycler GeneAmp PCR system manufactured by Applied Biosystems, the result obtained can be seen in Figure 5.15. The same samples were introduced to the prototype thermal-cycler and optimised according to the prototype thermal-cycler condition to achieve the best thermal-cycler programme. After several attempts, the optimum conditions were achieved. The conditions summarised in Table 5.9. At the end of amplification process on both techniques, the samples were applied on 1.5 % agarose gel in order to verify the PCR products obtained, the result obtained can be seen in Figure 5.16. The products obtained are not as successful as those from the conventional PCR due to the condition of the temperature control in prototype thermal-cycler. However, better results could be achieved by enhancing the quality of the temperature control system in the device in future work.

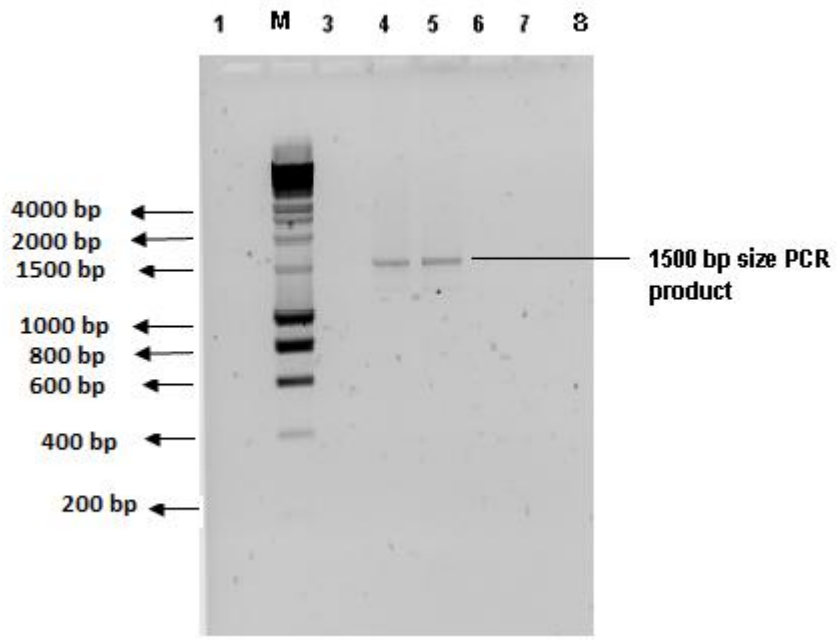

Figure 5.15 Sample resolutions on 1.5 % (w/v) of agarose gel electrophoresis at 90 V for 80 minutes. Agarose gel electrophoresis of the DNA fragment from *E .coli* was amplified by PCR using near complete 16S rRNA gene. 12.5 µl of PCR products were placed in each lane. Lane 5 was amplified using GeneAmp PCR system (9700 Applied Biosystems, UK) and Lane 6 contained the sample which was amplified using the prototype thermal-cycler, Lane 2 contains Hyper ladder 1, Lane 4 negative control, Lane 7 and 8 are empty

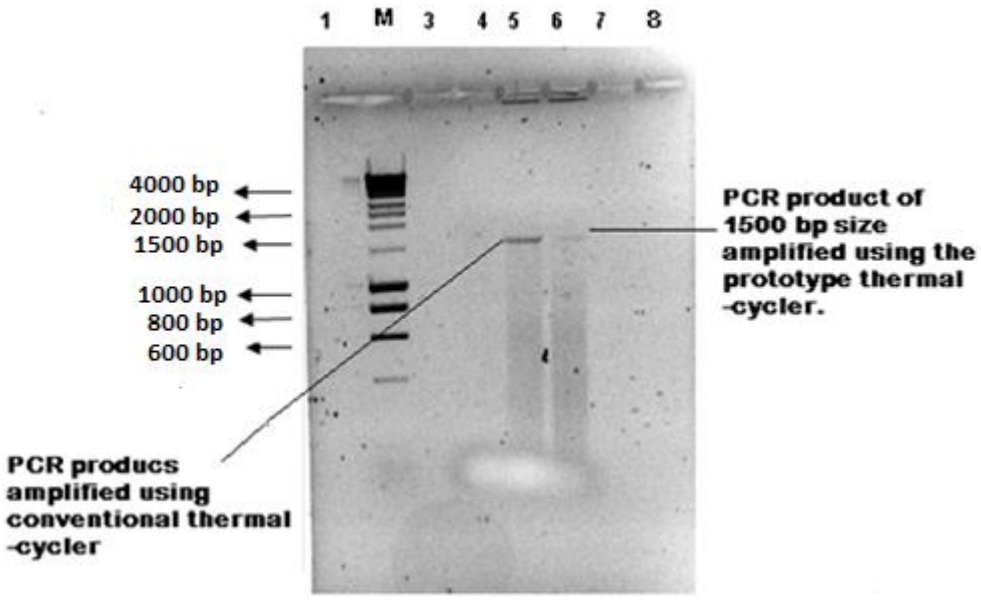

Figure 5.16 Sample resolutions on 1.5 % (w/v) of agarose gel electrophoresis at 90 V for 80 minutes. Agarose gel electrophoresis of the DNA fragment from *E .coli* was amplified by PCR using near complete 16S rRNA gene. 12.5 µl of PCR products were placed in each lane. Lane 5 was amplified using GeneAmp PCR system (9700 Applied Biosystems, UK) and Lane 6 contained the sample which was amplified using the prototype thermal-cycler, Lane 2 contains Hyper ladder 1, Lane 4 negative control, Lane 7 and 8 are empty.

The prototype device was set-up according to the protocol described in Table 5.9. The microbiological analyses were considered to be the "reference method" to evaluate the performance of the novel prototype device with clinical samples. Compared with conventional thermal-cyclers, the sample chamber of the prototype chip used in this project is characterised by significantly larger surface-to-volume ratio [2.6].

5.3.5.2 Fluorescence Results

The performance test of the device was done by fluorescence measurements for the sample chip before and after completing the amplification reactions. The PCR products were eventually analyzed by gel electrophoresis to confirm amplification of the appropriately sized fragment. For these controls, the entire sample chip and PCR reaction was performed for accurate comparison to the positive controls. These negative controls provide evidence that there is no amplification in the fluorescence signal. However, there is a significant fluorescence signal obtained in the positive sample as can be seen in Figure 5.17 as the H4000 Ocean Optic spectrophotometer was used to take the measurements and Figure 5.18 as the prototype photo-detector was used to take the measurements. The result of the positive sample was obtained after 35 cycles. As described in Chapter 4 the SYBR Green binds to any double stranded DNA, a non-specific increase in dsDNA can give rise to fluorescence signal. Therefore, the significant signal of the sample before adding the DNA template as can be seen in the small peaks (Figure 5.17 and Figure 5.18) and the effective limits of detection for this system are appropriate to reactions that reach the threshold fluorescence level within 35 cycles.

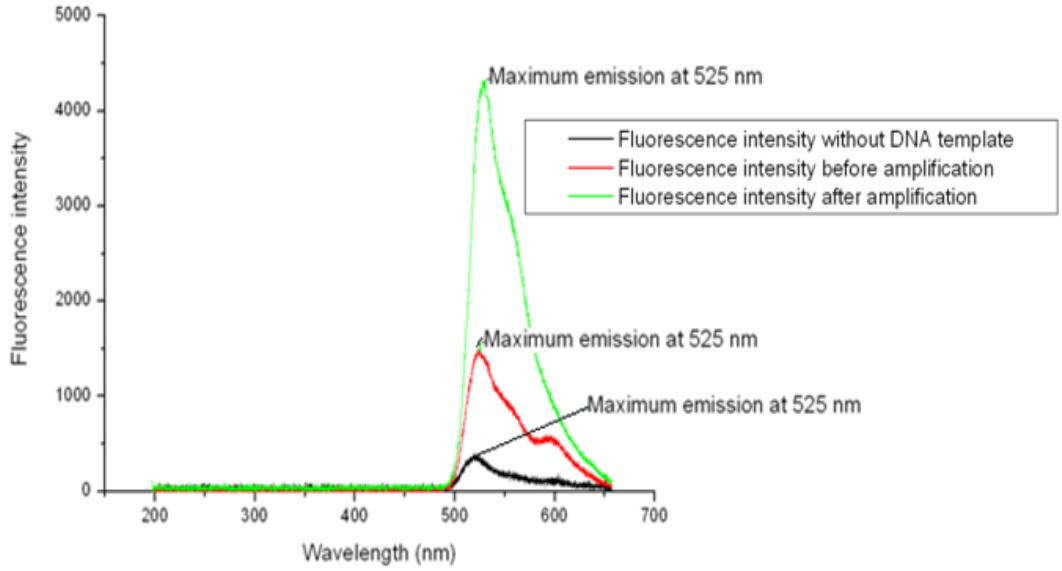

Figure 5.17 Fluorescence signal of the chip contains the PCR mix along with SYBR Green after the sample had been amplified in the device. The test performed using blue LED lamp and determined on (HR4000) spectrometer by means of 100 µm fibre optic.

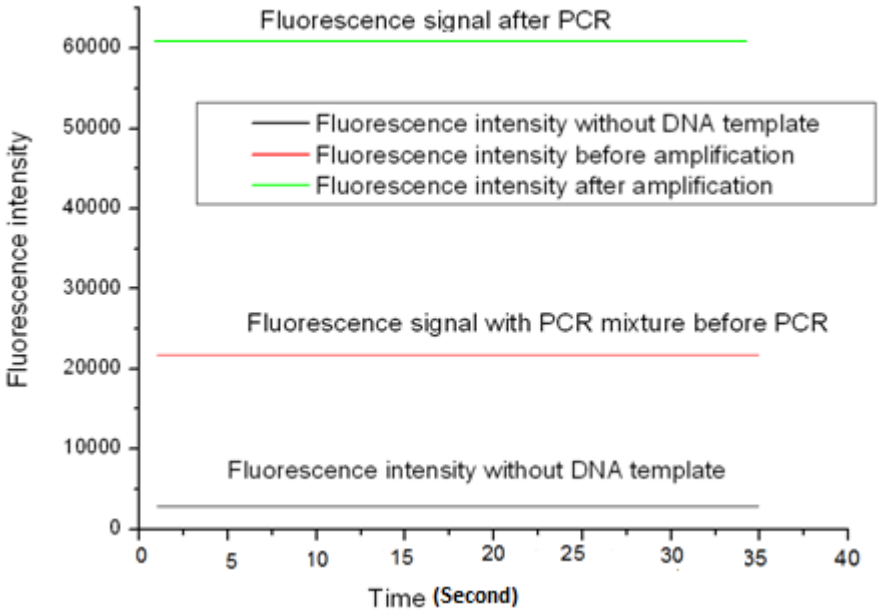

Figure 5.18 Fluorescence signal of the chip contains the PCR mix along with SYBR Green after the sample had been amplified in the device. The test performed using blue LED lamp and determined on the prototype photo-detector by means of 100 µm fibre optic.

5.4 Conclusion

Many types of chromosomal DNA have been used to evaluate the feasibility of PCR-on-a-chip devices produced by the researchers. The applications include pathogenic and non-pathogenic bacterial genomic DNA for example *E. coli* had been reported by Matsubara *et al*, (2005); Hu *et al*, (2006); Jia *et al*, (2005) and Niu *et al*, (2006), *Salmonella typhimurium* had been reported by Easley *et al*, (2006), *Neisseria meningitides* and *Staphylococcus aureus* had been reported by Liao *et al*, (2006). Wang *et al*, (2009), also tested viral genomic DNA for hepatitis C virus (HCV) and hepatitis B virus (HBV). Xing and Zhang (2009) had evaluated the ability to perform DNA amplification on a compact continuous-flow polymerase chain reaction (PCR) for rapid analysis of genetically modified organisms (GMOs) in genetically modified soybeans.

In this study, a miniaturized PCR system was developed to allow for nucleic acid amplification and on-line detection of infectious diseases. The chromosomal DNA used in this work was extracted from non-pathogenic K-12 subtype of *Escherichia coli*. The new shunting PCR system was comprised of a fine polycarbonate chip and double side heater thermal-cycler. The programmed servo was used as a control module to transfer the polycarbonate chip, which contains the PCR mixture, between the three reaction regions. With this approach, the time ratios of each reaction and cycle numbers for the entire PCR process can be adjusted to any optimal value. Moreover, the three double sides heating and temperature sensing were used to generate three specific reaction temperatures with high thermal uniformity. In this device, the time ratios of each reaction and cycle numbers for the entire PCR process can be adjusted to any optimal value. The investigations were shown that the proposed system was capable of performing PCR amplification with different annealing temperature range from 54 to 68°C, targeting three different sizes of PCR products 250, 552 and 1500 bp. The prototype thermal-cycler and PCR chip were successfully used to amplify the three sizes and the results were compared with same fragments amplified on a conventional PCR thermal-cycler machine. The method used for comparison was gel electrophoresis. In addition, a fluorescence detection system was employed for detecting of PCR products using SYBR Green I

fluorescent dye. Thus, the development of this miniaturized PCR system may provide a useful platform for molecular diagnosis.

Chapter 6 Future work

6.0 Introduction

In this project, a device for DNA amplification and end-point PCR detection was investigated. In an improvement over other systems, the device was robustness in method of amplifying DNA based on PCR technique and fluorescence detection. This approach of PCR thermal-cycling sample and detection is imperative for environmental or otherwise complex samples since a variety of contaminants can inhibit PCR amplification. Three different sizes of DNA fragments provided a benchmark for instrument performance. As reported here, the fluorescence detector limits of detection in the chip for this system are approximately 7.8 pM of FITC dye and 1.4 ng/ml of dsDNA .The average time required for DNA purification during these experiments was flexible and depended upon the application, but it is apparently shorter than conventional bench-top PCR mechanises.

6.1 Rational of the device

The motivation behind growing development of miniaturized systems is certainly due to their potential commercialization, but the challenge is the production of practical higher performance and throughput design. The key market for lab-on-a-chip or μ-TAS devices applications can be categorized into four consumers segments according to their market size: in vitro diagnostics, drug discovery, biotechnology, and ecology (Mark *et al,* 2010).

However, in vitro diagnostics can be subdivided into point-of-care testing either for self-testing or for marker testing in emergency medicine. The second user is central laboratory-based testing (e.g. core laboratory in a hospital). This market segment requires high sample throughput and low costs per test. Drug discovery in the pharmaceutical industry and ecology laboratories become in the third largest segment. The μTAS devices since the small reaction volumes per assay and partly the liquid control systems are based on microfluidic platforms. The significant market for repetitive analyses, which allows high development costs for proprietary, optimized systems, does not necessarily require a platform approach, but can benefit

from microfluidic production technologies and liquid handling systems (Mark *et al*, 2010).

Innovations technology can be ideal by identifying essential requirements of a certain application, e.g. portability, low reagent consumption and high precision for point-of-care diagnostics. This can be against the characteristics of the available devices.

This section will attempt to compare the strengths and limitations of the presented device with similar micro-fluidic devices published. The given plan characteristics are based on the reviewed literature and the experience of the authors, taking into consideration properties such as the material of the disposable, necessary processing equipment, production technologies, sensitivity and process speed.

The main contributions of this project are the design, implementation and demonstration of an end-to-end lab-on-a chip system for DNA analysis that is truly low cost to for mass production. The field of microfluidic total analysis systems promises low-cost solutions by miniaturizing and automating traditionally labour and reagent intensive processes. However, many of the innovations are complicated and expensive to manufacture and/or made of materials that are not robust for commercial application. To minimize the complexity and cost of the disposable component, completely passive chip was designed in a planar format that can be fabricated by injection moulding technique, as described in section [2.3.6]. Hence, this work describes a significant step towards the implementation of a μ-TAS to replace traditional clinical nucleic acid analysis, which has applicability in modern clinical labs as well as in more challenging environments such as at the patient point-of-care or in resource limited settings. The system described was designed as a proof-of-concept for a point-of-care setting. The device method is expected to be easily extendable to gram-negative bacteria targets or viral targets. Moreover, as the μ-TAS technology has been shown to be effective at isolating nucleic acids from physiological samples, as has been discussed in [2.5], the system potentially improved to be attached with miniaturised DNA purification system. Therefore, the system is also readily extendable to detect pathogens from clinical samples. Future work will be directed towards demonstrating it.

In comparison with the conventional thermal-cyclers, the prototype thermal-cycler device is intended to create uniform heating and fast thermal response times while minimizing the power required operating the device. The heaters were segmented into three temperature zones to allow for standardized temperatures, reducing the chances for over-shooting. The greater thickness of the sample reaction chamber and the double-side heater are necessary to reduce the power and to achieve uniformity in the temperature.

The chip was fabricated using Polycarbonate (PC), which is environmentally friendly plastic and could be recycled (Liu *et al*, 2009). The time consumption for amplification is feasible, as can be seen in Table 6.1. Furthermore, power consumption of the proposed thermal-cycler is small, and the device is capable of being integrated in battery supplied portable compact analysis or diagnostic systems. The device is practically portable and affordable for pathogen diagnostics.The proposed device will be integrated real time PCR system with florescence detection.

In this device, the disposal microchips were thermally cycled for 35 cycles using the same parameters described for purified DNA reactions, as has been described in section [5.2]. Fluorescence measurements were made at the end of the amplification phase and completed reactions were analyzed by gel electrophoresis to confirm amplification of the appropriately sized fragment. Because SYBR Green I bind to any double stranded DNA, a non-specific increase in dsDNA can give rise to fluorescence and potential false positive results. Therefore, the effective limits of detection for this system are limited to reactions that reach the threshold fluorescence level within 35 cycles. In this technique, an increasing fluorescence signal is measured online, which enables direct assessment of results after PCR without additional detection steps. The utility of this system can also be extended to other organisms and incorporate alternative fluorogenic PCR techniques. Compared with the conventional gradient PCR machine, the proposed system has several obvious advantages including, simple, inexpensive, faster amplification rate, easy operation and portable. Along with the thermal-cycler structure, a fine polycarbonate chip was fabricated. A fine disposable PCR chip was developed in this work for rapid DNA amplification.

Guttenberg *et al,* (2005) had reported a system based on Surface Acoustic Waves (SAW) method, which are mechanical waves with amplitudes of typically a few nanometres. The surface acoustic waves are generated by a piezoelectric transducer chip (e.g. quartz) fabricated by placing inter-digital electrodes (inter-digital transducer, IDT) on top of a piezoelectric layer. A PCR protocol has been implemented on the SAW platform, based on 200 nL droplets and an additional heating element placed underneath the substrate surface for temperature cycling while the droplet is at rest. The main advantages of the segmented flow microfluidic platform are the small volume liquid segments (controllable with high precision in the nanolitre range), acting as reaction confinements. This leads to little reagent consumption as well as a high number of different experiments that can be performed within a short period of time, which makes the platform a promising candidate for high-throughput screening applications, as in the pharmaceutical industry. The quasi-batch-mode operation scheme within nanolitre to microlitre-sized droplets is beneficial since it represents a consistent further development of classic assay protocols as in well plates. The large number of existing unit operations enables the effective manipulation of the liquid segments. Furthermore, the completely enclosed liquid droplets allow the incubation and storage of liquid assay results over a long period of time without evaporation. However, a limitation of the platform is that handling of small overall sample volumes is not possible due to the volume consumption during the run-in phase of the flow within the microchannels. This and the manual connection to external pumps renders the platform less suitable for point-of-care applications. Another drawback is the need for surfactants that are required for high stability of the plugs. They sometimes interfere with the (bio-)chemical reaction within the plugs and thus can limit the number of possible applications on the platform (Mark *et al,* 2010).

Easley *et al,* (2006) showed integrated DNA purification, PCR, electrophoretic separation and detection of pathogens in less than 30 minutes. The assay was performed on a pressure driven four layer glass/PDMS chip with elastomeric valves. Temperature cycling for PCR was achieved by IR radiation. Only the sample lysis step was not integrated in the microfluidic chip. Detection of Bacillus anthracis from

infected mice and Bordetella pertussis from a clinical sample was successfully demonstrated.

Budge *et al,* (2009) had reported an integrated μTAS system for the detection of bacteria including lysis, DNA purification, PCR and fluorescence readout has also been published recently. A microfluidic plastic chip with integrated porous polymer monoliths and silica particles for lysis and nucleic acid isolation was used for detection. A custom-made base device provided liquid actuation and off-chip valving by stopping liquid flow from the exits of the chip, utilizing the incompressibility of liquids. Detection of 1.25×10^6 cells of Bacillus subtilis was demonstrated with all assay steps performed on-chip.

Xing & Zhang (2009) had evaluated the ability to perform DNA amplification on a compact continuous-flow PCR system for rapid analysis of Genetically Modified Organisms (GMOs) in genetically modified soybeans. The continuous-flow PCR presented here has been shown to be a new technique for the detection of GMOs. The systems described are highly convenient for use in routine GMO identification analysis. The amplification of the P35S and the Tnos sequences could be successfully completed within approximately 9 min on this compact, spiral, channel-based, continuous-flow PCR microfluidics; thus, the amplification rate was much faster than that of the conventional PCR machine. In addition, the lower detection limit of DNA sample in the presented continuous-flow PCR microfluidics was estimated to be 0.005 ng /μl.

Budge *et al,* 2009 had presented a fully integrated lab-on-a-chip and associated instrument for the detection of bacteria from liquid samples. The system conducts bacterial lyses, nucleic acid isolation and concentration, polymerase chain reaction (PCR), and end-point fluorescent detection. The PCR thermal cycling was achieved with a ceramic heater and air-cooling, while end-point fluorescence detection was accomplished with an optical spectrometer; all integrated in the instrument. The integrated functionality of the chip was demonstrated using Bacillus subtilis as a model bacterial target. A Taq-man assay was employed on-chip to detect the isolated bacterial DNA.

Cady *et al*, 2005 A miniaturized, fully automated, PCR-based detection system has been developed for the rapid detection of bacterial pathogens. Monolithic DNA purification/real-time PCR silicon chips were fabricated and tested for their ability to purify and detect the pathogeneic bacterium *Listeria monocytogenes*. Using an automated detection platform with integrated microprocessor, pumps, valves, thermocycler and fluorescence detection modules, microchips were used to purify and detect bacterial DNA by real-time PCR amplification using SYBR Green fluorescent dye. Between 104 and 107 *L. monocytogenes* cells could be detected using this system with an average turnaround time of 45 min.

Wang *et al*, (2009) had described a moisturized PCR system similar to our design. The system categories as flow-through PCR chip, which was comprised of two micro modules for thermal and microfluidic control. This system is parallel to shunting design. The microfluidic control module with three S-shape micropumps could rapidly transport the PCR mixture through three reaction regions, as has been described in [2.6.3] and Figure 2.18. With this approach, the time ratios of each reaction and cycle numbers for the entire PCR process can be adjusted to any optimal value. This feature is also available in our system. However, the drawback of this model is the fabrication of the chip PDMS-based material may inhibit PCR amplification process, as has been described in [2.4].

Table 6.2 shows the complete comparison between our device and the same PCR devices proposed by other respect researchers.

Table 6.1: This table demonstrate comparison between our device with the similar proposed devices already published, the judgment based on the main key features required to built Point-Of-Care devices.

Device reference	Detection Technique	Sample Size	Speed (Heating /Cooling rate)	Disposability	Portability	Sensitivity	Drawback	Potential use
Lagally *et al*, 2001	Fluorescence	200 nL	20 °C/second	Reusable chip	Yes	20 starting DNA template copies/µl	Complex, difficult to use	Central Lab.
Bruckner *et al*, 2002	No detection unit	24 µL	Heating rate 3 °C/ second Cooling rate 1.6 ° C/ second	Renewable column (need washing)	Yes	Qualitative	No detection unit, limited usage	Point-Of-Care
Zou et al, 2002	No detection unit	20 µL	Heating rate 34-50 °C/ second Cooling rate 23-31 °C/ second	Reusable chip	NO	Qualitative	No detection unit, Fast but Similar to Conventional thermal-cycler	Central Lab.
Cheng *et al*. 2005	No detection unit	4.5 µL	~ 12 °C/ second	Reusable tube	Yes	Qualitative	No detection unit, Need washing.	Point-Of-Care
Chang *et al*, 2006	No detection unit	15 µL	Heating rate 38 °C/ second Cooling rate 7.9 °C/ second	Reusable	Yes	Qualitative	No detection unit, not easy to use	Point-Of-Care
Jia *et al*, 2007	No detection unit	25 µL	10 °C/ second.	Disposal chip	Yes	Qualitative	No detection unit, Thermal-cycler similar to conventional one.	Point-Of-Care
Budge *et al*, 2009	Fluorescence	7 µL	Heating rate ~ 10°C/ second Cooling rate ~5 °C/ second	Reusable system	Yes	end-point fluorescent detection	Complex and not practical	Point-Of-Care
Wang *et al*, 2009	Fluorescence	22 µL	Inevitable	Reusable system	Yes	10 copies/µl	Not easy fabricate	Point-Of-Care
Chung *et al*, 2010	No detection unit	40 µL	8.7 °C/ second	Disposable	Yes	External detection	Not easy to fabricate	Point-Of-Care
Our Prototype system	**Fluorescence**	**25 µL**	**Heating rate of 1.8 °C/ second Cooling rate of 2 °C/ second.**	**Disposable**	**Yes**	**end-point fluorescent detection, online can detect 100 pg/µl DNA**	**Advantage is easy to fabricate and low cost**	**Point-Of-Care**

As has been discussed in section [4.3], the sensitivity of the detection unit in comparison with a number of investigators works; there have been many attempts to integrate fluorescence detection with microfluidic chips. Edel *et al,* (2004) demonstrated the use of polyfluorine based (polymer LED) as light source, avalanche photodiode as a detector with Limit Of Detection (LOD) of 1 µM for fluorescein dye. Yao *et al,* (2005) had fabricated a microfluidic device with an integrated OLED excitation source and on-chip fluorescence detection using a pinhole and interference filter for masking the excitation light. A LOD of 3 µM was achieved for Alexa 532 dye. Kim *et al,* (2006) demonstrated a compact device using an Organic Light Emitting Device (OLED) a slight source and an integrated p-i-n photodiode as a detector, with interference filter to mask the excitation light and secured a LOD of 10 µM of TAMRA dye. Pagliari *et al*. (2009) recently demonstrated a promising new light source technology an inherently polarised light source using electro- spun light-emitting-polymer nano-fibres. Banerjee *et al,* (2010) had been able to successfully measure Rhodamine 6G down to 10 nM by means of a thin microfluidic chamber that used organic devices both as optical sources OLED and detectors (organic photodiode). A cross-polarisation scheme, placed on the both side of the chamber, was used to mask the pump light from the signal detector. However, our prototype photo-detector system has successfully secured a LOD of 19.7 pM of FITC.

Thus, the development of this miniaturized PCR system may provide a useful platform for molecular diagnosis. The main goal in the future work is developing modular PCR system appropriate for point-of-care (POC) application and could perform more efficient PCR process in less number of cycles.

6.2 Future work to improve the thermal-cycler design

Temperature control plays a crucial role in PCR successful amplification. Wang *et al,* (2012) have proposed a DSPIC based temperature controller especially for the micro-fluidic PCR system. This microcontroller consists of a high precision, stable performance sensor, in addition to an actuator, which can achieve a high heating and cooling rate. The system contains software programmed to control a PT100 temperature sensor. However, the proposed device only required a high performance control system to improve the stability of the temperature in each temperature zone of the system. Therefore, this system could be inserted in our proposed thermal-cycler in order to achieve a high precision temperature control system.

The thermal cycler design and control system can be improved according to the fundamental investigations discussed in Chapter 3. The three prototype models of a thermal-cycler provided the basic concepts to a greater extent in terms of a temperature control system and automation. Therefore, the study of the thermal-cycler could be improved as follows:

1) A temperature control system is essential part of the thermal-cycler operation system in order to maintain the PCR mixture at precise temperature in each single step of PCR process.
2) Improvement of the automation system is important to control the timing of each PCR operation step. The control unit of the system should to be able to organize transformations of the chip in between the three temperature zones according to the user prerequisite. This control unit can be achieved by integrating the unit with a built-in robot control system, which can be programmed by the user.

6.3 Future work in chip

The work done to create the sample chamber in the chip could be improved as follows:

1) The chip fabrication method.
2) The size of sample.

3) Multiplication of the sample chamber in the same chip.

The same sample chip described in [3.3.1] could be used as a base for improvement. In chip fabrication, the main improvement necessary in future work is to achieve efficient and rapid thermal control at the same time with micro-chip array. Accordingly, two main objectives will be investigated: scaling down the size of the sample chamber and improving the fabrication method.

The chip could be improved as follows: the sample chamber could be scaled down by reducing the thickness of the chip from 1 mm to 100 μm. In order to facilitate inserting the PCR mixture in this size of chip, 100 μm thickness, the suggested chip could be designed to have two main faces: a face with a thickness of 1 mm for the sample admission and the other face with a thickness of 100 μm, as can be seen in Figure 6.1. The fabrication methods could be used to achieve this design is hot-embossing and injection moulding method, which have been described in [2.3.4] and [2.3.6].

.

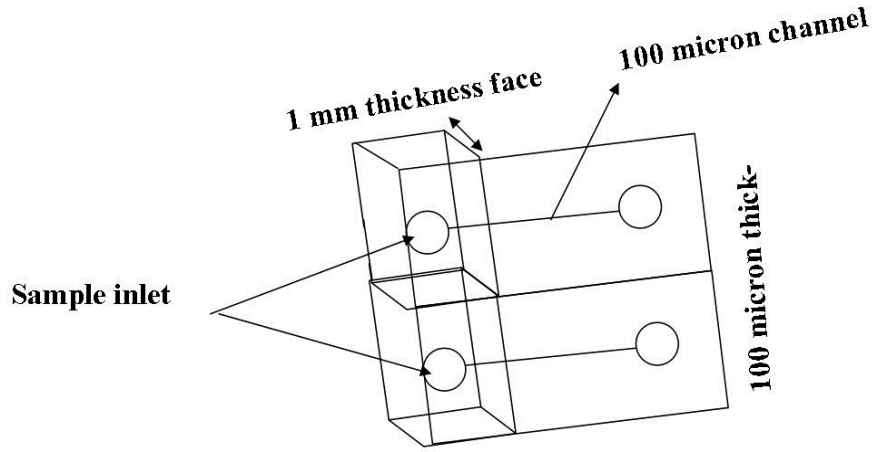

Figure 6.1 Schematic diagram is describing the suggested development in chip design.

6.4 Future work in the detection unit

The photo-detector used in this project is promising and novel and could be improved by different ways:

1) Signal enhancement: the fluorescence signal could be improved by placing a mirror at the bottom of the chip.
2) The expected change in the detector set up could take account of the geometry of excitation and emission. That is, the perfect excitation angle could be 45 degrees as an alternative of 90 degrees as in the current system.
3) As it has been discussed in [4.1.2], fluorescence-based optical detection measuring the intensity of the fluorescence signal resulting from the interaction between the fluorescent dyes/probes and an increasing amount of dsDNAs is commonly used for the quantification-PCR detection. This method provides a high sensitivity and can quantify the PCR products in real-time without performing slab gel or capillary electrophoresis. However, the accuracy of the fluorescence detection system and the discrepancy in the PCR efficiency induced by thermal cycling can influence the reproducibility of the miniaturized PCR system. The threshold (Ct) value and standard curves are usually used to determine the reproducibility and amplification efficiency of a PCR system. Therefore, the main objective of the future work is to develop a high accuracy micro system can perform nucleic acid amplification and real-time detection on a single chip.

6.5 Device application

The common problem of epidemic diseases is their ability to spread easily by either direct or indirect contact between patients or the environment, or via patients and medical personnel. It is considered to be an important risk factor for communicable infections, which continue to be a challenge for the general community but especially clinicians, hospital epidemiologists and administrators (MRSA, NHS, 2011).

In developing a pathogen detection system, efforts have been mainly focused on the detection of the pathogen genome very sensitively and accurately. In cases such as *Staphylococcus aureus*, gram positive bacteria that are responsible for a significant numbers of blood stream infectious diseases (Banada *et al*, 2012). Many strains of this bacterium have the ability to cause a variety of life-threatening diseases,

including: steomyelitis and septic arthritis, skin infections, endocarditis and meningitis. Moreover, *S. aureus* was one of the most rapidly growing bacterial pathogens in term of resistance to commonly used antibiotics. The most common pathogenic strains of this bacterium are methicillin-resistant *Staphylococcus aureus* (MRSA) and vancomycin-resistance *S. aureus* that are capable of growing in the presence of many commonly used antibiotics (Balaban *et al*, 2000).

Methicillin-resistant *Staphylococcus aureus* (MRSA) is a bacterium that causes infections in different parts of the body and it is spread by direct contact with the infected individual. It is carried by about 1 to 3 % of the UK population, although most of them are not infected (MRSA, NHS, 2011). Since it was discovered in 1961, MRSA has become one of the most common pathogens that cause nosocomial infections or hospital acquired infections (HAI) throughout the world. MRSA is commonly classified into two groups: hospital-acquired MRSA (HA-MRSA) and community acquired MRSA (CA-MRSA). The CA-MRSA is common in locations such as jails, gyms and day care facilities (Banada *et al*, 2012).

The staphylococcal chromosome cassette *mec* (SCC*mec*) is the genetic element that carries the methicillin resistance gene (Katayama *et al*, 2000). Methicillin resistance gene *mecA* is transferred from cell to cell if *SCCmec* is transmissible by phage transduction or if some other genetic transfer system specific for the movement of SCC*mec* exists. The *mecA gene is* integrated into the *orfX* gene in the *S. aureus* genome in a site specific manner (Hiramatsu *et al*, 2002; Katayama *et al*, 2000). The Staphylococcus cassette chromosome (*SCCmec*) genetic element of MRSA was characterised by Ito *et al* (1999) and Katayama *et al* (2000) which led to the elucidation of the entire *mec* region in the *mec* locus as a novel mobile (Hiramatsu *et al*, 2002).

According to Katayama *et al*,(2000) MRSA contains a class of genomic element designated SCC*mec* in a size of (52 kb) and SCC*mec* carries a set of unique recombinase genes, *ccrA* and *ccrB*, that are specifically involved in the recombination events (integration and excision)of SCC*mec* with the *S. aureus* chromosome. The ccr recombinases are also characteristic in that their NH2-terminal thirds had a substantial homology to the recombinases of the invertase/resolvase

family, whereas the integrases of bacteriophage lambda and conjugative transposons belong to the integrase family of site-specific recombinases. The characteristic serine residue that is considered to offer the hydroxyl group that attacks the DNA molecule in the strand exchange reaction is conserved among the recombinases of the invertase/resolvase family and in ccr proteins as well, but ccr proteins also differ considerably from the recombinases of the invertase/resolvase family in that they possess much larger COOH-terminal domains than those possessed by the recombinases belonging to this family.

Furthermore, Rago *et al* (2012) identified 5-types of SCC cassettes in the HA-MRSA types I to III and types IV and V in CA-MRSA strains. Specifically, methicillin resistance in staphylococci is caused by PBP2a protein encoded by the *mecA* gene. The *mecA* gene is located on a mobile genetic element, designated as staphylococcal cassette chromosome *mec* (SCC*mec*), which contains the *mec* gene complex (the *mecA* gene and its regulators) and the *ccr* gene complex encoding site-specific recompenses responsible for the mobility of SCC*mec* (Katayama *et al*, 2000).

In most cases, researchers have declared that culturing is the method used to diagnose the majority of bacterial infections, which can take many hours to days. Thus, physicians will typically prescribe a broad-spectrum antibiotic drug therapy at the initial examination and then change the therapy as needed upon receipt of the culture results (Huletsky *et al*, 2004). This practice has contributed to the rise of antibiotic resistance and is often ineffective at treating the patient. Moreover, some infectious agents are difficult to culture with standard laboratory procedures, contributing to the number of unidentified cases. To address these concerns, rapid diagnostics have been developed. Two main methods are now applied, immunoassays and nucleic acid tests. The immunoassays are often limited by inadequate sensitivity and/or specificity while nucleic acid-based tests are expensive (Huletsky *et al*, 2004). As a result, many DNA-based tests have been developed to detect MRSA.

During the past decade, a number of PCR and real-time quantitative PCR based assays have been employed and proposed for rapid detection of *mecA*. However,

disadvantages for PCR were raised as time required by post determination for each detection assay, high risk of cross contamination and low detection limit levels (Xu *et al*, 2011). The researchers found when clinical samples contain a mixture of coagulase negative staphylococci (CNS), methicillin sensitive S. aureus (MSSA), and MRSA, a positive *mecA* PCR can be generated by CNS while both MSSA and MRSA generate a positive PCR for the *coa* or the *nuc* gene. Only culturing could confirm MRSA. Huletsky *et al*, (2004) had described a real-time multiplex PCR assay that is useful for the detection of MRSA directly from specimens containing a mixture of staphylococci. This assay comprised five primers specific to the various SCC*mec* right extremity (SRE) sequences, including three new sequences, in combination with a primer and three molecular beacon probes (MBPs) specific to the *S. aureus* chromosomal *orfX* gene located to the right of the SCC*mec* integration site. This assay also increased awareness for the risk and hazard of MRSA and MRCNS strains and demands for tests capable of early, cost-effective, timely, and sensitive detection of *staphylococci* and associated antibiotic resistance. The determinants of the assay has made these tests an urgent necessity. Thus, its correct and rapid detection is essential for robust and timely control management strategies particular in hospitals.

As a result, one of the main future recommendations is particular focus on developing and evaluating a rapid and flexible testing method based on PCR assays for differentiation of MRSA and applying these assays to detect several strains from various clinical samples.

Most molecular methods for identification of *S. aureus* have been PCR-based and a range of primers designed to amplify species-specific targets were developed. The genes targeted include the nuclease (*nuc*), coagulase (*coa*), protein A (spa), femA and femB, Sa442, 16S rRNA and surface-associated fibrinogen-binding protein genes (Brown *et al*, 2005). For example, Liao *et al*, (2005) targeted the *coa* and *mecA* genes in *S. aureus* to generate amplicons of 816 and 533 bp, respectively. These primers Table 6.1 were, therefore, also used in the current study to test our PCR device.

Table 6.2 A summary of the *S. aureus* detection primer sets.

Name of the gene	Amplicon size	Primers sequence
coag	816 bp	F:5` CGAGACCAAGATTCAACAAG 3` R:3` AAAGAAAACCACTCGCATCG 5`
mecA	533 bp	F:5` AAAATCGATGGTAAAGGTTGGC 3` R: 5` AGTTCTGCAGTACCGGATTTGC 3`

Weller (1999) studied the distribution of *mecA*, *mecR1* and *mecI* in a genetically diverse collection of staphylococcal species. The researcher designed and tested a primer set of the following sequence: F 5'-GTGGAATTGGCCAATACAGG-3' R 5`-TGAGTTCTGCAGTACCGGAT-3` that detected the *mecI* gene by PCR and produced a 1339 bp fragment to. He showed that at least four *S. aureus* sub-species of the same strain fully expressed methicillin resistance despite the presence of an intact *mecI* gene and *mec* promoter region. Since, the reported method was suitable to detect MRSA, the detection of *mec*A gene by PCR was also considered as a practical standard for the device application in the present programme. Specifically, DNA positive control of MRSA strains should be used during test amplifications with specific primers.

Another approach for detection of MRSA was described by Xu *et al*, (2011) as they had developed and evaluated a testing method based on multiplex PCR assays for differentiation of MRSA, MSSA, MRCNS, MSCNS and non *staphylococci* strains, and applying these assays to detection of a large scale of MRSA and MRCNS strains from various clinical samples. The method used was based on detecting any *staphylococcal* species using as an internal control to the elimination of other bacterial pathogens. The primers used were corresponding to *Staphylococcus*-specific region of the 16S rRNA gene.

The primer sequence were as follows: (C1: 5'-GATGAGTGCTAAGTGTTAGG -3' and C2:5'-TCTACGATTACTAGCGATTC-3'), with an expected 542 bp amplicon. The method used to distinguish between *S. aureus* and CNS strains based on amplification of the *S. aureus* specific *femA* gene and the primers sequence were as follows: (F1:5'-AAAGCTTGCTGAAGGTTATG-3' and F2:5'-TTCTTCTTGTAGACGTTTAC-3', with an expected 823 bp amplicon. Moreover, to provide an indication of the possibility that the staphylococci present in the specimen

are resistant to methicillin, the method used was based on amplification of the *mecA* gene and primer sequence were: M1:5'-GGCATCGTTCCAAAGAATGT-3' and M2:5'-CCATCTTCATGTTGGAGCTTT-3' with an expected 374 bp amplicon.

Thus, the developed method can potentially be also used to differentiate between different types of MRSA especially the CA-MRSA and HA-MRSA strains. The end point detection could be accomplished by measuring the fluorescence signals from the interaction between the fluorescent dye e.g. SYBR Green1 and the increasing amount of dsDNAs. Furthermore, the system software could be improved to be used as a real time PCR system by measuring the fluorescence signal using the prototype photo-detector then calculating the Ct value as done for conventional real PCR system, see section [4.1.2].

References

Auroux, P.A., Koc,Y., deMello, A., Manz,A. and Day, P.J.R. (2004)' Miniaturized nucleic acid analysis', Lab Chip, 4(6), pp. 534-546.

Baier, T., Hansen-Hagge, T.E., Gransee, R., Crombé, A., Schmahl, S., Paulus, C., Drese, K.S., Keegan, H., Martin, C., O'Leary, J.J., Furuberg, L., Solli, L., Grønn, P., Falang, I.M., Karlgård, A., Gulliksen, A. and Karlsen, F. (2009) 'Hands-free sample preparation platform for nucleic acid analysis', Lab on a Chip - Miniaturisation for Chemistry and Biology, 9(23), pp. 3399-3405.

Balban N., L. Vincent Collins, James S. Cullor, Emma B. Hume, Enrique Medina-Acosta, Olney Vieira da Montta, Richard O'Callaghon, Paul V. Torres (2000) 'Prevention of diseases caused by *Staphylococcus aureus* using peptide RIP', Peptides 21, pp. 1301-1311.

Banada P.P., Soumitesh Chakravorty, Darshini Shah, Michele Burday, Fermina M. Mazzella, David Alland (2012)'Highly Sensitive Detection of *Staphylococcus aureus* Directly from Patient Blood', PLoS ONE, Volume 7 (2), e31126.

Banerjee, A., Shuai, Y., Dixit, R., Papautsky, I. and Klotzkin, D. (2010) 'Concentration dependence of fluorescence signal in a microfluidic fluorescence detector. Journal of Luminescence', 130(6), pp. 1095-1100.

Becker, H. and Gärtner, C. (2008) 'Polymer microfabrication technologies for microfluidic systems', Analytical and Bioanalytical Chemistry, 390(1), pp. 89-111.

Booth, C.S., Pienaar, E., Termaat, J.R., Whitney, S.E., Louw, T.M. and Viljoen, H.J. (2010) 'Efficiency of the polymerase chain reaction. Chemical Engineering Science', 65(17), pp. 4996-5006.

Brown. I.A (2001) Gene Cloning and DNA Analysis-An Introduction. Fourth Edition edn. Blackwell Science Ltd., Oxford, UK, pp. 176-194.

Brown Derek F. J., David. Edwards, Peter M. Hawkey, Donald Morrison, Geoffrey L. Ridgway, Kevin J. Towner and Michael W. D. Wren, (2005) 'Guidelines for the laboratory diagnosis and susceptibility testing of methicillin-resistant *Staphylococcus aureus* (MRSA)', Journal of Antimicrobial Chemotherapy 56, pp.1000–1018.

Berthier .J and P. Silberzan (2006) 'Microfluidics for Biotechnology', Artech Hause,INC. (UK).

Bruckner L.C.J., Tsukuda, T., Dockendorff, B., Follansbee, J.C., Kingsley, M.T., Ocampo, C., Stults, J.R. and Chandler, D.P. (2002) 'Renewable microcolumns for automated DNA purification and flow-through amplification: From sediment

samples through polymerase chain reaction', Analytica Chimica Acta, 469(1), pp. 129-140.

Bustin, S.A. (2010). The PCR revelution (Basic Technologies and Applications). First edition edn. UK: Cambridge University press.

Cady, N.C., Stelick, S., Kunnavakkam, M.V. and Batt, C.A. (2005) 'Real-time PCR detection of Listeria monocytogenes using an integrated microfluidics platform. Sensors and Actuators', B: Chemical, 107(1 SPEC. ISS.), pp. 332-341.

Chang, Y., Lee, G., Huang, F., Chen, Y. and Lin, J. (2006). Integrated polymerase chain reaction chips utilizing digital microfluidics. Biomedical Microdevices, 8(3), pp. 215-225.

Chen, J., Wabuyele, M., Chen, H., Patterson, D., Hupert, M., Shadpour, H., Nikitopoulos, D. and Soper, S.A. (2005) 'Electrokinetically synchronized polymerase chain reaction microchip fabricated in polycarbonate', Analytical Chemistry, 77(2), pp. 658-666.

Cheng, J., Hsieh, C., Chuang, Y. and Hsieh, J. (2005) 'Performing microchannel temperature cycling reactions using reciprocating reagent shuttling along a radial temperature gradient', Analyst, 130(6), pp. 931-940.

Cho, Y.-., Kim, J., Lee, Y., Kim, Y., Namkoong, K., Lim, H., Oh, K.W., Kim, S., Han, J., Park, C., Pak, Y.E., Ki, C.-., Choi, J.R., Myeong, H.-. and Ko, C., (2006) 'Clinical evaluation of micro-scale chip-based PCR system for rapid detection of hepatitis B virus', Biosensors and Bioelectronics, 21(11), pp. 2161-2169.

Christensen, T.B., Pedersen, C.M., Gröndahl, K.G., Jensen, T.G., Sekulovic, A., Bang, D.D. and Wolff, A. (2007) 'PCR biocompatibility of lab-on-a-chip and MEMS materials', Journal of Micromechanics and Microengineering, 17(8), pp. 1527-1532.

Chung, K.H., Park, S.H. and Choi, Y.H. (2010) 'A palmtop PCR system with a disposable polymer chip operated by the thermosiphon effect', Lab on a Chip - Miniaturisation for Chemistry and Biology, 10(2), pp. 202-210.

Dorrington, A. A.,Kunnemeyer, R.. (2002). A Simple Microcontroller Based Digital Lock-In Amplifier for the Detection of Low Level Optical Signals. 1st IEEE International Workshop on Electronic Design, Test and Applications (DELTA 2002), 29-31 January 2002, Christchurch, New Zealand, pp 486-488.

Duan, R., Zhou, X. and Xing, D. (2010) 'Electrochemiluminescence biobarcode method based on cysteamine? gold nanoparticle conjugates', Analytical Chemistry, 82(8), pp. 3099-3103.

Easley, C.J., Karlinsey, J.M. and Landers, J.P. (2006) 'On-chip pressure injection for integration of infrared-mediated DNA amplification with electrophoretic separation', Lab on a Chip - Miniaturisation for Chemistry and Biology, 6(5), pp. 601-610.

Edel, J.B., Beard, N.P., Hofmann, O., DeMello, J.C., Bradley, D.D.C. and DeMello, A.J. (2004) 'Thin-film polymer light emitting diodes as integrated excitation sources for microscale capillary electrophoresis', Lab on a Chip - Miniaturisation for Chemistry and Biology, 4(2), pp. 136-140.

Fang, T.H., Ramalingam, N., Xian-Dui, D., Ngin, T.S., Xianting, Z., Lai Kuan, A.T., Peng Huat, E.Y. and Hai-Qing, G. (2009) 'Real-time PCR microfluidic devices with concurrent electrochemical detection', Biosensors and Bioelectronics, 24(7), pp. 2131-2136.

Felske A,Wolterink A, van Lis R and Akkermans ADL (1998) 'Phylogeny of the main bacterial 16S rRNA sequences in a Drentse grassland soils (The Netherlands)', Appl. Environ. Microbiol. 54, pp 871–879.

Fiorini, G.S. and Chiu, D.T. (2005) 'Disposable microfluidic devices: Fabrication, function, and application', BioTechniques, 38(3), pp. 429-446.

Frey, O., Bonneick, S., Hierlemann, A. and Lichtenberg, J. (2007) 'Autonomous microfluidic multi-channel chip for real-time PCR with integrated liquid handling', Biomedical Microdevices, 9(5), pp. 711-718.

Ferguson1 A.S., W.E. Huang, K.A. Lawson1, R. Doherty, O. Gibert, K.W. Dickson,A.S. Whiteley, L.A. Kulakov, I.P. Thompson4, R.M. Kalin and M.J. Larkin. (2007) 'Microbial analysis of soil and groundwater from a gasworks site and comparison with a sequenced biological reactive barrier remediation process', The Society for Applied Microbiology, Journal of Applied Microbiology 102 ,pp1227–1238

Giese, H., Lam, R., Selden, R. and Tan, E. (2009) 'Fast multiplexed polymerase chain reaction for conventional and microfluidic short tandem repeat analysis', Journal of forensic sciences, 54(6), pp. 1287-1296.

Giordano, B.C., Ferrance, J., Swedberg, S., Hühmer, A.F.R. and Landers, J.P. (2001) 'Polymerase chain reaction in polymeric microchips: DNA amplification in less than 240 seconds', Analytical Biochemistry, 291(1), pp. 124-132.

Gong, H., Ramalingam, N., Chen, L., Che, J., Wang, Q., Wang, Y., Yang, X., Yap, P.H.E. and Neo, C.H. (2006) 'Microfluidic handling of PCR solution and DNA amplification on a reaction chamber array biochip'. Biomedical Microdevices, 8(2), pp. 167-176.

Guttenberg, Z., Müller, H., Habermüller H., Geisbauer, A., Pipper, J., Felbel, J., Kielpinski, M., Scriba, J. and Wixforth, A.,(2005) Planar chip device for PCR and hybridization with surface acoustic wave pump, Lab on a Chip, 5, pp 308–317.

Harris, S. and Jones, D.B. (1997) 'Optimisation of the polymerase chain reaction', British journal of biomedical science, 54(3), pp. 166-173.

Hashimoto, M., Chen, P.-., Mitchell, M.W., Nikitopoulos, D.E., Soper, S.A. and Murphy, M.C. (2004) 'Rapid PCR in a continuous flow device', Lab on a Chip - Miniaturisation for Chemistry and Biology, 4(6), pp. 638-645.

Higuchi, R.. (1993) Kinetic PCR Analysis- Real-time Monitoring of DNA', Amplification Reactions Bio-Technology, 11(9), pp. 1026-1029.

Hiramatsu K., Y. Katayama, H. Yuzawa, T. Ito. (2002) 'Molecular genetics of *Methicillin-resistant staphylococcus aurous'*, Int. J. Med. Microbiol. 292, pp 67-74.

Huber, M., Losert, D., Hiller, R., Harwanegg, C., Mueller, M.W. and Schmidt, W.M. (2001) 'Detection of single base alterations in genomic DNA by solid phase polymerase chain reaction on oligonucleotide microarrays', Analytical Biochemistry, 299(1), pp. 24-30.

Huletsky, A., R. Giroux, V. Rossbach, M. Gagnon, M. Vaillancourt, M. Bernier,F. Gagnon, K. Truchon, M. Bastien, F. J. Picard, A. van Belkum, M. Ouellette, P. H. Roy, and M. G. Bergeron (2004) 'New Real-Time PCR Assay for Rapid Detection of Methicillin-Resistant *Staphylococcus aureus* Directly from Specimens Containing a Mixture of Staphylococci', Journal of Clinical Microbiology,Vol. 42 (5) pp. 1875–1884.

ISO/IEC as the ISO/IEC 23270 Information technology Programming languages C# Second edition (2006-09-01)

Ito. T., Katayama Y., Hiramatsu, K. (1999) 'Cloning and nucleotide sequence determination of the entire mec DNA of pre-methicillin-resistant *Staphylococcus aureus* strain N315', Antimicrob. Agents Chemother. 43, pp 1449-1458.

Jackson, J.H. and MacCluer, C.R., (2010) 'Hyperbolic Saturation', Bulletin of mathematical biology, 72(5), pp. 1315-1322.

Ji, H.M., Samper, V., Chen, Y., Hui, W.C., Lye, H.J., Mustafa, F.B., Lee, A.C., Cong, L., Heng, C.K. and Lim, T.M. (2007) 'DNA purification silicon chip', Sensors and Actuators, A: Physical, 139(1-2 SPEC. ISS.), pp. 139-144.

Jia, G., Siegrist, J., Deng, C., Zoval, J.V., Stewart, G., Peytavi, R., Huletsky, A., Bergeron, M.G. and Madou, M.J. (2007) 'A low-cost, disposable card for rapid polymerase chain reaction', Colloids and Surfaces B: Biointerfaces, 58(1), pp. 52-60.

Katayama Y, Ito T, Hiramtsu K. (2000) 'A new class of genetic element, staphylococcus cassette chromosome mec, encodes methicillin- Resistant *Staphylococcus aureus*', Antimicrob. Agents Chemother., 44: pp 1549-1555.

Kim, J., Byun, D., Mauk, M.G. and Bau, H.H. (2009) 'A disposable, self-contained PCR chip', Lab on a Chip - Miniaturisation for Chemistry and Biology, 9(4), pp. 606-612.

Kim, Y., Shin, K., Kang, J., Yang, E., Paek, K., Seo, D.-. and Ju, B. (2006) 'Poly(dimethylsiloxane)-based packaging technique for microchip fluorescence detection system applications', Journal of Microelectromechanical Systems, 15(5), pp. 1152-1158.

Kopp, M.U., De Mello, A.J. and Manz, A. (1998) 'Chemical amplification: Continuous-flow PCR on a chip. Science', 280(5366), pp. 1046-1048.

Lab-on-chip. Gene-quantification.info (2010) Available at: http://www.gene-quantification .de/lab-on-chip.html (Accessed: 30 April 2010).

Lagally, E.T., Medintz, I. and Mathies, R.A. (2001) 'Single-molecule DNA amplification and analysis in an integrated microfluidic device', Analytical Chemistry, 73(3), pp. 565-570.

Larrick, J.W., (1997) 'The PCR Technique: Quantitative PCR. Eaton Publishing', U.S.A, pp. 3-13.

Lee, D., Wu, M., Ramesh, U., Lin, C., Lee, T. and Chen, P. (2004) 'A novel real-time PCR machine with a miniature spectrometer for fluorescence sensing in a micro liter volume glass capillary', Sensors and Actuators, B: Chemical, 100(3), pp. 401-410.

Lee, J.-., Cheong, K.H., Huh, N., Kim, S., Choi, J.-. and Ko, C. (2006) 'Microchip-based one step DNA extraction and real-time PCR in one chamber for rapid pathogen identification', Lab on a Chip - Miniaturisation for Chemistry and Biology, 6(7), pp. 886-895.

Lee G. B, Jung-HaoWang, Liang-Ju Chien, Tsung-Min Hsieh, Ching-Hsing Luo,Wen-Pin Chou,Ping-Hei Chen, Pei-Jer Chen, Da-Sheng Lee (2009) 'miniaturized quantitative polymerase chain reaction system for DNA amplification and detection', Sensors and Actuators B 141 ,pp 329–337.

Lee T.M., M.C. Carles, and I. Hsing, (2003) 'A Miniaturized DNA amplifier: its application in traditional Chinese medicine, Lab Chip. 3, 100–105.

Li, Y., Xing, D. and Zhang, C. (2009) 'Rapid detection of genetically modified organisms on a continuous-flow polymerase chain reaction microfluidics', Analytical Biochemistry, 385(1), pp. 42-49.

Liao, C.S., Lee, G.B., Liu, H.S., Hsieh, T.M. and Luo, C.H. (2005) 'Miniature RT-PCR system for diagnosis of RNA-based viruses', Nucleic acids research, 33(18),.

Lin Y.C., C.C. Yang, and M.Y. Huang (2000) 'A rapid micro-PCR system for hepatitis C virus amplification Sensor', Actuat. B-Chem. 71,127–133.

Liu, J., Enzelberger, M. and Quake, S. (2002) 'A nanoliter rotary device for polymerase chain reaction', Electrophoresis, 23(10), pp. 1531-1536.

Liu, F., Zhuo Li, Shitao Yu, Xiao Cui, Xiaoping Ge, (2009) 'Environmentally benign methanolysis of polycarbonate to recover bisphenol A and dimethyl carbonate in ionic liquids'. Journal of hazardous materials (impact factor: 4.14); 174(1-3), pp 872-875.

Madou, M.J. (2002) Fundamentals of Microfabrication: The Science of miniaturization 2nd Edition edn. UK: CRC Press.

Matsubara, Y., Kerman, K., Kobayashi, M., Yamamura, S., Morita, Y. and Tamiya, E., (2005) 'Microchamber array based DNA quantification and specific sequence detection from a single copy via PCR in nanoliter volumes'. Biosensors and Bioelectronics, 20(8 SPEC. ISS.), pp. 1482-1490.

Mehra, S. (2005) 'A kinetic model of quantitative real-time polymerase chain reaction', Biotechnology and Bioengineering, 91(7), pp. 848.

Meyer R., (1999) Development and application of DNA analytical methods for the detection of GMOs in food, Food Control (10), pp. 391-399.

McPherson .M and Simon Muller (2006) PCR., second edition edn. Taylor and Francis Group.

Miller J. C. and Miller J. N. (1993) Statistics for Analytical Chemistry, third edition, Ellis Horwood Limited.

Mullis, K., Faloona, F. and Scharf, S. (1986) 'Specific enzymatic amplification of DNA in vitro: The polymerase chain reaction', Cold Spring Harbor symposia on quantitative biology, 51(1), pp. 263-273.

Murray HG and Thompson WF (1980) Rapid isolation of high molecular weight plant DNA. Nucleic Acid Research (8), pp 4321-4325.

MRSA, NHS, (2011) UK Available at: http://www.nhs.uk/conditions/mrsa/Pages/Introduction.aspx (Accessed: 29 September 2011).

Nagai, H., Murakami, Y., Morita, Y., Yokoyama, K. and Tamiya, E. (2001) 'Development of a microchamber array for picoliter PCR', Analytical Chemistry, 73(5), pp. 1043-1047.

Obeid, P.J., Christopoulos, T.K., Crabtree, H.J. and Backhouse, C.J. (2003) 'Microfabricated device for DNA and RNA amplification by continuous-flow polymerase chain reaction and reverse transcription-polymerase chain reaction with cycle number selection', Analytical Chemistry, 75(2), pp. 288-295.

Park, K.H., Park, H.G., Kim, J. and Seong, K.H., (2006) 'Poly (dimethyl siloxane)-based protein chip for simultaneous detection of multiple samples: Use of glycidyl methacrylate photopolymer for site-specific protein immobilization', Biosensors and Bioelectronics, 22(5), pp. 613-620.

Rago J. V., Lieutenant Keith Buhs, Viktroija Makarovaite, Esha patel, Melissa Pomeroy, Christina Yasmine (2012) 'Detection and analysis of *Staphylococcus aureus* isolates from the Chicago metropolitan area', American jornal of infectious control 40, pp. 201-205.

Saiki, R.K., Gelfand, D.H., Stoffel, S., Scharf, S.J., Higuchi, R., Horn, G.T., Mullis, K.B. and Erlich, H.A. (1988) 'Primer-directed enzymatic amplification of DNA with a thermostable DNA polymerase', Science, 239(4839), pp. 487-491.

Saiki, R.K., Scharf, S. and Faloona, F. (1985) 'Enzymatic amplification of β-globin genomic sequences and restriction site analysis for diagnosis of sickle cell anemia', Science, 230(4732), pp. 1350-1354.

Saunders G C., Juliet Dukes, Helen C. Parkes, and Johanne H., Cornett (2001) 'Interlaboratory Study on Thermal Cycler Performance in Controlled PCR and Random Amplified Polymorphic DNA Analyses', Clinical Chemistry 47:pp147–55.

Sauer-Budge, A.F., Mirer, P., Chatterjee, A., Klapperich, C.M., Chargin, D. and Sharon, A. (2009) 'Low cost and manufacturable complete microTAS for detecting bacteria', Lab on a Chip - Miniaturisation for Chemistry and Biology, 9(19), pp. 2803-2810.

Schnell, S. and Mendoza, C. (1997) 'Theoretical description of the polymerase chain reaction. Journal of theoretical biology', 188(3), pp. 313-318.

Skoog.D.A, West.D.M, Holler F.J. and Crouch .S.R.. (2004) 'Fundamentals of analytical chemistry', eighth edition edn. USA: Thomson and Brooks/Cole,.

Soane D.S. (1992) 'Polymer Application for biotechnology', Prentice-Hall, Inc. USA.

Stryer Lubert (1981) Biochemistry. W.H. Freeman and company , San Francisco, USA.

Sun, Y., Kwok, Y.C. and Nguyen, N.T. (2007) 'A circular ferrofluid driven microchip for rapid polymerase chain reaction', Lab on a Chip - Miniaturisation for Chemistry and Biology, 7(8), pp. 1012-1017.

Tsai, M.H. and Saier Jr., M.H. (1995) 'Phylogenetic characterization of the ubiquitous electron transfer flavoprotein families ETF-α and ETF-β'. Research in microbiology, 146(5), pp. 397-404.

Vogel's (2000) Textbook of Quantitative chemical analysis. 6th edn. Harlow : Prentice Hall.

Walker, G.T., Little, M.C., Nadeau, J.G. and Shank, D.D. (1992) 'Isothermal in vitro amplification of DNA by a restriction enzyme/DNA polymerase system', Proceedings of the National Academy of Sciences of the United States of America, 89(1), pp. 392-396.

Wang, J., Chien, L., Hsieh, T., Luo, C., Chou, W., Chen, P., Chen, P., Lee, D. and Lee, G. (2009a) 'A miniaturized quantitative polymerase chain reaction system for DNA amplification and detection', Sensors and Actuators, B: Chemical, 141(1), pp. 329-337.

Wang, J., Chien, L., Hsieh, T., Luo, C., Chou, W., Chen, P., Chen, P., Lee, D. and Lee, G. (2009b) 'A miniaturized quantitative polymerase chain reaction system for DNA amplification and detection', Sensors and Actuators B: Chemical, 141(1), pp. 329-337.

Wang L.,H. Song, T. Chen and Z. Wang (2012c) 'A Design of DSPIC Based chip Temperature Controlling System', Applied Mechanics and Materials, 108, pp 206-211.

Weller TMA (1999) 'The distribution of *mecA*, mecR1 and *mec1* andsequence analysis of mec1and the *mec* promoter region in *staphylococci* expressing resistance to *methicillin*', J. Antimicrob Chemother., (43): pp 15-22.

Wittwer, C.T., Fillmore, G.C. and Garling, D.J. (1990) 'Minimizing the time required for DNA amplification by efficient heat transfer to small samples', Analytical Biochemistry, 186(2), pp. 328-331.

Woolley, A.T., Hadley, D., Landre, P., DeMello, A.J., Mathies, R.A. and Northrup, M.A. (1996) 'Functional integration of PCR amplification and capillary electrophoresis in a microfabricated DNA analysis device', Analytical Chemistry, 68(23), pp. 4081-4086.

Xiang, Q., Xu, B. and Li, D. (2007) 'Miniature real time PCR on chip with multi-channel fiber optical fluorescence detection module', Biomedical Microdevices, 9(4), pp. 443-449.

Xu Z., Lin Li1, Xihong Zhao, Jin Chu, Bing Li, Lei Shi, Jianyu Su and Mark E. Shirtliff (2011) 'Development and application of a novel multiplex polymerase chain reaction (PCR) assay for rapid detection of various types of staphylococci strains', African Journal of Microbiology Research Vol. 5(14), pp. 1869-1873.

Yang J., Y. Liu, C.B. Rauch, R.L. Stevens, R. Liu, R. Lenigk, and P.Grodzinski, (2002) 'High sensitivity PCR assay in plastic micro reactors', Lab. Chip. 2, 179–187.

Yao, B., Luo, G., Wang, L., Gao, Y., Lei, G., Ren, K., Chen, L., Wang, Y., Hu, Y. and Qiu, Y. (2005) 'A microfluidic device using a green organic light emitting diode as an integrated excitation source', Lab-on-a-Chip, Miniaturisation for Chemistry and Biology, 5(10), pp. 1041-1047.

Young, H.K., Yang, I., Bae, Y. and Park, S. (2008) 'Performance evaluation of thermal cyclers for PCR in a rapid cycling condition', BioTechniques, 44(4), pp. 495-505.

Zhang, C., Xing, D. and Xu, J. (2007) 'Continuous-flow PCR microfluidics for rapid DNA amplification using thin film heater with low thermal mass', Analytical Letters, 40(9), pp. 1672-1685.

Zou, Q., Miao, Y., Chen, Y., Sridhar, U., Chong, C.S., Chai, T., Tie, Y., Teh, C.H.L., Lim, T.M. and Heng, C.K. (2002) 'Micro-assembled multi-chamber thermal cycler for low-cost reaction chip thermal multiplexing', Sensors and Actuators, A: Physical, 102(1-2), pp. 114-121.

Zou, Z., Chen, X., Jin, Q., Yang, M. and Zhao, J. (2005) 'A novel miniaturized PCR multi-reactor array fabricated using flip-chip bonding techniques', Journal of Micromechanics and Microengineering, 15(8), pp. 1476-1481.

Appendix1

Thermistor was calibrated and linearised using the Steinhart-Hart equation

Thermistor Connection and Calculation with ADC-24:
The JT thermistor 0.5 mm 1 % tolerance as in instillation sheet was as follows:

Input voltage	0.1	0.15	0.2	0.25	0.3	0.35	0.4	0.45	0.5	0.55	0.6	0.65	0.7	0.75	0.8	0.85	0.9	1.0	1.05	1.1
Temp. °C	1.92	12.73	20.87	27.53	33.25	38.32	42.91	47.15	51.11	54.85	58.42	61.84	65.16	68.39	71.54	74.65	77.71	80.75	86.8	89.83

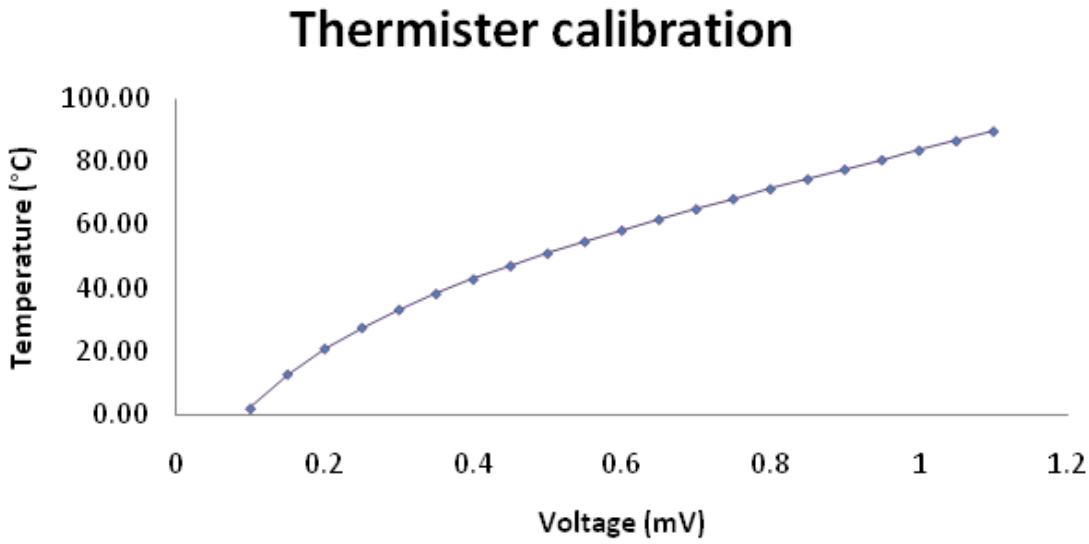

Calculation: with thermistorthermistor as upper (R_T) part of potential divider

$$\frac{V_{out}}{V_{in}} = \frac{R_2}{R_T + R_2} \qquad \frac{V_{in}}{V_{out}} = \frac{R_T + R_2}{R_2} = \frac{R_T}{R_2} + 1$$

$$\frac{V_{in}}{V_{out}} - 1 = \frac{R_T}{R_2} \qquad R_T = \left(\frac{V_{in}}{V_{out}} - 1\right) R_2$$

Temperature according to Steinhart and Hart equation then the equation was calculated from the software as in the web link below. (http://www.daycounter.com/Calculators/Steinhart-Hart-Thermistor-Calculator.phtml)

$$T = \frac{1}{a + b\ln R_T + c(\ln R_T)^3}$$ (T in Kelvin)

Combined equation:

$$T = 1/\left[a + b\ln\left((Vi/Vo - 1)R_2\right) + c(\ln\left((Vi/Vo - 1)R_2\right))^3\right]$$

Values for coefficients for 10k precision thermistor, using 50, 70, 90 ºC as obtained from YSI calculator spreadsheet 'ysi Steinhart _ hart calculator.xls' and data sheet

a = 2.68646E-03 for Temperature 50 ºC
b = 2.83964E-04 for Temperature 70 ºC
c = 1.44866E-06 for Temperature 90 ºC
With values entered for 10k thermistor, 10k R2 and 2.5V reference

$$T = 1/(2.68646E-03 + 2.83964E-04\ln((2.5/Vo - 1)*10) + 1.44866E-06(\ln((2.5/Vo - 1)*10))\text{\^{}}3)$$

Data logger is then programmed as follows;
Recording method is Real-time Continuous, setting sampling was set on 60 m second, readings per sample are single – Input Channel A is sited on Channel 1 only. Then, the Data-logger was connected via a USB cable with the software in personal computer.
The calibrated thermistor equation is:
1/(0.0026529+0.00033266*ln(1.0*(2500.00/A1.0))+0.0000010557*(ln(1.0*(2500.00/A-1.0)))power 3)-273.15

Appendix 2

Experimental data for Fluorescence measurements

Table A 4.1 FITC calibration data using the prototype photo-detector.

FITC (ng ml^{-1})	Fluorescence signal 1	Fluorescence signal 2	Fluorescence signal 3
Bl	0	0	0
0.05	2007.8	1923.6	1697.6
0.1	3942	3941.2	4230.4
0.15	6198.6	6382	6198.6
0.2	9019.4	9099	7775.2
0.25	11665.2	11470.4	11743.8
0.5	25126.2	25830.6	25988.6

Table A 4.2 FITC calibration data using H4000 Ocean Optic spectrophotometer.

FITC (ng ml^{-1})	Fluorescence signal 1	Fluorescence signal 2	Fluorescence signal 3
Bl	0	0	0
0.05	102	188	192
0.1	278	336	329
0.15	409	517	494
0.2	632	701	680
0.25	844	936	941
0.5	1829	1915	1869

Table A 4.3 The second FITC calibration data using the prototype photo-detector on lower concentrations

FITC (ng ml^{-1})	Fluorescence signal 1	Fluorescence signal 2	Fluorescence signal 3
Bl	0	0	0
0.0125	609.8	958.2	446.8
0.025	1367.4	1331	1364.4
0.05	2352.2	2331.8	2253.2
0.075	3462	3453.2	3256.2
0.1	4360	4337.2	3953
0.125	5699.4	5704.2	5536.8
0.15	6593	6570.8	6522.2

Table A 4.4 DNA calibration data using Micro-plate reader on lower concentrations

DNA (ng µl^{-1})	Fluorescence signal 1	Fluorescence signal 2	Fluorescence signal 3
Bl	0	0	0
0.5	3	3	4
1	7	7	8
2	17	17	16
4	38	38	39
6	55	54	53
8	74	74	75
10	81	80	80

Table A 4.5 DNA calibration data using the prototype photo-detector.

DNA (ng µl^{-1})	Fluorescence Sig.1	Fluorescence Sig.2	Fluorescence Sig.3	Fluorescence sig. 4
Bl	0	0	0	0
0.5	217	390.2	480.2	506
1	898.4	706	771.4	988.2
2	1553.8	1448.2	1539.4	2192
4	3424.8	3101	3181	2506.2
6	4990.4	4786.6	4868.4	3629.4
8	6322	7046.2	6988.8	5263.6
10	6810	8007	7853.6	6291.4

Table A 4.6 DNA calibration data using H4000 Ocean Optic spectrophotometer on lower concentrations.

DNA (ng µl^{-1})	Fluorescence signal 1	Fluorescence signal 1	Fluorescence signal 1
Bl	0	0	0
0.5	18	15	20
1	43	46	40
2	61	62	65
4	212	215	200
6	333	325	350
8	435	450	435
10	491	505	490

Table A 4.7 DNA calibration of Lambda Kit calibration data using the prototype photo-detector.

DNA (ng ml^{-1})	Fluorescence signal 1	Fluorescence signal 1	Fluorescence signal 1
Bl	0	0	0
100	1775	1767	1770.4
200	3241	3246	3245
300	4656	4657	4660.5
400	5598	5604	5601.8
500	8551	8554.5	8554.3
600	11020	11020.75	11020.55
700	13048	13044	13046.6
1000	18025	18032	18028.2

Appendix 3

NCBI Information of the designed primers

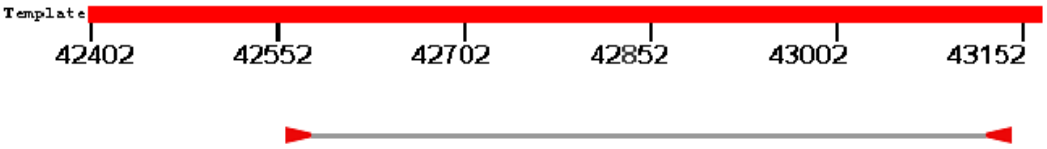

Escherichia coli str. K-12 substr. DH10B, complete genome >gi|169887498|gb|CP000948.1| *Escherichia coli* str. K12 substr. DH10B, complete genome . Features associated with this product `putative electron transfer flavoprotein FixA`

```
Forward primer 1   AGCAACAGGCAGCAGAGGCG 20

Template    42548 ..................... 42567


Reverse primer 1   GACGTTCGCGCTGTTTCGGC 20

Template    43099 ..................... 43080
```

Fit to GCCGAAACAGCGCGAACGTC.

Graphs of the gene:

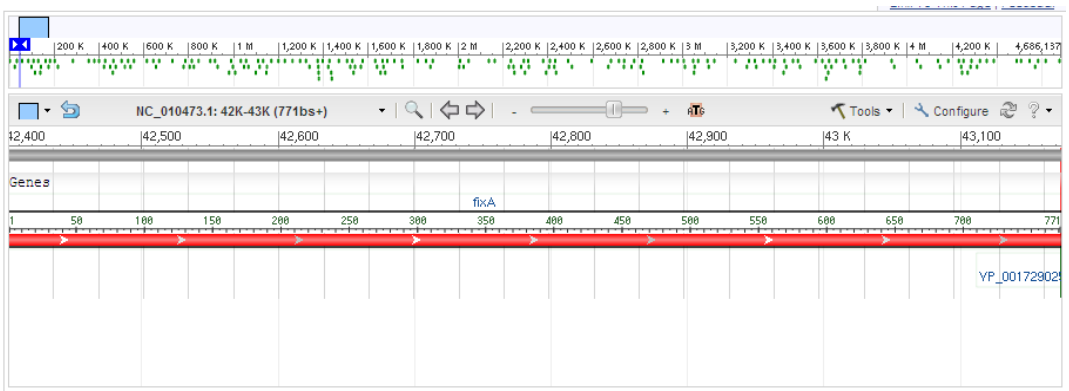

gi|170079663:42548-43099 Escherichia coli str. K-12 substr. DH10B chromosome, complete genome. products on allowed transcript variants

AGCAACAGGCAGCAGAGGCGCAGGTGACAGCCTTAAGTGTGGGCGGTAAAGCCCTG
ACCAACGCCAAAGGGCGTAAAGATGTGCTATCGCGCGGCCCGGATGAACTGATTGTG
GTGATTGATGACCAGTTCGAGCAGGCACTGCCGCAACAAACGGCGAGCGCACTGGCT
GCAGCCGCCCAGAAAGCAGGCTTTGATCTGATCCTCTGTGGCGATGGTTCTTCCGACC
TTTATGCCCAGCAGGTTGGTCTGCTGGTGGGCGAAATCCTCAATATTCCGGCAGTTAA
CGGCGTCAGCAAAATTATCTCCCTGACGGCAGATACCCTCACCGTTGAGCGCGAACTG
GAAGATGAAACCGAAACCTTAAGCATTCCGCTGCCTGCGGTTGTTGCTGTTTCCACTGA
TATCAACTCCCCACAAATTCCTTCGATGAAAGCCATTCTCGGCGCGGCGAAAAAGCCC
GTCCAGGTATGGTCGGCGGCGGATATTGGTTTTAACGCAGAGGCAGCCTGGTCAGAA
CAACAGGTTGCCGC CCGAAACAGCGCGAACGTC

Showing the complete gene sequence 771 bp region from base 42403 to 43173:

ATGAAGATTATTACTTGCTATAAGTGCGTGCCTGATGAACAGGATATTGCGGTC
AATAATGCTGATGGTTCATTAGACTTCAGCAAAGCCGATGCCAAAATAAGCCAA
TACGATCTCAACGCTATTGAAGCGGCTTGCCAGCTAAAGCAACAGGCAGCAGAG
GCGCAGGTGACAGCCTTAAGTGTGGGCGGTAAAGCCCTGACCAACGCCAAAGGG
CGTAAAGATGTGCTATCGCGCGGCCCGGATGAACTGATTGTGGTGATTGATGAC
CAGTTCGAGCAGGCACTGCCGCAACAAACGGCGAGCGCACTGGCTGCAGCCGCC
CAGAAAGCAGGCTTTGATCTGATCCTCTGTGGCGATGGTTCTTCCGACCTTTAT
GCCCAGCAGGTTGGTCTGCTGGTGGGCGAAATCCTCAATATT
CCGGCAGTTAACGGCGTCAGCAAAATTATCTCCCTGACGGCAGATACCCTCACC
GTTGAGCGCGAACTGGAAGATGAAACCGAAACCTTAAGCATTCCGCTGCCTGCG
GTTGTTGCTGTTTCCACTGATATCAACTCCCCACAAATTCCTTCGATGAAAGCC
ATTCTCGGCGCGGCGAAAAAGCCCGTCCAGGTATGGTCGGCGGCGGATATTGGT
TTTAACGCAGAGGCAGCCTGGTCAGAACAACAGGTTGCCGCGCCGAAACAGCGC
GAACGTCAGCGCATCGTGATTGAAGGCGACGGCGAAGAACAGATCGCCGCATTT
GCTGAAAATCTTCGCAAAGTCATTTAA